Urban Greenery Unveiled: A Knowledge-Based Approach to Characterizing and Mapping Urban Green Spaces

Inaugural-Dissertation

for the degree of

Doctor of Natural Sciences (Dr. rer. nat.)

in the

Faculty of Applied Computer Science

University of Augsburg

by

Irada Ismayilova

2025

Evaluation committee: Prof. Dr. Sabine Timpf
Prof. Dr. Jukka M. Krisp

Date of Defence: 14.03.2025

Abstract

Urban Green Spaces (UGS) significantly affect human well-being in growing cities, with even the sight of greenery enhancing mental productivity and reducing stress-related health issues. Research suggests that the impact of green spaces varies by type. However, existing UGS classifications often overlook small and heterogeneous UGS types due to limited understanding of them, which leads to a substantial portion of urban greenery being missed.

This thesis addresses gaps in UGS typologies by establishing a comprehensive list of UGS types present in southern German cities, which we incorporate into a UGS ontology. This ontology includes seven main UGS types- forest, park, grassland, cemetery, urban agriculture, green corridor, and amenity- divided into 28 sub-types. Unlike typologies, our ontology is extendable and machine-interpretable through its formalization. To support ontology-based UGS mapping, we further propose a UGS feature properties schema that is enriched with green space type-relevant semantic information.

We conduct a novel knowledge-based mapping approach that extracts semantic information relevant to UGS types using official definitions and legal documentation. By combining GIScience tools with machine learning techniques, we create spatial datasets for each semantic feature and perform semantics-based identification. Our findings include detailed semantic characteristics for four UGS types and suggest that while some characteristics effectively map specific green spaces, others require adjustments to enhance their specificity and geographic applicability. By further using Random Forest (RF) classification with Sentinel-2 data and digital orthophotos (DOP), we assess the distribution of urban green in Augsburg and Wuerzburg, achieving over 90% accuracy. Sentinel-2 with RF can accurately detect large, homogeneous green areas such as forests. In contrast, for more precise delineation of green areas, including individual tree crowns, DOP is a better data choice.

This thesis advances the UGS domain, offering a robust knowledge-based mapping tool for urban planners and decision makers. We, also identify areas for future research such as refining the ontology's feature parameters and extensively testing the developed spatial-semantic features across different regions to confirm their effectiveness. This can enhance the ontology's utility in urban planning, and help to establish new semantic features of UGSs that better reflect their dynamic nature.

Zusammenfassung

Städtische Grünflächen (Urban Green Spaces - UGSs) beeinflussen das menschliche Wohlbefinden in wachsenden Städten erheblich, wobei bereits der Anblick von Grün die mentale Produktivität steigern und stressbedingte Gesundheitsprobleme reduzieren kann. Die Forschung legt nahe, dass die Wirkung von Grünflächen je nach Typ variiert. Bestehende Klassifikationen von UGSs übersehen jedoch häufig kleine und heterogene Grünflächen-Typen aufgrund unseres begrenzten Verständnisses dieser, was dazu führt, dass ein erheblicher Teil städtischer Grünflächen unberücksichtigt bleibt.
Diese Dissertation adressiert Lücken in den UGS-Typologien, indem sie eine umfassende Liste von UGS-Typen erstellt, die in süddeutschen Städten vorhanden sind, und diese in eine UGS-Ontologie integriert. Diese Ontologie umfasst sieben Haupttypen von UGS-Wald, Park, Grasland, Friedhof, städtische Landwirtschaft, Grünkorridor und Gemeinbedarfsnutzung - unterteilt in 28 Unterarten. Im Gegensatz zu Typologien ist eine Ontologie erweiterbar und maschineninterpretierbar durch ihre Formalisierung. Zur Unterstützung der auf Ontologie basierenden Grünflächen-Kartierung schlagen wir darüber hinaus ein Schema von Merkmalseigenschaften vor, das mit typenspezifischen Informationen angereichert ist.
Wir setzen einen innovativen, wissensbasierten Kartierungsansatz ein, der semantische Informationen extrahiert, die für die UGS-Typen relevant sind. Dafür verwenden wir offizielle Definitionen und rechtliche Dokumentationen. Durch die Kombination von Geoinformatikwerkzeugen mit maschinellen Lernverfahren erstellen wir räumliche Datensätze für jedes semantische Merkmal und nutzen eine semantikbasierte Identifikation. Unsere Ergebnisse umfassen detaillierte semantische Merkmale für vier UGS-Typen und deuten darauf hin, dass einige Merkmale Grünflächen effektiv kartieren, während andere Anpassungen benötigen, um ihre Spezifität und geografische Anwendbarkeit zu erhöhen. Durch den weiteren Einsatz einer Random-Forest-Klassifikation (RF) mit Sentinel-2-Daten und digitalen Orthophotos bewerten wir die Verteilung der Grünflächen in Augsburg und Würzburg und erreichen eine Genauigkeit von über 90%. Sentinel-2 mit RF kann große, homogene Grünflächen wie Wälder genau identifizieren. Im Gegensatz dazu sind digitale Orthophotos die bessere Datenbasis für eine präzisere Abgrenzung von Grünflächen, einschließlich einzelner Baumkronen.
Diese Dissertation leistet einen Beitrag in der UGS-Forschung, indem sie Stadtplanern

und Entscheidungsträgern ein robustes, wissensbasiertes Kartierungswerkzeug bietet. Wir identifizieren jedoch auch Bereiche für zukünftige Forschung, wie die Verfeinerung der Merkmalsparameter der Ontologie und umfangreiche Tests der entwickelten räumlich-semantischen Merkmale in verschiedenen Regionen, um deren Wirksamkeit zu bestätigen. Dies kann die Nützlichkeit der Ontologie in der Stadtplanung erhöhen, indem neue semantische Merkmale integriert werden, die die dynamische Natur der UGS besser widerspiegeln.

Acknowledgment

Working on this thesis has been the greatest challenge of my life thus far. However, it would not have been possible to overcome this challenge without the caring support from my friends, family, and colleagues. I take this opportunity to express my sincere gratitude to Prof. Dr. Sabine Timpf, who encouraged me to choose a topic that genuinely interests me and shared her scientific and personal wisdom throughout. Without her assurance and help to stay on track, this thesis would not have seen the light of day. I also extend my gratitude to Prof. Dr. Jukka Krisp, who generously shared his knowledge and experience in countless GIG meetings and provided invaluable suggestions over the years.

This thesis is also the product of great support from my colleagues. Ana and Nikolina hold a special place, as they were beside me in biweekly meetings, patiently listening to my concerns and continuously offering help. I sincerely thank Eva, with whom I shared my office, for her continuous support, for sharing her experiences, and for always being available for discussions. Lika, Pablo, and Zulfa were there for me, whenever I needed a coffee break and were always open to discussions and suggestions. My Sion graduate retreat colleagues were an indispensable part of this journey, through countless Mensa meetings and end-of-semester celebrations. Thank you for always making me feel comforted that we all struggle in similar ways.

"The supreme happiness of life is the conviction that we are loved; loved for ourselves - say rather, loved in spite of ourselves; the conviction the blind have" (*Les Misérables*). I am deeply grateful to my husband, Christian, who consistently made me feel valued and loved, patiently supporting me through my moments of hesitation and confusion. He always reassured me that everything would be alright, while also generously sharing his expertise. I could not have pursued my dreams without the unconditional support of my mom and my sister. There are no words that can describe my gratitude to them. Thank you for loving me for who I am and never doubting what I can achieve.

Contents

List of Figures

List of Tables

Abbreviations

CIR	Color Infrared
CORINE	Coordination of Information on the Environment
DBSCAN	Density-Based Spatial Clustering of Applications with Noise
DL	Deep Learning
DOP	Digital Orthohoto
DSM	Digital Surface Model
DTM	Digital Terrain Model
ESS	Ecosystem Services
FAO	Food and Agriculture Organization
geoOBIA	Geographic Object-Based Image Analysis
GI	Green Infrastructure
GIS	Geographic Information System
GIScience	Geographic Information Science
GLCM	Grey-Level Co-occurrence Matrix
GLI	Green Leaf Index
IML	Interpretable Machine Learning
LC	Land Cover
LiDAR	Light Detection and Ranging
LU	Land Use
LULC	Land Use and Land Cover
ML	Machine Learning
MMU	Minimum Mapping Unit
nDSM	Normalized Digital Surface Model
NDVI	Normalized Difference Vegetation Index
NDWI	Normalized Difference Water Index
NGRDI	Normalized Green-Red Difference Index
NIR	Near-Infrared
OAT	One-at-a-time
OSM	Open Street Map
PUA	Peri-Urban Agriculture

RGBVI	Red-Green-Blue Vegetation Index
SA	Sensitivity Analysis
SAR	Synthetic Aperture Radar
SHAP	Shapley Additive Explanations
SVM	Support Vector Machine
SWIR	Short-wave Infrared
TN	Tatsächliche Nutzung (Actual LU)
UAV	Unoccupied Aerial Vehicle
UA	Urban Atlas
UGS	Urban Green Space

Chapter 1

On the Importance of Urban Green Spaces

"Who would want to live in a city made of only concrete?" asks the citizens' initiative "Preserve Green Spaces" in Munich[1]. Meanwhile, the intercultural garden "grow up" in Augsburg celebrates "our garden stays!"[2], as they manage not to fall victim for a re-planning initiative of the Reese park. Today, over half of the world's population lives in urban areas[3], even though these areas make up just 2% of the Earth's land surface [125]. Therefore, facilitating sustainable living conditions for every single human being is more important than ever before.

UGSs have long been known for their exceptional effect on human well-being. Studies show, that as little as looking out of a window and seeing green can already enhance mental productivity and reduce stress-induced adverse health effects [77]. Furthermore, it is also known, that different types of UGSs can have different well-being effects. For instance, parks and recreational areas play a significant role in enhancing physical health as they offer spaces for activities such as walking and jogging, which are instrumental in reducing obesity and other health problems [73]. Whereas, allotment gardens are associated with higher perceived subjective happiness [105]. Gardeners that are involved in gardening and production activities are also shown to have higher self-esteem and experience less depression and fatigue [148]. Moreover, community gardens provide excellent opportunity for social interaction and community engagement, thus facilitation strong community bonds [73].

However, not only availability but also accessibility appears to have an effect on human

[1] https://www.gruenflaechen-erhalten.de/ (accessed on 01.2025)

[2] https://www.growup-augsburg.de/ (accessed on 01.2025)

[3] https://www.un.org/en/development/desa/population/publications/pdf/urbanization/WUP2011_Report.pdf (accessed on 01.2025)

well-being. As such, in the existing literature, proximity and access to UGSs is associated with higher life satisfaction and perceived quality of life as well as lower anxiety and depression [56][73]. Inequalities in distribution of UGSs become especially evident in the times of crisis. For instance, during the COVID-19 pandemics, public UGSs were seen as "safe haven", where people could relax in fresh air without the fear of getting infected. This was particularly true for residents who did not own green space, e.g. garden [117]. Further, a study by Korpilo et al. [85] illustrated that during the pandemic, residents were more likely to visit UGSs close to their homes, and showed a preference for less crowded natural areas over crowded parks and recreational spaces. In addition, there was observed a noticeable shift towards exploring new types of UGSs such as agricultural land and areas with high tree density. Thus, once again, highlighting importance of not only the quantity but also variety, quality, and accessibility of UGSs.

In order to be able to support the full range of well-being services that UGSs provide, and to be be able to benefit from these services, it is important to know what type of UGSs exist, where they are located and who has the access to them. But how much green space does one person require in order to benefit from its service? Values might differ by countries. World Health Organization[4] sets 9 m^2 of green space per capita within 15 minutes of walking distance as a minimum required threshold. In the context of Germany, for instance, Taubenböck et al. [135] reveal, that green space distribution across german cities varies immensely. However, even cities with the least amount of green, provide more green space than the minimum suggested amount by the World Health Organization.

While availability of UGS might be important, only their accessibility by a general public will determine their service provisioning. Research shows that there are still inequalities in the access of UGSs by ethnicity, sex, and age. As such, in many European cities, immigrant communities frequently face restricted access to UGSs when compared to non-immigrant populations. This lack of access can result in unequal health advantages and a diminished overall well-being within these communities [30]. Furthermore, children and elderly are shown to be the groups with the highest demand of UGSs, due to increased screen time and disconnection from nature for former, and improved longevity and general health for the latter one [76].

Importance and necessity of UGSs are also mirrored within the Sustainable Development Goals of the United Nations. The goal 11.7 is particularly dedicated to UGSs, and encourages to provide "universal access to safe, inclusive and accessible, green and public spaces, in particular for women and children, older persons and persons with disabilities" by 2030[5]. Therefore, acknowledging human well-being effects of various types of UGSs can directly influence urban planning initiatives. In this regard, understanding what types of green cities store, where they are located, and whether they are capable

[4]https://www.who.int/docs/default-source/environment-climate-change-and-health/sustainable-development-indicator-cities.pdf?sfvrsn=c005156b_2 (accessed on 01.2025)

[5]https://www.un.org/en/development/desa/population/migration/generalassembly/docs/globalcompact/A_RES_70_1_E.pdf (accessed on 01.2025)

to provide expected services (e.g. due to size or spatial configuration) should be part for every sustainable urban planning activity.

1.1 Problem Statement

Currently, there is no universal agreement of what types of UGSs exist. This makes development of a common classification framework essential. This is especially vital from the human well-being perspective. Furthermore, methods for UGS identification can vary based on the green space type of interest. Disparity between UGS types can clearly be seen in the existing literature, particularly in common Land Use and Land Cover maps. As such, majority of studies, either consider overall green without particularly defining types of green like in Taubenböck et al. [135], or consider only open, public, and large green areas [127]. It is a common practice, that the overall scope of studies will define which types of green spaces will be taken into account. For instance, if focus is laid on hedonic house price estimation [15], selected UGS types will be different than if a conducted study is more interested in green infrastructure [74].

It is evident, that the choices we make when selecting information to represent on maps, will ultimately affect the stories we tell [100]. And this is particularly obvious in UGS maps. In order to understand how much green a city accommodates, where, and what type of green is there, one would commonly reach to Land Use and Land Cover (LULC) maps. However, these maps might not always represent the reality at a greater detail, or be purely only land use or only land cover maps [5]. In order to showcase limitations of existing LULC datasets in representing UGSs, we further will compare several LULC datasets in two sample cities, namely Augsburg and Wuerzburg. It is important to note, that we only focus on classes or sub-classes that clearly mean and represent green, and avoid e.g. blue spaces.

At the European level, Urban Atlas (UA) of the European Environment Agency provides users access to detailed LULC maps for 696 cities, in addition to street tree maps, building block height measurements, and population estimates. UA data relies on satellite imagery with a 2.5 meter spatial resolution and represents cities at a scale of 1:10000. It considers 20 distinct LULC classes, where green spaces appear under the "green urban area" class. Green spaces like grasslands can be identified within the "agricultural, semi-natural areas, and wetlands" category, while some other UGS classes appear under "sports and leisure facilities" category. UA has a minimum mapping unit (MMU) of 0.25 hectares [101].

The second LULC dataset we choose to investigate is the OpenStreetMap (OSM). It is a free and collaborative project that invites contributions from everyone to develop a digital map of the world. It uses a system of keys and values to facilitate searches for various objects on the map. UGSs are primarily categorized under the 'land use' key, though some may also be found under the 'natural' key. Although the OSM data is free, it is

Table 1.1: Comparison of UGS area in both Augsburg and Wuerzburg based on UA, OSM and TN datasets.

LULC	UGS Classes	Augsburg (km^2)	Wuerzburg (km^2)
UA	Green Urban Areas	6.0	4.3
	Forest	38.3	18
	Herbaceous	0.03	-
	Sport and Leisure	5.5	3.8
	Total	**49.8**	**26.1**
OSM	Park	1.6	2.0
	Forest	39.2	16.6
	Allotment	2.3	1.5
	Cemetery	0.8	0.4
	Grass	2.6	1.4
	Heath	0.9	0.1
	Meadow	4.5	1.9
	Recreational Ground	1.5	0.2
	Total	**53.4**	**24.1**
TN	Green areas	1.7	1.8
	Park	0.7	0.6
	Forest	38.2	17.7
	Gardens	2.5	0.8
	Cemetery	0.8	0.4
	Heath	0.2	-
	Grassland	10.6	3.9
	Recreational Ground	0.5	1.2
	Total	**55.2**	**26.4**

commonly known to have issues such as inconsistencies in mapping and missing data [92]. Majority of UGSs are listed as separate LULC classes (e.g. allotments, forests). However, some UGSs are subdivided into several parts comprised of forests, meadows and scrubs.
In Bavaria, detailed LU information can be found in the Actual LU data (Tatsächliche Nutzung, TN). It is organized in two levels: LU classes and detailed sub-classes. Under the umbrella of four main LU classes: settlement, traffic, vegetation, and water, this level is further subdivided into nearly 140 different sub-classes such as residential, road traffic, agriculture, flowing waters and others. The second level serves for providing more detailed information. For example, the sport and leisure facility class is further subdivided into botanical garden, parks, allotments and other classes.
Table 1.1 provides a per-class breakdown of various UGS types across three datasets. Here, we can observe considerable variations in the total UGS areas between the two cities across all datasets. However, there are even more significant discrepancies in categorization of UGSs. For example, the 'sport and leisure' category in UA does not correspond exactly to the 'recreational ground' category in the OSM or the TN datasets. In OSM, there is no

distinct 'botanical garden' sub-type and is instead included under 'recreational ground.' Conversely, in the TN dataset, botanical gardens are classified separately and included in our table along with other gardening areas like allotments. Additionally, while the OSM dataset records 0.1 km^2 of heath in Wuerzburg, the TN dataset does not list heath separately; it is likely grouped under another category such as grassland. Moreover, these datasets exclude residential/street level green spaces and green corridors at all.
Consequently, some UGS types, such as heath or grassland, might be small in area, but their cumulative distribution can change the whole picture of city green. By relying on common and freely available datasets, we not only overlook substantial green areas but also perpetuate confusion regarding the categorization and understanding of different types of UGSs. Therefore, there is a need for establishing a list of UGS types that includes all possible types of UGSs. This will eliminate underestimation of green in cities. Further, proposing methods that could help to identify these green spaces, would further reduce the ambiguity of their representation in LULC maps.

1.2 Knowledge-based Approach to Mapping Urban Green Spaces

The overarching goal of this dissertation is to address two main challenges currently facing UGSs, namely 1) absence of unified collection of UGS types and 2) exclusion of green space type-specific characteristics from common green space mapping procedures due to predominant use of "black box" approaches.
In order to come to a unified green space type collection, we propose a UGS ontology. Commonly this problem is addressed by providing a green space typology. Examples of such typologies are given by Bell et al. [15], Koc et al. [84], and Degerickx et al. [37]. Typologies organize concepts or terms into groups based on shared characteristics. As such, Bell et al. [15] organize green space types based on their effect on house price estimation. Typologies do not set a goal to include all possible green space types that can appear all around the world. These are topic-specific constructs and are more focused on what type is relevant for the topic of interest. In contrast, ontologies do not only establish a foundation for information sharing but also allow collaboration [58]. Unlike typologies, ontologies require well-defined concepts and constraints as well as represented knowledge must be universally accepted. This means, that by creating a UGS ontology, we search for a common UGS vocabulary applicable within the domain of interest. Selected UGS vocabulary, according to ontology definition rules, should contain all the essential knowledge within the domain [59]. Moreover, ontologies are extendable, meaning that even if they cover the basics of a domain, they can still be enriched if new classes or cite-specific categories appear. In contrast to typologies that are created once and do not consider ex-

tension later within the same typology, ontologies are "living" systems and can be adapted to new circumstances. Finally, additional advantage of an ontology over a typology is its formal conceptualization. Formal conceptualization means that an ontology can be comprehended by machines. Typologies are only human comprehendible. Conceptualization of a UGS ontology allows for machine-aided classification tasks. A use case for this can be ontology-based mapping of forests using e.g. remote sensing imagery.
Under-representation or exclusion of certain UGS types from common LULC maps is connected either to their size or to our limited understanding of them [127][63]. Mapping UGSs using machine or deep learning is a highly recognized and rapidly improving approach. They can manage large number of predictor variables, and can achieve good classification results [1][130]. The main challenge of these approaches is their interpretability. Here it is important to differentiate between classifying single pixels (green/non-green) versus whole objects (e.g. allotment). The early one is a very straightforward procedure and depending on the utilized model it can mostly be explained. Decision tree-based classifiers allow for tracing back and identifying particular value ranges or feature values that lead to the final classification outputs [93]. The latter one is much more complex. During object detection, high-level feature properties, in a varying order, can be used or complex descriptive properties can be calculated. These decisions are extremely difficult, to almost impossible, to trace back and explain [2][137].
The black-box problem in UGS mapping is addressed in this thesis by conducting knowledge-based mapping procedure. We use the knowledge-based and semantics terms interchangeably, with both referring to knowledge of the meanings. Knowledge-based mapping procedure refers to first understanding what certain UGS types mean. This involves, for instance, examining existing official definitions or regulations. Then, this procedure requires extracting spatial-semantic characteristics from the examined definitions. By performing semantics-based mapping, we are able to find answers to questions such as (1) which predictor variables are unique to the examined type of UGS, (2) what particular value ranges specifically describe certain type of UGS, (3) to what extend selected variables and values are reproducible and applicable to other regions. Unlike popular deep learning approaches, with knowledge-based approach we get more insights about various types of UGSs, which can lead to their better understanding and acceptance as valuable green space in urban areas.

1.3 Research Questions and Methodology

By being placed in a junction of geoinformatics, physical geography and informatics, this work showcases how the domain-specific knowledge can be combined in order to understand and address certain phenomena, i.e. UGSs. Consequently, we define two research questions that can lead us to addressing both challenges, described in the previous section. The first research question is defined as follows:

RQ 1: To what extent is it possible to develop a unified vocabulary for urban green spaces to form the basis of an ontology that facilitates domain-standardized knowledge sharing?

To answer this question, we will explore existing UGS typologies. Furthermore, by synthesizing these application-specific typologies, we will establish a common UGS vocabulary. This vocabulary will further be enriched and encompassed within a formalized UGS ontology.
Our second research question deals with identification of UGS specific semantic characteristics. Therefore, it states:

RQ 2: What unique spatial semantic characteristics of forests, allotments, peri-urban agriculture, and green corridors can be derived to assist their identification?

By answering this question, we aim towards identifying whether different types of green spaces own a special "face" like no other green spaces. Furthermore, are these characteristics quantifiable to an extent that it can be incorporated into mapping procedures to improve identification accuracy? To answer this question we will implement a mixed method approach, where we will combine techniques and methods from remote sensing, machine learning, and geoinformatics.
From the second research question we further derive three specific hypotheses that will be tested throughout the thesis:

- H1: Integrating the unique spatial semantic characteristics of urban green spaces into existing mapping methodologies enhances the effective identification of these spaces within urban areas.
- H2: The selected spatial semantic characteristics remain consistent across different spatial locations.
- H3: Utilizing freely available high-resolution Sentinel-2 imagery provides a comparable level of accuracy in identifying urban green spaces' coverage as does using freely available very-high resolution aerial imagery.

1.4 Contributions of the Research

We define our contributions in two broad directions, namely to Geographic Information Science (GIScience) in general and to the UGS domain in particular. This thesis contributes to GIScience through introducing a novel mapping approach that combines existing tools in the field. In addition, this work makes a number of contributions for recognition, understanding, and mapping of UGSs, thus further enhancing the UGS domain. Both scientific contributions are detailed hereafter.

Introduction and development of the UGS ontology is one of the main scientific advancement of the thesis. This ontology serves a crucial role by expanding the conventional categorization of UGSs beyond what is typically represented in LULC maps. Traditional LULC maps often overlook or oversimplify the variety of green spaces. By introducing a more nuanced ontology, this thesis highlights the existence and importance of previously unrecognized or underrepresented green space types. Through acknowledging a broader range of green space types, the ontology can aid city planners and decision makers in making informed decisions and influence policies and initiatives. This is particularly relevant if well-being of city dwellers is at stake due to urbanization.

By providing a dedicated UGS ontology, this thesis not only addresses a significant research gap but also demonstrates a practical methodology for creating and enhancing such an ontology to support machine-aided mapping procedures. This approach involves a detailed selection of green space object properties and data types, integrating them within the ontology in a way that is consistent and understandable. Furthermore, by providing this ontology, we set the stage for further dialogue and communication within this field. This thesis provides a robust ontological foundation that other researchers can build upon, whether they seek to refine the existing ontology, extend its application to other urban areas, or integrate it with other data sources and technologies like Geographic Information Systems (GIS) and remote sensing.

Our broader contribution encompasses practically showcasing how spatial-semantic information can be extracted from the existing legal definitions and how they can be improved to better suit spatial analysis. Furthermore, the thesis also contributes a step-by-step methodological framework that leverages the refined semantic information to identify and classify UGS types. This framework outlines how to systematically use the extracted and improved semantic information in practical spatial analysis, facilitating more accurate mapping and assessment of UGSs. In addition, our thesis contributes with practical examples of how traditional geoinformatics methods can be effectively combined with more modern approaches, such as machine learning, and reach good identification outcomes.

This thesis further contributes to GIScience by exhibiting the importance of method validation. We conduct comparative analysis in two study areas using exactly the same UGS features and asses transferability of these features. Through this procedure we not only verify feasibility of the proposed methods but also showcase how and which UGS features could be location-specific. As a consequence, the methodologies developed herein not only refine existing techniques but also elaborate new dimensions of analysis that are scalable and adaptable across different geographic contexts.

1.5 Related Publications by the Author

Throughout the development of this manuscript, parts of the implemented methods were peer-reviewed and published in proceedings of scientific conferences. Based on these publications, as well as the feedback we received through the publication process, we amended and improved our methodological approaches, and their final versions built the cornerstone of our knowledge-based identification workflows. In the following, we will present every publication as well as describe what part of them were utilized in this thesis.

Classifying Urban Green Spaces using a combined Sentinel-2 and Random Forest approach [68].

In this paper we explore pixel-based UGS mapping procedures using spectral bands and vegetation indices derived from Sentinel-2 data. By developing three various Random Forest (RF) models we achieve similarly good classification results. The normalized difference water index and soil-adjusted vegetation indices provide similar insights as the normalized difference vegetation index. RF model also proves itself to be a straightforward machine learning procedure to map green vegetation, by achieving over 90% identification accuracy. However, further visual validation procedure reveals, that the spatial resolution of the utilized data falls short in identifying fragmented heterogeneous vegetation in e.g. allotments or cemeteries. Although being cost effective and performing well with large homogeneous green areas, we propose to test the same methodology using higher resolution datasets.
Following suggestions and exploring limitations within this paper, we execute a slightly different and comparative green space mapping procedure, which is presented in Chapter 6. Here we compare a high resolution digital orthophoto and Sentinel-2 datasets as well as vegetation indices derived from them. Further, we also include the vegetation height for better separability of vegetation types. To compare applicability of RF model we perform transferability analysis and compare identification accuracy of a model trained with datasets from Augsburg in Wuerzburg.

Towards an Ontology of Urban Green Spaces [70].

This publication sets a starting point for elaborations on the existing gaps in UGS types and a need for development of an ontology. It presents comparative figures and discussions on how much of green space we are missing in cities, if we fail to consider all the potential UGS types. Therefore, content of this paper is further opened up and presented in this Chapter, under problem statement, whereas a new ontology is presented in Chapter 5. In the published paper we only explore Bell et al. [15]'s typology. In this thesis we explore two additional typologies to to acquire a complete list of UGS types. We also propose and then utilize the Protégé environment to build and formalize a new UGS ontology.

Semantic Identification of Urban Green Spaces: Forest [69].

Our first publication on the use of semantic information to map UGSs is presented on the example of forests. In this paper, we perform a rule-based classification in order to establish thresholds for descriptor variables. As descriptor, we take advantage of vegetation height, vegetation index, and textural homogeneity and dissimilarity. Our results demonstrate, that forests can be identified using a minimal set of parameters closely reflecting their semantics. Moreover, some thresholds, like NDVI, may be applicable in new study areas, but other like homogeneity and heterogeneity are specific to each scene and cannot be directly transferred to new locations. With slight modifications, such as using percentile-based thresholding instead of rule-based, we perform forest mapping again and present the workflow in Chapter 7.
In addition, this paper won the Best Short Paper Award in the Association of Geographic Information Laboratories in Europe (AGILE) conference in 2023 which was held in Delft, Netherlands.

Knowledge-Based Identification of Urban Green Spaces: Allotments [71].

This publication is evolving around mapping allotments both in Augsburg and Wuerzburg, using their semantic features. As semantic features, we define presence, density, and height of garden huts, proximity to water bodies and railroads, as well as presence of pathways within the allotment gardens. Using the proposed methodological workflow, we identify 78 percent of allotments in Augsburg and 88 percent in Wuerzburg. Therefore, we build upon this publication in this thesis. To better assess reproducibility of our approach, we include percentile-based thresholding of parameters as well as introduce feature sensitivity analysis.

Identification of Green Corridors as a type of Urban Green Spaces [72].

Commonly green corridors are mapped as ecological corridors. In this paper, for the first time, we explore potential approaches to map them as urban green corridors for human well-being. Here, we conduct a pre-trained deep learning approach to identify single trees and then associate them with nearby roads. After acknowledging limitations of this method, in this thesis, we execute a different approach. As such, we no longer limit green corridors to only trees. We also differentiate between various green corridor types and use existing green corridor rules to classify them both in Augsburg and Wuerzburg.

1.6 Outline of the Thesis

This work is structured as follows: Chapter 2 introduces the current research on the impact of UGSs on human well-being. It discusses the representation of UGSs on common land use and land cover maps and explores their limitations. This chapter also explores geographic information ontologies and their role in enhancing context extraction for remote sensing classifications. Chapter 3 describes the main methods used in our research. In Chapter 4, we describe two study areas where these methods are applied, as well as present datasets that are utilized in our studies. In Chapter 5, we present our UGS ontology. Our analysis progresses through various computational studies. Therefore, Chapter 6 features a comparative study using two different datasets to map UGSs. Chapters 7 through 10 focus on tailored workflows to identify forests, allotments, peri-urban agriculture, and green corridors, respectively. In each of these chapters, we provide study-specific discussions and draw conclusions from them. In Chapter 11, we synthesize findings and discussions from the performed studies and put them into perspective under the umbrella of the overarching research context. In this chapter, we also present answers to our research questions and hypotheses. We present our conclusions together with an outlook in Chapter 12. The bibliography complements the work.

Chapter 2

Related work

In this chapter we describe the importance of UGSs for human well-being, as well as their place in common land cover and land use maps. Following this, we elaborate on already established UGS typologies and describe geo-information ontologies. Moreover, we provide an overview of common UGS identification and mapping techniques.

2.1 Urban Green Spaces for Human Well-being

Human well-being is a multifaceted concept that encompasses various dimensions of health and quality of life within urban settings. In general this term is defined as "a state of human being that comprises on human (physical, psychological, mental) health, good social interaction, and overall life satisfaction (subjective well-being)" [73]. According to the World Health Organization, health is not merely the absence of disease but a state of complete physical, mental, and social well-being, and UGSs are capable to provide infrastructure to support that state [116][141]. There are many examples in the existing literature, where impact of UGS on humans is discussed. It is known, that as simple as a single view of greenery from a window can increase work performance and prevent adverse health effects from stressful life events [77]. Nevertheless, it is also important to categorize these effects of UGSs in terms of what aspects of well-being they affect, as well as understand if there are any differences between types of UGSs and their well-being effects.

According to Jabbar et al. [73], human well-being is broadly categorized into physical, psychological, mental, social, subjective, and environmental well-being. Physical well-being, for instance, refers to the state of physical health and the absence of disease. In his term, UGSs contribute significantly by offering areas for exercise, reducing pollution, and mitigating heat. Parks and recreational areas are particularly notable for their role in improving physical health, as they provide spaces for activities like walking and jogging. This can help reduce obesity rates and other health issues. Furthermore, psychological well-being involves positive self-esteem, personal growth, and happiness. These feelings are enhanced by UGSs through their restorative environments that reduce stress and enhance mood. Moreover findings of Wood et al. [148] reveal that allotment gardeners have a significantly higher self-esteem, and experience less depression and fatigue.

Jabbar et al. [73] define mental well-being as the ability to cope with stress, work productively, and contribute to the community. By providing tranquil environments, UGSs can hep to lower anxiety and depression. Other studies like Gascon et al. [56] show that long-term exposure to UGSs significantly reduces symptoms of depression and anxiety, emphasizing the importance of integrating green spaces into urban planning to support mental health.

Social well-being, which refers to the ability to interact positively within a community, is fostered by UGSs as they provide area for social interaction and community activities [73]. Community gardens, for example, encourage social interaction and community engagement, thereby improving social well-being while also offering opportunities for physical activity and healthy eating. Enssle and Kabisch [46] explore park visitation patterns and establish that older people with close social networks would attend parks more frequently than those who are more isolated in their daily lives.

While other types of well-being are important, subjective well-being might be the one that affects the most our day-to-day life. Proximity to green areas is associated with higher life satisfaction and perceived quality of life. For instance, an increased frequency of visits to gardening areas is shown to be positively related with greater subjective happiness [105]. Moreover, if people think that visiting UGSs is good for their health, they would visit them more frequently [46].

Finally, the last well-being category defined by Jabbar et al. [73], environmental well-being, considers the health of the natural environment and its capacity to sustain human life. This is enhanced by UGSs through their contributions to biodiversity and ecological balance.

Some other studies show, that e.g. cognitive recuperation, i.e., when the brain has a chance to rest and heal from cognitive fatigue, positively reflects on improving attention, focus, and overall mental functioning. According to the Attention Restoration Theory of Kaplan and Kaplan [78], this restoration can be achieved by spending time in inherently fascinating environments. And typically, it is natural environments that provide these restorative opportunities [79]. A comprehensive review by Beute et al. [17] further underlines the connection between urban and peri-urban green spaces and human well-being. This report concludes that visits to UGSs and the countryside are linked with different components of mental well-being. It highlights that natural environments with high biodiversity and good quality are particularly effective in promoting psychological restoration and connectedness to nature.

The benefits of UGS vary depending on their type and characteristics. Parks and recreational areas are associated with significant improvements in physical, social, and psychological well-being. Urban forests and green corridors are crucial for mental health, offering serene environments that promote relaxation and reduce stress. The presence of trees and natural landscapes in urban settings has been linked to lower levels of depression and anxiety [84].

The role of green spaces in human well-being is also explored through various methodological frameworks aimed at assessing their thermal performance and impact on microclimate. Bartesaghi Koc et al. [13] present a framework combining airborne remote sensing, field measurements, and numerical modeling to assess the thermal benefits of UGSs. This approach highlights the cooling effects of green spaces, which not only contribute to physical comfort but also to environmental well-being by mitigating urban heat island effects.

Additionally, the typology of green infrastructure (GI) plays a crucial role in understanding its benefits. The classification of green infrastructure into categories such as tree canopy, green open spaces, green roofs, and vertical greenery systems allows for a detailed analysis of their specific contributions to human well-being. Each type offers unique benefits: tree canopies provide shade and improve air quality, green open spaces offer recreational opportunities, green roofs enhance thermal performance and storm water management, and vertical greenery systems contribute to aesthetic and environmental benefit [13].

2.2 Urban Green Spaces within Land Use and Land Cover Datasets

For modeling features on the Earth surface, understanding two concepts is of immense importance, namely land use and land cover. The term land cover (LC) refers to the (bio)physical coverage on the Earth Surface [39]. It is the materials that we see, due to their distinct reflection at different wavelengths and with various frequencies of the waves in the electromagnetic spectrum [50]. Land use (LU) on the other hand, refers to the organization, actions, and resources employed by individuals within a particular LC category to generate, modify, or to sustain it [39]. Consequently, LC is about what is on the Earth surface, while LU refers to how a particular cover is used or modified by people. Thus, one reflects bio-physical wheres the other one socio-cultural and economic aspects of human-nature systems. Therefore, the logical inference is that when interpreting LU, the primary approach should involve using LC as the main substitute, alongside the image interpreter's usual points of reference like patterns, geographic location, or other similar factors.

In theory these two terms can clearly be distinguished from each other and described straightforwardly. However, in practice this is much more complicated as various types and applications may coexist. Therefore, when observing human-nature systems, clear many-to-many linkages can be noticed. For instance, a single area covered by forest LC might also serve as a site for various recreational activities such as hunting, hiking, and even livestock grazing [50]. However, many-to-many relationship can not always be directly identified, especially solely using one data source. Hunting, which is usually performed in a large area, cannot be extracted from LC information and requires supplementary knowledge of an area presented by e.g. local authorities [5].

An extended discussion of LULC confusion in existing classified products is presented by e.g. Anderson [5]. According to author, concepts related to LULC activities are closely connected and, in many instances, have been applied interchangeably. Moreover, there is no universally fitting categorization for LULC, and it's impossible that a single ideal classification could ever be created. The classification process incorporates various perspectives, and even when an objective numerical methodology is implemented, the process will still remain very subjective. Furthermore, in reality, there is no inherent justification for assuming that a single comprehensive inventory would remain relevant for an extended period, as LULC represent very dynamic systems. Therefore, each classification is tailored to fulfill a specific requirement of its intended user, and most users expect an inventory that adequately addresses the majority of their needs. The author further states, that challenges of aggregation of LULC information produced by different agencies are not only due to the differing classification systems and underlying task-specific requirements, but also due to continuous modifications in definitions of LULC categories.

Mapping the Earth's surface was and remains a desirable task, as it facilitates understanding its dynamics. Moreover, maps are tools used for sustainable planning purposes. Globally, there is a considerable number of programs that are dedicated for the creation of detailed and accurate LULC products at various scales. Formally relating different LULC datasets with inherent differences of class descriptions is highly problematic and there is a need to understand different LU ontologies. Due to the socio-economic dimension of LU, it may require connecting linguistic descriptors that carry diverse cultural, political, economic, or sociological connotations, in addition to the botanical or ecological definitions associated with LC [50].

In order to ease the confusion and varying implementations by different agencies, Anderson [5] proposes a four-level LULC classification approach shown in Table 2.1, that builds the base of the United States Geological Survey's classification scheme. The top two levels in the classification are clearly defined while the level three and four are meant to be customized by its users. With this approach, the author aims towards enabling the consolidation of detailed local data into consistent Level 1 and Level 2 land information, which align with the primary goal: establishing a classification system for LULC that can be applied in LU planning and management activities. As such, authors differentiate among urban and built-up, agricultural, rangeland, forest, water, wetland, barren, tun-

Table 2.1: The LULC classification proposed by Anderson et al., 1976.

Level 1	**Level 2**
Urban or Built-up Land	Residential Commercial and Services Industrial Transportation, Communications, and Utilities Industrial and Commercial Complexes Mixed Urban or Built-up Land Other Urban or Built-up Land
Agricultural Land	Cropland and Pasture Orchards, Groves, Vineyards, Nurseries and Ornamental Horticultural Areas Confined Feeding Operations Other Agricultural Land
Rangeland	Herbaceous Rangeland Shrub and Brush Rangeland Mixed Rangeland
Forest Land	Deciduous Forest Land Evergreen Forest Land Mixed Forest Land
Water	Streams and Canals Lakes Reservoirs Bays and Estuaries
Wetland	Forested Wetland Nonforested Wetland
Barren Land	Dry Salt Flats Beaches Sandy Areas other than Beaches Bare Exposed Rock Strip Mines, Quarries, and Gravel Pits Transitional Areas Mixed Barren Land
Tundra	Shrub and Brush Tundra Herbaceous Tundra Bare Ground Tundra Wet Tundra Mixed Tundra
Perennial Snow or Ice	Perennial Snowfields Glaciers

Table 2.2: The pan-European CORINE land cover classification.

Level 1	Level 2	Level 3
Artificial Surfaces	Urban fabric	Continuous urban fabric Discontinuous urban fabric
	Industrial, commercial and transport units	Industrial or commercial units Road and rail networks and associated land Port areas Airports
	Mine, dump and construction sites	Mineral extraction sites Dump sites Construction sites
	Artificial, non-agricultural vegetated sites	**Green urban areas** Sport and leisure facilities
Agricultural areas	Arable land	Non-irrigated arable land Permanently irrigated land Rice fields
	Permanent crops	Vineyards Fruit trees and berry plantations Olive groves
	Pastures	Pastures
	Heterogeneous agricultural areas	Annual crops associated with permanent crops Complex cultivation patterns Land principally occupied by agriculture, with significant areas of natural vegetation Agro-forestry areas
Forest and semi-natural areas	Forest	Broad-leaved forest Coniferous forest Mixed forest
	Scrub and/or herbaceous vegetation associations	Natural grassland Moors and heathland Sclerophyllous vegetation Transitional woodland-scrub
	Open space with little or no vegetation	Batches, dunes, and sands Bare rocks Sparsely vegetated areas Burnt areas Glaciers and perpetual snow
Wetlands	Inland wetlands	Inland marshes Peat bogs
	Maritime wetlands	Salt marshes Salines Intertidal flats
Water bodies	Inland waters	Water courses Water bodies
	Marine waters	Coastal lagoons Estuaries Sea and ocean

dra and perennial snow or ice. This classification scheme is adopted by many national mapping agencies as a base for LULC maps even though the scheme embodies LULC confusion at all four levels.
At European level, the coordination of information on the environment (CORINE) initiative provides the most comprehensive LULC classification system that is developed by the European Environment Agency. The motivation behind the CORINE LC inventory is articulated as a coordinated information gathering, environmental monitoring, and a consistent pan-European framework. The primary objectives include, firstly, the provision of quantitative LC data that is uniform and comparable throughout Europe. Secondly, it involves the development of an all-encompassing digital LC repository for all the 25 EU member states as well as other nations in Europe and North Africa. The mapping process adheres to the CORINE nomenclature and interpretation techniques, initially carried out at a scale of 1:100,000. This nomenclature includes 44 distinct LC categories organized into three hierarchical levels, with a minimum mapping unit of 25 hectares, as shown in Table 2.2. Each European Union member state is tasked with generating these datasets through on-screen interpretation and digitization of Landsat imagery within a GIS environment. The final European-wide dataset is assembled by merging the consistent national products into a unified dataset.

Table 2.3: The Urban Atlas nomenclature.

Class code	Nomenclature
11100	Continuous Urban Fabric (Sealing Degree > 80%)
11210	Discontinuous Dense Urban Fabric (Sealing Degree 50% - 80%)
11220	Discontinuous Medium Density Urban Fabric (Sealing Degree 30% - 50%)
11230	Discontinuous Low Density Urban Fabric (Sealing Degree 10% - 30%)
11240	Discontinuous Very Low Density Urban Fabric (Sealing Degree < 10 %)
11300	Isolated Structures
12100	Industrial, commercial, public, military and private units
12210	Fast transit roads and associated land
12220	Other roads and associated land
12230	Railways and associated land
12300	Port areas
12400	Airports
13100	Mineral extraction and dump sites
13300	Construction sites
13400	Land without current use
14100	Green urban areas
14200	Sports and leisure facilities
20000	Agricultural, Semi-natural areas, Wetlands
30000	Forests
50000	Water bodies

In the urban context, UA of the European Environment Agency provides users access to detailed LC and LU maps for 696 cities across Europe, in addition to street tree maps, building block height measurements, and population estimates. Thematic classes of UA are based on CORINE LC nomenclature and are presented in Table 2.3. UA data relies on satellite imagery with a 2.5 meter spatial resolution, enabling provision of consistent LULC information for all major European cities and their corresponding larger urban areas, with population figures exceeding 100,000 residents. The UA dataset represents cities at a scale of 1:10,000 and covers a total of 20 distinct LC classes. Among these, 17 pertain to urban environments and have a MMU of 0.25 hectares, while the remaining 3 classes relate to non-urban areas and are provided at MMU of 1 hectare. The dataset guarantees a minimum accuracy level of 85% for artificial surfaces and 80% for the remaining LC classes [101]. Urban areas are distinguished based on their imperviousness, which is derived from the high-resolution soil sealing layer provided by the Land Monitoring Core Service. This process combines Computer Aided Photo-interpretation and object-oriented classification methods.

UGS information can be extracted to a certain extent from all the three LULC products. Specifically, the CORINE LC dataset incorporates green areas within its third level of detail, categorized under "artificial and non-agricultural vegetated cities". Similarly, the UA dataset also includes a class denoted as "Green urban areas". Additionally, green spaces like grasslands can be identified within the "agricultural, semi-natural areas, and wetlands" category of the UA. It is worth noting that the level of detail varies depending on the specific datasets and the MMU.

2.3 Urban Green Space Typologies

Thoughtfully planned, effectively administered, and interconnected green areas carry considerable significance in well-functioning urban areas. Absence of a commonly agreed classification or topology of UGSs is not only a problem in terms of mapping of UGSs but also for understanding e.g. urban heat island [14] or biodiversity and ecosystem services [103]. Although UGSs have been studied for a very long time, for most of this time they have been treated as uniform structures [110]. However, UGSs exhibit remarkable diversity, spanning from urban parks to vertical gardens and rooftop horticulture, to city woodlands to community gardens. They essentially encompass all forms of vegetation in urban settings [35]. Given this wide array of green spaces, it is necessary to understand presence and span of various UGSs in cities and compile an inventory of UGS elements. In the context of LULC, UGSs can take on both roles. Hence, a forest occurring within an urban area represents a specific LC type, while an allotment garden is a classic example of LU, with a mixed function.

Due to growing interest in UGSs and their role in build-up environments, several inventories have been proposed, that organize UGS types into groups or hierarchies based on one or another purpose. For instance, Swanwick et al. [134] establishes a UGS typology consisting of 25 UGS sub-types within four main groups including amenity green spaces, functional green spaces, semi-natural habitats, and linear green spaces. However, in majority of instances, UGSs are created to serve certain purposes. Degerickx et al. [37] propose a functional urban green typology based on the main functions and services provided by UGSs. They categorize urban green elements into three main categories: trees, shrubs, and herbaceous plants that are later divided into 23 sub-types like forest, scrub path, lawn, pasture, flower bed. Moreover, Bell et al. [15] provide one of the broadest classification of UGSs and define explicit classes of UGSs for hedonic house price valuation. The authors propose the following UGS classes:

- Gardens and parks
- Natural and semi-natural spaces
- Green corridors
- Outdoor sport facilities
- Provision for children and young people
- Cemeteries and other burial grounds
- Amenity green spaces
- Allotments, community gardens and urban farms

This classification is further enriched with sub-classes such as various types of gardens and others.
In order to assess the functional linkages between UGSs and ecosystem services and biodiversity, Cvejić et al. [35] establish an inventory with a particular green infrastructure-perspective as compared to existing inventories. According to the authors, no inventory can ever be considered complete or static. Social initiatives, technological advancements, increased environmental consciousness, creativity of city planners and urban residents will always lead to occurrence of new types of UGSs. Typical examples mentioned are bioswales, guerrilla gardens and others. In their typology, the authors highlight following eight UGS categories that include:

- Building greens
- Private, commercial, industrial UGSs and UGSs connected to grey
- Riverbank green
- Parks and recreation

- Allotments and community gardens
- Agricultural land
- Natural, semi-natural and feral areas
- Blue spaces

Moreover, the typology contains 44 sub-categories of UGSs.
Variations in UGS typologies can be observed, even if they are created for very similar purposes. The typology by Jones et al. [74] include eight classes and 46 sub-classes of both urban green and blue spaces. The main eight UGS classes are mode of gardens, amenity areas, other public spaces, linear features/roads, constructed GI on infrastructures, hybrid GI for water, water bodies, and other non-sealed urban areas. The authors' main objective to create such a typology is to explore the ecosystem services provided by the green spaces. Further, with the proposed typology and multi-functionality matrix, they provide a valuable evaluation tool for GI types that have received less to no attention in the existing literature.
Even if the glossary differs, quite many similarities within UGS typologies can be observed. For instance, while some authors differentiate between linear green and consider riverbank green as sub-category of linear green [134], others call them straightforwardly "riverbank green" [35]. Some differentiate between linear green and do not consider riverbank green as a sub-type of this category [74]. Therefore, there is a potential for further exploration and unification of UGS types.

2.4 Geographic Information Ontologies

An ontology with its term taken from philosophy, represents an explicit specification of a conceptualization [58]. Ontologies establish a foundation for information sharing and collaboration. They clearly define the terminology specific to a particular application domain. By capturing the essential meanings within this domain, ontologies facilitate semantic consistency and understanding across different systems [139]. Ontologies are constructed using a set of representational primitives, with the final aim of modeling domain knowledge. These representational primitives typically consist of classes, attributes of these classes, and relationships among the classes [58]. In order for a conceptualization to be considered as an ontology it should be explicit, shared and formal. Being "explicit" entails having well-defined concepts and constraints (e.g. height above 5 meters). A "shared" conceptualization implies that the knowledge is universally accepted (e.g. common LULC classification system). And finally, "formal" conceptualization means that it can be comprehended by machines.
In the context of GIScience, ontologies provide a structured framework for representing,

categorizing, and interpreting the complex knowledge inherent in this domain. In this sense, ontologies within GIScience focus on creating effective tools for specific geographical purposes rather than uncovering the nature of the world. As a result, it aligns more with engineering than with conventional empirical science [31].

In order to represent a knowledge base, different types of ontologies exist. For instance, top-level ontologies encompass very broad concepts such as spaces, time, matter, objects, events, and actions. They are universal and not specific to any one problem or domain and ideally serve as a shared foundation that can be used by a wide range of people. Whereas, domain ontologies refer to the specialized vocabulary of a particular field or domain. They refine the general concepts from the top-level ontologies to make them relevant to specific areas. Moreover, task ontologies relate to the specific vocabulary used in particular activities. They adapt the general concepts from the top-level ontologies to suit specific tasks. Finally, application ontologies merge elements from both domain and task ontologies. They define concepts that are specific to both a certain field and a particular activity. These concepts often describe the roles or functions that entities perform in specific scenarios [60].

GIScience ontologies are created to systematically represent geographic data by defining the relationships between various geographic entities, thus enabling data sharing and interoperability. Therefore, they can be created at all ontological levels described above. According to Guarino [59], the ontology creation process involves several critical steps such as domain specification, concept extraction, hierarchical structuring, and formalization. During the domain specification the scope and boundaries of the domain, that will be covered by the ontology, need to be defined. Here, identifying the main concepts, entities, and relationships that are relevant within the domain is critical. At the second stage, relevant concepts and terms from existing literature and databases will be extracted. This way it is possible to make sure that all significant concepts within the domain are identified and documented. At stage three, the extracted concepts will be organized into a hierarchical structure, typically involving a top-level ontology that provides general concepts such as "entity", "object", and "event", and lower-level ontologies that specify more detailed domain-specific concepts. Then, the ontology needs to be formalized, where formal language will be used to define the relationships and properties of the concepts. Description Logic or Web Ontology Language (OWL) are only few of the formal languages. The final, step around ontology creation is validation and refinement. Authors emphasize that iteratively testing the ontology with real-world data and refining it based on feedback helps to ensure, that the ontology accurately represents the domain and is useful for the intended applications [59].

In the fields of LULC classification or remote sensing, task or application level ontologies appear more often than others. This is not surprising, as commonly the goal of such ontologies, apart from formalizing concepts, is usability in practical applications. Arvor et al. [7] emphasize the importance of using formal ontologies to enhance the in-

terpretation of remote sensing data, which allows for more accurate land classification and analysis. However, representing geographic concepts in ontologies is connected with a range of challenges. Geographic entities can carry multiple meanings for different users. For instance, when mapping a river, one should be aware that it isn't just a body of water; it might be a crucial transportation route or a boundary between two countries. This in turn results in difficulties of semantic interoperability among databases [31]. Nevertheless, unlike traditional remote sensing approaches that focus on numeric data (e.g., specific NDVI values for forest classification), ontologies integrate symbolic knowledge (e.g., "Forest" has "HighNPP" or "HighNDVI" values) with numeric thresholds to enhance knowledge representation and sharing [23].
Arvor et al. [8] argue that analyzing satellite images is a complex task involving selecting relevant data, analyzing image content, and considering user skills. While Geographic Object-Based Image Analysis (geoOBIA) became more popular in this regards, the rules and methodologies developed in geoOBIA are often specific to particular datasets or scenarios and may not be easily transferable to other contexts. GeoOBIA is somehow similar to ontology in terms of use of expert knowledge and in aiming to enhance semantic interpretation of images. Nevertheless, only ontologies are capable to and facilitate sharing and provide a formal, explicit specification of knowledge that encompasses both symbolic and numeric information and facilitate sharing and reusing of knowledge.

2.5 Urban Green Mapping

Historically, diverse methods have been utilized to gather data regarding UGSs. Field campaigns, visual interpretation and manual digitization are among the most accurate as well as the most time and cost intensive methods. Nowadays, remote sensing (RS) offers a precise, fast, and cost-effective method for extracting information about UGSs, such as location, vegetation types, and coverage [127]. However, its demands and cost-effectiveness vary depending on UGS classes and applications, with the balance between data costs, processing expenses, and application purposes influencing its usability. In terms of RS data specifications, high-resolution data like hyperspectral and Light Detection and Ranging (LiDAR) is used for detailed mapping of observations. Less expensive options like Landsat or Sentinel imagery are often used for overall UGS mapping across cities [127].
Mapping UGSs presents its unique set of challenges. These stem from the spatial and spectral diversity and the intricate three-dimensional structure of urban areas. These challenges include extensive shaded regions, numerous instances of light scattering, and complexities in geometric aligning of different data sources [108]. Furthermore, parts of UGSs might be located on private grounds, which would make it difficult to map from ground, and if their area is too small, it would complicate to map them from satellite im-

ages [127]. Therefore, attempts were made to understand the effect of spatial resolution particularly on UGS identification. In this regard, Sun et al. [133] perform up-scaling of WorldView-2 multi-spectral images from two to up to 40 meters, and explore accuracy decrease by lowered spatial resolution. Their findings reveal, that UGSs can be accurately mapped using images with spatial resolutions ranging from two meters to 16 meters, while imagery of lower resolutions yields less effective outcomes. In contrast, Huang et al. [66] achieve good UGS mapping accuracy by using images with 30 meter resolution. However, to maximize the extraction of UGS information, authors delve into sub-pixel rather than pixel-level analysis.

Due to the increased availability of satellite images, growth in usage of more high resolution Sentinel-2 imagery [27], and very high resolution imagery [63][67] can be observed. The latter approach appears to be particularly helpful to identify small-scale UGSs. As such, Haase et al. [63] focus on urban front and backyard green spaces, particularly around residential buildings on privately owned ground, and implement spectral unmixing technique. Using very-high resolution RapidEye data they calculate sub-pixel vegetation fractions for the entire study area. The authors achieve very good classification accuracy and discover that front and backyards make up to 40% of the UGSs in the study area. However, they acknowledge that the utilized RapidEye dataset, although providing high resolution, is not freely accessible and thus transferability of the method to elsewhere with the same dataset might be a limiting factor.

The complexity of UGSs mapping, it terms of size, within-class heterogeneity, and common RS data challenges, such as shadows, requires more detailed procedures of fusion of various data sources with other complementary information [118]. For instance, Degerickx et al. [37] establish an extended typology of UGS first, and then apply a UGS mapping workflow by using hyper-spectral APEX, Worldview-2 datasets in combination with Airbone LiDAR datasets. As a complementary information source, authors include vegetation indices such as the Normalized Difference Vegetation Index (NDVI), Normalized Difference Water Index (NDWI), a grass index highlighting the difference between trees and lawn and others. Their findings show that incorporation of the LiDAR dataset substantially increases the UGS identification. However, it also requires additional spectral data, preferably hyper-spectral, for accurately identifying UGSs with high thematic detail. Furthermore, high spectral similarity among various UGS types and the complex urban environment interactions, e.g. shadow effects, are the main sources of errors, where shrub and herbaceous class show the highest misclassification rate. Use of vegetation indices even with images of limited spectral resolution is shown to be advantageous for vegetation identification. According to the analysis of Motohka et al. [104], simple green-red difference index is an effective phenological indicator, because it provides a universal threshold for detecting leaf green-up and autumn coloring phases, and it distinctly responds to subtle disturbances and differences in ecosystem types.

Generally, UGS mapping, as any other LULC mapping, involves a spectral image classification procedure. In this approach, each pixel within RS data is rigorously analyzed and is categorized into a distinct spectral class, which is then linked to a existing real-world concept. This method assumes that the LC to be mapped exhibit identifiable spectral characteristics that can be effectively extracted. However, some complications may arise as certain types of LU exhibit intricate arrangements of LC [127]. Traditional per-pixel classification methods might encounter challenges when attempting to classify such cases, primarily due to the inherent spectral diversity associated with a specific LU in question [119]. Therefore, modern image classification approaches involve machine learning (ML) or deep learning (DL) techniques [1][130]. Thus, precise methodology and dataset selection will depend on the final goal of the research and the level of detail required.

In the existing literature, ML methods, such as support vector machine (SVM) and random forest (RF) are two of the most frequently used UGS mapping methods. In a study conducted by Ju et al. [75], the authors use an SVM classifier together with Sentinel-2 imagery to map UGSs across the major Latin American cities and reach 87 % classification accuracy. They utilize OSM data as a training data source and therefore note that the variability and availability of OSM data, especially for smaller cities, is the main limiting factor for automatization of the mapping procedure. Indeed, availability of training, testing and validation datasets play a crucial role in how well ML/DL methods work [75]. Similar to the previous authors, Chen et al. [27] propose a work around this issue by utilizing crowd-sourced information for training purposes. As such, they perform UGS mapping through neural network-based automatic mapping method where they integrate Sentinel-2 images and crowd-sourced geospatial big data. By achieving over 94% identification accuracy, the authors successfully showcase the potential of a low-cost UGS mapping workflow performed on free training samples created from crowd-sourced OSM data. Similarly, Ludwig et al. [92] identify public UGSs with 95% accuracy, by utilizing Sentinel-2 as imagery source and OSM data as training data source.

Due to the extensive application of object-based image analysis in the field of computer vision, its usage in the geospatial context has also significantly increased, particularly for high-resolution image analysis. Image-objects formed of clustered neighboring pixels with similar attributes and shared meaning, form the core of geoOBIA. Unlike traditional per-pixel analysis, geoOBIA focuses on image-objects, created through segmentation, as a primary unit of analysis [25]. Since segmentation reduces single pixel information by grouping and forming objects, its use to identify UGSs is obvious. Use of geoOBIA can affect processing times, and be handy if limited resources to process high resolution images are available [18]. Furthermore, geoOBIA allows introduction of additional descriptive information, that can in turn improve identification results [61].

Typically, geoOBIA also involves post-segmentation classification using ML methods. As such, Zylshal et al. [156] extract UGSs in Jakarta, Indonesia using a combination of SVM, geoOBIA as well as expert knowledge. The implemented technique reaches 86% classification accuracy. However, the applied classification rule set appears to be limited to

the selected area, thus requiring further tests for transferability purposes. Furthermore, Puissant et al. [115] focus on mapping areas covered by urban tree crowns, referred to as wooded elements, with the help of very high resolution optical images. They perform geoOBIA in combination with RF classification method and their result illustrate that RF together with geoOBIA is highly robust for the urban green element classification.
Further examples of accurate UGS classification with geoOBIA include e.g. Labib and Harris [87]. They implement geoOBIA to identify green infrastructure and compare its applicability on an example of Sentinel-2 and Landsat 8 images. Their results show, that this approach yields reliable results in terms of UGS identification. Furthermore, they observe that geoOBIA performs better with Sentinel-2 images that have slightly higher spatial resolution than Landsat 8 images. However, the authors also note, that geoOBIA faces difficulties of identifying GI in areas affected by tree and building shadows.
From the investigated literature it is obvious that there is an increasing trend of use of the ML and DL methods. This is particularly due to the capability of such models to handle multidimensional data, learn patterns within it, and interconnections between variables. However, this opens up a plethora of discussions around the "black box" problem. On one hand the capabilities of ML methods is difficult to resist. The lack of transparency, on the other hand, makes it difficult to explain these complex interconnections as well as why certain results are acquired. Therefore, there is a need for interpretable machine learning (IML) methods for especially mapping urban vegetation [137]. This is driven by the complexity of urban landscapes and the necessity of understanding how models make their predictions [2].

2.6 Detection of Various Urban Green Space Types

In the previous section we describe the state of art in overall green space mapping. However, further we focus particularly on three types of UGSs, namely forests, urban agriculture, and green corridors. We explore which methods and data are the most used ones in terms of their detection and what kind of insights authors gained through their utilization.

Forest

It's widely recognized that forest ecosystems have a profound impact on both humans and the environment around us, across all scales, including local, regional, continental, and global [120]. Therefore, a forest inventory is critical due to various reasons including but not limited to planning, fire management and conservation. Inventorying forest through mapping could be challenging as forests might exhibit large variability in composition, volume, quality and topography [81]. Previously, forest mapping hugely relied on manual digitization of forest boundaries using aerial imagery. Manual forest inventories are time

consuming and expensive, what makes their repetition at regular intervals very difficult [40]. With an increase of earth monitoring satellite missions, forest mapping practices became highly automated and cost efficient. As the literature on UGS mapping shows, it is the combination of various datasets and extraction techniques that yields the best mapping results. Therefore, forests are not different in this regard, and are mapped using various datasets, including but not limited to optical RS images [83], LiDAR datasets [128] a well as synthetic aperture radar (SAR) imagery [120].
In their work, Simard et al. [128] showcase an innovative use of space-borne LiDAR data from the Geoscience Laser Altimeter System (GLAS) on board of ICESat to map forest canopy height on a global scale with 1 kilometer spatial resolution. This study highlights the potential of LiDAR technology in capturing detailed vertical structures of forests, which is crucial for understanding biomass distribution, primary productivity, and biodiversity. By combining GLAS-derived canopy height data with ancillary variables like tree cover, elevation, and climatology maps, authors achieve high accuracy despite GLAS data's sparse coverage. Validation of their results against field measurements further emphasizes LiDAR's robustness in forest canopy assessment.
In contrast to LiDAR data use, the Global Rain Forest Mapping project, led by the National Space Development Agency of Japan, represents a pioneering effort in utilizing SAR technology to produce spatially and temporally contiguous datasets over the tropical belt. Due to the low L-band frequency sensitivity of the utilized SAR imagery to aboveground biomass, they are able to detect e.g. standing water beneath the forest canopy. This sensitivity is shown to be particularly relevant in urban forests, where the ability to distinguish between different types of vegetation and other LC types can be especially challenging.
Unlike the previous studies, Sun et al. [132] explore the fusion of LiDAR and SAR data to enhance biomass estimation by leveraging strengths of both techniques. LiDAR, with its capability to provide detailed vertical profiles of canopy structure, offers accurate measurements of canopy height, while SAR data, particularly sensitive to canopy volume and biomass, adds spatial continuity across the landscape.
However, use of tree height information to map trees or forests is showcased to be particularly practical for forest mapping. As such a study by Kim [83] demonstrate how a normalized digital surface model (nDSM) derived from stereo photography at 25 centimeter resolution can be utilized to estimate forest stand volume based on crown density and stand height. This method presents a cost-effective alternative to LiDAR or SAR. This study further illustrates the capability of RS to provide detailed and actionable forest metrics beyond mere canopy cover, including tree heights and volume estimates, essential for urban forestry management. Similarly to Kim [83], Balenović et al. [10] investigate the application of digital photogrammetry for estimating forest stand heights using stereo models from color infrared (CIR) digital aerial images. Therefore, they first create a digital surface model (DSM) from aerial photographs, followed by the extraction

of nDSM to represent tree heights. Furthermore, they explore the importance of high spatial resolution in the accuracy of photogrammetric estimates. By comparing images with different resolutions (10 and 30 centimeters), the study demonstrates that higher resolution images are capable to precisely identify tree tops, which is critical for accurate height measurement. However, they also indicate, that lower resolution (and thus less expensive) imagery is sufficient for operational purposes, assuming a high-precision digital terrain model (DTM) is available.

Urban Agriculture and Urban Gardens

Urban agriculture can be generally defined as growing food in cities [136]. While this definition includes large agricultural fields that are located in urban areas, it also considers small-scale gardening in allotments, front and backyard gardens, or even balcony and rooftop gardens. In large cities agricultural land is not included in the public green space data, as it is usually not clear how this land will develop [63]. However, in some countries, it is integrated into urban economic and ecological systems [38]. Urban agriculture is crucial for enhancing food security, promoting sustainable LU, and supporting local economies. It also serves social and ecological functions, including recreational spaces, enhancing biodiversity, and improving urban climate [136].
Mapping urban gardens is critical for understanding the spatial distribution and potential of these spaces in enhancing urban food systems, biodiversity, and community well-being. Despite their importance, accurately mapping these areas is challenging. This is primarily due to varied vegetative cover within the gardens, which complicates classification [127]. One notable effort in this field is conducted by Taylor and Lovell [136], who manually analyze high-resolution Google Earth imagery to map agricultural sites in Chicago. They categorize sites by type: residential gardens, community gardens, urban farms, and by size, from small to very large. Despite achieving high accuracy, they note the process being exceedingly labor-intensive. Contrasting, Mathieu et al. [95] conduct an geoOBIA method with Ikonos imagery to map private gardens in New Zealand. The four meter spatial resolution imagery, enhanced with four spectral bands, appears effective in identifying green spaces. This approach not only differentiates various garden types but also provides crucial ecological data, highlighting the significance of spatial resolution in revealing detailed characteristics of garden spaces. The method is also highlighted for its efficiency in generating garden-relevant datasets. Moreover, there is no evident research that focuses on extracting garden-relevant features, like sheds, using height information. Nevertheless, the approach of height thresholding is commonly performed for the extraction of residential buildings. For instance, Vu et al. [143] utilize LiDAR height thresholding of both pre- and post-event data to identify new constructions or demolitions of buildings. Selected thresholds are based on the standard deviation from the mean difference, helping to distinguish height changes from normal variance due to factors like environmental changes.

The authors note that height thresholding is effective in detecting significant structural changes, whereas minor extensions or modifications that do not significantly alter buildings' height profile might not be detected. Similarly, Matikainen et al. [96] use height information obtained from a laser scanner for building detection. They utilize the height difference between DSM and the DTM to distinguish buildings from other structures or vegetation, using a 2.5 meter height threshold. Although this method is advantageous in reducing misclassifications and enhancing accuracy of building detection, it struggles to identify low-rise buildings or structures with minimal elevation differences from their surroundings.

The utility of very-high-resolution RS imagery for mapping small, fragmented green spaces is further evidenced by Haase et al. [63] who achieve a 96% accuracy rate using a 5 meter spatial resolution Rapideye dataset combined with spectral unmixing techniques. In a similar vein, Freire et al. [54] utilize a 0.61 meter resolution QuickBird dataset for urban agriculture mapping. Despite a lower accuracy rate of 52%, attributed to the varying vegetation stages within a single site, the semi-automated process marks a significant step forward in urban agricultural identification. Advancements in garden mapping continue with the use of unoccupied aerial vehicles (UAVs) and an RF ML method by Wagner and Egerer [144]. The UAVs, flying at lower altitudes, offer enhanced visibility and produce highly detailed 5 centimeter resolution images, ideal for calculating spatial metrics at plot level, a task difficult with larger scale images like those from Sentinel-2. Achieving an 80% prediction accuracy, this method is deemed highly suitable for urban garden mapping. However, Abdi [1] executes a combination of aerial and Sentinel-2 imagery to map urban gardens in Yazd city, Iran. His methodological approach, using vegetation indices and DSM alongside geoOBIA, achieves over 80% accuracy. The integration of the SVM method within geoOBIA proves particularly effective in distinguishing urban gardens from other LUs. This approach not only enhances mapping accuracy but also reveals vulnerability of smaller gardens due to urban development. Mentioned research articles make it clear that mapping urban gardens is a complex but critical task, greatly aided by the availability of high-resolution data to precisely identify these valuable urban areas.

The process of mapping urban agriculture in general involves similar approaches as with urban gardening areas, namely combination of GIS, RS, and ML methods. An example of this is the work by Taylor and Lovell [136], who utilize Google Earth images to map potential urban agriculture locations, supplemented by data from local non-profits and food policy councils. Their method involves a combination of RS and manual checks via Google Earth, categorizing urban agriculture sites based on their visibility and determining their accessibility and ownership. The accuracy of these maps is largely influenced by the spatial resolution of the data used, highlighting that manual verification and reliance on third-party data can introduce bias or errors if the data is outdated or incomplete. To enhance the reliability of these maps, Delgado [38] employs aerial photographs coupled with field surveys, despite its higher cost and time investment, results in significantly more precise data than that obtained from medium or low resolution satellite imagery alone. This approach includes field validations to confirm agricultural activity, followed by integrating these findings with urban maps to analyze the urban-rural gradients and the impacts of urbanization on farming practices. Although highly accurate, field validation is noted to be labor-intensive, potentially limiting its applicability for larger-scale projects or frequent updates.

An alternative to intensive field surveys is the use of very high-resolution RS images, as demonstrated by Forrest [52]. The author utilizes Quickbird satellite imagery and the geoOBIA technique to segment and classify urban and peri-urban agricultural areas, offering a better management of the spatial complexity typical for urban settings. However, this method faces challenges in accurately marking field boundaries due to the fragmented nature of urban landscapes, and it may struggle to keep up with the dynamic shifts in urban agriculture without regular data updates. Similarly, combination of multi-spectral UAV data and OBIA to map agricultural sites is explored by El Hoummaidi et al. [44]. This study utilize DL algorithms to analyze high-resolution drone imagery, achieving notable success in vegetation cover classification and crop health assessment. Here, the authors as well note that the use of UAVs enables capturing of detailed, real-time data, offering insights into crop health that were previously unattainable with traditional RS methods. This method proves particularly effective in urban settings where traditional field surveys are logistically challenging and time-consuming.

Urban agriculture often presents itself differently in imagery; crop fields generally appear more uniform than smaller gardening areas, making reliance on a single data source inadequate. Therefore, to capture the dynamic nature of urban agriculture, involvement of multi-temporal data is preferred over single-date observations. Such an approach helps in aligning phenological development with varied crop types and management practices in crop production systems, thus improving the accuracy of cropland maps. Addressing this, Blickensdörfer et al. [19] integrate optical and radar data from satellites like Sentinel-2, Sentinel-1, and Landsat 8 with environmental data that includes topographic and climatic elements. Using an RF classifier, they analyze dense time series data from these sources to enhance classification accuracy, particularly under varied weather conditions. While the integration of multiple data sources broadens the scope of mapping, it also escalates the complexity and computational demands of the process. This comprehensive approach depends on the availability of consistent, high-quality time-series data, which may not be universally accessible or applicable in all regions. Similarly, Forster et al. [53] recognize that different crops and their phenological stages exhibit distinct spectral, textural, and morphological characteristics. Therefore, using Quickbird imagery in combination with OBIA, they map peri-urban agriculture (PUA) in Hanoi, Vietnam. The study demonstrates that per-field vector segmentation and classification are more effective for mapping PUA compared to traditional pixel-based methods. However, it also highlights the need

for advanced segmentation techniques and multi-temporal imagery to improve accuracy and efficiency.
Perennial crops can sometimes be challenging to identify, as they showcase varying temporal changes compared to annual crops. In order to identify such crops, in particular vineyards, Simonneaux et al. [129] perform NDVI thresholding to map them in Morocco. They set 0.15 as a minimum threshold between bare soil and tree-like vegetation while 0.45 as a maximum threshold. Although the authors reach 85% identification accuracy, they highlight confusions due to overlapping spectral signatures of different crops as well as underdetection of young tree plantations due to low NDVI values. Peña et al. [112] use spectro-temporal indices derived from Landsat 8 images to map perennial plants in Chile. The authors utilize the full spectral range of the used images, as well as NDWI, and NDVI indices. However, they achieve the best result, by especially utilizing the visible and Short-wave infrared (SWIR) bands. In contrast, NDVI produces the poorest outcomes. They further examine the significance of different dates and establish that the early (greenness) and late (senescence) stages of the growing cycle are the most critical for differentiation.

Green Corridors

The importance of green corridors from an ecological perspective is well known. Therefore, they are mainly mapped to understand connectivity of core areas and rarely are mapped as a part of UGSs. They serve to connect major landscape elements in urbanized regions [24], thus integrating different LU classes like industrial areas and residential sites. Their primary role is to maintain a green landscape structure and ensure ecological continuity [62]. As such, Guneroglu et al. [62] map green corridors in Trabzon and Rize, Turkey. Using the SVM classification approach with combination of multispectral digital aerial images, Ikonos, and Quickbird images, the authors identify severe fragmentation of green spaces in both study areas. In order to understand the fragmentation level as well as disconnection of green spaces, they utilize metrics such as the Largest Patch Index, Area Weighted Mean Patch Fractal Dimension and others. Based on the their findings, the authors propose a network of green corridors for each city and showcase how the proposed networks can serve as ecological links between fragmented landscapes. They apply three main rules to design green corridors:

- Connectivity - ensuring that the corridors connect major patches of green spaces
- Continuity - corridors are designed to provide continuous green space, avoiding interruptions that could hinder their ecological function
- Accessibility - making the green corridors accessible to the public to enhance recreational opportunities while maintaining their ecological integrity

In the existing literature, there are also other examples of how green corridors are identified, especially from the urban planning perspective. For instance, Popescu et al. [114] develop a methodology to identify ecological corridors for large carnivores, specifically the brown bear, in various Romanian landscapes. With a three step approach, authors first perform habitat suitability analysis to map core habitat areas of the species of interest. They utilize DEM and CORINE LC datasets as a base for GIS analysis. They then create a connectivity model that establishes or adds linear structures at the critical points where infrastructure disrupts ecological flows. And finally, they explore ecological corridors at two scales and identify critical areas in the network.

The effects of urban expansion, or changes in urban areas on the pattern of urban green corridors is further investigated by Wang and Pei [145]. Their study conduct morphological spatial pattern analysis techniques and socio-ecological analysis methods to evaluate the spatial patterns of urban green and blue areas over time. With the selected method, they categorize green infrastructure into different structural classes like core, edge, and bridge patterns, which allows for a detailed examination of how urbanization has reshaped ecological landscape. Using Landsat data and an atlas of urban expansion, they first identify water, built-up, and other/open space and later fore-and background classes for the morphological analysis. The findings of the analysis highlight a tension between urban development and ecological conservation. Therefore, the study advocates for integrating GI planning in urban development to maintain and enhance ecological networks.

Use of morphological image processing to map ecological corridors is very common technique among ecologists. As such, Vogt et al. [142], discuss the importance of landscape corridors for biodiversity conservation and present a method for automated mapping using morphological image processing and a CORINE LC dataset. They introduce a technique that differentiates between "line" and "strip" corridors by considering their width and connectivity, which is crucial for practical conservation efforts [24]. Further, the authors emphasize that structural connection, does not necessarily imply a functional connection. However, a knowledge of structural corridors is certainly valuable from a biodiversity assessment viewpoint. The authors also acknowledge limitations of RS data and the need for ground validation to validate identified corridors.

Various techniques are implemented to identify these corridors, which range from RS imagery and ML classification to habitat suitability, network analysis and morphological image analysis. Zhang et al. [154] seek to improve landscape connectivity through mapping of potential green corridors. The authors first identify core patches that consist of 16 parks with more than 12 hectares area. Then they utilize least-cost path technique to identify the easiest route that wildlife can take from one core area to another. By assigning suitability scores and weights to LU types (e.g., prioritizing vacant lots with trees), they create a cost surface map to identify the “easiest” or most feasible routes. This allows the placement of corridors by calculating paths with minimal ecological “costs” (resistance) across the landscape. Furthermore, by using a gravity model, they also rank corridors that

would provide the most significant connections with the least investment. The authors, however, encounter problems due to the resolution of the utilized data. Therefore, they emphasize the necessity of high-resolution data for accurately mapping UGSs and vacant parcels. Assignment of resistance values to different land types and suitability scores for various LUs is based on expert judgment and existing literature. Therefore, the authors also acknowledge that this subjectivity in scoring can lead to bias, as it might not fully represent the true ecological costs of each LC type for all species.
Use of satellite data and GIS for green corridor mapping is a common practice. Cui et al. [33] focus on constructing and optimizing green space ecological networks in urban fringe areas. They use a combination of Landsat satellite imagery and GIS to classify LC in the study area. By dividing green spaces into categories (e.g., parks, protective green spaces, and regional green spaces), they create a spatial layout of the area's green network. The authors utilize the minimum cumulative resistance model to map potential corridors. Resistance values are assigned based on LC, with urban and developed areas presenting higher resistance and green or natural areas showing lower resistance. The least-cost path analysis then identifies feasible ecological corridors with the least cumulative resistance. Similarly to the study of Zhang et al. [154], the authors define subjectivity in assigning resistance values as a drawback of the applied methodology. Moreno et al. [102] focus on using RS data to assess and plan green corridors and explore the potential of urban forests for green corridor development. The authors use Sentinel-2 satellite imagery, specifically implementing NDVI to assess vegetation health, vigor, and density. Areas with NDVI values close to or above 0.3 are considered high-quality vegetation zones, characterized by healthy, vigorous plants and sufficient canopy cover. These high-NDVI areas are identified as core green spaces that could serve as hubs or anchor points in the green corridor network. This approach provides a detailed picture of green space distribution and quality across a urban landscape. As a result, they select parks, urban forests, and other large, public green areas as core areas. They further conduct a detailed assessment of vegetation in the field, focusing on a street-level vegetation quality within 100 meter transects. For each 100 meter segment, the authors evaluate health and structural quality of the vegetation to determine its suitability as a connector within the corridor. They also acknowledge, that due to the satellite's resolution, some smaller vegetation patches may not have been captured accurately, potentially leading to underestimations of vegetative cover.

Chapter 3

Methods

In this chapter, we describe methods executed throughout the thesis. Application of selected methods, or their outputs, across various chapters is depicted in Figure 3.1. In the following we introduce the Random Forest model, grey-level co-occurrence texture metrics, mean-shift segmentation, density-based clustering, and convex hulls. Additionally, we detail architecture of interpretable machine learning techniques, focusing specifically on Shapley Additive Explanations, and discuss the one-at-a-time sensitivity analysis approach.

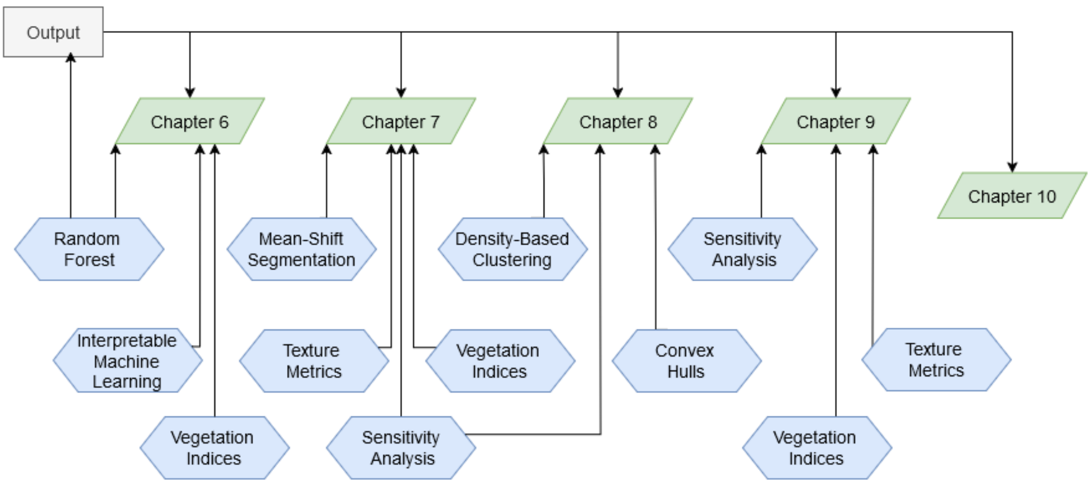

Figure 3.1: Flowchart depicting utilization of methods across various Chapters.

3.1 Random Forest

In most modern ML approaches, a classifier is produced by a learning algorithm using a collection of training examples in a set S. The classifier represents a hypothesis about the

true function f. When presented with new x values, it predicts the associated y values [41]. When preforming a classification task, such as classifying UGSs, we are not only interested in the most accurate results, but also in uncovering which variables contribute the most to the classifier. However, many ML techniques, including k-nearest neighbors, SVM, and neural networks, while excel in classification tasks, offer little understanding of which variables are most influential in the resulting classifier [6]. Classification trees, which are structured as binary trees, stand out for their ability to predict an observation's class using a wide array of covariates and bring light on which covariates serve as key predictors. It is, however, observed that classification trees can be unstable regarding the changes in training sets. Therefore bagging techniques are introduced to reduce and/or eliminate this instability [41]. Bagging can be represented as follows: in each iteration, bagging introduces a training set to the classifier that comprises of randomly selected m training examples from the original set of m items. This sample is known as a bootstrap replicate of the initial training set, a process referred to as bootstrap aggregation or bagging by Breiman [21]. On average, each bootstrap replicate includes about 63.2% of the original training set's examples, with some appearing more than once [41]. Furthermore, an alternative approach to creating training samples is to form them by excluding separate portions of a training data. For instance, this data can be split at random into 10 distinct segments. Subsequently, 10 interlinked training sets can be generated, each time omitting one of these 10 segments. This method mirrors the one employed for tenfold cross-validation. As a result, ensembles built using this method are often referred to as cross-validated committees [41].
RF, introduced by Breiman [22], is a specific instance of bagging [6]. It is also referred to as an ensemble learning technique. Ensemble classifiers consist of multiple single classifiers whose individual judgments are aggregated to categorize new instances. Experiments show, that ensembles frequently surpass the accuracy of single classifiers that they are build on. Therefore, creation of robust ensemble classifiers is a particularly dynamic field of supervised ML [41]. In order to grow ensembles, random vectors with the previously described bootstrap sampling technique are created. The procedures of voting for a common class, based on the generated large number of trees, is called random forests [22]. Consequently, RF can be described as a classifier consisting of tree-structured classifiers assembly $\{h(x, \Theta_k), k = 1, \ldots\}$, with $\{\Theta_k\}$ being independently distributed random vectors, and each tree giving a unit vote for the most popular class at input x [22].
An important procedure incorporated into RF is a feature selection, where the most contributing features can be calculated. Commonly, feature selection techniques shift through various subsets of features to identify the optimal and the smallest subset out of the potential 2^N candidates, based on a specific evaluation metric [36]. Feature selection not only enhances model performance but also allows for the creation of simpler and more efficient models through the use of a limited set of features. Additionally, it provides deeper insights into the data's underlying processes by concentrating on a chosen subset

of features [121]. The calculation of variable importance in RF, however, involves assessing the mean decrease in accuracy by utilizing the out-of-bag (OOB) observations. Since RF is developed from a bootstrapped sample, around one-third of the observations in the dataset are not used in the development of each tree, and these unused observations are termed OOB observations for that particular tree [6]. Therefore, these OOB observations effectively serve as a natural test set for each tree, offering a simpler and less resource-intensive alternative to the traditional cross-validation method for estimating RF error rates. Variable importance, otherwise also called permutation importance, is calculated following three general steps described by Archer and Kimes [6]:
for a series of bootstrap samples indexed by $b = 1, \ldots, B$:

1. Identify the OOB observations, designated as $\mathcal{O}_b$, where $\mathcal{O}_b$ is the complement of the b-th bootstrap sample within the full dataset $\mathcal{D}$;
2. For $\mathcal{O}_b$, utilize the tree T_b to determine class memberships and count the instances where T_b accurately identifies the correct class;
3. For each predictor variable indexed by $j = 1, \ldots, p$:
   (a) Shuffle the values of predictor x_j within $\mathcal{O}_b$;
   (b) Apply T_b to classify $\mathcal{O}_b$ using the shuffled x_j, and count the correct classifications;
   (c) The vote difference for the correct class between the shuffled and original OOB data is computed by $V_{\text{diff}} = V_{\text{correct, orig}} - V_{\text{correct, shuffled}}$.

When the quantity of trees is fixed, a variable that receives higher importance score, compared to others, is the most important variable for the classification. Hence, instead of calculating an exact relationship between the independent variables and the outcome, like in conventional data modeling, measures of variable importance offer a strong statistical reflection of a variable's role in the RF classification [6].
Apart from permutation feature importance, it is also common practice to calculate the Gini impurity measure [21]. Gini impurity explains how "mixed" the classes are in a node. It ranges from 0 (pure, all samples in the node belong to a single class) to a maximum value when the classes are evenly mixed. For a node t with K classes, the Gini impurity is calculated based on Equation 3.1:

$$G(t) = 1 - \sum_{k=1}^{K} p_k^2 \tag{3.1}$$

where p_k is the proportion of samples of class k in the node. As the tree is constructed, the Gini gain for every split will be recorded. Then, for each feature x_j, the Gini gain across all the nodes where the feature is used to split the data in the current tree will be summed as follows in Equation 3.2:

$$G_{\text{importance}}(x_j) = \sum_{t \in T_j} \Delta G_t \tag{3.2}$$

where T_j is the set of all nodes in the tree where x_j was used to split.
Since RF consists of multiple decision trees, the Gini importance will be averaged over all the trees in the forest as shown in Equation 3.3:

$$G_{\text{forest importance}}(x_j) = \frac{1}{B} \sum_{b=1}^{B} G_{\text{importance},b}(x_j) \tag{3.3}$$

where B is the number of trees in the forest.
In order to optimize classification accuracy, RF allows parameter tuning. When building an RF classifier, two key parameters for classification need to be set: number of variables used to split a node (*mtry*) and number of trees grown in the forest (*ntree*). When determining number of variables for split, a typical approach is to take a square root of m, where m represents sum of the number of predictor features. Unlike many other classifiers, an increase in *ntree* leads to an improved classification performance [22]. Thus, this parameter must be adjusted wisely.

3.2 Mean-Shift Segmentation

Mean-Shift segmentation, proposed by Fukunaga and Hostetler [55], is a non parametric and iterative clustering method designed to detect modes, or peaks, of a dataset's probability density function. The algorithm focuses on estimating the gradient of the density function. By pinpointing areas of highest density, mean shift segmentation effectively divides the dataset into distinct clusters or segments. This method has been widely utilized across various fields, especially in image processing, for tasks like edge detection, image segmentation, and analysis of feature spaces [155]. It is used for locating maxima of a density function given discrete data is sampled from that function [29]. The main advantage of this segmentation technique is its ability to adapt to an actual data distribution, allowing it to handle arbitrary shapes and numbers of clusters without requiring prior knowledge of these clusters [55]. This procedure works by iteratively shifting each data point towards the region of the highest data point density until convergence. Comaniciu and Meer [29] describe the process of the mean-shift segmentation with the following five steps:

- Initialization: Each data point x_i in the feature space is given a kernel function. Typically, the Gaussian kernel $K(x)$ is used to weight the influence of surrounding points. The bandwidth parameter h of the kernel determines the size of the neighborhood considered for mean computation.

- Mean Shift Vector Calculation: The mean shift vector is computed as:

$$m(x) = \frac{\sum_{i=1}^{n} K\left(\frac{x-x_i}{h}\right) x_i}{\sum_{i=1}^{n} K\left(\frac{x-x_i}{h}\right)} - x$$

  where x is the current position, x_i are the neighboring data points, K is the kernel function, and h is the bandwidth. The mean shift vector $m(x)$ points toward the direction of the maximum increase in the density.

- Shifting the Window: The current position x is shifted by the mean shift vector:

$$x \leftarrow x + m(x)$$

  This step moves the data point towards the region of higher density.

- Convergence: The iterations continue until the shift $m(x)$ is smaller than a predefined threshold, indicating that the point has reached a mode of the density function.

- Cluster Formation: Once convergence is achieved, data points that converge to the same mode are assigned to the same cluster. This results in the segmentation of the data into clusters.

Mean-shift segmentation has been widely incorporated into various spatial libraries due to its ease of integration into GIS workflows. The Mean Shift Segmentation tool in ArcGIS Pro not only executes the algorithm but also offers the flexibility to adjust specific parameters for improved segmentation outcomes. For example, adjusting spectral detail parameter allows for more refined segmentation, while the spatial detail parameter introduces spatial dependency among grouped pixels. Additionally, defining the minimum segment size can help better distinguish spatial objects with known dimensions, effectively managing the separation of large and small patches.

3.3 Density-Based Clustering

Density-based clustering is an approach that identifies clusters within a dataset by looking at regions of high object density. The core idea is that a cluster is a contiguous region of high density, separated from other clusters by areas of lower density. Points that lie in regions of low density are considered noise or outliers [86]. The density of a point is typically estimated using methods like kernel density estimation or nearest neighbor density estimation. A density-based cluster is formed by connecting points that have a higher density than a given threshold and are reachable through a contiguous path.

Consequently, for each point x first the local density $p(x)$ is estimated by means of kernel or nearest-neighbor approaches. Points are considered connected if they are within a specified distance ε of each other. Finally, the cluster is formed as the maximal set of points directly or transitively connected to each other with densities exceeding a given threshold λ [86].
Density-Based Spatial Clustering of Applications with Noise (DBSCAN) is one of the most well-known density-based clustering algorithms [48]. It identifies clusters by finding regions in a data space where the density of points exceeds a certain threshold. DBSCAN is particularly suitable for datasets with clusters of varying shapes and sizes, and it can help to effectively identify noise and outliers. It uses two key parameters: radius ε and minimum number of points (*minPts*). The procedure of DBSCAN can be described as follows:

- Core Points A point p is classified as a core point if there are at least *minPts* points within its ε-radius neighborhood. Formally, the density of a point p is the number of points within a radius ε around p:

  $$k_p = |\{x \in D \mid \text{distance}(p, x) \leq \varepsilon\}|$$

  A point p is a core point if $k_p \geq minPts$.

- Direct Density Reachability: A point q is directly density-reachable from point p if q is within the ε-radius of p and p is a core point.

- Density Connectivity: Two points p and q are density-connected if there is a path through other core points such that each point on the path is directly density-reachable from the next point. This transitive relation allows DBSCAN to form clusters of arbitrary shape.

- Cluster Formation: The algorithm starts by selecting an arbitrary point in the dataset. If this point is a core point, a new cluster is created by adding all points density-reachable from it. This process is repeated until all points have been assigned to a cluster or labeled as noise.

- Noise Identification: Points that do not belong to any cluster are considered as noise.

While DBSCAN exhibits advantages in distinguishing noise and not requiring number of clusters as input, its performance still depends on the choice of ε and the *minPts*. Furthermore, it might struggle to form clusters of varying densities, as the mentioned parameters cannot adapt to the differences in density within the same dataset [86].

3.4 Texture Metrics

In classical RS classification tasks, it is common to consider unique spectral characteristics of objects. Spectral information reflects chemical or biophysical properties of these objects. However, measuring spatial characteristics of objects can be equally important. This is especially true as the level of detail improves with increased spatial resolution, which can also lead to an increase in potential noise. [64].
Texture of objects, similar to color and shape, can be crucial for their identification. While texture can be described in many ways and can have many forms like 'smooth' or 'rough', for a computer to understand it or be able to represent it, numeric representation of a texture must be defined and/or provided. There are numerous standard methods for texture processing. Mostly studies have concentrated on texture measures obtained by sliding a fixed-size window with an odd number of dimensions across an image and analyzing various pixel relationships. The grey-level co-occurrence matrix (GLCM), introduced by Haralick [65] in 1979, is by far the most commonly used technique for deriving texture measures [28]. Furthermore, it is a method that can provide a numeric, computer understandable representation of various textures.
GLCM implements a spatial co-occurrence matrix to calculate relationships between pixel values, and uses these relationships to derive second-order statistical properties from the matrices. Features extracted from the GLCM are based on the premise that the texture information in an image is encapsulated in spatial relationships among the grey levels of adjacent pixels [57]. Therefore, GLCM examines each pair of pixels separated by a distance d in a given direction θ and computes how often different combinations of pixel intensities (gray levels) occur in an image. There are eight texture indices that can be grouped into 3 main classes, namely statistics, contrast, and orderliness group [149]. The statistical group provides descriptions of the fundamental statistical variables associated with the texture's gray value, and includes texture metrics such as mean, variance, and correlation. Furthermore, the contrast group quantifies local variations within a patch and contrasts these with the adjacent pixels, and focuses on metrics such as contrast, homogeneity, and dissimilarity. Finally, the orderliness group evaluates the regularity and randomness of pixel values, using measures like angular second moment and entropy metrics [149]. Short descriptions and equations to calculate some of the most commonly used GLCM metrics are given in Table 3.1. Even if many attempts to modify or propose new texture extraction methods were made, GLCM remains the most utilized one. Until now, the most changes to GLCM were done in terms of improved calculation algorithms, while the calculation statistics behind it still remains the same [146].
Studies show, that the information extracted by texture analysis from visible and infrared wavelengths is independent from spectral reflectance values. This in turn, can be an extremely advantageous information source from RS images whose wavelength distribution is limited only to visible or infrared part of the spectrum [64]. Consequently, recognizing

and measuring the variations in texture within an image can aid distinguishing between types of vegetation. This distinction can, in turn, assist in characterizing different types of UGSs. This is particularly relevant for species with similar spectral characteristics but with different spatial patterns [99].

Table 3.1: Equation and short description of commonly used GLCM indices.

GLCM Metrics	Equation	Description
Dissimilarity	$\sum_{i,j=0}^{N-1} iP_{i,j}\|i-j\|$	Measures the variation of grey level pairs in an image
Homogeneity	$\sum_{i,j=0}^{N-1} \frac{iP_{i,j}}{1+(i-j)^2}$	Quantifies the consistency of the non-zero elements within the GLCM
Contrast	$\sum_{i,j=0}^{N-1} iP_{i,j}(i-j)^2$	Measures the intensity contrast between neighboring pixels over the whole image
Entropy	$\sum_{i,j=0}^{N-1} iP_{i,j}(-InP_{i,j})$	Measures the disorder of grey levels in the image

The selection of the the most appropriate GLCM metrics for UGS characterization can be challenging. However, from the mentioned indices, the most commonly associated ones with land cover patches are contrast, dissimilarity, entropy, and variance [64]. These indices excel in identifying edges, capturing spatial dynamics and exchanging of resources between various UGSs and their adjacent areas [149].

3.5 Vegetation Indices

In RS, scientists use vegetation indices to assess vegetative covers both qualitatively and quantitatively through spectral data. These indices help distinguish various types of vegetation based on their unique spectral properties compared to the surrounding ground elements [151]. For example, visible light in the red spectrum (630-690 nm) is absorbed by chlorophyll, and near-infrared light (760-900 nm) is reflected by the cellular structures of leaves. The noticeable difference in reflectance between these two wavelengths is indicative of the presence of green vegetation. Specifically, the red spectral response correlates with chlorophyll levels, while the near-infrared response depends on the leaf area index and the density of the green vegetation. By analyzing these spectral responses, vegetation indices enable the differentiation of vegetation from soil and the assessment of photosynthetically active biomass based on vegetative cover density. Overall, these indices provide a more sensitive measure of vegetation health and biomass than individual spectral bands [11].

In the Chapter 2 we describe how various authors identify urban green. It is no surprise

that majority of them utilize vegetation indices as well [37][112]. Therefore, in the following we present how selected vegetation indices can be calculated to assist a vegetation mapping.
NDVI is one of the most commonly used vegetation indices to highlight vegetation. It is based on the knowledge that chlorophyll absorbs the red light while the mesophyll leaf structure scatters near-infrared light (NIR). NDVI values range from -1 to +1, where positive values represent healthy vegetation and negative values indicate an absence of or sparse vegetation [106]. It is calculated using red and NIR bands of the Sentinel-2 images based on Equation 3.4.

$$NDVI = \frac{NIR - Red}{NIR + Red} \tag{3.4}$$

Vegetation indices are not only calculated from multi-spectral data. Some very-high resolution aerial images can frequently be provided as only three band image with red, green, and blue bands. Consequently, to increase an information gain from limited spectral resolution, RGB-based vegetation indices can be calculated.
Green Leaf Index (GLI) is recognized as one of the most robust RGB-based indices for areas dominated by vegetation, built-up, or sparse vegetation [3]. It utilizes all three bands of aerial imagery, with values ranging from -1 to +1. Negative values indicate soil and non-living features, while positive values represent green leaves and stems [90]. GLI is calculated using Equation 3.5, where green, red, and blue represent spectral bands of an aerial imagery.

$$GLI = (2 * green - red - blue)/(2 * green + red + blue) \tag{3.5}$$

In addition to the GLI index, two common RGB indices are the Red-Green-Blue Vegetation Index (RGBVI) as well as the Normalized Green-Red Difference Index (NGRDI). The idea behind RGBVI index is based on the knowledge, that green vegetation has high reflectance in the green spectrum (around 540 nm) and the absorption in the red and blue regions of the visible spectrum (400–700 nm) caused by plant chlorophylls. Therefore, to account for reflectance differences due to chlorophyll a absorption (420, 490, and 660 nm) and chlorophyll b absorption (435, 643 nm), Bendig et al. [16] propose the RGBVI index. The RGBVI is formulated as the normalized difference between the squared green reflectance and the product of blue and red reflectance and is calculated based on Equation 3.6.

$$RGBVI = \frac{(RG \times RG) - (RR \times RB)}{(RG \times RG) + (RR \times RB)} \tag{3.6}$$

The NGRDI index is also designed to differentiate green vegetation from other ground cover types [140]. It is calculated as the normalized difference between green and red reflectance bands of aerial imagery, based on a straightforward Equation 3.7.

$$NGRDI = \frac{RG - RR}{RG + RR} \tag{3.7}$$

It effectively distinguishes between three main ground cover types:

- Green Vegetation: Characterized by higher green reflectance than red, resulting in positive NGRDI values.
- Soils: Have higher red reflectance than green, leading to negative NGRDI values.
- Water/Snow: Show similar reflectance in both green and red wavelengths, producing NGRDI values near zero.

NGRDI ranges between -1 and +1, where the value of zero serves as an effective threshold to separate green vegetation from other types of ground cover. Additionally, changes in the balance between green and red reflectance can be used to detect phenological events, such as the timing of leaf green-up and autumn coloring [104].

3.6 Convex Hulls

The convex hull of a set of points in a plane is the smallest convex polygon that can completely contain all the points in the set. It can be visualized as a shape formed by stretching a rubber band around the outermost points of a set; when the band is released, it snaps into the shape of the convex hull [82]. The process of creating a convex hull using a set of points can be described as follows:

- Start with three non-collinear points to form the initial convex hull. Let's denote these points as p_1, p_2, and p_3. These points are arranged such that they form a counter-clockwise triangle.
- Calculate orientation of these three points to ensure they form a convex polygon. The orientation of points p, q, and r can be determined using the determinant:

$$\begin{aligned}\text{orientation}(p, q, r) &= \text{sign}\left(\det \begin{vmatrix} 1 & p_x & p_y \\ 1 & q_x & q_y \\ 1 & r_x & r_y \end{vmatrix}\right) \\ &= \text{sign}\left((q_x - p_x) \times (r_y - p_y) - (q_y - p_y) \times (r_x - p_x)\right).\end{aligned}$$

If orientation$(p_1, p_2, p_3) > 0$, the points form a counter-clockwise turn, indicating a convex shape.

- For each new point r in the set check if r lies inside the current convex hull. A point r is inside the convex hull if, for every edge (p_i, p_{i+1}) of the hull, the orientation of the triplet (p_i, p_{i+1}, r) does not indicate a right turn:

$$\text{orientation}(p_i, p_{i+1}, r) \geq 0.$$

If r is outside the current hull (i.e., for at least one edge (p_i, p_{i+1}), orientation$(p_i, p_{i+1}, r) < 0$), identify the sequence of edges that are visible to r. This involves finding tangents to the current hull from point r.

- If r is outside the current hull, find the edges of the hull visible from r. This is done by finding the range of indices $[i, j]$ where:

$$\text{orientation}(p_i, p_{i+1}, r) < 0.$$

- The edges that are weakly visible from r form a consecutive subchain. Let this subchain be from vertex v_i to v_j. Replace this subchain with the new point r, thus creating new edges (v_i, r) and (r, v_j).
- Find the tangents from point r to the current hull. The tangent lines are determined by the edges where the orientation changes from positive to non-positive as you traverse the hull.
- Update the list of vertices that form the convex hull.

A primary challenge in convex hull computation arises when using floating-point arithmetic. Kettner et al. [82] demonstrate that the result of convex hull algorithms can be unreliable due to the limited precision of floating-point arithmetic. Especially rounding errors can lead to misclassification of points, causing the algorithm to miss points that should be included in the hull or include points incorrectly. Furthermore, the algorithms rely on geometric properties such as the orientation of points (whether a set of points forms a left or right turn). Floating point errors can cause these properties to be violated, resulting in failures like a point outside the convex hull might seeing no edge of the hull, leading to its incorrect exclusion. Points inside the hull might be erroneously classified as being able to see an edge, leading to incorrect updates to the hull. In addition, a computed convex hull may not be truly convex, or in severe cases, the algorithm might even fail to terminate.

3.7 Interpretable Machine Learning Techniques

Various approaches to explain ML and DL methods exist. However, Shapley Additive Explanations (SHAP) by Lundberg [93] is one of the most frequently used one in LULC related studies. SHAP facilitates to understanding the contributions of each feature to predictions made by a model. SHAP uses Shapley values, originally developed for cooperative games, to allocate the "payout" (in this case, model prediction) among "players" (input features) according to their contribution. To compute SHAP values, a model is trained with and without each feature, and differences in the model's output are calculated to determine that feature's contribution. SHAP provides both local and global explanations, which allows to understand both individual predictions and overall model behavior [93].
Lundberg [93] describes SHAP values as follows. Let $f(x)$ be the prediction model, where x is a vector of input features. SHAP values represent how much each feature contributes to the difference between the actual prediction $f(x)$ and the mean prediction $E[f(z)]$. A SHAP value for each feature i is computed by taking average of the marginal contributions of that feature over all possible subsets of features S that do not contain i. SHAP values ϕ_i for feature i are calculated based on Equation 3.8 as follows:

$$\phi_i(f,x) = \sum_{S \subseteq F \setminus \{i\}} \frac{|S|!(|F|-|S|-1)!}{|F|!} \left[f_{S\cup\{i\}}(x) - f_S(x) \right] \tag{3.8}$$

where F is a set of all features, S is a subset of features excluding i, $f_S(x)$ is the model's output when only features in set S are known, and $f_{S\cup\{i\}}(x)$ is the model's output when feature i is added to the subset S.
Computational complexity of exactly calculating SHAP values for models with many features could be a limiting factor, since it requires evaluating the model for all possible subsets of features. Therefore, several approximation methods are used, such as Kernel SHAP and Tree SHAP. In Kernel SHAP, SHAP values can be estimated by solving a weighted linear regression problem where the weights are chosen to match the Shapley values. Loss function for the regression is calculated based on Equation 3.9:

$$L(f,g,\pi'_x) = \sum_{z' \in Z} \left[f(h_x^{-1}(z')) - g(z') \right]^2 \pi'_x(z') \tag{3.9}$$

where π'_x is a weighting kernel based on the size of the subset S, ensuring that the solution satisfies the Shapley properties.
Calculating SHAP values for tree-based classifiers, as described above, becomes computationally infeasible. However, when applied specifically to tree-based models like RF, SHAP values can be computed much more efficiently. This is because tree models have a structure that can be exploited to avoid directly computing contributions for every possible feature subset. Instead of brute-force summation over all feature subsets, Tree SHAP

exploits the structure of decision trees to compute exact SHAP values [94]. Tree SHAP of the feature i will therefore be calculated based on Equation 3.10:

$$\phi_i(f,x) = \sum_{S \subseteq N \setminus \{i\}} \frac{|S|!(|N|-|S|-1)!}{|N|!} [f_x(S \cup \{i\}) - f_x(S)] \tag{3.10}$$

where S is a subset of features that does not include i, and N is the set of all features. This equation calculates weighted marginal contribution of feature i across all possible feature subsets S.

Consequently, permutation feature importance provides a global importance measure indicating how crucial a feature is across the entire dataset, whereas Gini importance shows a global importance score summarizing how often and effectively a feature splits a data across all trees. However, SHAP values offer both local explanations for individual predictions and global importance by aggregating these local explanations.

3.8 Sensitivity Analysis

Information that is fed into spatial models may contain various forms of uncertainty, such as measurement errors, insufficient data resolution, absence of information or presence of out-of-date information. Additionally, models may incorporate conceptual uncertainties, which include uncertainties in the structure, assumptions, and specifications of the model. Therefore, mathematical modeling of natural and man-made systems must be accompanied by a sensitivity analysis (SA) [122], in order to increase the confidence in model itself and its predictions [32][88]. Uncertainty analysis help to associate model behavior based on the quality of the fed input data and generally tries to answer the question "how uncertain is the inference". SA tries to find an answer to the question "where the uncertainty is coming from" and thus explains variations in the output due to the variations in the input data [122]. Both tasks, although they follow different objectives, are usually combined in practice and are called SA.

SA estimates can be generally categorized into two groups: global and local estimates. Global SA involves varying all inputs at the same time and performs multi-dimensional averaging to evaluate the interactions between these inputs. It is based on the premise that all the included variables are uncertain, and thus it is not adequate to investigate this system through what-if simulations, altering only one variable at a time [123]. Global SA is conducted through six methodical steps

- Define objective function of the study
- Identify input variables of interest
- Assign both range and a statistical distribution to these selected inputs

- Choose and implement a sampling strategy to produce an N-sized sample from the input distributions
- For each sampled set of input values, compute the model to derive N outcomes for the objective function

Utilize the findings from step 5 for uncertainty analysis and conduct a sensitivity estimation technique to ascertain the relative significance of the input variables [88]. The Monte Carlo technique is the most common global SA technique. It relies on conducting numerous assessments of the model using randomly selected input variables. This process, however, can be computationally very expensive, especially if a large number of input variables is considered [32].
Another approach to global SA estimation includes variance based estimations. They perform sensitivity index generation for a given variable based on the model output's variance attributable to this factor [32]. Variance-based approaches can determine sensitivity indices independently of common model assumptions such as linearity or monotonicity [88]. These methods model prediction's variance V by breaking it down into partial variances. These partial variances, then, quantify the portion of V, which can be attributed to the model inputs, whether they are considered individually or in combination, like in Equation 3.11.

$$V = \sum_{i} V_i + \sum_{i<j} V_{ij} + \sum_{i<j<m} V_{ijm} + \ldots + V_{12\ldots k} \tag{3.11}$$

where V_i denotes the fraction of the output variance accounted for by the i^{th} model input and the fraction of the output variance accounted for by the Y to X_i. V_{ij} represents the fraction of the output variance due to the combined influence of the i^{th} and j^{th} inputs, indicating the sensitivity of Y to the interaction among X_i and X_j. While the symbol k corresponds to the total count of model inputs. Therefore, the first-order sensitivity indices of variables can be written using Equation 3.12.

$$S_i = \frac{\mathrm{Var}\left(\mathbb{E}\left[Y|X_i\right]\right)}{\mathrm{Var}(Y)} \tag{3.12}$$

where $\mathrm{Var}(Y)$ is the total variance of the output and $\mathbb{E}\left[Y|X_i\right]$ denotes the expected value of Y given X_i. Methods for estimating S_i include the Fourier Amplitude Sensitivity Test introduced by Cukier et al. [34] in 1973, and Sobol' method, developed by Sobol' [131] in 1990.
On the other hand, local SA focuses on quantifying how small changes in the models inputs affect the models output. The word 'local' signifies that derivatives are computed at a specific point, often referred to as the 'baseline' or 'nominal value' point, within the multidimensional space of input variables [122]. The local, one-at-a-time (OAT) type of SA is probably the most commonly used local SA method [49], even if it s heavily criti-

cized by various authors. According to Saltelli and Annoni [122], OAT fails to recognize interactions between factors since such detection requires the variation of multiple factors at a time. When factors are altered sequentially in the OAT approach, their interaction remains inactive and thus cannot be detected. This means, it is nearly impossible to discern if the combined effect of changing both X_1 and X_2 simultaneously differs from their individual effects observed by first adjusting X_1, returning to the starting point, and then altering X_2. Furthermore, the choice of OAT SA stands strong, only if the model under analysis is proved to be linear [124].
Although the OAT technique is criticized, there is a clear understanding why it still remains one the most frequently used SA approaches. For natural scientists, a critical concern involves the concept of a "baseline" - a reference point within the input factor space where all input factors are set to their optimal estimates, which is known as the "nominal value". There is a noticeable reluctance to deviate from this baseline, as statistical sampling methods would commonly suggest, due to its perception as a reliable anchor. Shifting from this baseline can lead to the model moving into unknown territory, metaphorically described as "terra incognita" which, in practical terms, means becoming unreliable or potentially failing when moved away from this established reference point. Adjusting one factor at a time, as practiced in the OAT method, means that any observed impact on the output, whether it's an effect or the absence of one, can confidently be linked to that specific factor [49].

Chapter 4

Study Area and Data

In this chapter, we will be presenting our study areas as well as utilized datasets.

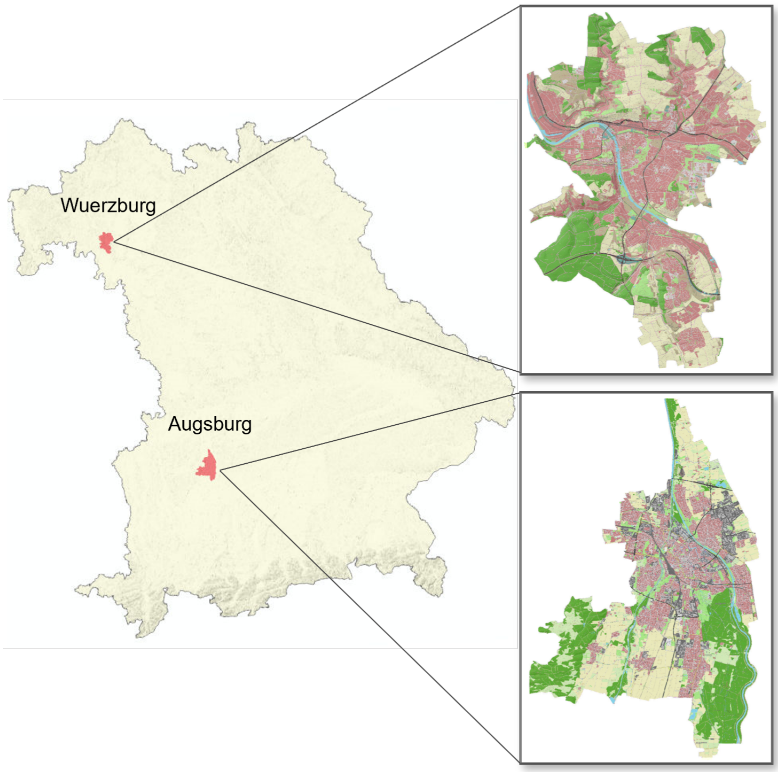

Figure 4.1: A map illustrating both study areas in Bavaria, Germany at a greater detail.

In this thesis, we aim towards knowledge-based mapping of various UGS types by establishing reproducible workflows. Therefore, we select two study areas: one to develop methodology on, and the second one to test reproducibility of the proposed methodology. In defining our study areas, we focus on Bavaria, Germany. To account for possible differences as well as to make sure that both areas do contain some similarities, we choose

the cities of Augsburg and Wuerzburg. Figure 4.1 illustrates their location in Bavaria, Germany as well as provides an overview of both at a greater detail.
Since we are interested in identifying UGSs, we refer to the "greenest city" ranking developed by Taubenböck et al. [135], to see how the selected cities perform. Their findings reveal, that all cities in Germany with at least 100.000 inhabitants, provide more than 50 m^2 of green space per capita, which is the advised minimum amount by the World Health Organization. This finding also apply to the selected study areas. However, in a more detailed ranking, Wuerzburg is noted for providing more green space per capita, securing the 30th position. In contrast, Augsburg offers less green space per capita and ranks 50th in this assessment. In the following, we provide a more detailed overview of historical importance, geographical conditions as well as green space composition of both study areas.

4.1 Augsburg

Located at the northern foothills of the Alps, the city's geological, morphological, and climatic conditions have been greatly influenced by this major mountain range. Situated in a valley once occupied by the Lech glacier, the city's landscape is characterized by sediment deposits from glacial times, which have been further shaped by the Lech and Wertach rivers. Dominated by lighter brown soils, fertile loams, and reddish-brown rendzina soils, the area's topography is defined to the west by a mountainous and valley-rich landscape, while to the east it features rolling hills that have been gradually eroded by the waterways [80].
With a population of nearly 300,000 inhabitants, it is the third major city in Bavaria. However, it is most prominent for its historical value, from holding the Roman cultural heritage to impressive water supply infrastructure in the 13th century. The network of water infrastructure in Augsburg evolved into a cohesive urban water management system starting in the 13th century. In the 14th century, towns across central Europe began developing intricate mechanisms designed to utilize the readily available river water. By the early 15th century, places like Augsburg had installed waterwheels beneath their bridges to power piston pumps. These pumps elevated river water to high-rise storage tanks. Augsburg's Rotes Tor (Red Gate), constructed in 1416, stands as one of the oldest water systems in central Europe. It featured reciprocating pumps powered by three waterwheels, which transferred water to various reservoirs and supplied public fountains. In the 19th century, as industrialization progressed and cholera outbreaks occurred, the city transitioned from using surface water channels from the Stadtwald (city forest) to extracting water from deep wells. This shift led to the decommissioning of old water towers and the construction of the Neubach waterworks in 1879 [42].
Spanning a total area of 146 km^2, Augsburg accommodates two major forests in the south-

east and southwest of the city, which are called the city forest (Stadtwald) and western forest (Westliche Wälder), respectively. Further woody vegetation is located alongside the rivers Wertach and Lech and covers approximately 36 km^2 of the area of Augsburg. Nearly 9% of the total area is dedicated to recreational spaces such as parks, gardens, and sports fields. Agricultural areas, located to the northeast and south of the city, cover around 38 km^2 and further contribute to the city's green belt. From a biogeographical standpoint, the limestone dry grasslands spanning parallel to the river Lech are exceptionally valuable. They serve as crucial links within the Lech valley "corridor," a pathway of international ecological significance that connects the limestone habitats of the dry grasslands and forests of the Alps in the south with the Swabian Jura Mountains to the north. These environments are vital for the sustainability of 80 different species [80].
The most common vegetation species in Augsburg are dominated by grass and herb species with very high regeneration capacity, such as Common Yarrow, Ground Elder, Mugwort, and others. A survey conducted in 2004 found that the most common deciduous species are the Silver Birch, Common Ash, Small-leaved Lime, London Plane, Sycamore Maple, Field Maple, Hornbeam, Horse Chestnut, Black Locust, and European Beech. In terms of the conifers, 24 species were identified, with the most prevalent being the Norway Spruce, followed by the European Yew, Black Pine, Serbian Spruce, and Scots Pine [80].
Augsburg's average elevation is recorded at 489 meters above sea level. The local climate is a blend of moderate Atlantic and continental influences, resulting in an average yearly temperature of 8.1 degrees Celsius and an annual rainfall of 831 millimeters [80].

4.2 Wuerzburg

The city of Wuerzburg encompasses around 88 km^2 and is situated along the Main River in Lower Franconia. Franconia is located in the northern part of Bavaria, Germany. The town's center lies on the eastern (right) bank of the river. Its hillside location, climatic conditions, and other local factors have established Wuerzburg as a distinguished wine-producing region.
Wuerzburg's climate is significantly influenced by its topographical features. The average annual temperatures are at around 10 degrees Celsius, and the average annual precipitation is nearly 757 millimeters. The pronounced basin-like topography enhances the risk of temperature inversions, which predominantly occur during the winter months in the area. According to the 2004 Air Quality Plan data, temperature inversions up to 1000 meters above sea level occur on 70% to 80% of days annually. These inversions typically disperse by mid-morning during the summer months, but in winter, approximately 70% of all inversions persist until noon. Of the inversions observed during the autumn and winter months, about 20% to 30% of those detected at night are still present at noon the

following day[1].
On a limestone plateau stands the Nikolausberg, which accommodates Wuerzburg's highest point at 360 meters above sea level. The city's lowest points, at 166 meters, are located at Alte Kranen and Neuer Hafen.
The most prominent features of open space in the city include the river Main, the Ringpark, the botanical garden, and the surrounding vineyards. The Ringpark is a large green space that encircles the city center. Other UGSs, including gardening areas, parks, sport, and leisure facilities, make up almost 8% of the total area. To the southwest, large forest areas contribute to the "greenness" of the city and cover nearly 16% of the area. Agricultural areas that lie outside the built-up city center constitute 27% of the total area of Wuerzburg. Furthermore, Wuerzburg accommodates approximately 2.5 km^2 of vineyards.
The soil type in the area is predominantly dark gray-brown soil with a mulch humus layer. This soil generally has a good supply of nutrients that are available to plants. However, there are areas with poor root penetration due to densely packed clay layers. Additionally, this soil type has low to moderate water storage capacity within the main root zone, which impacts agricultural practices and plant growth [2]. Although soil types slightly differ, the vegetation composition of Wuerzburg is quite similar to that of Augsburg. The forests in Wuerzburg are comprised of species like spruce, pine, ash, birch, beech, and oaks[3]. However, more exotic tree species can also be found in, e.g., the Ringpark. As such, giant sequoia, Japanese pagoda tree, sugar maple, Amur cork tree are among others[4].

4.3 Data

Mapping UGSs poses a significant challenge due to their potential representation through a combination of various LU elements and LC types. Selection of datasets for UGS mapping, therefore, necessitates careful consideration. We take into account three key aspects when choosing appropriate datasets: (a) whether the resolution of the dataset permits the identification of even the smallest UGS elements, (b) whether the datasets have sufficient temporal resolution, and (c) whether the dataset is freely accessible and allows for the unrestricted sharing of results. Therefore, in the following we describe raster datasets utilized to map UGSs, as well as vector datasets used to refine the results, and to produce validation datasets.

[1]https://www.wuerzburg.de/media/www.wuerzburg.de/org/med_509759/574508_bericht_klimaplanatlas_wuerzburg_final.pdf (accessed on 01.2025)
[2]https://www.lwf.bayern.de/boden-klima/umweltmonitoring/104336/index.php (accessed on 01.2025)
[3]https://www.bmel.de/DE/themen/wald/wald-in-deutschland/waldzustandserhebung.html (accessed on 01.2025)
[4]https://www.wuerzburg.de/media/www.wuerzburg.de/org/med_512918/553300_baumsteckbriefe.pdf (accessed on 01.2025)

4.3.1 Earth Observation Imagery

To analyze vegetation cover, observe phenological shifts, and explore their relationships with specific types of green spaces, we utilize remotely sensed imagery. We differentiate between two types of images: those that enable us to monitor changes over time, albeit with a lower spatial resolution, and those that offer higher spatial resolution but lack a temporal dimension. Since we perform the analysis in two study areas, we ensure to utilize the same type of datasets. However, data acquisition dates differ due to environmental conditions present in each study area. For example, as discussed earlier, Wuerzburg is significantly impacted by temperature inversions, which obstruct the visibility of distant satellites. Consequently, it is extremely challenging to find cloud-free datasets in this area. Moreover, aerial image capture missions are typically conducted on a sectional basis, meaning that different parts of the region are photographed at various times. As a result, it is impossible to obtain digital orthophotos or digital surface models of both cities on overlapping dates.

4.3.2 Multi-Spectral Sentinel-2 Data

To map overall green and comprehensively analyze phenological changes in UGSs, we utilize a sequence of Sentinel-2 multi-spectral images, sourced from both the Sentinel-2A and Sentinel-2B satellites. These images, classified as Level-2A products as presented in Table 4.1, are selectively acquired over the course of 2022, aiming for a monthly frequency. In order to achieve the most accurate depiction of green spaces, a selection criterion is applied, limiting the selection to images with less than 10% cloud cover. Consequently, data from January, September, and November are excluded due to prevalent cloudiness or snow coverage.

We achieve the uniformity in the dataset through the consistent capture of images on relative orbit 65, a parameter that ensures stable viewing angles and consistent illumination conditions. Additionally, all images correspond to the geographic tile T32UPU. To further enhance the data's applicability and coherence, each image is undergone precise adjustments to its extents, ensuring alignment with the boundaries of the study area. Subsequently, the images are reprojected into the ETRS89 / UTM zone 32N coordinate system. This way we ensure uniformity and comparability across all datasets.

We further produce temporal normalized difference vegetation index (NDVI) using the acquired datasets. To do so, we follow the Equation 3.4 presented in Chapter 3.

The Sentinel-2 images obtained for Wuerzburg are listed in Table 4.2. Similar to our approach in Augsburg, we aim to acquire images with less than 10% cloud coverage to ensure a clearer representation of vegetation. However, due to Wuerzburg's unique topographical and climatic conditions, cloud cover is more prevalent here than in Augsburg. To maximize the number of cloud-free images, we utilize imagery from both Sentinel-

Table 4.1: Temporal Sentinel-2 datasets acquired for Augsburg.

Date	Level	Relative Orbit	Tile Number
10.02.22	2A	R065	T32UPU
27.03.22	2A	R065	T32UPU
21.04.22	2A	R065	T32UPU
11.05.22	2A	R065	T32UPU
15.06.22	2A	R065	T32UPU
25.07.22	2A	R065	T32UPU
14.08.22	2A	R065	T32UPU
18.10.22	2A	R065	T32UPU
17.12.22	2A	R065	T32UPU

2A and Sentinel-2B sensors. Although they orbit on different relative paths, both sensors provide bottom-of-atmosphere corrected images, ensuring compatibility between datasets. Nonetheless, images from January, August, October, and November are excluded from our analysis due to very high cloud coverage. Moreover, acquired images are undergone to their extent adjustment and reprojection to the ETRS89 / UTM zone 32N coordinate system.
Sentinel-2 data is a multi-spectral data. This means that it captures reflectance values at various parts of the electromagnetic spectrum. However, not all the bands are captured at the same spatial resolution. As such, Band 2 (Blue), Band 3 (Green), Band 4 (Red), and Band 8 (NIR) are provided at 10 meters resolution, which is the highest available. Band 5, Band 6, and Band 7, all of which are Vegetation Red Edge bands, as well as Band 8a (Narrow NIR) and Bands 11 and 12 (both SWIR) are available at 20 meters resolution. Finally, Band 1 (Coastal Aerosol), Band 9 (Water Vapor), and Band 10 (SWIR - Cirrus) have the lowest resolution of 60 meters.

4.3.3 Aerial Imagery

To extract finer information than Sentinel-2 allows, we utilize digital orthohotos (DOP) acquired from the Bavarian State Office for Digitization, Broadband and Surveying webpage[5]. The bigger portion of the aerial imagery of Augsburg is captured on the 18th of June 2022, while a smaller portion of the area of the city in the South is captured on the 14th of June 2022. DOP of Wuerzburg is acquired on the 28th of May 2023. Both images

[5] `https://geodaten.bayern.de/opengeodata/` (accessed on 01.2025)

Table 4.2: Temporal Sentinel-2 datasets acquired for Wuerzburg.

Date	Level	Relative Orbit	Tile Number
28.02.21	L2A	R108	T32UNA
07.03.21	L2A	R065	T32UNA
26.04.21	L2A	R065	T32UNA
31.05.21	L2B	R065	T32UNA
13.06.21	L2B	R108	T32UNA
18.07.21	L2A	R108	T32UNA
03.09.21	L2A	R065	T32UNA
20.12.21	L2B	R108	T32UNA

are orthorectified and are outcome of the Bavarian biennial aerial surveys. They are freely available as a three band RGB - imagery with ground pixel size of 20 centimeters. We pre-process them by setting the right coordinate reference system as well as adjusting the correct extent.
The spectral resolution of the aerial imagery is limited to only three bands. Therefore, to enhance the information gain, we calculate indices from these three bands. As mentioned in the Chapter 3, the GLI, RGBVI, and NGRDI are the most used RGB-based indices and are capable to provide additional insights into the vegetation cover. Consequently, we calculate the GLI, RGBVI, and NGRDI using Equations 3.5, 3.6, and 3.7 respectively.

4.3.4 Digital Terrain and Surface Models

In order to understand and utilize height dimension of green spaces in our analysis we make use of two main datasets: digital terrain model (DTM) and digital surface model (DSM). DTM represents the Earth's surface without vegetation and man-made structures with the help of point clouds of known location and elevation. The data for Bavaria's DTM is collected using Airborne Laser Scanning since 1996 and is updated as needed through new aerial surveys. It comes as a raster dataset at different spatial resolutions. The highest and freely available resolution is one meter. This dataset is freely available to download, and is distributed under the CC BY 4.0 license.
The DSM depicts the Earth's surface, including all objects on it such as vegetation and buildings, in a grid format. The current grid size is 40 centimeters, which corresponds to 6.25 points per square meter. The basis for calculating the DSM are the aerial images from the Bavaria aerial survey, which have a ground pixel size of 20 centimeters. It is generated through dense correlation of the stereo images. Each grid point (XYZ) in the

DSM calculation is assigned a color value directly derived from the oriented aerial images. Quality of the DSM is assured through determining the height accuracy at selected areas and points. DSM with 40 centimeters resolution is not a freely available dataset yet, and all rights belong to the Bavarian State Office for Digitization, Broadband and Surveying.

Table 4.3: Overview of the datasets derived from row Sentinel-2 and DOP images.

Augsburg	Wuerzburg
NDVI - 10.02.22	NDVI - 28.02.21
NDVI - 27.03.22	NDVI - 07.03.21
NDVI - 21.04.22	NDVI - 26.04.21
NDVI - 11.05.22	NDVI - 31.05.21
NDVI - 15.06.22	NDVI - 13.06.21
NDVI - 25.07.22	NDVI - 18.07.21
NDVI - 14.08.22	NDVI - 03.09.21
NDVI - 18.10.22	NDVI - 20.12.21
NDVI - 17.12.22	-
GLI - 18.06.2023	GLI - 28.06.23
RGBVI -18.06.2023	RGBVI - 28.06.23
NGRDI -18.06.2023	NGRDI - 28.06.23
nDSM	nDSM

We utilize the DTM and the DSM datasets in order to calculate height of objects above earth surface. Commonly, the above ground height of objects can be represented with the normalized digital surface model (nDSM). nDSM is a derivative elevation product, which we obtain by subtracting DTM from DSM, using Equation 4.1.

$$nDSM = DSM - DTM \tag{4.1}$$

Consequently we not only utilize raw RS images, but also produce derivative products based on these images. An overview of these derivative datasets is given in Table 4.3. Here, once again acquisition date differences are highlighted, although they cover at least one date in every season.

4.3.5 Auxiliary and Validation Data

In Bavaria, detailed LU information can be found in the Actual Land Use data (Tatsächliche Nutzung (TN)). It is the distributed under CC BY 4.0 license and can be accessed and downloaded free of charge. TN dataset is organized in two levels: LU and detailed designation of these LUs. In other words, it consists of LU classes and sub-classes. Under the umbrella of four main LU types, i.e. settlement, traffic, vegetation, and water, this level is further subdivided into nearly 140 LU classes. These include residential, road traffic, agriculture, flowing waters and others. The second level provides more detailed information as what exact sub-types the LUs contain. For example, the sport and leisure facility LU class is further subdivided into botanical garden, parks, allotments and other sub-classes. Consequently, there are nearly 50 sub-classes for the main LU types.

Table 4.4: "Tatsächliche Nutzung"(TN) classes containing UGS types.

Land Use Class	Sub-class
Agriculture	Arable Land, Tree Nursery Grassland, Pasture, Orchard
Sports, Leisure and Recreation Area	Botanical Garden, Zoo Recreational Area, Leisure Facility Garden, Allotment Garden Green Space, Park, Playground Safari and Wildlife Park
Forest	-
Cemetery	-
Heath	-

Usage areas in the TN dataset must be formed up to a maximum size of 5 hectares and a maximum length of 1 kilometer. The boundaries of classes are established according to the actual conditions on site and do not consider cadastral division boundaries. Additionally, municipal boundaries are always considered as boundaries between different types of LU. The TN dataset is regularly updated using a combination of aerial imagery, data from agricultural and forestry administrations, and on-site surveys conducted during cadastral surveys. As a result, the dataset is typically no more than three years old, with urban areas being updated even more frequently. The TN dataset is provided at a scale of 1:1000. However, it only includes information on state-owned LUs, meaning areas such as privately owned forest land are generally not represented.

The TN dataset uses a more streamlined classification scheme, which, for example, does not include a separate category for UGSs. Table 4.4 presents LU classes and their sub-classes from the TN dataset that are associated with or are representative of UGSs. The largest mixed class, encompassing 10 different UGS types, is the "Sport, Leisure, and Recreation" category. This is followed by the "Agriculture" category, which includes four UGS types. Moreover, the TN dataset also contains distinct classes for forest, cemetery,

moor, and heath, all of which largely represent UGSs as well.
TN also provides definitions for LU classes and sub-classes. We examine especially the sub-classes that appear under the sport and leisure facility class. As such, green space designation refers to a facility with trees, shrubs, lawns, flower beds, and paths that primarily serves for recreation and the beautification of the cityscape. Park is defined as a landscaped green space that serves for representation and recreation. Allotment is considered to be a facility consisting of garden plots that are managed and leased by associations. Whereas, garden designation refers to an area used for growing vegetables and fruits that is not associated with 'residential building area' and does not include allotment gardens. Furthermore, this class includes uses that also store green space such as botanical garden and zoo, recreational and leisure areas, playground, safari and wildlife park.
In this study, the TN dataset serves not only as a reference dataset but also as a validation dataset. Validation is a standard procedure used to assess the accuracy of utilized methods. This process involves comparing identified features against a known dataset that contains these features. Therefore, t is essential for the entire UGS mapping procedure. In Chapter 2, we acknowledge the absence of accurate UGS maps for the study areas, which would typically serve as a basis for validation. Therefore, we create a validation dataset that includes selected classes from the Table 4.4, and is comprised of:

- Forest: forestry operation area
- Sports, recreational, and leisure areas: botanical garden, zoo, green space, grassland, allotment garden, park
- Agriculture: arable land, tree nursery, orchard, vineyard
- Industrial and commercial areas
- Mixed-use areas
- Cemetery
- Heath

This list of LU classes only slightly differs per study area. For instance, vineyards appear only in Wuerzburg while Zoo appears only in Augsburg's validation dataset.
The forest validation dataset contains all polygons from the forest class in the TN dataset, while the allotment validation dataset includes polygons from the allotment garden subclass within the sport, leisure, and recreational area class. Similarly, the validation dataset for urban agriculture consists of polygons representing all sub-classes within the agriculture class.
Unfortunately, none of the existing TN classes or sub-classes adequately represent urban green corridors. Therefore, it is impossible to create a validation dataset using the TN dataset. To validate green corridors we will be utilizing UGS datasets that we will create using RF classification procedure.

Chapter 5

Urban Green Space Ontology

In the previous chapters we describe limitations of the existing UGS classifications and how they fail to capture the full spectrum of UGS types. Therefore, in this chapter we propose a new UGS ontology and describe a procedure to create and formally conceptualize this ontology.

5.1 Definition of Ontological Classes

Frequently when performing studies on UGSs we are interested in two aspects; what types of UGSs exist and how can they semantically be described. The first aspect requires establishing all possible UGS classes in a classification or in a typology. The second aspect is more descriptive and allows gaining knowledge on UGSs on top of typology or classification. This could include, for instance, exploring a particular tree composition, defining characteristic urban furniture, establishing presence/absence of walking paths or calculating proportion of vegetated areas to sealed parts. This is particularly relevant if we want to better understand and plan green spaces for human well-being.

Organization of UGS types in a classification or typology has already been done before. For example, allotment is a type of UGS and can be placed at various levels in a typology depending for what propose this typology will be used. However, allotment is a product of combined natural and anthropogenic factors. As such, allotments contain biotic land cover (e.g. woody and herbaceous vegetation), abiotic cover (e.g. sheds, paths, pool) and with it associated land use (e.g. horticultural/ornamental crop production, leisure activity place). Therefore, we see a need for a conceptual basis in UGS mapping procedure. Consequently, we avoid providing yet another typology that is limited in scope of its application and provide a semantic translation of UGS types on top of UGS classification.

The semantics of 'things' (e.g. UGSs) and related expert knowledge can be represented in an ontology which we describe in detail in Chapter 2. As extensively presented by Arvor et al. [8], use of ontologies for RS datasets can tremendously improve the understanding of concepts as well as enhance mapping procedures. Given, no UGS ontology exists, in this chapter we propose an extensive UGS ontology.

We define two key factors that we should take into consideration when creating a UGS ontology. Firstly, we need to know a complete list of UGS types that can exist, if not globally, then at least in certain regions. Secondly, the created ontology should conform to basic ontological rules. Therefore, in the following, we first describe how we collect and assess a full list of UGS types. We then explore main requirements for complete ontologies and assess whether our ontology fits these requirements. Finally, we present our ontology implementation and formalization using the Web Ontology Language (OWL) in the Protégé software.

Well-designed formal ontologies provide a common vocabulary that is necessary for communication between computer applications as well as between computer applications and users [58]. Therefore, our aim is to state what exists in terms of UGSs and provide a common vocabulary for further research and analysis around UGSs. Consequently, to achieve a comprehensive list of UGS types, we examine existing published literature on UGS typologies. One drawback of such typologies is that their field of application is usually limited to certain topics. In this regard, we explore one of the most known UGS typologies by Bell et al. [15], Jones et al. [74], and Degerickx et al. [37]. Class and subclass distribution of all three typologies is shown in Figure 5.1 and is color coded with yellow lines representing the typology by Jones et al. [74], pink dashed lines representing the typology by Bell et al. [15], and purple dotted lines representing the typology by Degerickx et al. [37].

Bell et al. [15]'s typology is broad and its main application field evolves around hedonic house price estimation. Therefore, it includes all the possible green space types that could somehow improve livelihood of areas and thus affect house pricing. In this classification, the authors delineate 9 UGS classes that are further subdivided into 35 sub-classes. Typology of Jones et al. [74] focuses on GI rather than purely on UGS types. GI is a planned network of green spaces. Therefore, by exploring GI types we enrich our ontology with UGS classes that have already been tested to be suitable within urban planning. The authors divide GI into nine classes which are further subdivided into 45 sub-classes. The third typology by Degerickx et al. [37] explores yet another aspect of UGSs, namely vegetation composition. The authors define three vegetation classes, namely trees, shrubs, and herbaceous plants. They further categorize 23 UGS types under the umbrella of these three classes.

We proceed in the creation of a comprehensive UGS type list by examining every single class composition in all three typologies. For example, Bell et al. [15] classify allotments, community gardens, city farms, and urban agriculture. Whereas, Jones et al. [74] under garden class considers only balcony, private and shared common gardens. Allotments are

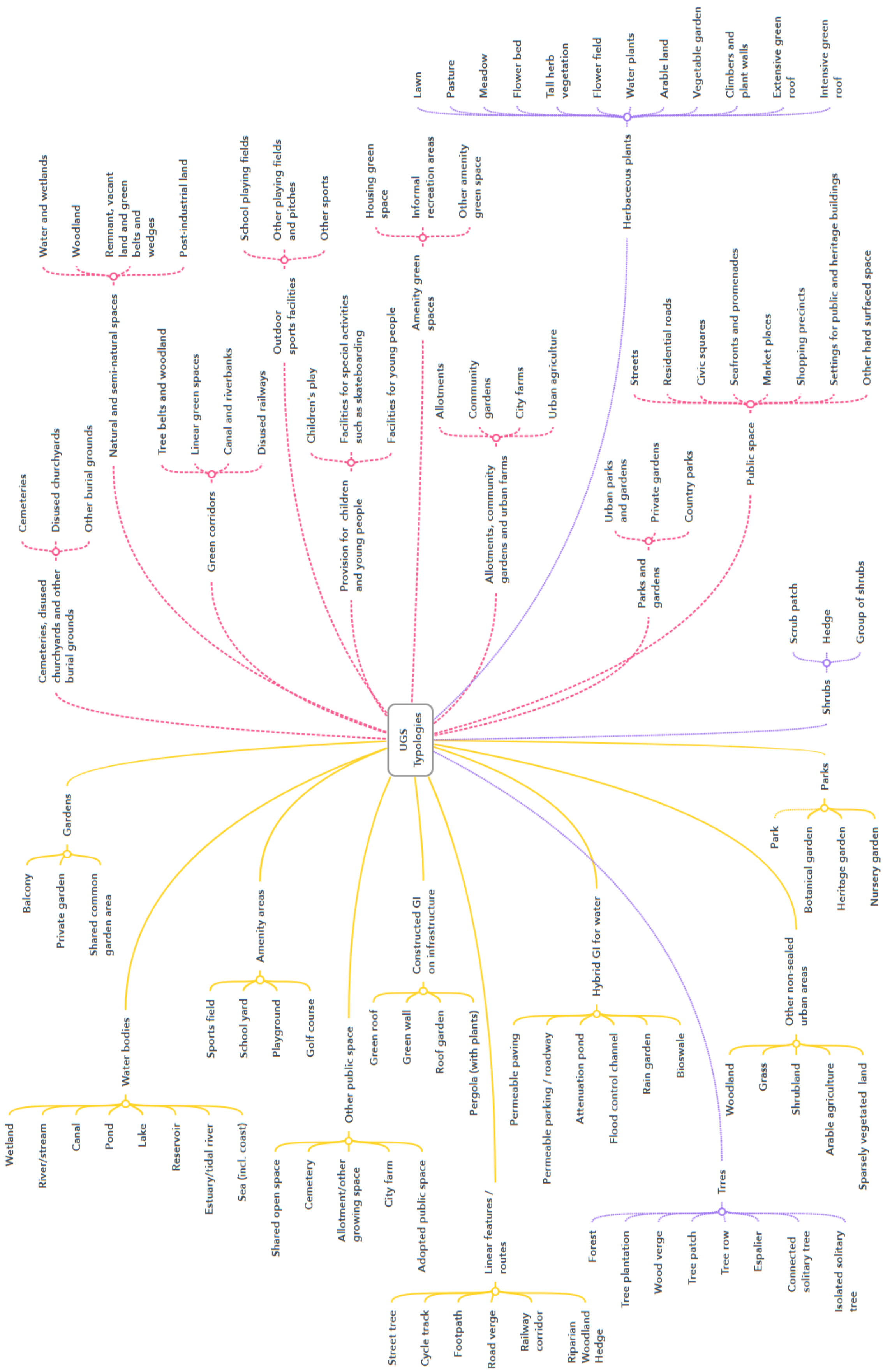

Figure 5.1: Mind map of UGS typologies based on works by Bell et al. [15] (pink dashed), Jones et al. [74] (yellow), and Degerickx et al. [37] (purple dotted).

classified as other public spaces while crop lands as other non-sealed urban areas. From over 100 UGS types (including duplicates), we extract class names that appear in all and then enrich our list by including the ones that appear in one and not all typologies. Furthermore, we perform a re-categorization of the selected classes and establish which types of UGSs belong together or can be included under the same class. Through this process we harmonize sub-classes that semantically belong together but are organized differently in various typologies. Here, we do not try to correct any possible conceptual mistakes in the existing UGS typologies, but rather have them addressed in the structure of the proposed ontology.
Following the described procedure we end up with seven UGS classes. These classes include forest, park, grassland, cemetery, urban agriculture, green corridor, and amenity. Sub-classes of the selected UGSs are organized as follows. Forest, grassland, and cemetery are non-complex classes with no further subdivisions. We subdivide amenities into institutional green, neighborhood green, playground, and sport fields. Green corridors, in our harmonization, are made of water body corridor (both river and standing water), railroad corridor, road corridor, pathway corridor, and ecological corridor. The largest subdivision is happening in terms of urban agriculture. Here, we distinguish between herb garden, rooftop garden, front yard garden, backyard garden, community garden, allotment, nurseries, orchards, arable land, city farm, and permanent crops. Finally, the park class is comprised of city park, botanical garden, zoological garden, pocket park, dog park and skate park. This synthesized list of UGS classes will be building stone of a UGS ontology in the following section.

5.2 Construction of a Urban Green Space Ontology

To build a UGS ontology, we follow steps proposed by Guarino [59], and start by domain specification, where we define scope and purpose of our ontology. The proposed ontology is placed within the domain of UGSs and the primary aim of this ontology is to facilitate mapping and classification of various types of UGSs. The scope of the proposed ontology is geographically focused on southern German cities. This means that the ontology is tailored to address specific characteristics, or types of UGSs that are relevant or unique in the given geographic location.
The second requirement of the ontology development is that it should include core concepts of a domain. Yet, ontologies should be extendable [58]. When selecting UGS classes and sub-classes we try to stay as neutral as possible and be as inclusive as possible. However, the overarching purpose of the created ontology as well as UGS mapping in this dissertation is human well-being. Thus, we do use a "human well-being filter" when viewing the selected classes in the ontology. Consequently, by using established seven UGS classes and 28 sub-classes, we provide a foundational model that can be extended

into a more specific or task-oriented ontology if needed.
Ontologies express what is there. This also includes relationships in between. Therefore, we define hierarchies and connections between our ontological classes. There are several approaches for this, that are usually domain dependent. We choose to perform a top-down approach to organize the entities into hierarchies.
During the organization of the hierarchical structure, entities must be connected with objects. Depending on which entities we connect and for what purpose, varying properties can be established. For instance, if we say forest consist of woody vegetation and want to connect these two together, then e.g. "hasCharacteristics" could be used. However, for the first part of the ontology creation we choose to use the "is-a" property, denoting that one entity has an object (or class has a sub-class). Figure 5.2 illustrates intermediary results of the first two ontology creation steps, where UGS is defined as and OWL thing, and "is-a" property is used to connect it with the selected UGS classes.

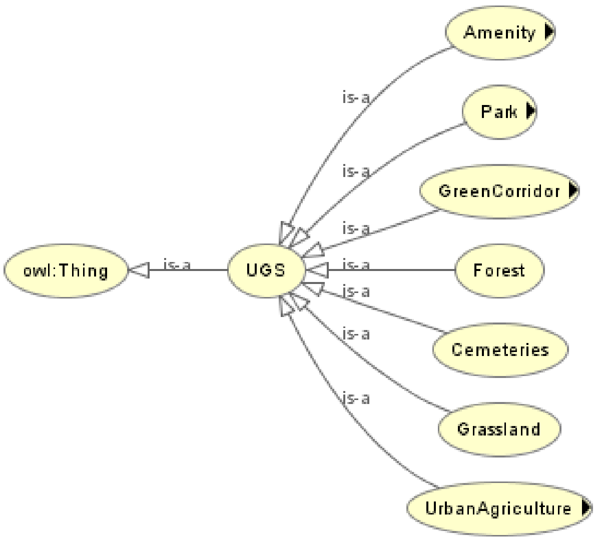

Figure 5.2: Figure of hierarchical organization of the selected UGS classes using "is-a" connector property.

We further add our selected sub-classes into the ontology as another hierarchical level. Visually, this step is presented in Figure 5.3. As it can be seen here, cemetery, grassland, and forest remain as a single level class, while the other classes are extended with their corresponding sub-classes. All the sub-classes are connected with classes using the same "is-a" object connector.
At the beginning of this chapter, we state that we are not only interested in providing yet another UGS typology but are also interested in semantic translation of the selected UGS types. Given semantic translation helps to uniquely describe green spaces, this can also facilitate RS image analysis using ontology as a classification tool. Consequently, we integrate these concepts by enhancing our ontology with precise object property specifications. Such specifications are essential for describing hierarchical relationships within the

Figure 5.3: Figure of hierarchical organization of all UGS classes in Web Ontology Language.

ontology. We illustrate this detailed decomposition of the ontology's hierarchical structure through object properties in Figure 5.4. Although shown here separately, these descriptive entities are part of the UGS ontology.

Figure 5.4: Illustration of detailed object properties that are incorporated into the UGS ontology.

The idea behind object property enrichment is that we can use property instances to characterize a single UGS type, and later use the content of the matching instances to identify UGSs. We enrich the ontology with four principal object properties: geometry, texture, position, and thematic aspects. These properties are then augmented with specific characteristics to provide a detailed description. Geometry includes attributes such as height and shape, with further subdivisions of the shape into circularity and rectangularity. Furthermore, texture property describes texture metrics. In our example, we encompass Haralick [65]'s (GLCM) texture metrics. Here, we specifically include dissimilarity and homogeneity metrics from this matrix. Position property, defined broadly as proximity, indicates the relative closeness of various features.
A detailed distinction of object properties is done within the thematic property class. Here, we start by differentiating between anthropogenic and natural properties. We then define paths, paved areas, recreational facilities and urban furniture as elements of the anthropogenic properties. Further refinement is done to paved areas by distinguishing terraces. Recreational areas are enriched with pool and umbrellas, whereas urban furniture contains fences and sheds. Natural object properties are comprised of vegetation,

water body, and soil types. Here, we follow the same logic to refine the object properties. As such, vegetation property contains elements such as tree cover, NDVI, and GLI.
In our ontology, we structure relationships among object property classes using the "is-a" relationship, which defines each class as a subtype of a more general class, ultimately linking back to the root class, "Thing". This hierarchy allows a clear and logical classification system. The object property hierarchy follows the same ontological rules, as it should be extendable. This means, that here we only capture object properties that we will further be using for green space mapping. However, the ontology can be extended with further features, to accommodate other use cases. For example, here we include only GLCM texture metrics. If needed, another texture metrics class such as Fourier transform can be used and added to the ontology. Similarly, we only utilize circularity and rectangularity shape measures. But if needed, one could extent the ontology with e.g. aspect ratio, compactness or convexity. During object property creation we follow the same rule as for the ontology. This means, that we select only four properties and some sub-properties, that are also used throughout the dissertation. However, these properties can further be extended in order to better fit other use cases.
Beyond this "is-a" hierarchical structure, we introduce specific relationships that connect our defined classes to various UGS types through specialized object properties. These relationships are crucial for detailing the characteristics of each UGS type and are defined by properties such as "hasFeature", "hasGeometry", "hasProximity", and "hasTexture". The "hasFeature" property allows us to link UGS types such as allotments, to specific features they contain. These could include sheds, paths, and other thematic elements, thus contextualizing allotments within the ontology. "hasGeometry" is used to associate physical shapes with UGS types. This is relevant, for instance, when describing crop fields as rectangular with a specific rectangularity value. Finally, "hasProximity" details the closeness of various features or elements relative to each other within the UGS. This is a useful characterization in case of e.g. allotments, that commonly appear nearby rail tracks. These connections illustrate a complex network of relationships within the UGS ontology. An example of two connections, namely "hasFeature" and "hasTexture" can be seen in Figure 5.5. While this complexity may be challenging for human interpretation, it is suited for machine processing. The structured format of the ontology allows for advanced querying capabilities. Such queries are particularly useful in tasks like image classification, where specific characteristics of UGS types are identified and analyzed based on these relational properties.
In this ontology, certain object properties are quantifiable, allowing for precise measurement and representation. For example, NDVI and GLI are numerical indices that range from -1 to +1. Further, height and proximity are also numeric values measured in meters. To effectively incorporate such quantitative data into our ontology, we include data properties that capture specific values. Here we use two primary types of data properties, namely "v_measurement" and "v_logical". The former property is defined as a float

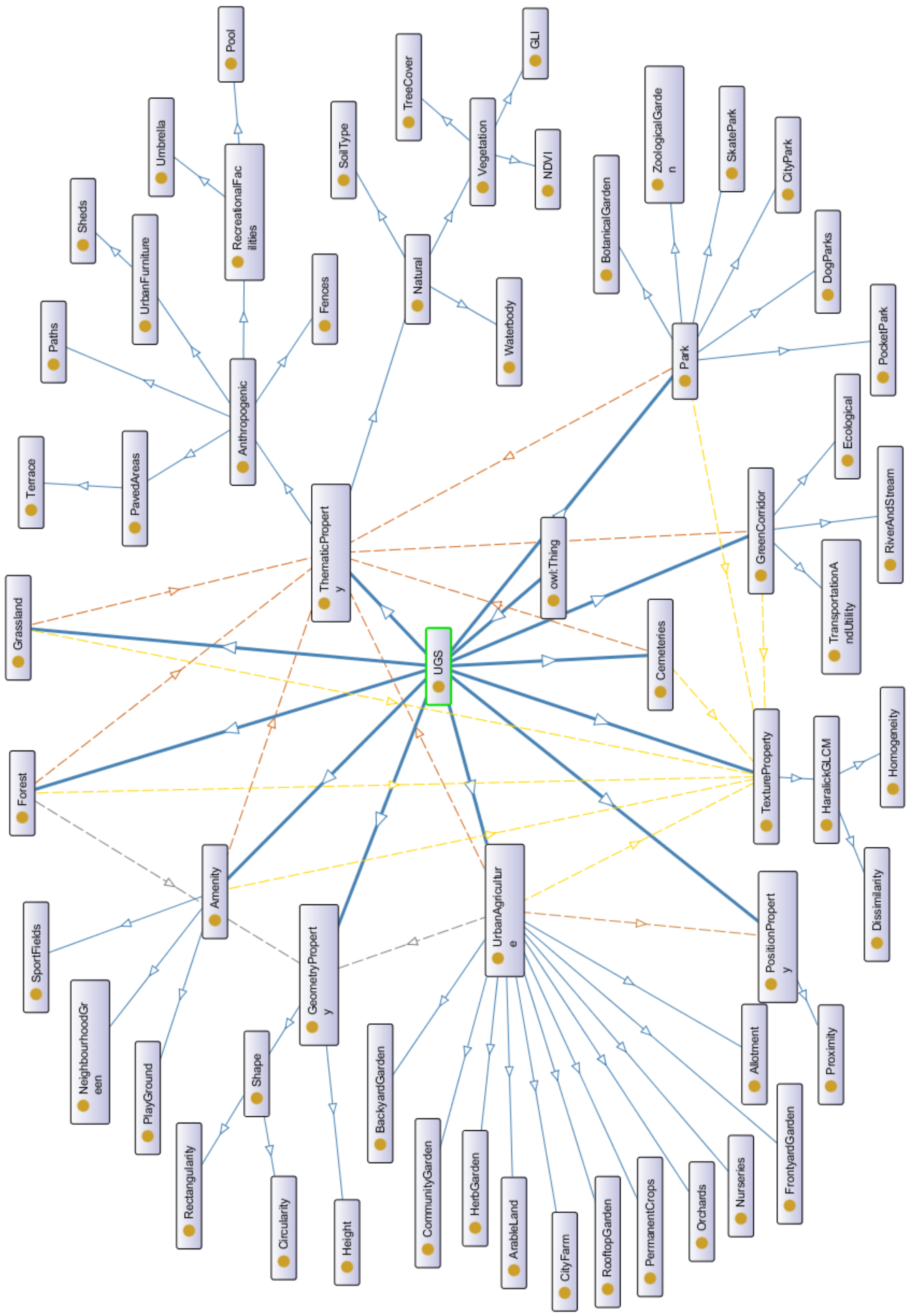

Figure 5.5: Graph showcasing connected feature properties, like hasFeature(red), hasTexture (yellow) within the UGS ontology.

type and is versatile enough to represent various numerical indices and measurements, such as distance or height. The latter property is utilized for binary logical values, stored in string format. It is particularly useful for verifying the presence or absence of features, such as determining whether fences exist or if paths are present. These data properties enable us to maintain straightforward yet powerful data representations within our ontology, facilitating accurate and efficient queries.

The final step in developing our ontology involves its formalization [58]. This process considers using a formal language to clearly define the relationships and properties of the concepts within our ontology. For this purpose, we execute the OWL in Protégé version 5.5.0. This allows us to create a structured, well-defined UGS ontology that can be used effectively in semantic web applications.

In this thesis, we develop and introduce the UGS ontology. However, we do not perform ontology-based UGS mapping. To map UGSs, we use a knowledge-based approach. Nevertheless, insights gained from the further performed procedures can be used to update and extend this ontology to bring it to a complete, ontology-based mapping, format.

Chapter 6

Mapping Urban Green with Sentinel-2 and Aerial Imagery

In the previous chapters we already describe the potential difficulties of mapping UGSs. Particularly the size of UGS patches as well as complex urban settings with similar looking and fragmented objects are the most challenging aspects of UGS identification [127]. However, accurate UGSs maps are utterly important, because they play a crucial role for data-driven decision making in the context of sustainable urban planning. The long history of LULC mapping gives us insights in terms of general requirements for LULC mapping such as necessity of adequate spatial and spectral resolution of the utilized datasets. Nevertheless, in the context of UGSs, there have not yet been any systematical comparisons done among datasets to identify what particular characteristics of these datasets might yield the best identification outcomes. However, the implementation of ML and DL methods, in hopes of overcoming the spatial and spectral limitations of datasets, has grown significantly over the past decade. These approaches have their own limitations, with the 'black box' problem being one of them. While such models enhance prediction accuracy, they often obscure the relationships between the predicted results and the variables used in the process [137]. This is suboptimal, as understanding the underlying relationships is essential for making informed decisions, reducing feature overload in future model designs, and ultimately saving both time and computational resources. Here, it is important to distinguish between identifying single pixels and classifying whole objects. As we describe in Chapter 3, one way of shedding light on these "black boxes", is the usage of IML techniques. This is particularly relevant in the case of pixel-based mapping as the process is much more straightforward.

Consequently, in an attempt to fill this research gap, we conduct a comparative study showcasing advantages and disadvantages of various datasets for UGS mapping, and strive

to answer two research questions: (1) to what extent the spatial and spectral resolution of the selected datasets influences the accurate identification of greens in urban areas, and (2) how effective is the transfer of trained models to different study areas. In addition to producing accurate UGS maps, we are also interested in exploring whether saving certain intermediate steps in the ML process can yield results comparable to a more complete workflow. To achieve this, we compare datasets with varying spatial and spectral resolutions, i.e., a high spatial but lower spectral resolution digital orthophoto versus Sentinel-2 imagery, which has lower spatial but higher spectral resolution. By following data fusion and ML techniques, we explore different derivative features and derive key statistical metrics that allow us to compare both and create accurate UGS maps of the study areas. Furthermore, we test a RF model trained in Augsburg on Wuerzburg, to establish the precision of the trained model as well as assess importance and necessity of unique, study area-tailored training datasets.
In the following sections, we describe steps of the proposed identification workflow in detail. We then apply the proposed workflows to two study areas, present their results, discuss these results, and draw conclusions from them.

6.1 Modeling Approach

To identify UGSs, we follow the exactly same procedure in both cities to ensure the comparability of the results. To do so, we follow the mapping workflow given in Figure 6.1.

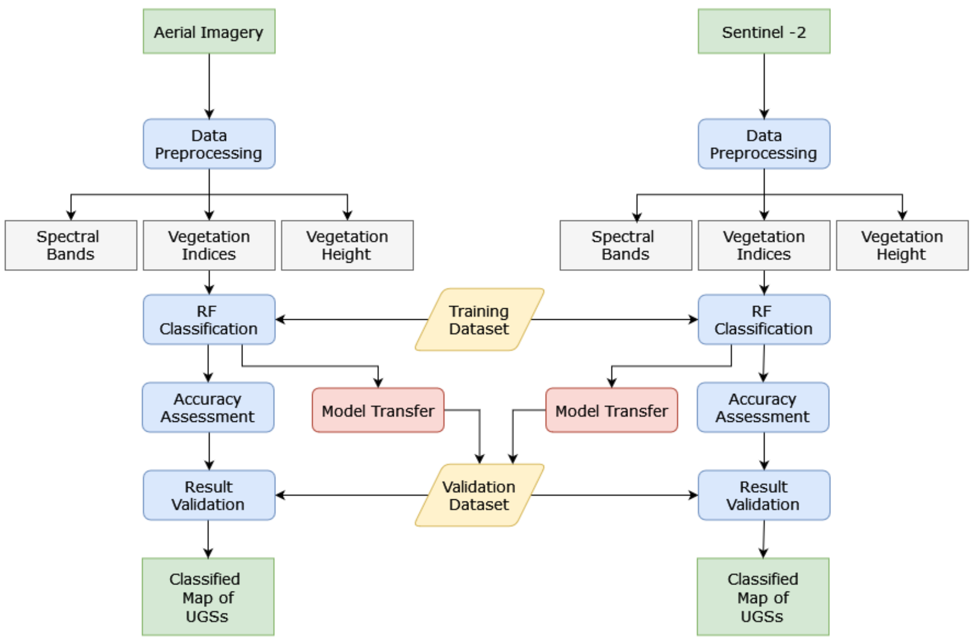

Figure 6.1: Workflow to identify UGSs using two different data sources.

We start the procedure, as described in Figure 6.1, with digital orthophoto (DOP) data preparation. These aerial datasets are three band images with 20 centimeters ground resolution and are collected on the 14th, 18th of June 2022, and the 28th of May 2023 in Augsburg and Wuerzburg, respectively. These images include only red, green, and blue spectral bands. In order to enhance green space relevant information, we utilize a number of vegetation indices i.e. GLI, RGBVI, and NGRDI calculated based on Equations 3.5, 3.6, 3.7 accordingly. Similar to NDVI, RGB-indices are based on the premise, that vegetation reflects the most in the green band, while absorbs in the red and blue band. Consequently, these should facilitate for vegetation to stand out more than any other non-green object on the urban scenes.

Apart from DOP we also Use Sentinel-2 images. Spectral bands of Sentinel-2 data, described in Chapter 4, have varying spatial resolution, ranging between 10-60 meters. Therefore, we choose to use only four spectral bands with the highest resolution: red, green, blue, and near-infrared. It is known, that chlorophyll absorbs the red light while the mesophyll leaf structure scatters NIR [151]. Therefore, especially these two bands must be advantageous to identify UGSs. Used Sentinel-2 images of Augsburg are captured on the 10th of February, 27th of March, 21th of April, 11th of May, 15th of June, 25th of July, and 17th of December 2022. Whereas, images of Wuerzburg are collected on the 28th of February, 7th of March, 26th of April, 31th of May, 13th of June, 18th of July and the 20th of December 2021. Exact details of the utilized imagery have previously been provided in Chapter 4. Due to the atmospheric conditions, it is generally difficult to acquire images taken on exactly same dates with e.g. similar cloud cover, over different locations. In addition to single spectral bands, we also make use of a vegetation index (VI), namely NDVI. Since VIs are mathematical combinations of spectral bands, they help to enhance vegetation information by reducing soil and atmospheric effects. We choose to use NDVI, because it is the most commonly used VI in terms of LULC and UGS mapping. NDVI is calculated based on the Equation 3.4, and ranges from -1 to 1, with healthy and dense vegetation values being close to 1.

In addition to spectral information, we also utilize height information to distinguish greens from the rest. The height dataset, that we use, is the nDSM data calculated in Chapter 4, based on DSM and DTM. Since this dataset comes in 40 centimeters resolution, we resample it once to 20 centimeters to fit the DOP, as well as to 10 meters to fit the Sentinel-2 datasets.

The overall aim of this workflow is to precisely identify green. Therefore, we lay focus on different green space classes, while generally ignoring how well e.g. buildings are differentiated from roads. Consequently, we perform a binary classification task with two target classes i.e. green and non-green. To achieve this goal, we choose to conduct RF classification described in detail in Chapter 3. This classification approach requires training data, that is a dataset that contains a representative distribution of predicted variables. Furthermore, it also requires a testing dataset that will be used to evaluate how well the

classification task performs and to what extent the developed model manages to capture patterns and relationships between predictor and predicted variables. Training data collection is a manual procedure, where a point shapefile is created by collecting data from both green and non-green locations. The quantity and quality of training data is defined as a crucial factor for the classification process and can significantly influence the actual classification accuracy [98]. Yet, there is no fixed rule as of how many training points need to be collected to achieve the best results. Thus, we collect approximately 900 pure training points for each class in each study area, making in total 1800 training points per study area. When collecting training data, we ensure that our training samples encompass all possible types of greenery, such as deciduous and coniferous trees or herbaceous plants. Following the recommendations of Millard and Richardson [98], we randomly distribute the training points across the study areas.
In Chapter 3 we describe that there are different ways of implementing training and testing an RF model. Here, we choose to perform train/test instead of cross validation. We split the collected training data into two parts in 70 to 30 proportion. The 70% of the dataset is utilized to train the RF model and the 30% is used to assess how well the trained model performs. Furthermore, hyperparameter tuning is an essential step in building reliable ML models. This process includes, among others, finding optimal number of trees to grow in the forest (ntree) and setting number of variables that will be randomly selected at each node to split that node (mtry). However, this step is an iterative procedure and repetitively testing values might be time-intensive. We provide specifications of the created models in Table 6.1.

Table 6.1: Specifications of utilized parameters settings to evaluate goodness of the built RF models

Training Data	1800 points
Train/Test Splits	70/30
Number of Trees (ntree)	700-1000
Number of Predictor Variables (mtry)	1; 3; 5;
Sentinel- 2 predictor variables	Red, Green, Blue, NIR, NDVI, Height
DOP predictor variables	Red, Green, Blue, GLI, RGBVI, NGRDI, Height

In Rstudio, the default number of trees grown by the RF is 500. However, it might be that the number of training samples and the number of utilized predictor variables could be explained with less, or slightly more trees than 500. Moreover, our final aim is to make predictions to the whole study area. From this perspective it is advantageous to build a simple model as possible to reduce the processing time during predictions. Thus, we first train our RF model with 1000 trees and one predictor variable. We then assess the error rate of this model. Based on the error rate we modify the number of trees accordingly. Once we set the number of trees, we then explore if increasing the number of mtry would improve the classification accuracy. For this purpose we test three and five mtrys.

The performance of the RF classifier is evaluated using overall classification accuracy, OOB error rate, sensitivity, and specificity measures. These measures are described in detail in Chapter 3. The OOB error represents internal error rate of tested sub-samples, whereas the sensitivity expresses accuracy of predicting positive class (green). The specificity describes accuracy of the negative class (non-green) prediction. Furthermore, we also explore which of the chosen predictor variables play the most important role to identify green areas. This can be done in two ways; first looking into overall feature importance based on the mean decrease in accuracy and/or decrease in Gini impurity. It is also possible to look into the influence of predictor variables on single features, which is done using SHAP values. Details of both approaches are presented and elaborated in Chapter 3. Once we identify the most optimal model parameters using train/test datasets, we make predictions over the whole study areas. The described RF classification procedure is applied to both Sentinel-2 as well as the aerial imagery. Exactly same training and testing datasets are utilized in both cases to ensure the consistency in the workflow.

To address the second research question regarding the transferability of RF models, we introduce an additional step in our workflow. After training the RF model using DOP and Sentinel-2 data from Augsburg, we apply the model to predict green areas in Wuerzburg. Complete modeling workflow is conducted using RStudio version 4.3.1.

Based on the final predictions, we calculate the total amount of greenery identified through the RF classification. Crucial part of RF classification is result validation. Validation is a procedure when identified results are compared to known results to derive performance statistics. Known results in this sense could be already existing green space maps created by local authorities, or LULC maps that contain detailed green space categories. However, there are currently no UGS maps of the study areas. Consequently, we rely on the TN dataset. We extract the following classes from the TN datasets in order to form a validation dataset: forest, parks, botanical garden, garden, grassland, arable land as well as permanent crops (orchards, vineyards). We use this dataset to validate results of classification with both Sentinel-2 and DOP datasets. We then compare results of classification in Wuerzburg once using RF model trained on training data from Wuerzburg and once trained on Augsburg. This helps us to establish the transferability of the trained model to different study areas. However, we acknowledge, that this dataset while helping to validate our results can also cause over- or under-estimation of the greenery.

6.2 Results

In this section we provide results of the performed RF classification, using both Sentinel-2 and aerial imagery. To identify UGSs in two study areas, we use red, green, blue and NIR bands with 10 meter resolution as well as temporal NDVI datasets derived from them. Furthermore, we use red, green, and blue bands of the DOP images with 20 centimeters resolution and the GLI, RGBVI, and NGRDI indices derived from them for both study areas. To highlight vegetation height, we additionally use the nDSM dataset. Further, we separately present results of both classification models.

6.2.1 Random Forest Classification using DOP

We start the procedure by determining the optimal number of trees to grow in the forest. Figure 6.2 showcases that in Augsburg, after developing around 400 trees, the OOB error begin to remain stable at around 0.005 and 0.10. We therefore search for the best mtry using only 400 trees in the forest.

Table 6.2: RF accuracy results in Augsburg, based on DOP and various hyperparameters.

ID	split_ratio	ntree	mtry	OOB_error	Accuracy	Sensitivity	Specificity
1	0.7	700	1	0.48	0.98	0.98	0.98
2	0.7	400	1	0.56	0.98	0.98	0.98
3	0.7	400	3	0.63	0.98	0.98	0.98
4	0.7	400	5	0.79	0.98	0.98	0.98

An overview of the results for all possible combinations is given in Table 6.2. For all the combinations, the RF model reaches a classification accuracy higher than 98%, making nearly perfect predictions. Although very minimal changes in OOB error take place, these do not affect the final overall prediction accuracy. Furthermore, the prediction rate of true positives (sensitivity) and negatives (specificity) is 98%, meaning both classes are identified at a similar rate. Therefore, we select the best model based mainly on possible prediction time over the study area. Training and prediction time using training/testing samples in Augsburg is less than a minute. However, the area of Augsburg is large. Consequently, we select the model with one mtry and 400 trees (ID 3) as the most suitable for large area predictions.

We explore the feature importance of the selected model, to establish which variables are the most influential predictors. It turns out, as shown in Figure 6.3, that GLI and Height are the most important predictor variables affecting the overall prediction results. Furthermore, GLI is also the most important variable to decrease the Gini impurity, meaning observations in each group after the split at node are more homogeneous. The

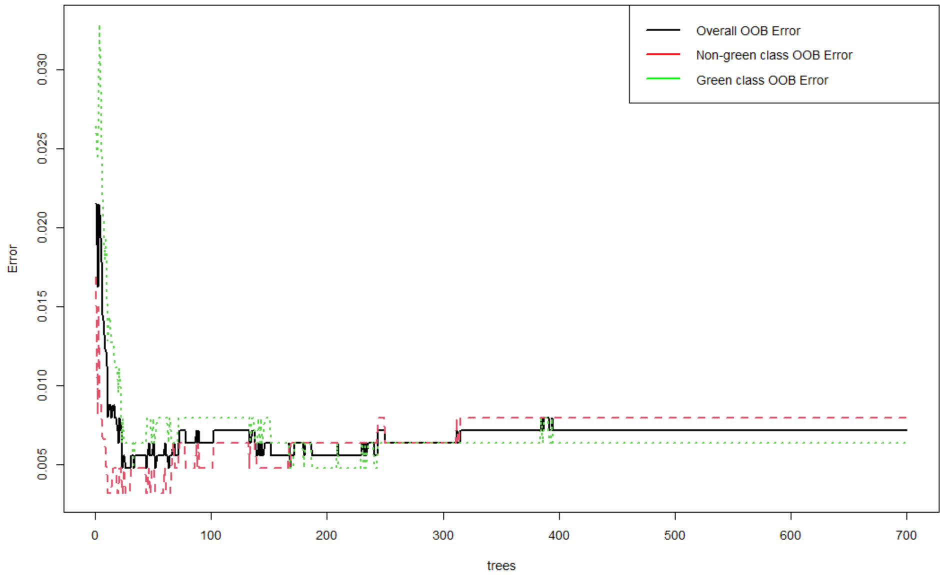

Figure 6.2: Plot illustrating decrease in OOB Error rate, based on the DOP in Augsburg, as the number of trees increase.

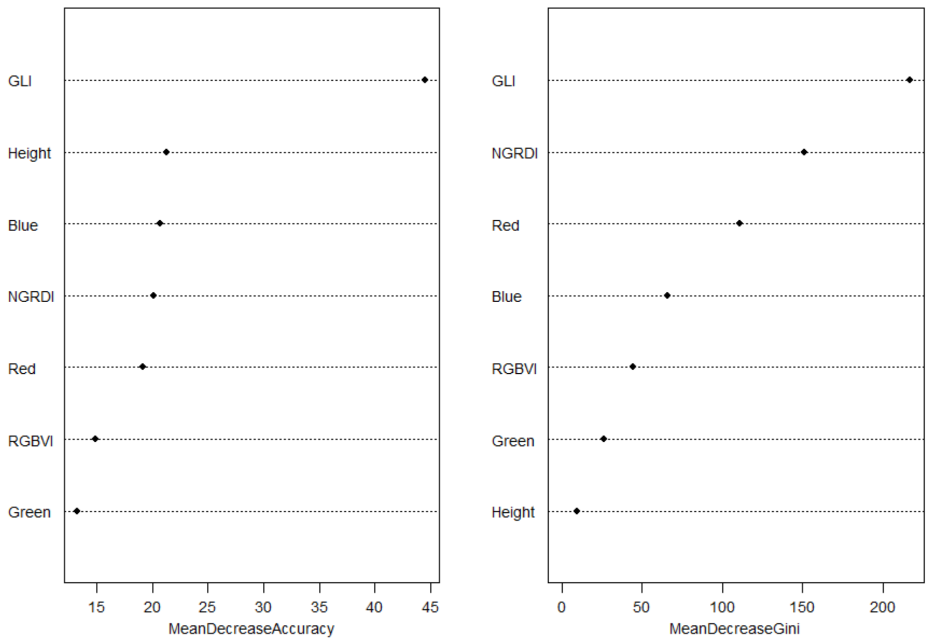

Figure 6.3: Variable importance plot of RF prediction in Augsburg using DOP dataset.

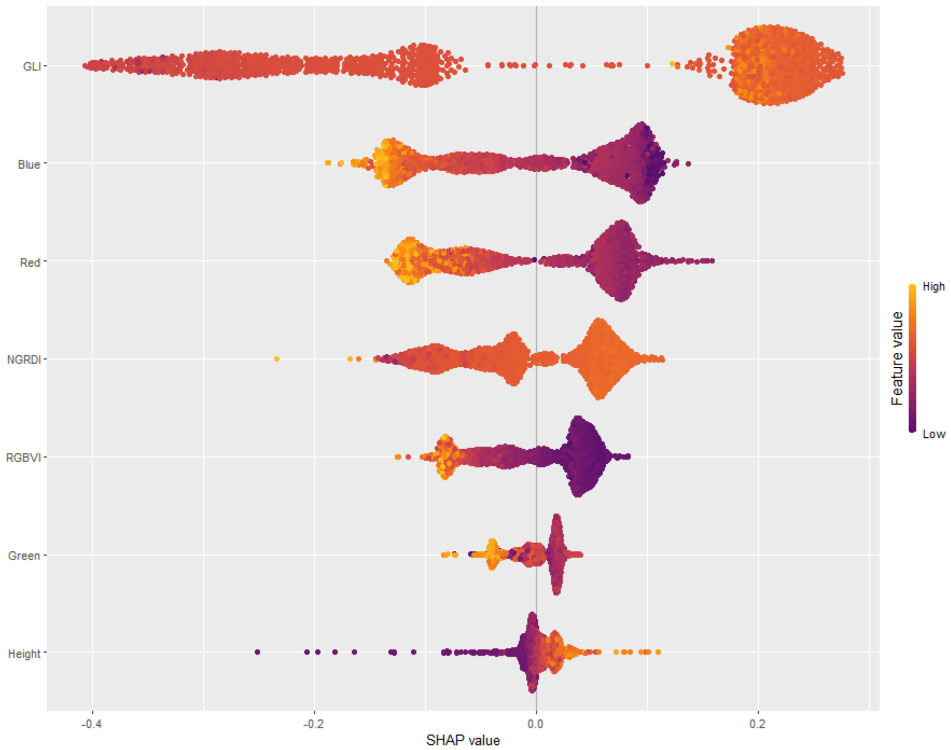

Figure 6.4: SHAP feature importance of RF prediction in Augsburg calculated using DOP dataset.

second most important variable for Gini impurity is the NGRDI index.
Yet, we are also interested in exploring how single features in the dataset are predicted. Therefore, we use SHAP values presented in Figure 6.4 to describe the co-dependencies. The color gradient from purple to yellow indicates the actual value of the feature, with purple representing low values and yellow representing high values. This allows us to see not only the impact of the feature but also how common different values are. According to the figure, GLI shows a broad spread of SHAP values, mostly on the positive side, indicating it generally increases the likelihood of a location being classified as urban green. Furthermore, blue, red, and green bands show varying degrees of influence with both positive and negative SHAP values, indicating these features can either increase or decrease the likelihood of positive class classification depending on their values. The NGRDI and RGBVI indices show a mixture of positive and negative influences, with NGRDI having a smaller impact compared to RGBVI, which shows a significant positive influence particularly at higher values. Finally, height predominantly shows negative SHAP values, suggesting higher values of height decrease the likelihood of an area being classified as urban green.
By using aerial imagery and predictor variables derived from it, we classify total of 75.1 km^2 of urban green in Augsburg. Distribution of identified urban green as well as comparative distribution of green spaces in the TN dataset is shown in Figure 6.5. Moreover,

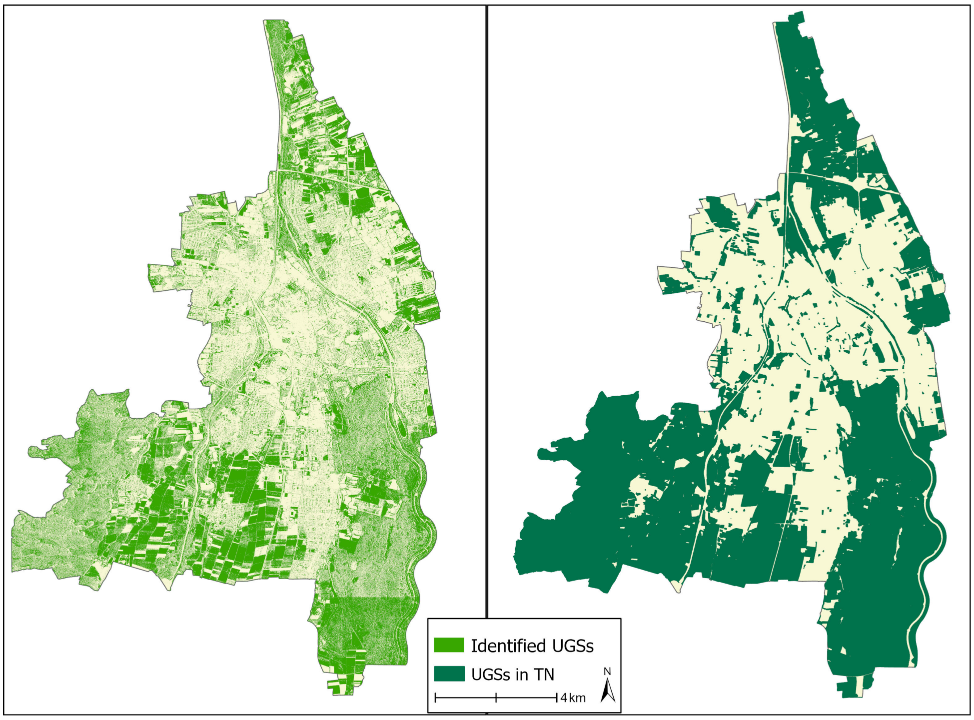

Figure 6.5: Comparative map of identified UGSs using aerial imagery and RF against TN dataset in Augsburg.

we calculate the area of identified UGSs that overlap those in the TN dataset. This validation procedure establishes that 67 km^2 of UGSs overlap in both datasets. There is a cut line visible on the south of Augsburg in Figure 6.5. This problem originates from the original DOP. Largest part of Augsburg was captured on the 18th of June, while this tiny part in the South was captured on the 14th of June. Due to different lighting condition, reflectance values here appear slightly lower. Therefore, RF fails to delineate tree crowns as well as it does in the rest of the area. We observe here shadows also being classified as urban green.

Using the DOP dataset we perform exactly the same RF classification procedure in Wuerzburg. Similarly to Augsburg, we first test the minimum number of trees required to achieve adequate results. We then test whether mtrys do affect the prediction accuracy. Decrease in the OOB error based on the number of trees is shown in Figure 6.6. As it can be seen on the figure, after 200 trees are grown, OOB error rate drops to almost 0.0 and remains stable afterwards. Consequently, we test usefulness of increasing the number of random variables to split nodes, using 200 trees.

The accuracy values for all the model parameter combinations are given in Table 6.3. As it can be seen in this table, OOB error remains exactly the same over all the tested combinations. Furthermore, prediction accuracy for all the tests is above 97%. In comparison to Augsburg, the area of Wuerzburg is not as large. Nevertheless, we select the optimum hyperparameters exactly the same way: minimum number of ntree and mtry. Thus, the

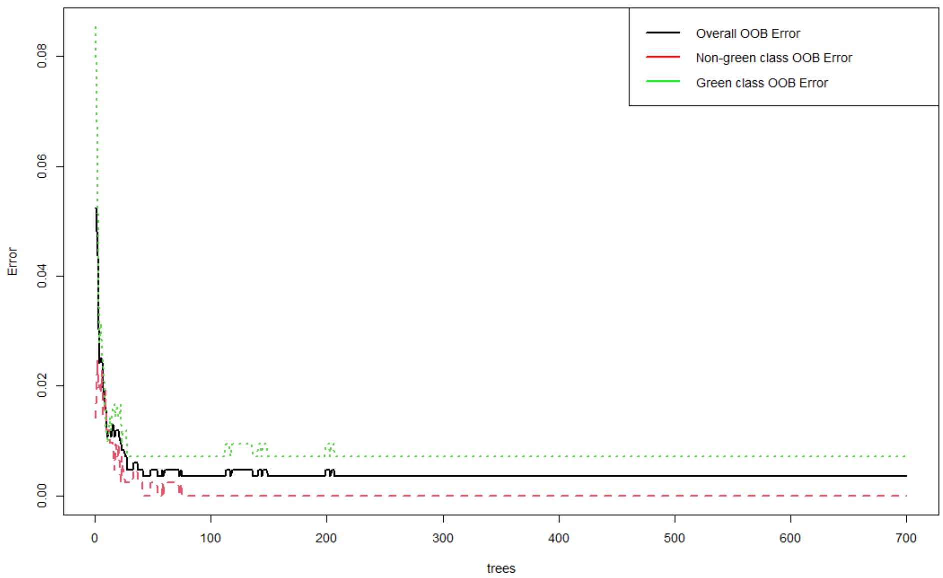

Figure 6.6: Plot showcasing decrease in OOB Error rate, based on the DOP in Wuerzburg, as the number of trees increase.

Table 6.3: RF accuracy results in Wuerzburg, based on DOP and different hyperparameters.

ID	split_ratio	ntree	mtry	OOB_error	Accuracy	Sensitivity	Specificity
1	0.7	700	1	0.36	1	1	1
2	0.7	200	1	0.36	0.99	1	0.99
3	0.7	200	3	0.36	0.98	0.97	0.98
4	0.7	200	5	0.36	0.98	0.97	0.99

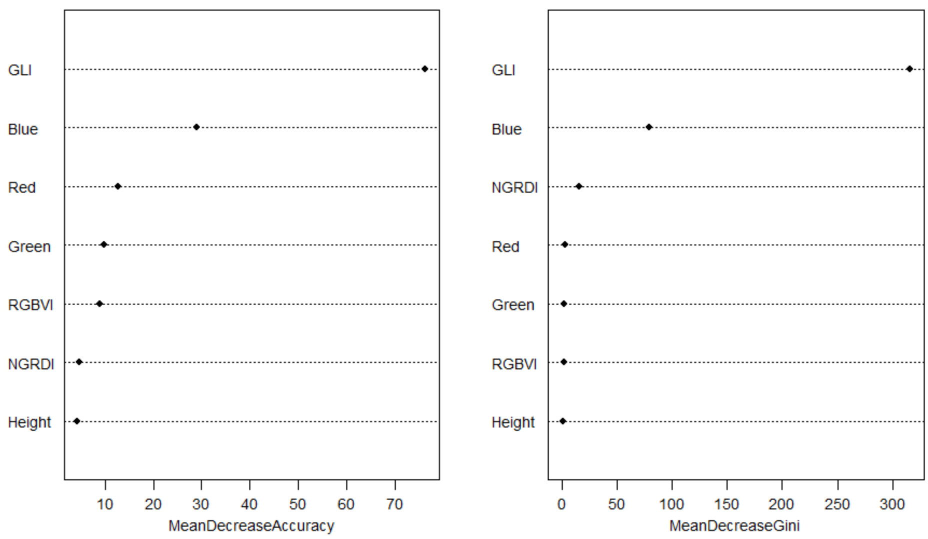

Figure 6.7: Variable importance plot of RF prediction in Wuerzburg using DOP dataset.

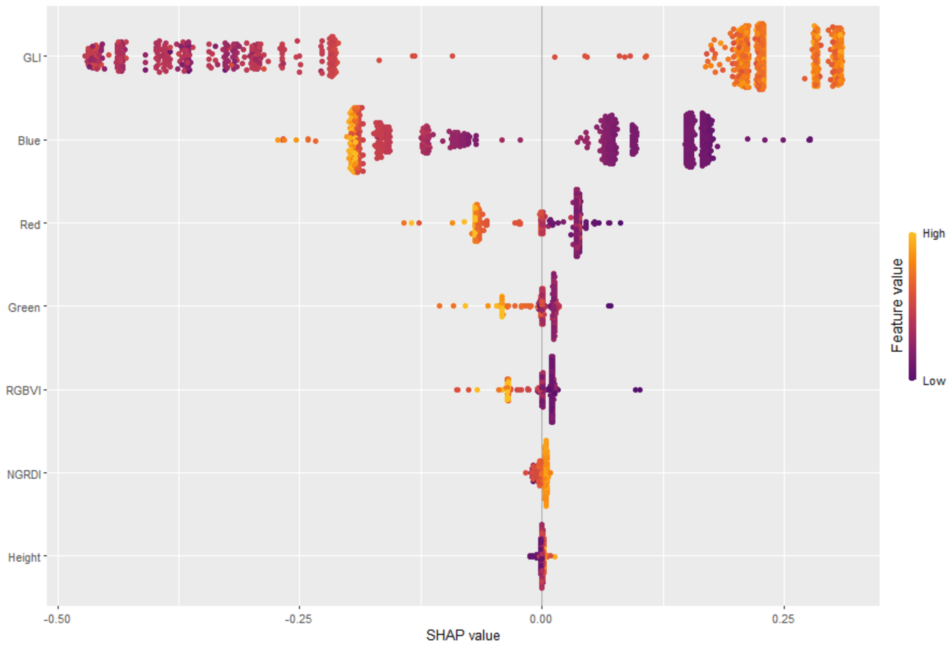

Figure 6.8: SHAP feature importance of RF prediction in Wuerzburg calculated using DOP dataset.

RF model that uses 200 trees and single random variable to split nodes is the most suitable RF model. This model reaches 99% prediction accuracy, and it can perfectly identify the green class (sensitivity) in comparison to the non-green class (specificity).
We further explore the variable importance as well as the SHAP values of this model. The variable importance plot given in Figure 6.7 illustrates, that GLI is yet again the most influential factor for improving overall accuracy as well as decrease the Gini impurity. However, unlike in Augsburg, the blue band is the second most important predictor variable, followed by the red band for overall accuracy, and NGRDI for Gini impurity. Figure 6.8 illustrates the importance of predictor variables on single features in the dataset. The GLI mainly shows positive SHAP values, especially for higher feature values, confirming its strong positive influence in predicting urban green. Both blue and red bands exhibit both positive and negative SHAP values, indicating a complex influence on the model's prediction. The Green band exhibits a significant spread of SHAP values but tends to show more positive influence, particularly at higher feature values, which supports predictions of an area being urban green. The RGBVI index shows a strong negative influence when the feature values are low and a positive influence at higher values. This dual influence suggests that RGBVI's high values support the classification of an area as urban green, while low values discourage it. NGRDI primarily shows positive SHAP values, especially at higher feature values, indicating that higher NGRDI values strongly push the model towards predicting urban green. Whereas, height mostly exhibits negative SHAP values, suggesting that higher heights generally decrease the likelihood of an area being

classified as urban green.

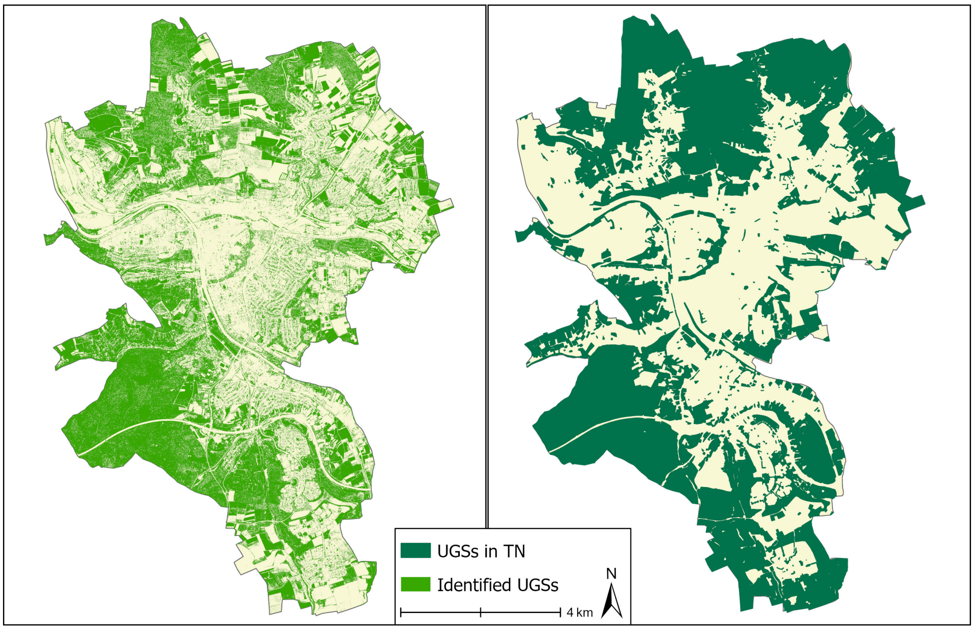

Figure 6.9: Comparative map of identified UGSs using aerial imagery and RF with TN dataset in Wuerzburg.

Figure 6.9 illustrates both green identified using aerial image as well as UGSs within the TN dataset. In total, we identify 43.8 km^2 of UGSs. 38 km^2 of the identified green areas overlap those in the validation dataset. As in case of Augsburg, here we also establish, that much more green is identified than the TN dataset accommodates. Furthermore, when examined at a grater detail like in Figure 6.18, we establish that street level green is identified with a high precision, that does not appear in TN dataset and thus cannot be validated.

6.2.2 Random Forest Classification using Sentinel-2

To identify UGSs using Sentinel-2 imagery, we implement the same RF classification procedure as with DOP imagery. Here, we use the red, green, blue and NIR bands with 10 meter resolution, as well as NDVI datasets derived from them. Following the workflow, we first identify which hyperpyrameter settings of RF can yield the most reliable classification results. We first explore prediction performance using 1000 trees and one mtry. Change of OOB error for this model is given in Figure 6.10. It can clearly be seen, that 400 trees is a cut point, until which the model learns and produces the OOB error. After growing 400 trees, the OOB error remains stable at 0.01.
We then test whether a change in mtry would affect the prediction accuracy. For this, we present all accuracy values of the RF classification in Augsburg in Table 6.4. Here, we

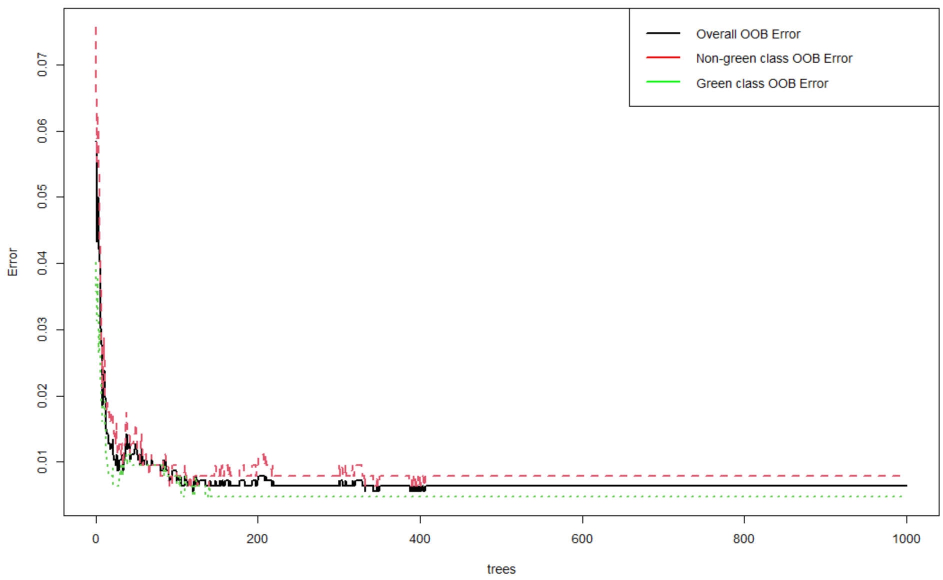

Figure 6.10: Plot illustrating decrease in OOB Error rate, based on the Sentinel-2 data in Augsburg, as the number of trees increase.

observe a similar picture as with DOP. The OOB error changes slightly depending on the selected mtry, but remains quite low. Accuracy values are all above 98%, with prediction of non-green class reaching 100% for models 3 and 4. Therefore, we select model 2 with 400 trees and 1 mtry as the most optimal model for making a prediction for the whole study area.

Table 6.4: RF performance metrics in Augsburg, using Sentinel-2 imagery and NDVI.

ID	split_ratio	ntree	mtry	OOB_error	Accuracy	Sensitivity	Specificity
1	0.7	1000	1	0.63	0.99	0.98	0.99
2	0.7	400	1	0.56	0.99	0.98	0.99
3	0.7	400	3	0.48	0.99	0.98	1
4	0.7	400	5	0.56	0.99	0.98	1

We assess importance of each variable using two metrics: Mean Decrease in Accuracy and Mean Decrease in Gini as shown in Figure 6.11. This helps us to understand how crucial these variables are in the overall classification process. NIR band of June imagery (Jun_B08) as well as green band of June imagery (Jun_B04) rank highest, suggesting they are the most critical predictor variables for accurate prediction of urban green. The subsequent most important variables are NIR band of May (May_B08), NDVI of June and May (NDVI_06 and NDVI_05). The Mean Decrease Gini chart focuses on how each feature contributes to the homogeneity of the nodes in the trees. However, NDVI

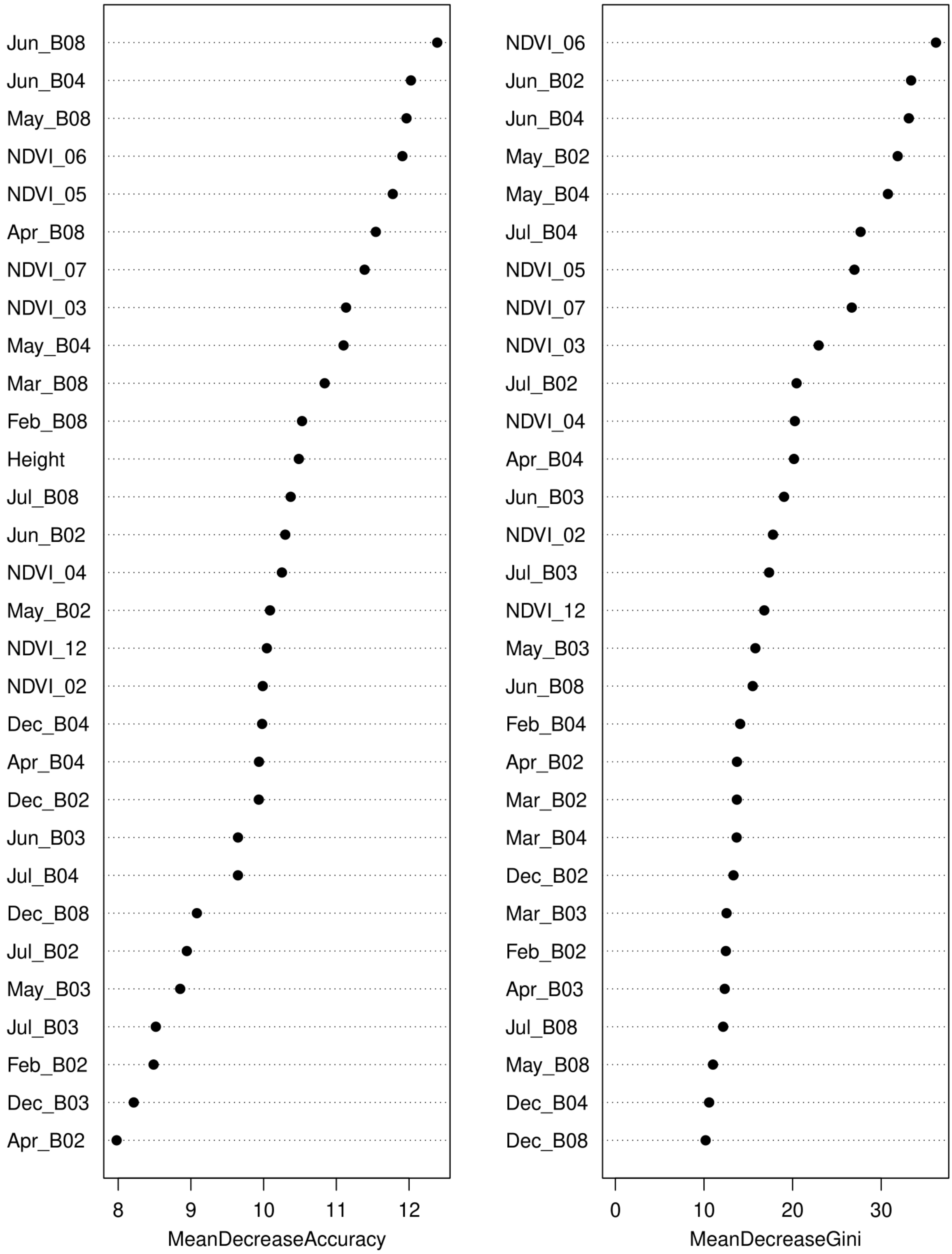

Figure 6.11: Feature importance graph of the utilized Sentinel-2 imagery and predictor variables to map UGSs in Augsburg.

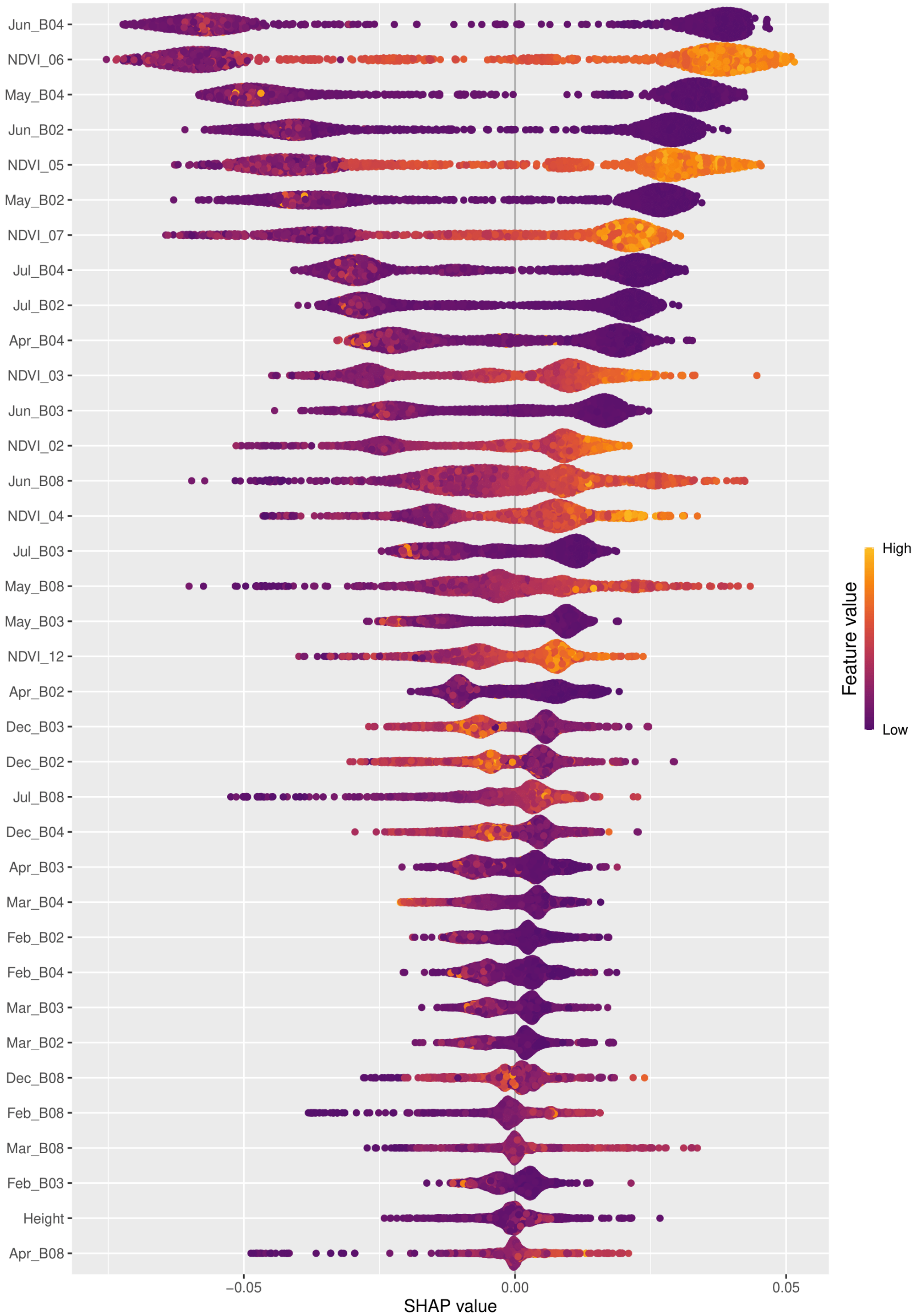

Figure 6.12: SHAP feature importance of RF prediction in Augsburg calculated using Sentinel-2 datasets and their derivatives.

of June imagery appears to have the highest contribution, followed by blue band of June (Jun_B02). This indicates that they are influential in defining node splits that lead to more homogeneous subgroups. The next three important variables for node homogeneity are red band of June (Jun_B04), blue (May_B02) and red band of May (May_B04).
The SHAP plot in Figure 6.12 provides insights into the magnitude and direction of the impact each variable has on predicting green class. Here as well, red band of June imagery has a substantial influence on the model predictions. This band shows a prominent spread of SHAP values. Lower red band values typically correlate with positive SHAP values, suggesting that areas with less red light absorption (which could correspond to denser green vegetation) are strong predictors for identifying green. The NDVI index created from June imagery follows closely in importance, with higher NDVI values consistently showing positive SHAP impacts. This aligns with the expectation that higher NDVI values, indicating more vigorous vegetation, push the model towards predicting green class. Although less influential than the red bands or NDVI indices, lower values in this band, which may indicate less absorption by non-vegetative surfaces, have a positive impact on model predictions. Finally, higher NDVI values in May correlate with positive SHAP values, pushing the model towards predicting urban green. This underlines the importance of vegetation vigor in May for predicting green areas. Starting from the blue band of May, all the following variables show a very similar and limited spread in SHAP values and rather cluster around zero. Except, the opposite is true for the NIR band. For all months, the NIR band shows the strongest spread of higher values within positive SHAP range. This indicates that in all cases high NIR band values will be a strong predictor of urban green.
Although the sensitivity and specificity values and overall accuracy express to what extend the utilized training dataset is capable to predict each class, we further visually investigate the outcome of the classification. In addition to the visual inspection, we use the enriched TN validation dataset, described in Chapter 4, to understand the performance of our classification. Figure 6.13 illustrates the comparison between identified and TN UGSs. The performed RF classification identifies around 85.9 km^2 of green. 80.3 km^2 of this area overlaps with the area of UGS in the validation dataset. While a majority of the areas between identified and TN dataset overlap, additional green appears in the RF classification. These areas are particularly street-level green between residential areas, or open areas that look green and have fine grass coverage.
In Wuerzburg, we perform exactly the same procedure to select best performing hyperparameters for RF. We explore 36 predictor variables, that include single temporal Sentinel-2 bands, NDVI indices derived from them as well as vegetation height. Accuracy results over various hyperparameters options are given in Table 6.5. We follow the same model selection approach as previously. In the given set up, the OOB error of model predictions reaches its lowest at around 150 trees and remains stable afterwards. This can clearly be seen in Figure 6.14.

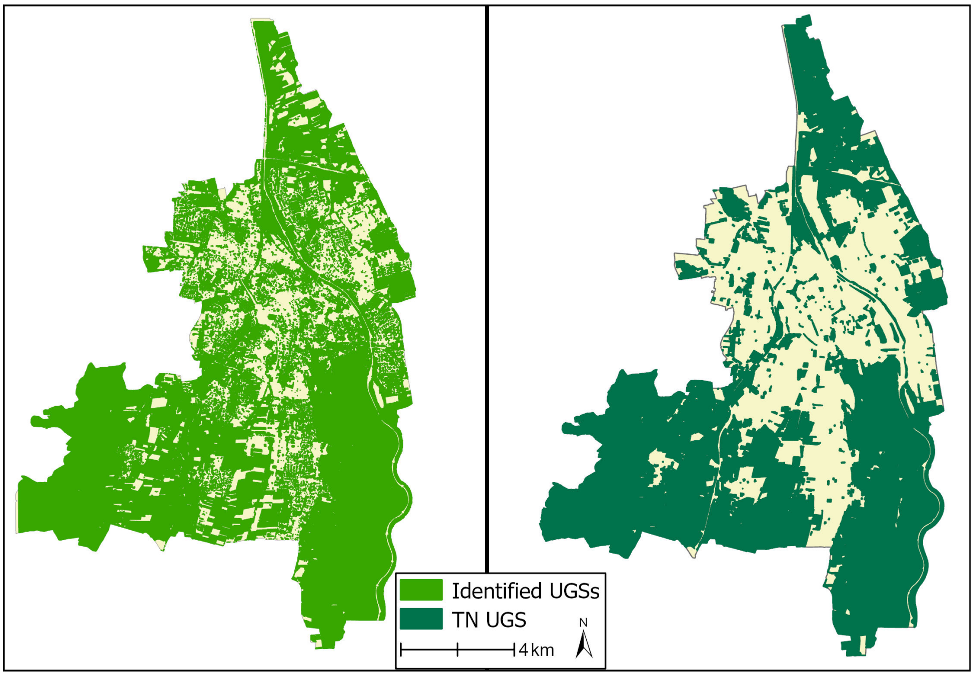

Figure 6.13: Comparative map of identified UGSs using Sentinel-2 and RF with TN dataset in Augsburg.

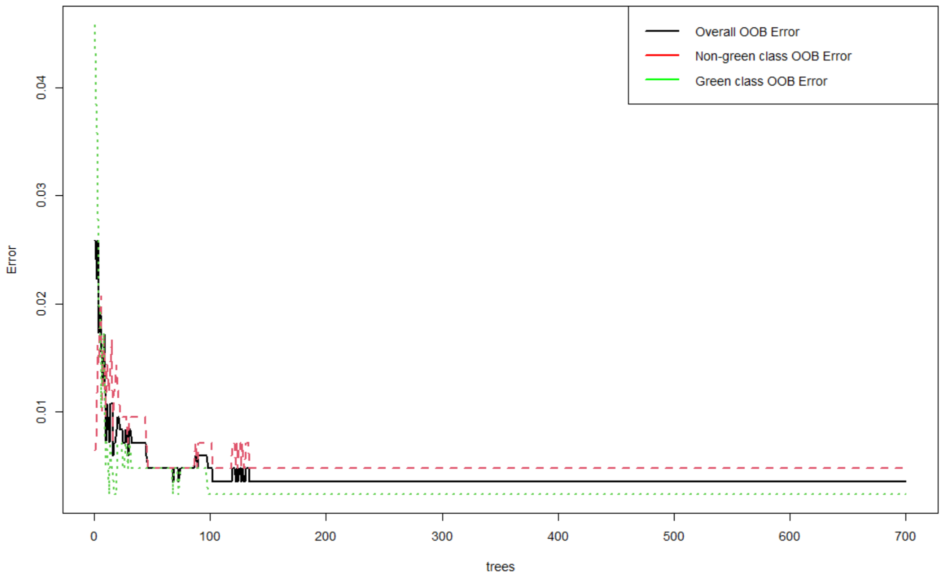

Figure 6.14: Plot illustrating decrease in OOB Error rate, based on the Sentinel-2 data in Wuerzburg, as the number of trees increase.

Table 6.5: RF performance metrics in Wuerzburg, using Sentinel-2 imagery and temporal NDVI.

ID	split_ratio	ntree	mtry	OOB_error	Accuracy	Sensitivity	Specificity
1	0.7	700	1	0.36	1	1	1
2	0.7	150	1	0.36	1	1	1
3	0.7	150	3	0.36	1	1	1
4	0.7	150	5	0.12	1	1	1

Considering the overall aim of making predictions over the whole area of Wuerzburg, we select 150 trees and 1 mtry as the most appropriate model parameters.
We further examine variable importance in the build RF setup. Therefore, we once again explore the impact of each variable on the model's overall accuracy (mean decrease in accuracy), variable contribution to node splits in the decision tree (decrease in Gini), as well as direction and magnitude of influence for each variable (SHAP). We first present the results of the overall feature importance in Figure 6.15.
The NDVI variable derived from the June imagery is the highest-ranked variable in terms of mean decrease in accuracy. Removing this variable has the greatest negative effect on model accuracy. It is also the second most important variable for Gini, showing it is used in many tree splits and contributes to pure decision making. NDVI of May is the second most important variable affecting overall accuracy, and the most important variable resulting in decrease of Gini impurity. This suggests that NDVI in May is a key for distinguishing between green and non-green labels. Interestingly, NDVI of July is important for overall accuracy as for Gini impurity, although ranked slightly lower than the previous two variables. For both overall importance and Gini importance, this trend of modest influence is followed by the red bands of June and July images.
The SHAP values for the selected RF classification are presented in Figure 6.16. Here, we can also establish more dominant influences of certain variables to predict the class 1, which is the green class. Consequently, higher NDVI values in May, June, and July (yellow points) consistently have positive SHAP values, indicating that higher values of these variable push the model to predict the green class. Contrary, lower values of red band of both July and June images impact the RF model to predict urban green. The red band of the June imagery, and several bands afterwards, illustrate double spikes either in negative or positive SHAP values. For the rest of predictor variables, there is clustering of SHAP values around 0, indicating these variables will not substantially contribute, neither positively nor negatively, for a pixel being classified as green or non-green.
Apart from examining the statistical measures of identifying green/non-green labels, we also explore to what extent the values represent the reality. Therefore, we utilize the TN

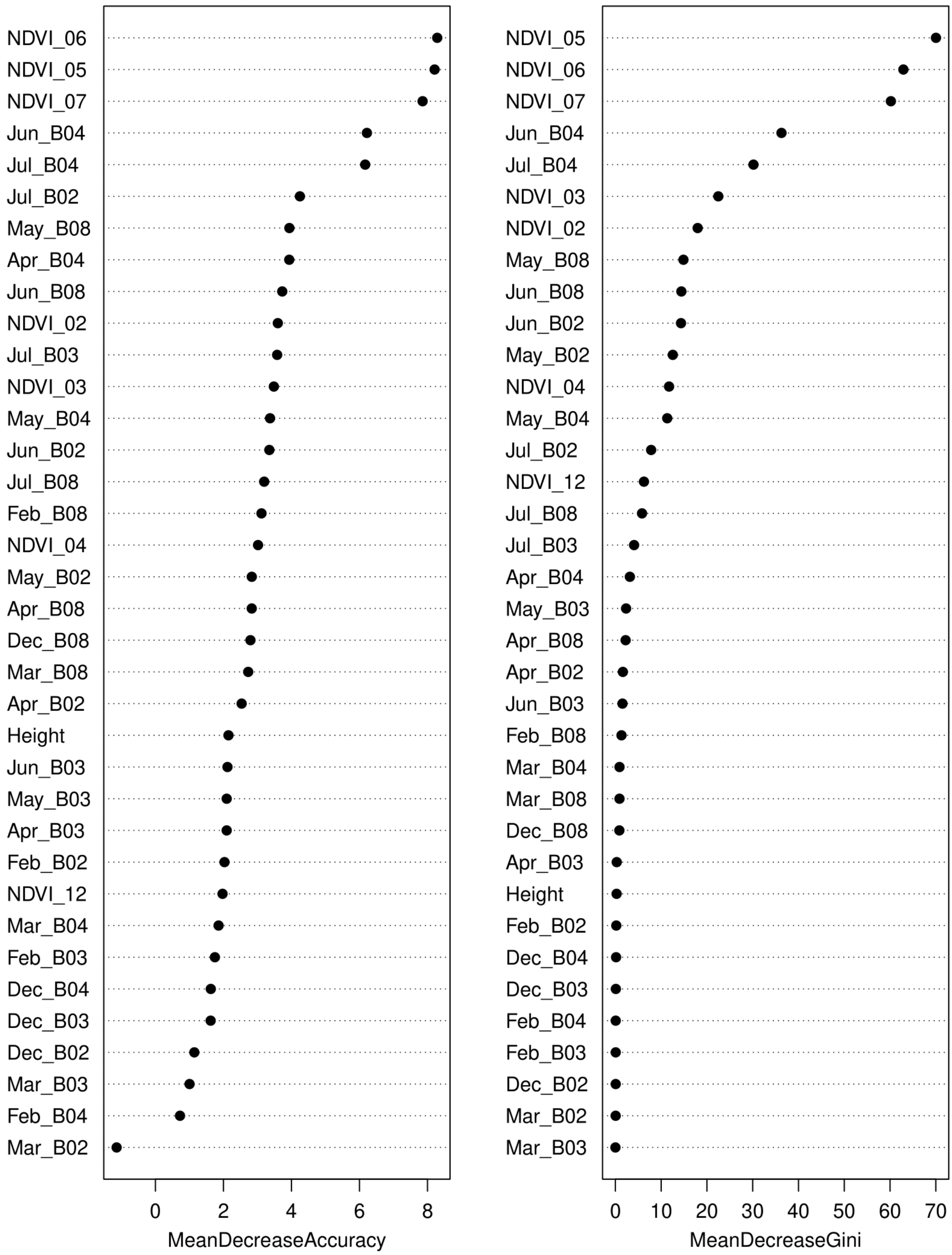

Figure 6.15: Feature importance graph of the utilized Sentinel-2 predictor variables to map UGSs in Wuerzburg

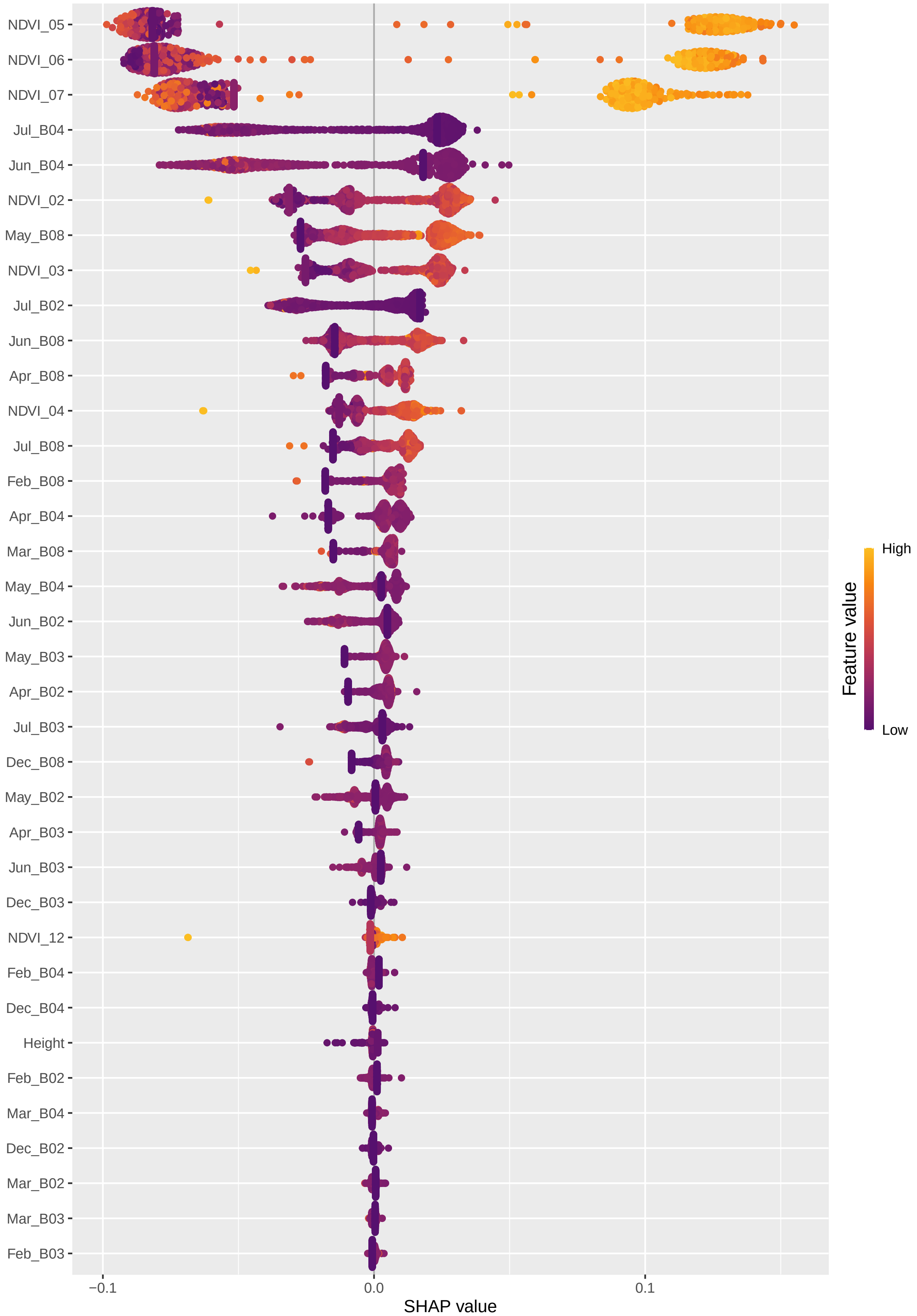

Figure 6.16: SHAP value graph of the utilized Sentinel-2 imagery and predictor variables to map UGSs in Wuerzburg.

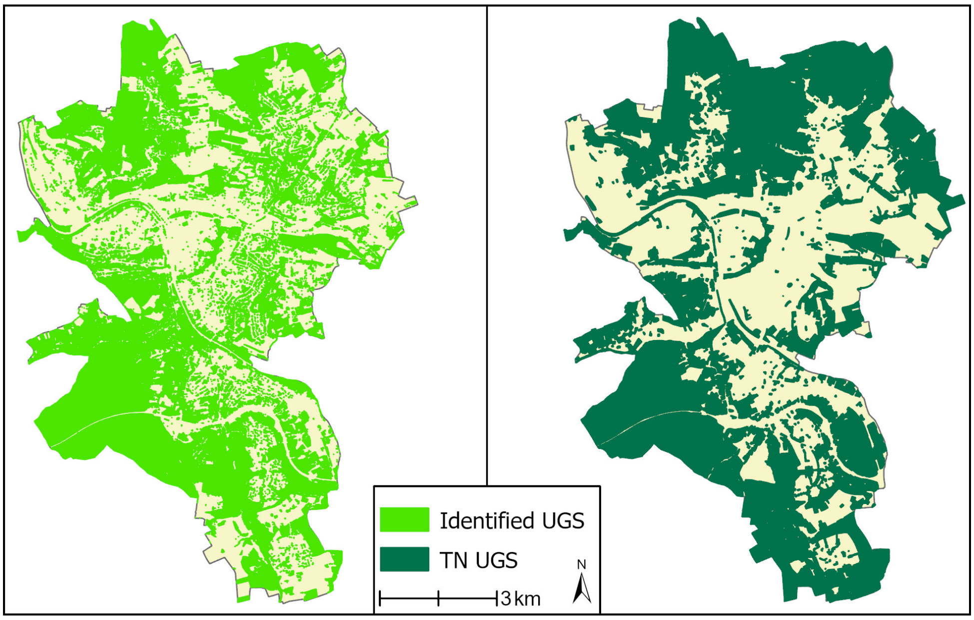

Figure 6.17: Comparative map of identified UGSs using Sentinel-2 and RF with TN dataset in Wuerzburg.

dataset to validate our results. By utilizing the best performing RF settings, we identify 48.9 km^2 of green in the city. 46.2 km^2 of the identified urban green overlap the TN validation dataset. A comparative map of identified green with RF as well as green space distribution based on the TN dataset is shown in Figure 6.17. Similarly to Augsburg, we also identify intermediate green areas like street trees or grassy areas that do not typically appear in the TN dataset.

In addition, we visually compare how well singular features are identified based on different data sources. Hence, we present a snippet of an area in Figure 6.18 to illustrate to what extent spatial resolution affects precise green identification. It can clearly be seen on this figure, that with 20 centimeters resolution street level greenery is identified with much higher precision than with 10 meters resolution. This is even more striking, given that Sentinel-2 contains NIR band, which is advantageous for highlighting green vegetation.

Finally, we asses how well green is identified in Wuerzburg using the RF model that was trained in Augsburg. We first examine the precision of using DOP and Sentinel-2 imagery. When the RF model is trained on 1800 training points in Augsburg and predicted on the DOP imagery of Wuerzburg, it identifies 51 km^2 of greenery in Wuerzburg. This number is nearly 8 km^2 more than when we train and predict an RF model using training dataset collected from Wuerzburg. We also examine whether there is an overlap between over-predicted areas and the TN validation dataset. It turns out that 24.5 km^2 of green areas predicted by transfer learning technique actually overlap the TN dataset. A visual comparison between predicted urban green in Wuerzburg is given in Figure 6.19. Here it is clearly seen that the majority of overlaps appear within agricultural production areas.

Figure 6.18: Comparative map illustrating visual differences in UGS identification, between DOP (upper) and Sentinel-2 (lower) imagery, due to spatial resolution differences.

The other source of over-prediction is in the outlines of green areas. As such, when DOP is trained on the Wuerzburg dataset, it can precisely distinguish outlines of urban green, such as crowns. However, the transfer learning approach predicts slightly larger areas around e.g. crowns also as green.

Our examination of the results of transfer learning using Sentinel-2 dataset reveals, that it identifies 57.4 km^2 of green in Wuerzburg. This number is almost 9 km^2 higher than when we train the RF model with training data from Wuerzburg itself. 35.7 km^2 of the predicted green overlap with the TN validation dataset. Moreover, nearly 3 km^2 from the over-predicted green (9 km^2) appears in the TN validation dataset. A comparative map of predicted green using RF trained on the training data from Wuerzburg (left) and RF model trained on the training data from Augsburg (middle) is presented in Figure 6.20. The right map in this figure illustrates the areas that do not overlap in the predictions of two models.

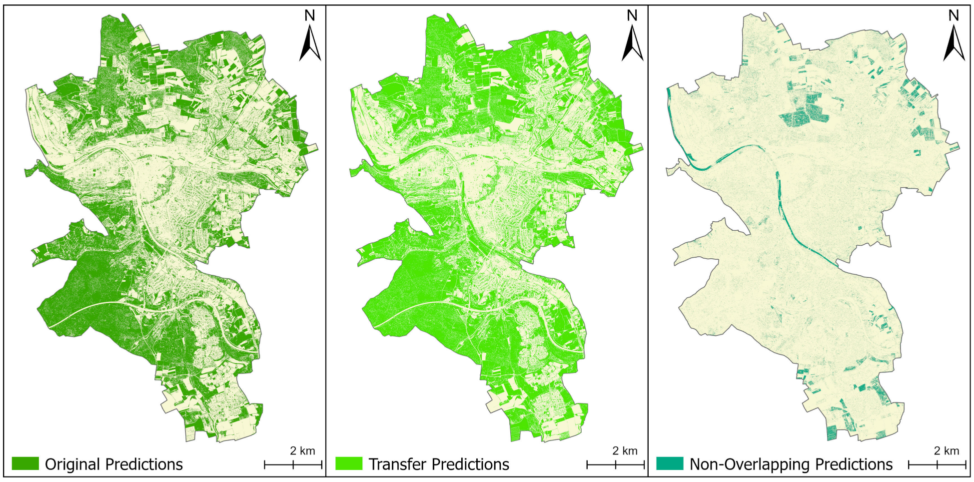

Figure 6.19: Comparative map that illustrates the differences of urban green predictions using RF model trained on DOP data from Wuerzburg (left), RF model trained on DOP data from Augsburg (middle), as well as detailed areas that do not overlap between predictions (right).

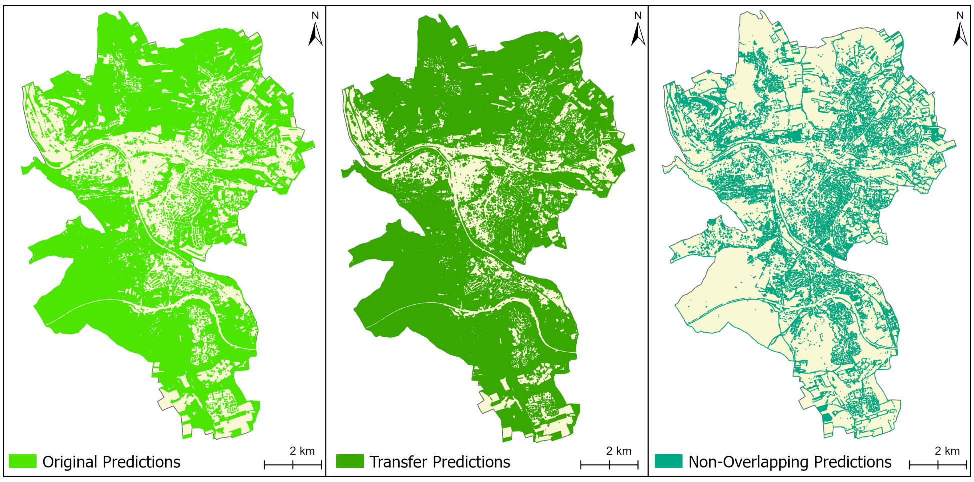

Figure 6.20: Comparative map that illustrates the differences of urban green predictions using RF model trained on Sentinel-2 data from Wuerzburg (left), RF model trained on Sentinel-2 data from Augsburg (middle), as well as detailed areas that do not overlap between predictions (right).

6.3 Discussion and Conclusions

Acquiring accurate maps of UGSs is challenging due to the inherent confusion surrounding different types of UGSs and the level of generalization in existing LULC maps. In this computational experiment, we use a combined approach of RF and RS to identify UGSs, demonstrating that cities contain far more green than what is typically represented in LULC maps. Recognizing that different types of UGSs exist and that some may be too small to be detected in RS imagery, we compare high-resolution Sentinel-2 data with very-high-resolution aerial imagery. Moreover, we test the transferability of the trained RF models to new study areas. To ensure the comparability of results, we apply the exact same procedure to both datasets, using identical training and validation sets. This approach is consistent across both study areas.

The first question that arises is whether it is possible to determine which selected data sources and their derivative products can aid in identifying UGSs. To explore this, we focus on vegetation indices, which have already been shown to be valuable in green space mapping [104][1]. Moreover, Abdi [1] illustrates, that temporal datasets can facilitate vegetation identification. Therefore, to capture and utilize changing phenological characteristics of vegetation, we also utilize temporal Sentinel-2 datasets.

The first challenge in comparing selected data sources between two cities is the difficulty of obtaining data for the exact same time period. Sentinel-2 provides freely available data with a revisit time of five days, making it generally possible to capture images for both locations on the same or nearly the same date. However, cloud coverage presents significant challenges due to the altitude at which these satellite constellations fly. Therefore, we only select Sentinel-2 images per month throughout a year with less than 10% cloud coverage. This results only in seven images for both Augsburg and Wuerzburg (January, August, September, October, and November are excluded). While it is possible to get imagery for some extra months in Augsburg, it is challenging to do so in Wuerzburg. This is mainly determined by the topography of the two study areas. Wuerzburg's center is surrounded by hills. This means that fog would typically remain in the valley, thus making the area underneath invisible for satellites. Conversely, imaging authorities that provide DOPs have a better control over the acquisition date. It means, that these images will be taken on the clearest days to allow visibility of all the objects on the surface. One major problem could be that parts of cities are captured on different days and different pre-processing steps are applied to combine images. This might not only affect how the images look, but also result in differences of reflectance values. However, DOPs are captured near-annually around the same time each year, making monthly DOPs too expensive to obtain and therefore unavailable for the study areas.

Apart from the temporal factor, spectral qualities of images are also important for green space mapping. Sentinel-2 images provide much wider spectral resolution, whereas DOPs contain only three visible bands. In contrast, DOPs have extremely high spatial resolution of 20 centimeters, while spatial resolution of Sentinel-2 data ranges from 10 to 60 meters depending on the bands used. Consequently, when comparing identified urban green, we do take into consideration all the possible differences inherent to the selected datasets.

Many ML methods exist that can be utilized for RS image classification, where RF is among the most frequently used ones [27][115]. Therefore, we choose to implement RF classification by Breiman [22]. Determining factors of goodness of the classification are how well utilized dataset represents objects of interest and how good is the training data that will be used to identify these objects. Moreover, model engineering steps can also play a crucial role in avoiding e.g. overfitting of the model. This could include the train and test split, number of trees as well as the number of variables to split nodes. Consequently, we choose to test some of the variables in a changing order to observe the accuracy change. In case of both datasets, we split training data into 70/30 train/test proportions, and choose to grow only as many trees as absolutely necessary for adequate classification. However, depending one the dataset and the indices derived from them, we test between one and five variables to split the nodes. Unlike to many other examples in the existing literature, we achieve both for Sentinel-2 and DOP classification extremely high accuracy, that is constantly above 95%. In a similar set up of using Sentinel-2 for UGS mapping, Chen et al. [27] achieve 94% accuracy, whereas Abdi [1] reaches 80%. Furthermore, in a study of using 5 centimeters resolution DOP in combination with RF, Wagner and Egerer [144] achieve 80% prediction accuracy. While all the mentioned studies have different focus ranging from UGS mapping to LULC mapping to more specific urban garden mapping, all of them utilize either DOP or Sentinel-2 data and build RF classification workflows. Considering our exceptionally high classification accuracy, we further explore the possibility of overfitting. The out-of-bag (OOB) error, an internal measure of accuracy, uses sub-samples of data to evaluate both training and testing performance. The consistently low OOB error across all hyperparameter tuning combinations indicates that the likelihood of overfitting is very minimal.

RF classification can be time-intensive, especially with the very high resolution of the DOP datasets, which impacts the selection of hyperparameters. If similarly good results can be achieved with only 500 trees, it is more cost-effective to avoid growing, for example, 1500 trees. The same principle applies to the number of predictor variables: if using just one predictor variable per split yields the same accuracy as using all seven, it is more efficient and meaningful to use only one. Looking at our results, we find that equally good classification outcomes for both Sentinel-2 and DOP data in both cities can be achieved using under 500 trees. This can be explained by the straightforwardness of the decision making. In the example of an eight bit DOP image there are only 256 values available to describe every pixel. Given green areas represent unique portions of these values, RF does not need to build too many decision trees to come to a clear outcome. The same, to a certain extent, applies to the Sentinel-2 datasets. Although they represent reflectance intensities with a wider range of values, NDVI derived from them is limited to a range between -1 and 1. Our results clearly show that in most cases NDVI values are the determinant variables, therefore RF can easily distinguish green in this small NDVI range.

Here, it is also important to note the precision of the training dataset. Quality of training data is a widely discussed aspect in ML classifications. The principle of "rubbish in and rubbish out" is understandable, since ML can only learn from the data that we provide. Therefore, we pay extra attention to collect pure, green area representative training points. This improves the pattern recognition of the RF model substantially, since it does not require extra effort to delineate noise from the actual data. This is also reflected in how well true positive and negative labels are recognized.

We observe differences in the predictor variables used for node splitting, as they vary depending on the dataset. Unfortunately, RF does not provide a straightforward way to identify the exact variable used to split a specific node, since this information is spread across many trees in the forest. Nevertheless, variable importance can be used as an indirect method to infer which variables are most frequently chosen for splits. When DOPs and their derivative indices are used, the GLI index consistently emerges as the most important variable for RF predictions, which likely contributes to the model's high accuracy. For Sentinel-2 datasets, there is some variation in the ranking of important variables across study areas. However, in both cities, the NDVI values from June, July, and May, along with the red and NIR bands from June consistently rank among the top five most important variables. The NDVI index is specifically designed to highlight healthy vegetation, so its prominence as the most important variable is not surprising. This finding aligns with existing literature, such as Degerickx et al. [37], Simonneaux et al. [129], and Abdi [1]. There are, however, some exceptions, such as the publication by Peña et al. [112], where the use of NDVI does not yield significant contributions. It is worth noting that the authors use Landsat-8 data with a 30 meter resolution, which could be an underlying reason for the unsatisfactory results. Additionally, the relatively high importance of red band values for identifying green spaces can also be easily explained by the expected behavior of chlorophyll, which strongly absorbs red light in healthy vegetation [106].

DOP images, as previously described, contain only three bands, that potentially could be not enough for identifying green areas. However, some studies, such as by Agapiou [3], utilize RGB indices to identify various vegetation types. This analysis reveals that GLI is capable to outperform across all vegetation types. Furthermore, NGRDI index of Motohka et al. [104] is similarly shown to be profiting for the vegetation delineation, if only three band information is available. Our results are also in line with the existing literature, as GLI turns out to be the most important variable in both study areas. Furthermore, NGRDI is the second most important band in Augsburg. However, in Wuerzburg, the blue band appears to influence more than the NGRDI index. NGRDI already includes red and green band information, therefore its importance to a certain degree is expected. Although first appearing controversial, chlorophyll also absorbs in blue band, and like the red band, the blue band will show low reflectance in areas with healthy, green vegetation. Other indices and bands we use appear to have minimal to no influence, which may be because individual red and green bands do not contribute much to RF classification unless combined in indices.

What we expected to be important but did not turned out to be, is the vegetation height. Only in the trial of RF classification using DOP in Augsburg, height variable appears to have slightly higher importance, which is still much lower than the importance of GLI.

In all other set ups the importance of the height variable is extremely low. It could be, that GLI is highly representative of vegetation and thus it is repeatedly used as a variable to split the nodes. But it could also be that there is a very large variation between height values for different vegetation, i.e. tall trees in forests and low grass vegetation. Consequently, RF can not establish patterns based on this variable and therefore does not consider it during decision making.

Variable importances from the trained RF models provide valuable insights into which variables are most significant in a given context. However, it is also useful to examine how the distribution of variable values influences RF accuracy. This is referred to as an IML approach, and in this study, we utilize SHAP values from Lundberg et al. [94]. Our analysis confirms that, for DOP images, the GLI increases the likelihood of a location being classified as green. The higher the GLI value (closer to 1), the greater the probability that a pixel will be classified as green. Consistent with our earlier discussion on chlorophyll absorption of blue light, SHAP values show that lower values in both the blue and red bands increase the chances of a pixel being identified as green. These findings hold true for both Augsburg and Wuerzburg. For Sentinel-2 data, higher NDVI values from May, June, and July drive the model to predict urban green. Similar to the DOP data, lower values in the red band also indicate a higher probability that a pixel will be classified as green.

Interestingly, in Wuerzburg, the SHAP values for some variables illustrate more than two peaks in value distribution. These are obvious for variables, such as red band of June, NDVI of February, NIR of May and others. This suggests that the mentioned variables have two different value ranges that contribute to positive or negative predictions. This phenomenon could be attributed to the training dataset. For instance, if the training data includes sparse or less healthy vegetation, the red light may not have been absorbed as effectively as in healthy vegetation. Consequently, the model identifies two distinct value ranges for the red band that represent green space. This behavior, stemming from the training dataset, can also be attributed to other variables with several value peaks.

When we express that our classification yields high accuracy, we rely only on the model statistical measures. Since study areas are much larger that the size of the training data, to be able to conclude on the precision of the classification, a validation procedure is a must. Nevertheless, the absence of accurate UGS maps makes the validation procedure almost impossible. In order to counteract this disadvantage, we do create validation map from the TN dataset. Yet, this dataset is missing privately owned green areas, such as private forests. Moreover, none of the existing datasets captures back and front yard green, or street level trees and grasses.

Based on the acquired results, we observe considerable differences not only in terms of how much green is identified, but also in how well certain green spaces are identified. As such, in Augsburg we identify 75.1 km^2 of green using DOP and 85.9 km^2 of green using Sentinel-2 imagery. Moreover, based on the green space validation dataset, that is com-

prised of various green space types from the TN dataset, the area of green in Augsburg constitutes 79 km^2. The RF classification encounters slight problems due to a mismatch occurring in the DOP image. A very small part in the south of Augsburg was captured on different dates. Due to the varying lighting conditions, reflectance values here appear slightly lower than in the rest of the DOP. Therefore, we suspect that variations between e.g. vegetated pixels and pixels that represent shadows is not high enough. Therefore, some shadows of trees are classified as green. In the rest of Augsburg, we do not encounter such issues. It is important to note, that the validation dataset is not as detailed as the classified image. This means, that in the area of the DOP tile mismatch, RF failed to delineate single tree crows (as RF did elsewhere) and classified shadows as green. But when comparing to the TN dataset and looking at the total identified area, RF did not over-predict vegetation.
In Wuerzburg, predicted values equal to 43.8 km^2 and 48.9 km^2 of green identified using DOP and Sentinel-2 data respectively. In comparison, the TN validation dataset accommodates 40.7 km^2 of green in Wuerzburg. Although identified values differ from the TN dataset, we identify a considerable amount of small-scale green that is not captured elsewhere. Especially when examining the Figure 6.18 at a greater detail, we can see differences in identified UGSs based on Sentinel-2 and aerial image. It is clear that fine green information cannot be captured as precisely with 10 meters resolution, like it could be with 20 centimeters resolution. However, it is also important to note, that at such a fine scale, open areas with no particular purpose, that visually appear green, are also classified as UGS. In the existing literature, there are hints that the classical per-pixel classification techniques might be less advantageous to identify green areas, than e.g. OBIA, due to spectral diversity associated with a specific LU in question [119]. Consequently, combination of pixel and object based classification can counteract the over-identification in some areas and reduce effects associated with the absence of e.g. NIR band in the DOPs.
Based on the acquired results, we consider some optimization options. Firstly, we collect 1800 training points, with a special emphasis on including all possible types of green spaces. A training dataset of a similar size utilized by Abdi [1] was adequate to achieve good classification output. However, collection of pure training points in two study areas is a manual and time consuming process. It is possible to acquire training data from others sources, like Chen et al. [27] use crowd-source information for training purposes, or Weigand et al. [147] uses LUCAS data points as a training dataset. However, none of these approaches can provide as detailed green space information as we require for the purpose of creating detailed green space maps. Thus, this makes collection of training data manually our only option. Secondly, we consider different processing requirements as it determines the feasibility of performing an ML classification. Number of collected training data, especially when divided into 70/30 proportion is not as time-intensive. Nevertheless, making prediction on huge study areas is computationally heavy. Considering these aspects, it would be wise to train such a model that can make accurate predictions

in new study areas. This is called transfer learning, when a trained model is applied to a totally new area. Furthermore, parameters of this model need to be repeatedly tested so that they are generalizable to other spatial contexts.
Our results show, that the RF model trained with under 500 trees and only one mtry in Augsburg, has great potential for predicting green areas in Wuerzburg. However, we do observe differences in total predicted areas. Under a detailed examination, these differences appear particularly in agricultural areas as well as in tree crowns. When RF is trained on the training data from Wuerzburg, it is much more capable to delineate single crowns. However it fails to do so, when RF is trained on the Augsburg data. We assume, that the pixels surrounding crowns or shadows have similar reflectance as some green areas in Augsburg. Similar behavior can also be observed alongside the river. Here as well, reflectance values could be very similar to some green areas in the training dataset. Spatial resolution of Sentinel-2 datasets appear to have even more influence during transfer learning. We notice these especially in its complete disability to separate e.g. shadows from green. However, we also establish that forest areas do not have as high overestimation as build up areas. This is probably because forests are homogeneous areas with even distribution of green intensities. It contrast, build up areas are very heterogeneous with sparse tree distribution in between. In could be that sometimes a 10 meter sized pixel includes green space, sometimes does not. Such abrupt changes from green to non-green might make it difficult for the RF model that learned slightly different values in Augsburg, to make proper predictions.
In conclusion, this study aims to address challenges in accurately mapping UGSs due to the limitations of existing LULC maps and the diverse nature of UGS types. By combining RF classification and RS data from Sentinel-2 and very-high-resolution aerial imagery, we demonstrate that urban areas contain significantly more green than LULC maps typically represent. Our comparison of Sentinel-2 and DOP imagery highlights variations in UGS detection accuracy between these data sources, with high-resolution imagery identifying smaller green that lower-resolution data often misses. Our findings reveal that vegetation indices, particularly NDVI and GLI, play a crucial role in detecting green, with high accuracy rates achieved for both Sentinel-2 and aerial imagery classifications. However, cloud coverage and the limited temporal availability of aerial imagery present challenges in data acquisition, particularly in maintaining seasonal consistency across different locations. Additionally, RF classification's sensitivity to spatial resolution emphasizes the importance of balancing spectral and spatial qualities in UGS mapping.
This study also demonstrates that transfer learning can reduce the time required to create training data in new study areas. However, usefulness of transfer learning depends on the specific research questions. For example, if the goal is to produce a UGS map showing the general distribution of various green without needing precise boundary delineation, DOP imagery with a transfer RF model could be used. This map would appear similar to generalized TN maps but would also include street-level greenery. On the other hand, if

the objective is to delineate green areas more precisely including individual tree crowns, training data specific to the study area for classifying DOP data is essential. The use of Sentinel-2 with RF can accurately identify large, homogeneous green areas such as forests, though it struggles to identify scattered green spaces. Therefore, for mapping large green areas, Sentinel-2 and RF may be a more time-efficient choice. Overall, DOP imagery with RF produces the most precise green distribution maps, but it is a cost-intensive procedure.

The main limitation of this study is the lack of an accurate UGS validation dataset. While we demonstrate the methodology's applicability statistically, our ability to validate the results is limited. Creating accurate validation datasets, which would likely involve a manual digitization process, is essential for future research. Improving the transfer learning approach could facilitate a scalable solution to UGS mapping. Although this study shows that the proposed approach is promising, it does not fully explore tuning opportunities. Furthermore, combining pixel-based and object-based classification methods could mitigate over-identification in open green areas while improving the detection of specific UGS types - an area that also requires further exploration.

Chapter 7

Urban Forest

Starting from this chapter, we present our approach to knowledge-based UGS mapping. Therefore, we first present how forests are described in the existing local and global definitions. Moreover, we synthesize presented forest definitions to create one that makes it more suitable for spatial analysis. We then conduct a workflow to showcase how urban forests can be identified using their unique semantic characteristics. To asses efficacy of the proposed approach, we conduct an analysis in two study areas, and describe transferability of the proposed workflow.

7.1 Definition of Urban Forest

What is a forest? How do we define it? While the questions are clear, answers to them are not always straightforward. From a botanical perspective, forest is characterized as a vegetation dominated by trees, covering an area large enough to enable development of a forest climate[1]. This distinguishes forests from, for example, tree-lined avenues, parks or tree nurseries. In order to understand the complexity of defining forest, we present two different forest definitions: one at a more general and the other one at a national level.

The Food and Agriculture Organization (FAO) of the United Nations defines forest as a land area larger than 0.5 hectares, populated with trees surpassing height of five meters and possessing a canopy coverage exceeding 10 percent, or having the potential to meet these criteria in situ. This definition specifically excludes areas primarily used for agricultural or urban purposes, emphasizing importance of tree presence and the exclusion of dominant alternative LUs. It encompasses regions where young trees have yet to grow, but are anticipated to reach the expected canopy cover and tree height. Additionally, it

[1] hhttps://www.bundeswaldinventur.de/vierte-bundeswaldinventur-2022/hintergrundinformationen (accessed on 01.2025)

accounts for areas temporarily devoid of trees due to forest management activities like clear-cutting or natural calamities, with the expectation of regeneration within five years. Though local circumstances may support an extension of this period.
The FAO definition further covers forest infrastructure such as roads and firebreaks, as well as small clearings, and extends to forests within protected areas like national parks and reserves that hold particular environmental, scientific, historical, cultural, or spiritual value. It includes linear tree formations like windbreaks and shelterbelts if they cover an area larger than 0.5 hectares and wider than 20 meters, as well as abandoned lands from shifting cultivation practices showing signs of tree regeneration meeting the specified canopy and height criteria. Moreover, it recognizes forests outside legally designated areas that satisfy the forest criteria. However, it distinctly excludes tree stands in agricultural production systems like fruit trees, oil palm plantations, olive orchards, and certain agroforestry systems where crops are cultivated under tree cover[2].
Under German forest legislation, forest is broadly defined to encompass any land area populated with forest plants. This definition extends beyond merely tree-covered areas to include lands that have undergone clear-cutting or thinning, forest pathways, strips designated for forest division and protection, clearings, glades, meadows within forests, areas for wildlife feeding, places used for wood storage, and other lands linked to and serving the purposes of the forest. An area is only classified as a forest, if it is at least 0.1 hectares in size and 10 meters wide.
However, certain areas do not qualify as forest according to this law. These exclusions include lands where trees are planted with the intention of swift timber removal, particularly if such stands are managed on a cycle of no more than 20 years, known as short rotation plantations. Agroforestry lands, which combine tree cultivation with agricultural production, are also excluded. Small plots within open fields or urban areas, if they are populated with scattered trees, tree lines, hedges, or are utilized as nurseries, also do not meet the forest criteria under this law. Similarly, lands populated with forest plants but located on or adjacent to railway paths - including those within service facilities and extending to a specific width alongside the tracks - are also not classified as forests.
Furthermore, this legislation provides flexibility for states to adapt these definitions by potentially including additional lands as forests or excluding certain types of cultivated areas, such as Christmas tree farms as well as parks linked to residential zones, from the forest definition. This nuanced approach allows for a degree of customization in how forest land is categorized, reflecting the diverse nature of LU and management practices across different regions[3].

[2]`https://openknowledge.fao.org/server/api/core/bitstreams/531a9e1b-596d-4b07-b9fd-3103fb4d0e72/content` (accessed on 01.2025)
[3]`https://www.gesetze-im-internet.de/bwaldg/BJNR010370975.html` (accessed on 01.2025)

7.2 Semantic Features of Forests

In previous section we present the FAO as well as the German national definition of forest. As our focus is on mapping forested areas, it is important to note that these definitions are intricate, encompassing details that may not be entirely quantifiable or depictable through spatial datasets. Consequently, to enable mapping of forests based on these definitions, we synthesize elements from both the FAO and German definitions. This synthesis helps highlighting fundamental features of forests that shape their semantic essence and contribute to their semantic profile while facilitating their identification. In this work, forests are:

- Areas populated with tree species.
- Areas larger than 0.5 hectares.
- Areas populated with trees with height higher than five meters.
- Areas not covered by other LUs, e.g. agriculture and urban LU.
- Areas where young trees have yet to achieve expected tree height.
- Areas covered with tree stands that are not in agricultural production systems like olive orchards or vineyards.
- Areas covered with woody vegetation that do not follow scattered tree, tree lines, and hedges pattern.
- Areas covered with forest plants that are not adjacent to railway paths.
- Areas covered with linear tree formations like windbreaks and shelterbelts with an area greater than 0.5 hectares and wider than 20 meters .

We pay attention to incorporate a comprehensive range of elements from the existing definitions into our analysis, carefully choosing or redefining aspects that can be quantified or recognized through spatial datasets. Consequently, in the following we describe how exactly we derive representations of forest semantics from spatial datasets and how we combine them together to create final forest areas.

7.3 Forest Modeling

Upon establishing criteria for an area to be identified as a forest, our next step involves generating spatial features that facilitate its mapping. This process demands the acquisition of datasets that can accurately capture the vertical extent of spatial elements, ensure a uniform distribution of these elements (specifically trees), and distinguish forested areas from non-forested LUs like agriculture. The process of identifying forests within the designated study areas adheres to the methodology depicted in Figure 7.1. We first test the workflow in the city of Augsburg. Afterwards, we use thresholds for the most important variables, identified through the SA, to map forests in Wuerzburg.

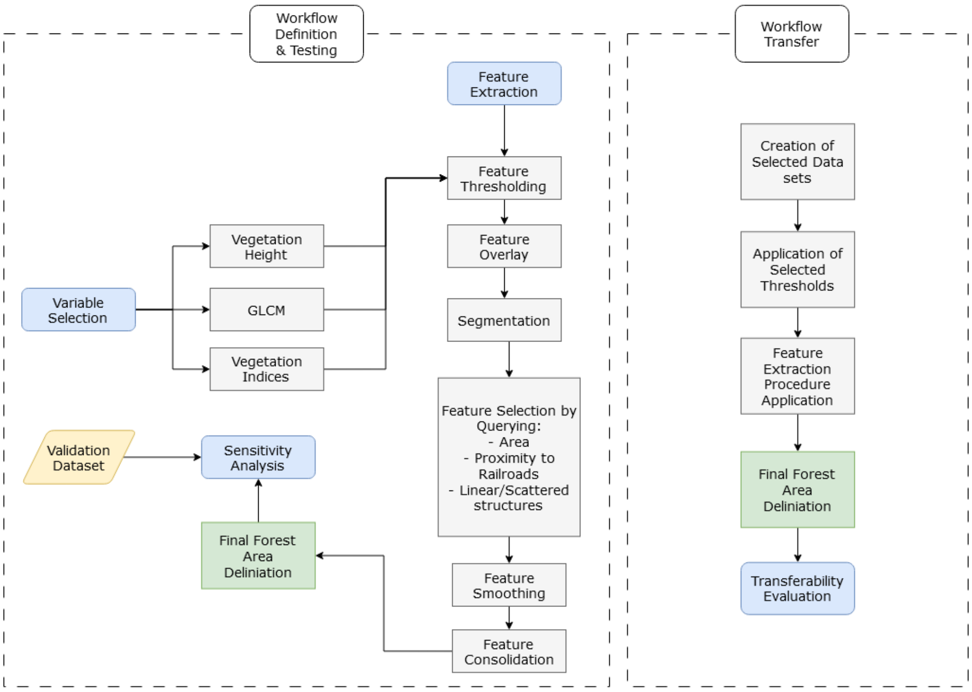

Figure 7.1: Forest identification workflow in both study areas.

The forest definition we propose indicates that the trees in a forest should be taller than five meters. Therefore, the first parameter to be identified is tree height. In order to achieve this we utilize the nDSM dataset, as outlined in Chapter 4. Urban scene can be very complex since it hosts various features that might exceed five meters in height, not limited to trees alone. Furthermore, forests are living habitats, where older trees might be cut, while younger trees are yet to grow and reach five meters. Hence, it's crucial to grasp the general variations in height within forested regions, as a singular height measurement is insufficient for distinguishing trees from other objects or including younger trees within the same forest. Therefore, we first determine the variations of heights within known forest locations. These known forest locations are extracted from the TN dataset. TN captures all the publicly owned LUs, including forests. While the private forests are not included into this dataset, the area of public forests is large enough to understand height variations.

The process of identifying forest height distribution involves extracting pixel by pixel height value from the nDSM dataset within each forest polygon. The nDSM dataset is a product of DSM and DTM datasets with varying spatial resolutions. Thus, there might be inherent uncertainties in the height information. In order to exclude outliers from the extracted dataset and encapsulate the central 90% of the height variations, we cut off

the dataset below the 5th and above the 95th percentiles. This way we produce a binary height dataset, for both study areas, that is thresholded using the values above 5th and below 95th percentiles.
In addition to the pre-defined height range, the proposed forest definition also states that forests are areas covered with tree species and are larger than 0.5 hectares. This means that forests appear as patches with similar tree coverage. It is known to us that the forests in both study areas are mostly mixed forest of both deciduous and coniferous species. As a result, these regions exhibit distinct textural features, characterized by the intermingling of large deciduous tree crowns with the slimmer crowns of coniferous trees. Textural characteristics of spatial objects can be described using the GLCM method proposed by Haralick [65] and described in Chapter 3. In this work, main usage of the GLCM is in understanding forest area. Forests, especially those with a mix of coniferous and deciduous trees, exhibit significant texture variability due to the differences in tree canopy structure and density. Coniferous trees tend to have a more uniform texture compared to the varied texture of deciduous forests. Therefore, from the existing texture metrics, we select the dissimilarity as the texture metric to understand the change of grey levels in forest areas. GLCM metrics are typically derived from gray scale images. Frequently, images depicting a variety of vegetation indices are used, particularly for UGS analysis [149]. However, we argue that vegetation indices like NDVI are calculated from spectral bands and consequently represent a condensed form of information. Additionally, their value typically range from -1 to 1, which further limits the variations in the data. To capture more detailed gray scale levels beyond what vegetation indices can offer, we utilize raw spectral bands. Forest, as any other vegetated area, undergoes phenological changes throughout the seasons. However, mixed forests demonstrate even more peculiar changes due to the mixture of evergreen and deciduous vegetation. To be able to adequately capture these changes, we utilize temporal Sentinel-2 imagery in both cities.
In order to include sufficient amount of information, yet to reduce the amount of data and processing time, we use one image from each spring, summer, and winter season. Consequently, for Augsburg, we select Sentinel-2 images captured on the 27th of March, 15th of June, and 17th of December of 2022. We produce exactly the same datasets also for the second study area. Here, we use as well the Sentinel-2 images from the 7th of March, 13th of June and 20th of December 2021. A detailed description of all included Sentinel-2 images is given in Chapter 4 in Table 4.1 and 4.2 for Augsburg and Wuerzburg respectively. Moreover, we calculate GLCM only on bands two and three. This is because both of these bands have 10 meters resolution and allow a higher information gain. Further, these bands are not part of vegetation indices that we included into the analysis. This way we reduce the possible correlation between the bands and indices. Therefore, similar to our approach with the height dataset, we generate binary dissimilarity datasets for three dates utilizing a thresholding method. We establish the lower and upper thresholds at the 5th and 95th percentiles of dissimilarity values that occur solely within forested

areas. To achieve this, we first extract dissimilarity values for forest polygons and then calculate the percentile values and use them as thresholds.
Other than the choice of grey scale image, size of the moving window to calculate GLCM must be carefully selected. Size of the window matters, as it should be able to capture fine grey level changes within the window, yet be able to ignore the present noise. Commonly, the size of the moving window will be set similar to the utilized image resolution [149]. Nevertheless we utilize a 3x3 window size, the smallest possible in most modern, GLCM implemented, software. With the selected window size we try to compensate on the 10 meters resolution of the utilized images. It is also important to note, that texture analysis is based on descriptive statistics that varies across different contexts, and can be influenced by changes in image scale and window size [64]. In order for the analysis to be comparable across both study areas, we perform regional GLCM analysis [149]. We implement in RStudio software version 4.2.2.
Tree height and density significantly distinguish forests, yet presence of vegetation in these areas is a primary identifier. Therefore, it is vital to emphasize areas that are genuinely "green" and further meet specific criteria for height and homogeneity. To accentuate vegetation in our study areas, we choose the NDVI index and compute it following Equation 3.4. Similar to the approach taken with the GLCM index, we incorporate temporal NDVI analysis into our study. We calculate NDVI for more than three dates, which is an extension of our previous approach with the dissimilarity index. This enhances our understanding of the overall vegetation status and its changes over nearly a year in the study areas. Hence, for Augsburg, we calculate NDVI indices using Sentinel-2 images captured on the 10th of February, 27th of March, 21th of April, 11th of May, 15th of June, 25th of July, and 17th of December 2022. For Wuerzburg, we calculate NDVI indices using images captured on the 28th of February, 7th of March, 26th of April, 31th of May, 13th of June, 18th of July and the 20th of December 2021. The slight temporal differences occur due to the availability of the cloudless datasets in both study areas. Here, once again, we produce binary NDVI datasets using exactly the same approach as for the nDSM and dissimilarity datasets. We first extract NDVI values of each date under forest polygons, calculate the 5th and 95th percentiles, and finally use these values as the lower and higher thresholds to reclassify the initial NDVI datasets in both cities.
We proceed in the forest identification workflow by combining the reclassified binary nDSm, NDVI, and dissimilarity datasets. Since our final goal is to identify forest and non-forest areas, we produce a multiplication product of the selected layers. This product serves as a base to create final forest polygons. However, this procedure produces a pixel by pixel binary image and it is necessary to group these pixels into forest objects. Therefore we create forest objects using Mean-Shift Segmentation by Fukunaga and Hostetler [55], which is describe in detail in Chapter 3. We use ArcGIS Pro Version 2.3 to carry out the segmentation. Through a process of trial and error, we identify the most appropriate values for the segmentation parameters. We determine that a spectral detail of 15.5, a

spatial detail of 15, and a minimum segment size of 20 produce the most accurate results, especially, in terms of eliminating small non-forest pixels.
The next step of the post-processing is to identify polygons that meet the 0.5 hectares criteria. Thus, we select every polygon that does not meet this criterion and exclude it from the forest dataset. In order to establish whether further forest rules are met, namely presence of agricultural production systems on identified forest areas, presence of woody coverage that follow scattered tree, tree lines, and hedges pattern as well as adjacency of forest polygons to railway paths, we perform three additional steps. We first identify the proportion of forest polygons laying over the agricultural polygons by erasing non overlapping polygon parts. Here we use the TN agriculture dataset as a base for overlay operations. We further calculate how many forest polygons are located in at least 100 meter proximity to railroads. And finally, we describe the forest polygons' shape using the circularity index given in Equation 7.1.

$$Circularity = \frac{4\pi \times \text{Area}}{\text{Perimeter}^2} \tag{7.1}$$

Circularity values span from 0.0 to 1.0, with values near one indicating a shape that is more circular. Conversely, values approaching 0 indicate that the shape is more elongated. In order to improve the appearance of the resulted forest polygons we smooth out their borders using 100 meters smoothing tolerance. We also close possible holes within the forest polygons by dissolving them with their adjacent polygons.
What we identify using the knowledge-based approach, is forest objects. However, just like in case of TN polygons, these objects do not express how much green they store, but rather how large areas they cover. Consequently, we use the urban green map created in Chapter 6 using DOP, and calculate the amount of green stored within identified forest polygons.
Aforementioned processes, including binary raster merging and subsequent result refinement, are initially carried out only in Augsburg. Upon determining the most important variables, we apply established thresholds to detect forested areas in Wuerzburg. Therefore, we create binary datasets in Wuerzburg by only utilizing thresholds from Augsburg. Consequently, we perform transferability analysis and assess the potential of the proposed workflow to map forests in two different cities.

7.4 Feature Importance Determination

We describe and select a number of variables to identify forests. Especially, we include temporal information into the analysis to ensure the highest information gain. However, this produces a large number of variables that may or may not improve the identification accuracy. Therefore, we perform a local feature SA in order to identify which of the selected variables have the highest impact on the identification accuracy. We perform SA separately first for dissimilarity indices and then for vegetation indices. We keep nDSM as a constant variable in both groups, as vegetation height is the most prominent forest indicator.

We calculate sensitivity of each selected variable following the OAT feature selection approach. In Chapter 3 we already described various possibilities of feature importance determination. Here, we examine the deviation of the model's accuracy from the actual accuracy observed in the validation dataset as a result of excluding variables from the model one-at-a-time. The procedure is set up as following: Let each raster be represented as R_i, where i equals the number of rasters. The first step involves creating a composite product P_{-i} by multiplying all the rasters except R_i, following Equation 7.2.

$$P_{-i} = \prod_{\substack{j=1 \\ j \neq i}}^{n} R_j \tag{7.2}$$

where n is the total number of variables and j represents the index of these variables while making sure that all rasters except the *i-th* one are included in the multiplication. Furthermore, for each P_{-i} the identification accuracy A_{-i} is calculated and evaluated against the accuracy of the validation dataset, denoted by V. Unlike the ML methods where only 100% accuracy can be reached, this task may result in overestimation or underestimation of forest identification accuracy. In order to account for bidirectional accuracy changes relative to V, we derive percentage deviations of A_{-i} from V. This method enables us to quantify the extent to which accuracy diverges from V, when one or more variables are excluded from the analysis. Consequently, the percentage deviation, D_i of A_{-i} from V is calculated using Equation 7.3.

$$D_i = (\frac{|A_{-i} - V|}{V}) \times 100 \tag{7.3}$$

We use the TN forest dataset as a reference for accuracy assessment. Consequently V, that we use to assess accuracy deviation, is the area of forests in this dataset. Based on the deviation calculation, we define those variables whose exclusion from the analysis results in the largest deviation, as the most influential variables.

7.5 Results

We identify forests in Augsburg by combining height, texture, and vegetation indices along with their derived thresholds. Additionally, through the use of the OAT SA, we determine the most influential variables for forest mapping. By utilizing thresholds, derived from datasets of Augsburg, we extract forest areas in Wuerzburg and assess the transferability

of the proposed workflow.
To derive thresholds, we utilize TN forest dataset as reference data. This data is comprised of approximately 600 polygons in total with an area of nearly 35 km^2. As a minimum and maximum threshold, we extract the 5th and 95th percentiles accordingly. Our results, shown in Table 7.1, present a comprehensive overview of minimum and maximum thresholds across all the utilized predictor variables.

Table 7.1: Threshold values of all the utilized predictor variables in Augsburg, extracted using the 5th and 95th percentiles.

Variables	Minimum Threshold	Maximum Threshold
nDSM	0.712	28.935
March B2 dissimilarity	0	0.333
March B3 dissimilarity	0	0.556
June B2 dissimilarity	0	0.333
June B3 dissimilarity	0	0.555
December B2 dissimilarity	0	1.333
December B3 dissimilarity	0	1.445
NDVI 02	0.176	0.451
NDVI 03	0.188	0.415
NDVI 04	0.226	0.433
NDVI 05	0.332	0.606
NDVI 06	0.340	0.655
NDVI 07	0.378	0.612
NDVI 12	0.047	0.180

We first explore the height dataset and establish, that the height distribution over the existing forests in Augsburg is between 0.08 and almost 30 meters. This wide range showcases the significant variability in forest canopy heights within Augsburg, highlighting the diverse forest structures ranging from young to mature wooded areas.
Textural dissimilarity in the green and blue bands during March, June, and December shows a uniform minimum threshold of 0 across all instances, indicating a baseline textural similarity in forested areas. Furthermore, the maximum thresholds of March and June constitute to 0.333 and 0.555 for band two and band three, respectively. In contrast, December's maximum thresholds reach up to 1.333 and 1.445 for band two and band three accordingly. This suggests a significant textural deviation in forested areas during

this month, in comparison to other examined months, potentially due to seasonal changes affecting leaf-off conditions in deciduous forests.
NDVI, a critical index for assessing vegetation health and coverage, presents thresholds that progressively increase from February (NDVI 02) through June (NDVI 06), with minimum values gradually rising from 0.176 to 0.047 and maximum values stretching from 0.415 to 0.655. This trend indicates a growing vegetation density and health leading into the summer months. The slight decrease in May (NDVI 05) and July (NDVI 07) to a maximum threshold of 0.606 and 0.612, followed by a drop to 0.180 by December (NDVI 12) highlights the phenological characteristics of vegetation growth within the study area.

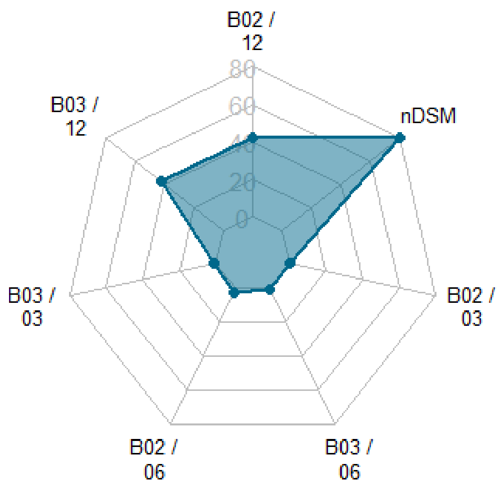

Figure 7.2: A star-plot illustrating variable importance of temporal dissimilarity indices as well as nDSM, derived using OAT technique in Augsburg.

We conduct a SA using the OAT technique to determine the impact of excluding individual variables on the identification accuracy. We use the TN dataset to establish how much accuracy will deviate from the TN's accuracy, if one of the variables is dropped. We first evaluate the effect of excluding height (nDSM) and dissimilarity texture metrics for bands two and three, which is illustrated in Figure 7.2. We observe that the omission of the nDSM variable results in the most significant deviation, with an estimated change of approximately 60% from the TN forest areas. This is indicates that the nDSM variable plays a critical role in the forest area estimation.
Following this, the exclusion of the December band 2 and band 3 variables shows a moderate impact on the results, with deviations around 10-15%. The sensitivity of the estimations of the June and March variables is lower, suggesting a lower influence of these temporal metrics on the final forest area estimations.

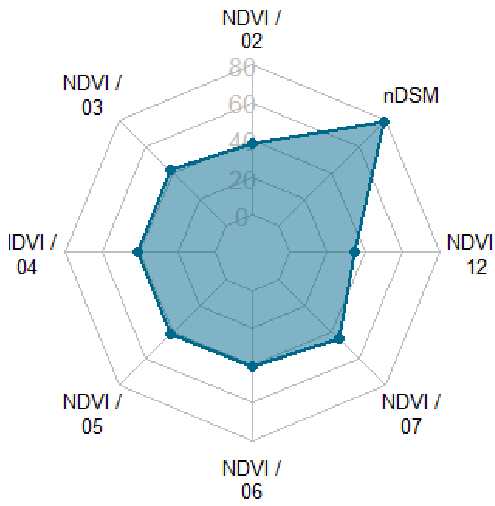

Figure 7.3: A star-plot showing variable importance of temporal NDVI indices as well as nDSM, derived using OAT technique in Augsburg.

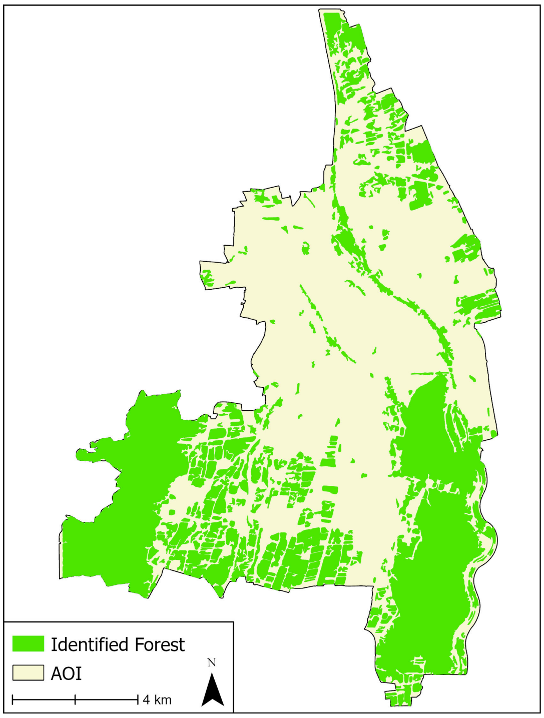

Figure 7.4: Map of the identified forest in Augsburg with nDSM variable dropped.

Furthermore, we investigate the impact of temporal NDVI indices on the forest identification accuracy, given in Figure 7.3. Here, we also include the nDSM variable to explore to what extent its influence remains if vegetation indices are incorporated. Similar to the case with texture metrics, the nDSM variable once again holds the highest sensitivity,

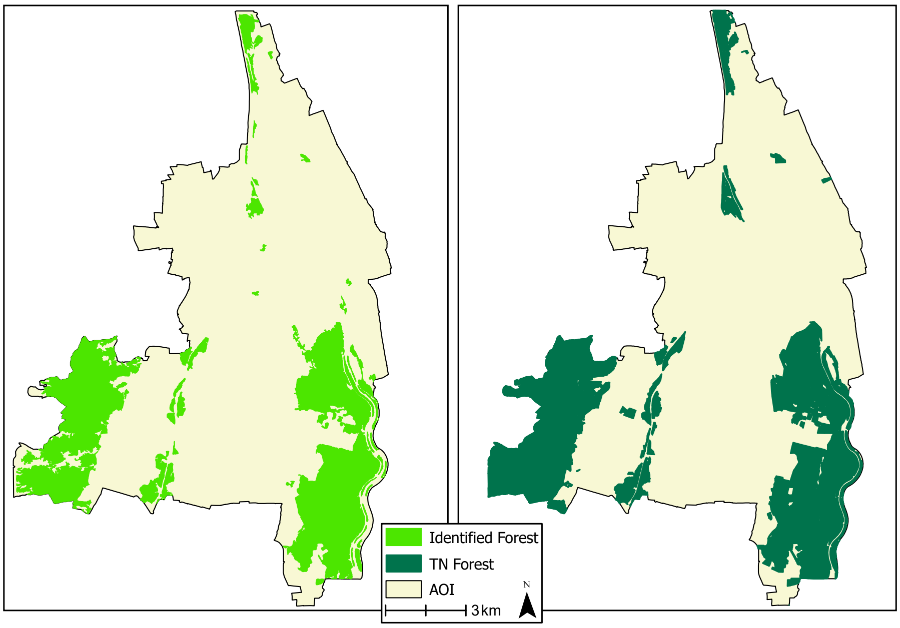

Figure 7.5: A comparative map of the results of forest identification workflow versus the TN forest polygons in Augsburg.

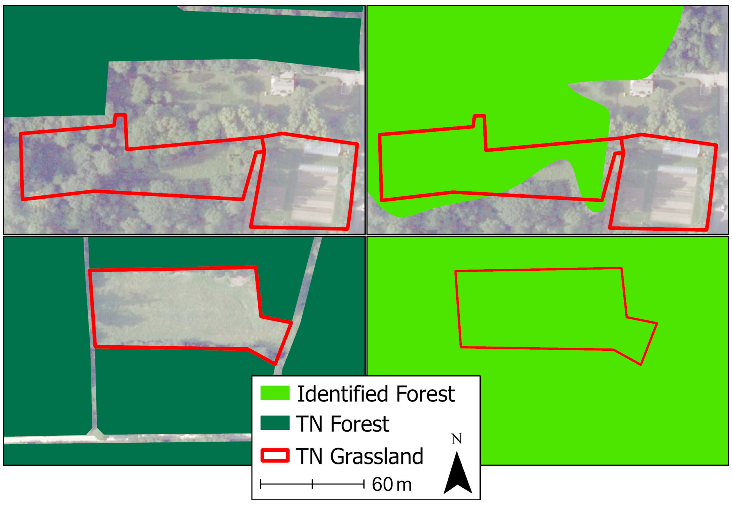

Figure 7.6: An explorative map of sample identified forest polygons as well as TN agriculture polygons in Augsburg.

indicating a potential deviation of around 60%. Among the NDVI variables, NDVI of July and March indicate higher sensitivity, with deviations exceeding 20% and 15%, respectively. The other NDVI values show variations for July and March variables, though this variation is negligible.
The importance of the nDSM variable is visually represented in Figure 7.4. In this particular example we drop the nDSM variable and utilize the remaining temporal NDVI indices to map the forest areas. As the figure suggests, a considerable amount of false predictions

is made. However, we observe a trend in the misclassification concerning agricultural areas. All the false predictions in the North-East as well as Southern areas of Augsburg are crop fields, that visually appear very similar to forest areas, despite being much lower in height. Therefore, particularly when summer season indices are used, height is the most distinguishing parameter between green vegetated areas and forests.

We establish that nDSM, dissimilarity metrics of bands two and three for December, as well as NDVI values of July are the most influential variables to identify forests. Using these variables as forest identifiers, we identify and calculate approximately 37.8 km^2 of forest area in Augsburg as shown in Figure 7.5. The map on the left showcases distribution of forests based on the performed analysis. while the map on the right illustrates forest distribution according to the TN dataset. We identify a moderately larger forest area compared to the TN dataset, totaling 35.43 km^2.

Our forest definition states, that forests should not be in agricultural production systems or be covered with woody vegetation that follows scattered trees, tree lines, and hedge patterns as well as be adjusted to railway paths. Consequently, the results of the proximity analysis reveal that there are only four forest polygons in Augsburg that emerge in lees than 100 meters closeness to local railroads. Since we already filter forest polygons with less than 0.5 hectares area, none of these four polygons show scattered tree patterns but are rather areas with densely growing trees.

In addition, we use the circularity index to describe how elongated or circular forest polygon shapes are. The circularity indices of the four polygons span from 0.13 to 0.37, indicating that the shapes are not circular but are also not exclusively elongated. This also eliminates the forest criteria of classified areas being windbreaks or shelterbelts as such areas represent tree formations planted in rows and having elongated form.

Our analysis reveal that approximately 0.4 km^2 of identified forest areas are overlapped by agricultural production areas. By further visually investigating we reveal that most of the overlapping areas are designated grasslands in the TN datasets. Sample areas of such overlap are illustrated in Figure 7.6. As shown in the figure, such misclassifications appear in areas either with gaps within the forests or in areas that are indeed covered with woody vegetation but classified as grassland in TN. Lastly, using the urban green map from Chapter 6, we calculate approximately 22 km^2 of green stored within identified forest polygons.

Finally, we utilize variables selected as important for Augsburg, and their threshold values, and apply them to Wuerzburg. In order to establish to what extend the threshold values are transferable to the new area, we use the TN forest datasets of Wuerzburg as a validation dataset. A comparative map of Wuerzburg, showing identified forests and forest distribution in TN dataset, is given in Figure 7.7. Consequently, using the nDSM, the dissimilarity texture index of bands two and three of December, as well as the NDVI values from July, we identify 19.6 km^2 of forest in Wuerzburg. In the TN dataset the forest area in Wuerzburg equals to 13.7 km^2.

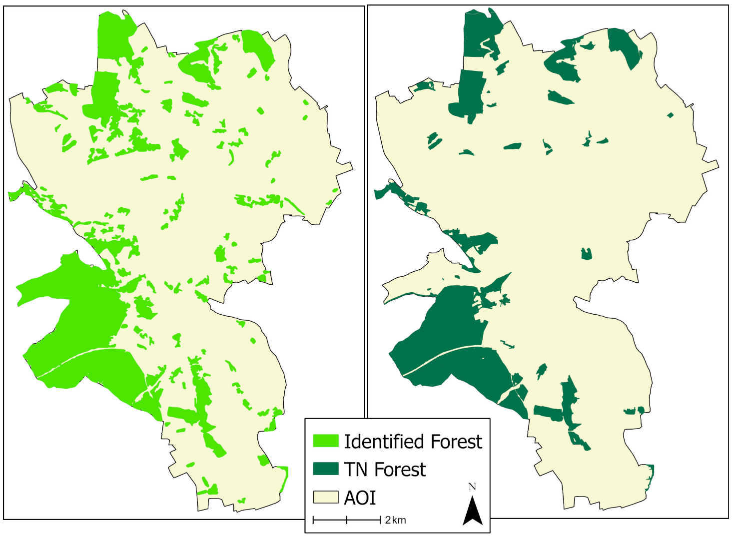

Figure 7.7: Map illustrating comparison of identified forest polygons with TN forest polygons in Wuerzburg.

In Wuerzburg, we also explore how close the identified forests are to railroads, how elongated these polygons appear, and whether some agricultural production sites are falsely identified as forests. Consequently, from the 126 identified forest polygons, only 16 are located in 100 meter proximity to local railroads. The circularity of these polygons ranges from 0.13 to 0.89, indicating shapes are in a middle range, not exactly elongated but also not circular. From the identified forests, nearly 1.5 km^2 of identified forest polygons overlap agricultural production sites.

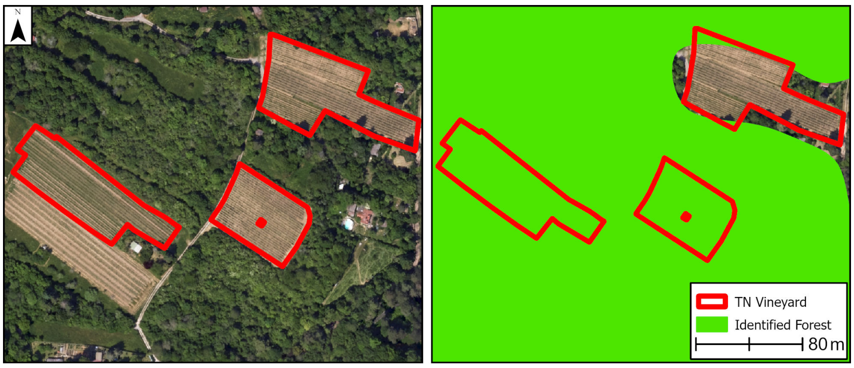

Figure 7.8: Map of the misclassified forest polygons at a greater detail in Wuerzburg.

After a detailed examination, we observe that a great number of polygons are falsely classified as forests. Upon visual examination, we establish that a majority of these false classifications appears in agricultural production sites, particularly in vineyards. Figure 7.8 represents a snippet of vineyards that are classified as forests while clearly being crop production cites. Forest-like appearance of viticulture, as well as a broad range of height threshold values make it challenging to eliminate such false classifications. When compared to the urban green map produced in Chapter 6, identified forest polygons in Wuerzburg accommodate nearly 11 km^2 of urban green.

7.6 Discussion and Conclusions

In this chapter, our aim is to identify forests as a specific type of UGSs, executing spatial and semantic features derived from established forest definitions. To achieve this, we begin by combining two pre-existing definitions of forests into a singular, more spatial analysis-oriented definition. This newly synthesized definition then guides us in the creation of spatial datasets for each forest descriptor, enabling us to map forests within our selected study areas.

We conceptualize forests as regions populated by tree species that achieve a minimum height of five meters. This definition is inclusive of areas where trees have not yet reached this height but are anticipated to do so. Considering the significant height variation, from completely barren areas to those with trees surpassing five meters, it is important to first extract the height variations in existing forests and use these thresholds to map forests. While Airborne LiDAR systems represent the forefront in measuring forest height distributions [128][132], digital photogrammetry offers a more cost-efficient alternative [107][10]. Consequently, due to its availability and cost efficiency, we utilize the nDSM dataset to monitor height variations within existing forests in Augsburg. Our findings reveal a broad range of height variations in these forest locations, spanning from as low as 0.7 meters to nearly 29 meters. A comparative study, conducted by Balenović et al. [10], examines to what extent tree height can be adequately predicted using photogrammetric stereo-measurements and evaluates their results with the help of field measurements. For tree species that can also commonly occur in the southern German forests, e.g. sessile oak, European beech, wild cherry, and European aspen, tree height is in a range between around 19-22 meters. It is critical to note that this study measures heights of individual trees rather than an entire forest area, as our study does. Despite the challenges in identifying individual trees using aerial images with a 30 centimeters spatial resolution, the study successfully predicts trunk heights. Given that our nDSM dataset incorporates DSM data acquired through similar photogrammetric methods, and by checking predicted tree height at random locations, we state that the nDSM dataset makes realistic predictions of tree heights.

In addition to adequately representing tree heights in forests, based on the OAT feature selection, nDSM showcases the highest importance among all the predictor variables. This is particularly relevant when distinguishing forest from other green homogeneous areas such as agricultural fields. A clear example of such a confusion is illustrated in Figure 7.4. Here we can observe, that every single crop field which is vegetated throughout the selected temporal span, is misclassified as a forest once the nDSM variable is dropped.

Therefore we can clearly state that, in the implemented setup, removing the nDSM layer will drastically reduce the identification accuracy and will lead to a great confusion of forests with other UGSs.
Furthermore, we utilize NDVI as a primary metric for assessing "greenness". Observations of temporal NDVI value changes in forests, from 0.4 in February to 0.65 in June, followed by a decrease to 0.18 in December, demonstrate a clear alignment with seasonal greenness variations. Which in turn reflects mixed species composition of the forests. Furthermore, Aryal et al. [9] highlight that NDVI values between 0.19 - 0.5 represent sparse or shrubby vegetation, whereas values above 0.5 are allocated for tree species. Therefore, we can explain our NDVI values of around 0.18 - 0.4 with the leaf-shedding season in deciduous forests from fall to winter. Moreover, summer NDVI values of approximately 0.6 are also inline with existing literature, clearly representing tree species in the forests.
The SA of temporal NDVI datasets suggests that the NDVI data from July plays a more significant role in identifying forests compared to other months. However, upon examining the feature importance in Figure 7.3, we find that the differences in importance among the NDVI data from different times are minimal. We attribute these negligible differences to the diverse composition of tree species within forests. Mixed forests consist of coniferous trees, which usually have narrower crowns, and deciduous trees, which have larger crowns. As a result, even when deciduous trees shed their leaves in winter, the coniferous trees do not occupy enough space to significantly alter NDVI values during the colder months. Consequently, single NDVI readings (e.g. 5th percentile) for a large forested area remain relatively stable and homogeneous across seasons, showing higher values in summer and lower values in winter.
Our definition of a forest states that the area must be at least 0.5 hectares in size, should not be comprised of isolated individual trees, and must not be characterized by linear formations. This means that visually forests appear as homogeneous and large polygons with more of a rounded form than a linear shape. Therefore, by taking into account mixed forest composition and homogeneous distribution of trees, we represent these semantic nuances with the help of texture metrics. Dissimilarity is one of the common texture metrics used to understand LC patches and is superior in expressing spatial dynamics within UGSs [149]. The minimum threshold we derive for dissimilarity is 0 meaning they have a completely uniform texture where all pixel pairs have the same intensity. The maximum threshold spans from 0.3 to 1.4. The maximum value typically depends on the type of the grey image utilized. However, closeness to 0, once again, indicates more homogeneous areas. According to Park and Guldmann [111], presence of large, dense forests with complex shapes leads to higher dissimilarity values, especially along the peripheries. Thus, the increase of the dissimilarity value in December to 1.4 from 0.3 in March and June, can be attributed to the foliage change that affects forest outlines.
The SA outputs, that dissimilarity indices calculated for December have higher information gain than of June and March. We can explain this phenomenon by the visual and

textural appearance of forests in December. Once the deciduous trees loose their foliage, the visibility and distinguishability of the forest structure can be enhanced. This can make it easier to identify forests based on the structural differences rather than on the color or density of foliage that might be more evident in other months.
The workflow we define is complex but it mirrors the complexity of the forest definition. As a result, we undertake an initial selection of descriptive variables for use in the analysis. Despite reducing variable count, the remaining 14 descriptors still represent a significant quantity, potentially leading to longer processing times and difficulties in replicating the analysis in different study areas. Consequently, we perform a feature selection procedure based on the SA in order to further cut down the number of predictor variables. This process helps us to identify a minimal yet effective set of variables for forest mapping, including the nDSM, dissimilarity indices of bands two and three from December, and the NDVI index for July. Therefore, we use the selected four variables and replicate the forest identification workflow in Wuerzburg.
While being located in the same state and nearly similar climatic belt as Augsburg, Wuerzburg has varying topographic differences. This is the reason why we choose to test the proposed workflow in Wuerzburg in the first place. It allows us to observe how well the similarities can be captured while tolerating the differences. Since we use exactly the same threshold values as in Augsburg, the only transferability assessment is calculating the identification accuracy in comparison to the TN dataset. In Augsburg, we calculate very close figures for both identified forest and forest in the TN dataset, with 37.8 and 35.43 km^2 respectively. However, our workflow overestimates the forest area in Wuerzburg by nearly 7 km^2. During a detailed visual examination we discover that some of the identified forest polygons are designated as "green space" or park. However, these areas fit our forest description, such as densely growing trees, low textural dissimilarity, and absence of agricultural production. Moreover, we establish that two viticulture polygons are identified as forests although being categorized as a agricultural class in the TN. Another closely located vine growing site is however correctly classified as a non-forest. This indicates that the selected threshold values, even if being capable to identify most of the forest areas, might require some fine tuning in order to be applicable in Wuerzburg.
In addition, the utilized datasets might also have shortcomings in terms of identification precision. The TN dataset, chosen for its open access and relatively high ground resolution, omits privately owned LUs. This exclusion is particularly significant in Wuerzburg, where large forested areas in the South-West are situated on private properties, thus absent from the TN dataset. Given these constraints, it is challenging to assess the efficacy of our methodology. Identifying forest areas and comparing them to the TN dataset, does not conclusively determine the inadequacy of our applied methods. To make realistic evaluations of the effectiveness of our workflow, we see a necessity to utilize a more comprehensive LU dataset or manually digitize all forest polygons.
Fluctuations in the identification of forest polygons from the TN dataset, particularly in

Wuerzburg, may also stem from the post-processing steps. To transition from a pixel-by-pixel representation of forests to more coherent forest objects, we perform a segmentation process. This process involves grouping individual pixels into larger units known as superpixels, where the choice of parameters is crucial. In this instance, we use default parameters for segmentation. One of the known downsides of segmentation is the parametrization, which is often difficult and highly case-sensitive [108]. However, differences in the final maps might be a result of parametrization settings and for the purpose of enhancing transferability to different urban settings, it might be beneficial to adjust these parameters to better suit other cities. Similarly, the smoothing of polygons to achieve a final forest representation involves setting specific parameters, such as distance. We use a 100 meter distance, which may lead to the unintended merging of some polygon parts, and thus results in false overlaps with other LUs. Such overlaps we experience, for instance, in areas where agricultural fields and forests share a common border.

Our aim in this study is not only to create a methodological workflow that allows us to precisely identify forests, but also to make this workflow transferable. In order to include all unique characteristics of forests it is necessary to select a multistage workflow. Although this workflow produces reliable results, it is very time and cost intensive. This is especially true for the feature selection procedure. The intensity of the OAT SA has many times been suggested by e.g. Saltelli et al. [124]. We first hand experience this intensity as for all the 14 variables nearly 10 spatial analysis steps are performed. Therefore, for future use of OAT, application of it on only selected features might be more appropriate to choose.

In conclusion, this study introduces a robust methodology for identifying urban forests by integrating spatial and semantic features tailored from synthesized forest definitions. By using the nDSM dataset, we achieve reliable tree height estimations that, coupled with NDVI and texture metrics, allow us to accurately distinguish forests from other types of UGSs. Feature selection and sensitivity analyses highlight the significance of nDSM and seasonal NDVI, which are vital for improving classification accuracy across different temporal conditions. Testing the methodology in Wuerzburg, however, reveals some limitations, especially in areas with privately owned lands that are omitted from the TN dataset and in topographical differences that impact threshold transferability. In total, selected semantic features are representative of forests and allow their identification with good precision. However, overestimation in Wuerzburg indicates a need for threshold fine-tuning and consideration of alternative segmentation parameters to improve transferability. Therefore, in the future work, it is important to focus on refining the feature selection process by conducting optimized sensitivity analyses on key steps, potentially making the process less resource-intensive. Additionally, using a more accurate and inclusive LU dataset may further enhance accuracy and applicability of this workflow to diverse urban settings, supporting urban planners in mapping green spaces more effectively.

Chapter 8

Allotment Gardens

In this chapter, we present the semantic mapping procedure of allotment gardens. Therefore, we first start by exploring existing allotment laws and definitions. We then establish representative semantic characteristics of allotments and further present a methodological workflow to map them. In order to assess the reproducibility of the proposed workflow, we develop and test it first in Augsburg and then apply it to Wuerzburg.

8.1 Definition of Urban Gardens

Urban gardens, also known as allotment gardens, have over a hundred years history and a heterogeneous development pattern stretching from the pre- and post-war initiatives in Northern Europe to post-economic crisis action plans in Southern Europe. Urban gardens have not always been a part of spatial planning activities but are reaction to the established political, social and economic conditions. Throughout Europe and until short after World War II, historical development of allotment gardens had a lot of similarities to each other. However, after the 1945 urban garden development pattern split into two major directions: loss of interest and negligence of allotment gardens in the West and becoming a major part of a food program to alleviate starvation in the East (e.g. Poland, USSR) [43]. Post-war urbanization trends have also affected development of allotment gardens. In Ireland, due to post war city development actions, centrally located gardening areas were turned into private housing areas. This lead to a dramatic decline in the interest in allotment gardens [52].

In Germany, despite having over 200 years of history, the booming of allotment gardens started as a response to the post-industrialisation unemployment rise. The first "Schrebergarten" was established in the 1860es by a school teacher and named after Moritz Schreber. The main goal of this gardening practice was to establish a communication

and cooperation between parents and students and to provide a playground for children of factory workers. However, the following two World Wars would turn these gardens into critical areas to produce desperately needed food. Moreover, The Goettingen gardens were established in 1996 when the local government allocated a piece of land to a group of female refugees from Bosnia for cultivation. Members were offered on-site basic German language lessons, or helped to obtain e.g. driver's licenses. Consequently, these gardens evolved into a hub for building social capital through educational initiatives and this model has since inspired most intercultural gardens in Germany [97].
According to the memorandum by the Department of the Environment Transport and the Regions of the United Kingdom, the term "allotment" is described in the Allotments Act 1925 as an "allotment garden" or a land parcel not larger than five acres, intended for cultivation either entirely as a garden farm or partly garden farm and partly farm. The Allotments Act 1922 specifies "allotment garden" as a plot no bigger than 40 poles (or 1,000 m^2) primarily used by the occupiers to grow fruit and vegetables for their own family consumption. The term allotment garden refers to a larger agglomeration of single allotments. This definition is consistent across various statutes[1].
In Germany, the federal law of allotment gardens was adopted in 1983[2]. According to this act, an allotment garden is a garden that is dedicated for non-commercial production of horticultural products for personal use, and for recreation. Furthermore, for an area to be called allotment garden, it must fulfill two man criteria: a garden must be used for gardening purposes, and it must be a part of a complex that includes multiple individual gardens and communal facilities such as a clubhouse, play areas, and pathways. The jurisprudence of the Federal Court of Justice in 2005 mandates that an allotment garden, in addition to communal facilities, must contain at least five individual gardens (verdict from the 27.10.2005– Az.: III ZR 31/05).
The size of an allotment garden is also regulated by this federal law. According to it, an allotment garden must not exceed 400 m^2 in size. In addition to specifying the size of allotment gardens, the same law sets regulations also for garden sheds. A garden shed may have a maximum size of 24 m^2. However, this limit applies only to the shed itself; terraces or covered seating areas are not included in this measurement. The regulation concerning the size of garden sheds has been in effect since April 1, 1983. Consequently, sheds built before this date may exceed the maximum size of 24 m^2. Furthermore, permanent residency is not permitted in allotment gardens, which is why garden sheds must not be equipped to allow permanent living.
There are further specifications on the exact usage of single allotments. As such, this regulation requires that at least one-third of the area in an allotment garden is dedicated to growing garden produce for personal use, like fruits and vegetables. Another third

[1] `https://publications.parliament.uk/pa/cm199798/cmselect/cmenvtra/560-iii/560iii02.htm` (accessed on 01.2025)
[2] `https://www.gesetze-im-internet.de/bkleingg/BJNR002100983.html` (accessed on 01.2025)

of gardens should be allocated for pathways, garden sheds, and terraces. The remaining third of a garden area is intended for landscape design, ornamental plants, and lawn.

8.2 Semantic Features of Allotments

In both selected study regions different types of gardening areas are present. These gardening spaces share certain similarities while also display distinct differences in both their appearance and functional purposes. For instance, community gardens showcase a collective spirit, typically featuring a mosaic of vegetable patches, communal compost bins, and occasionally several shared sheds for storing gardening tools. These spaces are not just for cultivating produce; they also act as center for community engagement. In contrast, herb gardens are often situated in public spaces like parks and are primarily focus on cultivating a variety of herbs. These gardens serve both culinary and educational purpose. Balcony or rooftop gardens are usually comprised of individual pots or small vegetable beds placed on balconies or roof terraces. Despite these distinct visual elements, translating such varied semantic data into a spatial analysis framework is challenging. Therefore, we focus only on allotment gardens.

In order to derive allotment semantics, we rely on the official allotment garden law in Germany. Here, it is crucial to note, that when we further talk about allotment garden, we consider the whole agglomeration of single allotments. When looking at allotment gardens from a bird's-eye view perspective, as illustrated in Figure 8.1, certain key features become evident: each allotment contains one, nearly uniformly sized shed within individual plots throughout the entire cluster; notably larger facility management buildings are situated at the primary entrance; a network of unpaved trails originates from this main access point, providing connectivity to every plot. When exploring overall spatial locations of allotment gardens in both study areas, it is notable that many gardens are positioned adjacent to railways or near rivers. In visual comparison, these plots tend to be smaller or more elongated near these features, whereas allotment gardens located further from rivers and railways are generally larger and more square or rectangular in shape.

The characteristics outlined can be traced back to historical developments and current national regulations governing allotment gardens. Historically, allotment gardens were allocated to railway workers for cultivating produce, leading to their frequent placement near rail tracks. Nowadays, these plots are available for rental by the general public, which has led to the emergence of more allotment gardens within urban areas. Additionally, under the "small garden" law, allotment gardens are restricted to 400 m^2 with at least five single allotments within it, and garden huts not exceeding 24 m^2 in floor area. Although there are no exact height restrictions for these huts, those constructed without an official permit typically must not exceed 3.5 meters.

Consequently, we establish the following semantic characteristics, essential for the map-

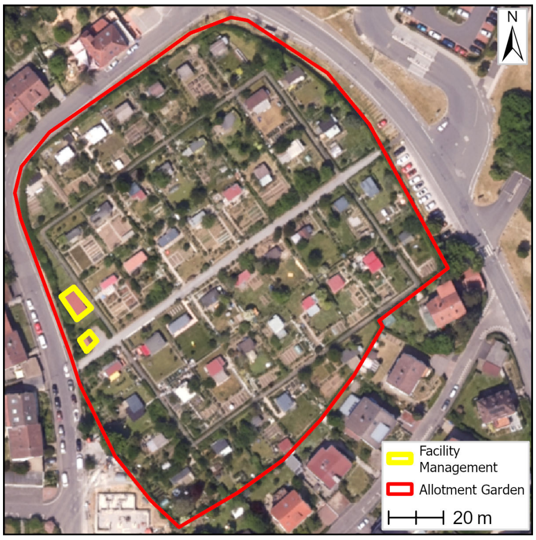

Figure 8.1: Sample allotment garden in Wuerzburg, Germany.

ping and identification process of allotment gardens:

- Shed presence: Every allotment should contain at least one garden shed.
- Shed size: The area of garden sheds must not exceed 24 m^2.
- Shed cluster: There should be at least five garden sheds within an allotment garden, indicating five separate allotments.
- Shed height: The height of garden huts should not exceed 3.5 meters.
- Path network: There should be a network of intersecting paths present.
- Road intersection: Allotment gardens should not be intersected by major roads.
- Proximity: The majority of allotment gardens should be located in close proximity to railroads and/or water bodies.

8.3 Allotment Garden Modeling

We map allotment gardens using the previously defined semantic criteria. In order to adequately capture all the fine details in small allotment gardens, we only utilize very-high resolution datasets and a three step identification workflow shown in Figure 8.2. The workflow begins by initially thresholding images of garden sheds and enhancing these thresholded regions using a map of green spaces. In the second stage, we apply techniques for delineating areas to identify the boundaries of allotment gardens. The final part of the model is focused on knowledge transfer, where we test our methodology in Wuerzburg.

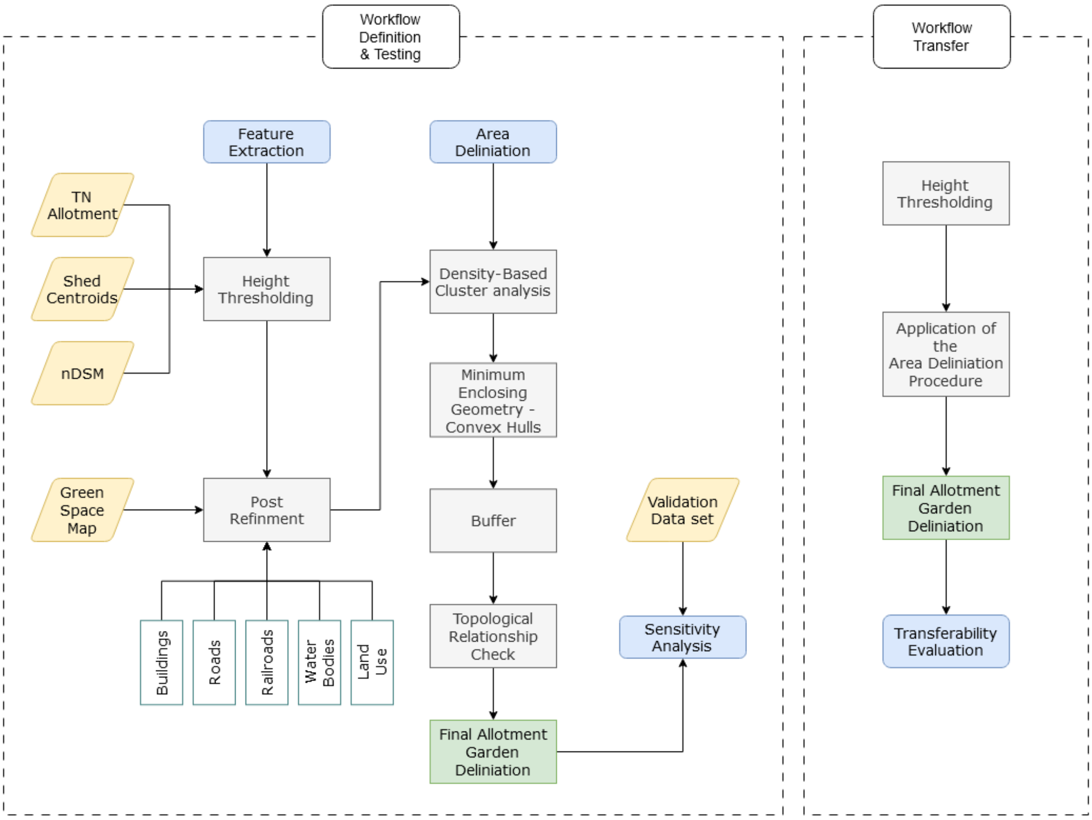

Figure 8.2: Methodological workflow to map allotment gardens.

To analyze the general height variations in allotment gardens, we manually collect approximately 200 hut centroids and extract height data from the nDSM dataset created in Chapter 4. We then calculate various percentiles for the minimum and maximum thresholds.

To effectively identify sheds, we examine four different sets of percentile thresholds: the 5th, 25th, 75th, and 95th percentiles. We conduct four testing attempts to analyze how sensitive our results are to different threshold settings:

- In the first test, we use the 5th percentile as the lower threshold and the 95th percentile as the upper threshold.
- In the second test, we set the 25th percentile as the lower threshold and the 75th percentile as the upper threshold.
- In the third test, we apply the 5th percentile for the lower threshold and the 75th percentile for the upper threshold.
- In the fourth test, we use the 25th percentile as the lower threshold and the 95th percentile as the upper threshold.

We apply all the subsequent steps in the workflow to all four test sets and explore allotment garden identification accuracy to determine the best performing threshold combination.

It is generally difficult to extract pure garden sheds by using two threshold values, because in urban settings there could be many more objects falling within the same thresholds. Therefore, we utilize supplementary datasets to improve the thresholding outcomes. These datasets include the urban green dataset created in Chapter 6 and the TN dataset. Importantly, we exclude the sport and leisure class from the latter dataset to prevent unnecessary elimination of garden objects. Additionally, we remove any thresholded objects that overlap with infrastructure elements like railroads, rivers, and roads, and building footprints. Finally, we eliminate all the remaining objects that are larger than 24 m^2 as per the allotment garden definition.

In the second stage, we refine selected "shed" objects by determining their spatial clustering. Initially, we identify sheds that have at least one other shed within a 15 meter radius. Therefore, we create buffers around them and eliminate those with an area less than 707 m^2, which is the area of a single buffer. We determine the 15 meter radius based on the findings of how close garden sheds are to each other in few gardening areas in Augsburg. For the remaining garden sheds, we use the DBSCAN algorithm. This technique is particularly effective for clustering spatial points, especially with noisy data as discussed in Chapter 3. However, specific parameters must be set before use to ensure an adequate clustering output. Since the allotment garden law stipulates a minimum of five allotments, we use this figure as our base for creating shed clusters. Additionally, we use a 50 meter cluster search radius, based on our observations of allotment gardens in Augsburg.

Once we have identified clusters of sheds, we draw minimum enclosing convex hulls around these clusters and add an additional one meter buffer to expand the hulls. This buffering process is based on the understanding that garden sheds tend to be positioned closer to the inner parts of the allotments. As a result, created convex hulls may be smaller than actual boundaries of allotment gardens.

According to the semantic criteria we define, the identified allotment gardens should be intersected by paths but not by main roads, and they should primarily be located near railroads and water bodies. To determine if the identified gardens meet these criteria, we use road, railroad, and water body datasets from the TN database. By performing spatial selection techniques, we filter out allotment gardens that either lack a path network or are intersected by main roads. Given, that the smallest allotment garden must host at least five gardens, we define the path network as a network with at least five paths. We check presence of a path network, using the TN path dataset. As this dataset lacks precision, we manually digitize missing paths within known allotment garden locations. Additionally, we use proximity analysis to determine the closeness of identified allotment gardens to railroads and water bodies.

In order to test the applicability of the proposed workflow and the identified thresholds in other study areas, we test our methodology in Wuerzburg. We utilize the nDSM dataset and the TN dataset of Wuerzburg, described in Chapter 4, and the urban green map

created in Chapter 6 using DOP and RF, to perform thresholding, refine the results and create allotment garden polygons.
We evaluate the accuracy of the proposed methodology by using the "small garden" subclass in the TN dataset. This assessment focuses on two key aspects: (1) the proportion of existing allotment gardens that are successfully identified, and (2) the accuracy with which the outlines of allotment polygons are delineated. We use both of these parameters to calculate the overall accuracy using Equation 8.1.

$$Accuracy = \frac{\text{Identified Area}}{\text{Validation Area}} \tag{8.1}$$

where identified area excludes false positives, as well as portions of polygons that do not overlap with actual polygons.
As we explore four different test cases, we perform an accuracy assessment for each one and select the test with the best-performing threshold for further transferability analysis. Finally we also explore how much green is stored within each identified allotment area. To do so, we utilize the urban green map from Chapter 6.

8.4 Results

We develop our identification workflow centered around garden sheds, starting by examining height variations of shed centroids. For this, we utilize the 5th, 25th, 75th, and 95th percentiles. Our findings reveal that shed heights at these percentiles equal to 1.93 meters, 2.22 meters, 2.62 meters, and 2.98 meters, respectively. Subsequently, we conduct four test trials to explore different percentile thresholds: Test 1 uses the 5th and 95th percentiles, Test 2 uses the 25th and 75th percentiles, Test 3 uses the 5th and 75th percentiles, and Test 4 uses the 25th and 95th percentiles.
With test 1 we identify 1.59 km^2 of allotment garden area in Augsburg. Area of allotment gardens in the TN dataset is nearly 1.7 km^2. Of the area identified, 0.5 km^2 falls into the false positive category, meaning this area is incorrectly identified as allotment when there is none. Our analysis reveals a nearly 0.8 km^2 discrepancy between the actual allotment polygons and those identified with the proposed workflow. Furthermore, 57% of the identified allotment gardens are not crossed by a path network, previously defined as a mandatory semantic criteria. Test 2 identifies 1.4 km^2 of allotment area in Augsburg, with 0.3 km^2 being false positives. We also note a 0.7 km^2 mismatch between the TN polygons and identified polygons. Within the identified allotment gardens in test 2, 37% are not intersecting a path network.
In a more detailed exploration of test 3, we identify 1.8 km^2 of allotment gardens in Augsburg. Of this, 0.35 km^2 are classified as false positives. Our analysis shows a 0.4 km^2 difference, or border mismatch, between the spatially overlapping true positive polygons.

For this test scenario, we also explore how many of the identified allotment gardens are crossed by paths. Our results reveal, that 52% of the identified allotment gardens are not crossed by a path network. Finally, test 4 results in the identification of 1.9 km^2 of allotment gardens in the study area. Of this total, 0.4 km^2 are false positives. Moreover, there is a 0.6 km^2 mismatch between the validation and the identified allotment polygons. From all the identified polygons in this test case, 47% are not intersected by a path network.
Using the aforementioned figures, we calculate the identification accuracy for all four test sets and represent it in a star plot in Figure 8.3.

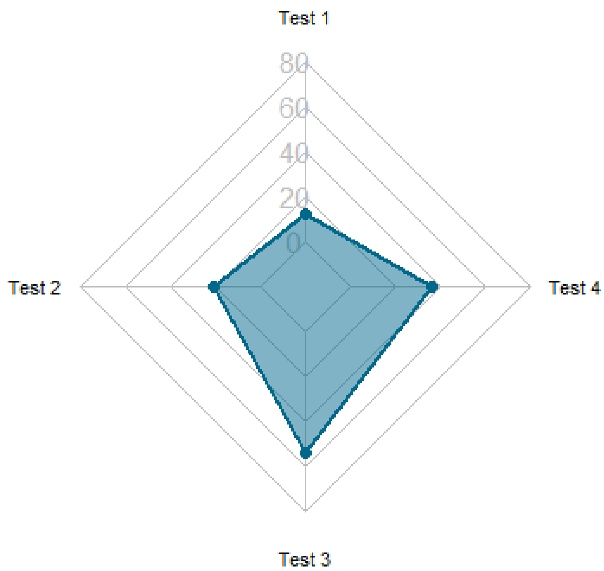

Figure 8.3: A star-plot illustrating the accuracy of four implemented threshold test cases to identify allotment gardens in Augsburg.

Test case three, which uses the 5th and 75th percentiles as the minimum and maximum thresholds, achieves the highest accuracy at 66%. In contrast, test case one attains only 15% accuracy. Test cases two and four make the second and third positions, achieving 25% and 44% accuracy, respectively. Based on the accuracy assessment, we determine that shed heights in the study area range between 1.93 and 2.62 meters. This range proves to be the most accurate for their identification. Consequently, these height values serve as a base of allotment shed thresholding in both study areas.
Apart from the statistical validation, we also perform visual confirmation. As such, we pay attention to how well linear allotment gardens are identified, as well as how well the minimum convex hulls perform. In Figure 8.4 we present sample allotment gardens in Augsburg, and compare identified against actual TN-allotment gardens. We can see that linear allotment gardens are identified well, although in some cases two or more polygons are drawn instead of a single allotment. Furthermore, we also observe that the proposed

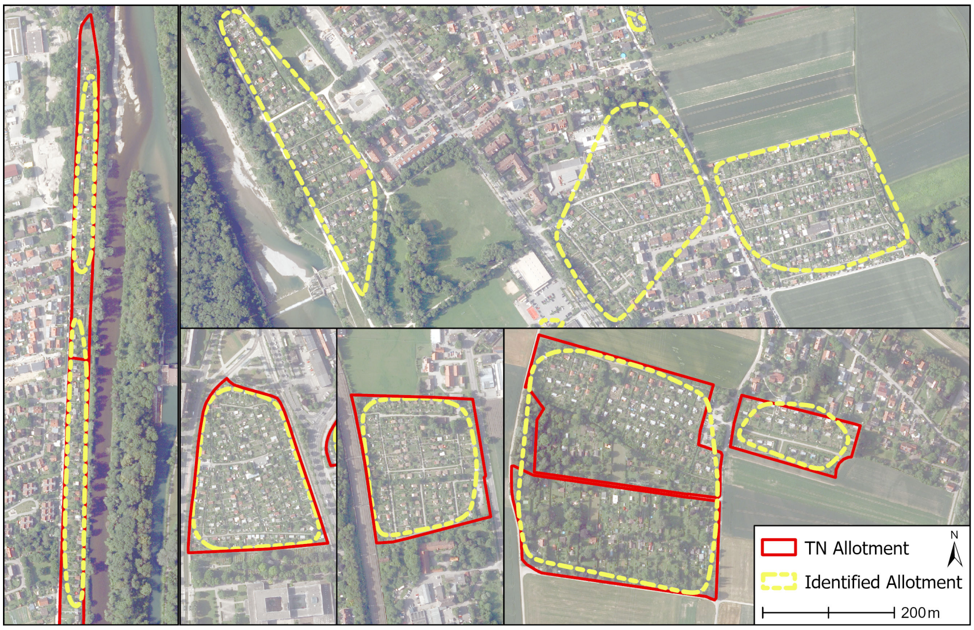

Figure 8.4: Figure showcasing various sample areas with identified and actual allotment polygons in Augsburg.

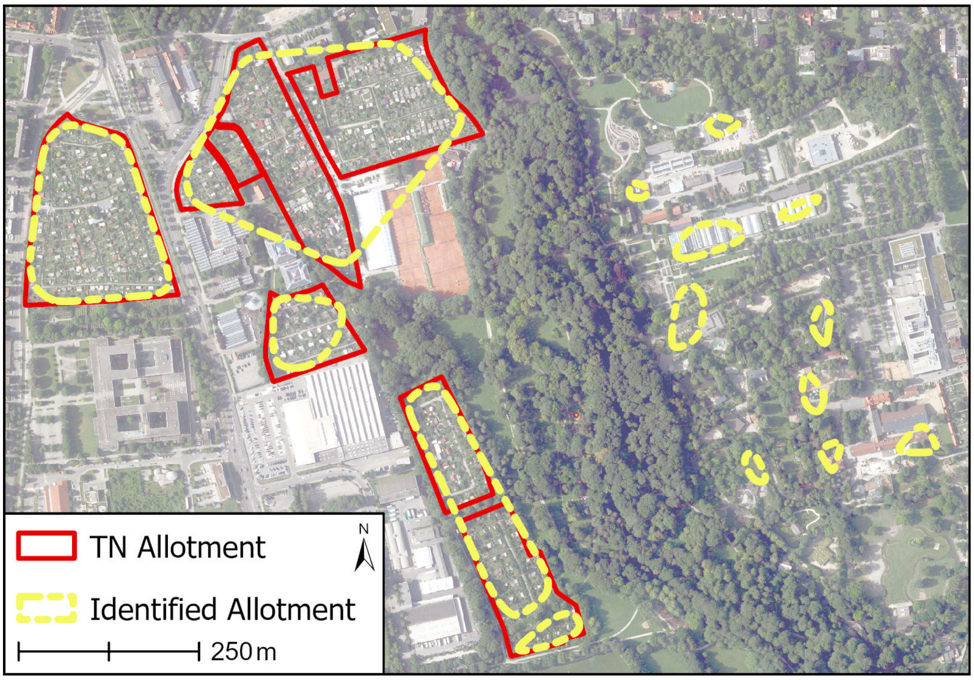

Figure 8.5: Figure illustrating various sample areas with identified and actual allotment polygons with a focus on overlapping borders in Augsburg.

methodology identifies allotment gardens that are not classified as allotment in the TN dataset. Some similar areas appear as just garden or are missing totally in the TN dataset. For the selected test trial, the area of such false positives is 0.4 km^2. However, as it can

be seen on the figure, some of the false positive polygons are indeed allotment gardens, just do not appear as such in the TN dataset.
In addition, we explore how well borders of identified and actual allotment gardens overlap. This can particularly be seen in in the middle of Figure 8.5, that actually includes three single allotment gardens from the TN dataset.
Based on the calculated statistics as well as the visual inspection, we determine test three as the best performing thresholding scenario. Therefore, we check the results of this scenario for their proximity to railroads and rivers. From all the identified allotment gardens, 56 are closer than 50 meters to water bodies, and five are located in a distance between 50 to 100 meters to water bodies. The remaining 29 allotment gardens are located further than 100 meters from water bodies. Moreover, 30 of the identified allotment gardens are situated in less than 50 meters proximity to railroads, whereas 17 are located in a proximity between 50 to 100 meters. The remaining allotment gardens are located further than 100 meters. Based on the urban green map, we calculate almost one km^2 of green stored within identified allotment gardens in Augsburg.
Using the exact threshold values as of the test 3 in Augsburg, we identify allotment gardens in Wuerzburg.

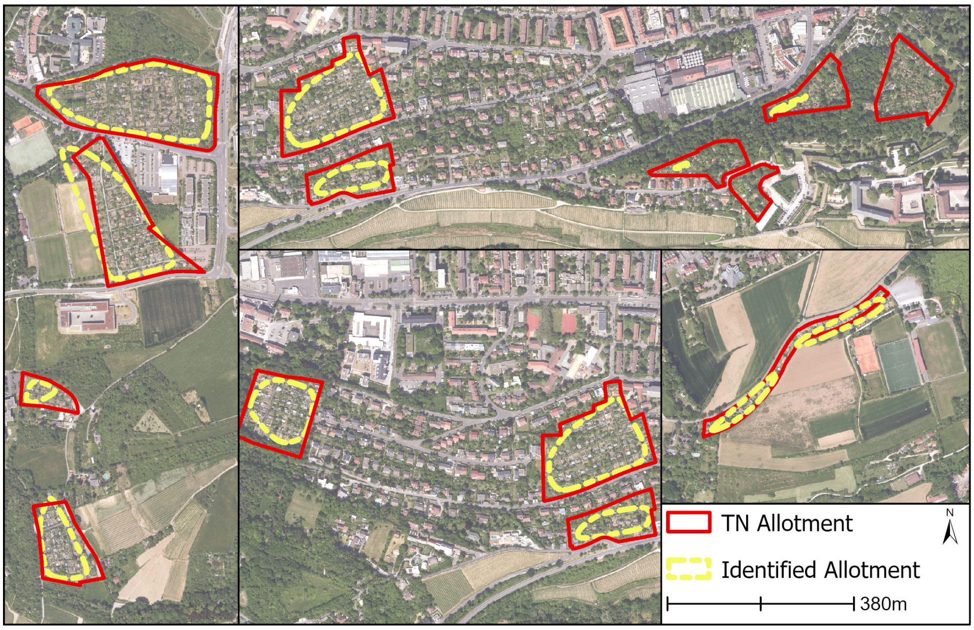

Figure 8.6: Figure showcasing various sample areas with identified and actual allotment polygons in Wuerzburg.

According to the TN dataset there are nearly 0.5 km^2 of allotment gardens in the city of Wuerzburg. Based on the threshold transfer, we identify 0.42 km^2 of allotment gardens in Wuerzburg. Example of some identified areas in Wuerzburg are illustrated in Figure 8.6. The area of false positive polygons in Wuerzburg equals to 0.13 km^2. Furthermore, we establish 0.18 km^2 of areal mismatch between identified and TN allotment gardens.

Moreover, 38% of the identified allotment gardens are not crossed by a path network. Application of the thresholds, established for Augsburg, in Wuerzburg, yields 65% of identification accuracy. However, the quality of the drawn convex hulls is much lower than in case of Augsburg.
Similar to Augsburg, we calculate how close the identified allotment gardens are located to railroads and water bodies. As such, 14 out of 31 identified allotment gardens are located closer than 50 meters to water bodies and two are located in a proximity of 50 to 100 meters. Additionally, 14 are situated in a distance of less that 50 meters to railroads while three of them are located in a proximity of 50 to 100 meters. In Wuerzburg, identified allotment gardens store nearly 0.7 km^2 of green.

8.5 Discussion and Conclusions

In this section, we utilize a semantic mapping procedure for allotment gardens. Initially, we examine the existing legislation on allotment gardens and conduct visual inspections using aerial imagery. These examinations aim to identify unique semantic characteristics that distinguish allotment gardens from other types of UGSs. We determine that the most distinctive feature of allotment gardens is the presence of sheds within each allotment. Unlike backyard and front yard gardens, where sheds are also common, sheds in allotment gardens are typically clustered in a larger area without any adjacent private housing. Furthermore, size and height of sheds are also unique determining characteristics as they must not exceed 24 m^2 in area and 3.5 meters in height.
To extract huts in the study areas, we chose to conduct height thresholding technique. While there are no examples specifically for shed thresholding, this method is commonly used for extracting residential buildings. For instance, Matikainen et al. [96] set a 2.5 meter height threshold to distinguish buildings from surrounding features like vegetation. In contrast, we test various thresholds to identify the most suitable minimum and maximum values. Our results indicate that the 5th and 75th percentiles, extracted from sample garden shed heights, equal to 1.93 and 2.62 meters. These height values appear to be the most promising threshold values. These figures closely align with the height thresholds utilized by Matikainen et al. [96]. Additionally, the maximum height of 2.62 meters is also consistent with the semantic criteria derived from the allotment legislation.
Another dominant characteristic of allotment gardens is presence of a path network within a large allotment area. We test whether identified allotment gardens are indeed intersected by paths. It turns out that nearly 52% of the identified allotment gardens, despite meeting the criteria for shed presence, height, and size, are not intersected by a network of paths. An example of such misclassification can be seen in Figure 8.5 on the right-hand side. This area is part of the Zoo and Botanical Garden in Augsburg, where small structures such as glasshouses or seating areas with umbrellas appear. Similar false positives also

occur in camping areas in Augsburg, where stationary campers are located, and along the riverside in Wuerzburg, where summer events take place and beaches are present. We can attribute this high rate of false positives to the temporal factor of the utilized datasets. The DSM dataset is derived from the DOP, which is taken on June 14th and 18th in Augsburg and May 28th in Wuerzburg. During the warm spring-summer months the number of objects that match the height range of the utilized shed threshold can significantly increase, leading to false shed detection and thus decreasing the overall identification accuracy. Therefore, the availability of a winter-time dataset, when broad-leaf trees have lost their foliage and umbrellas, campers, or other seasonal objects are not present, might considerably improve the identification rate. However, by incorporating other allotment-specific criteria, such as path presence, we can eliminate the majority of false positives and thus enhance the overall identification accuracy.

While misclassifications due to shed heights can be addressed using path networks, we find that the fixed shed size poses an even greater challenge. According to allotment legislation, the size of a garden shed must not exceed 24 m^2. This limit applies solely to the shed itself, excluding any additional terraces or covered seating areas from this measurement. Moreover, this size restriction has only been in effect since April 1, 1983, meaning older allotment gardens might still feature much larger garden sheds. When applying the 24 m^2 size criterion, we observe elimination of quite a few shed objects. This is due to the nDSM imagery used, where large tree crowns might cover parts of sheds, or terraces attached to sheds might be at the same height and thus be misclassified as one object. While shed eliminations due to the challenges of distinguishing between shed roofs and terraces reduce the number of potential sheds for clustering, even more significant mismatches arise in delineating borders of allotment gardens. This phenomenon can be clearly observed in Figure 8.5, where three TN allotment gardens are marked as a single allotment based on our analysis. During the refinement process, some huts close to the allotment borders are eliminated due to vegetation coverage or the size limit, and consequently, the convex hull is snapped to the next possible hut centroid in the neighboring allotment area.

In addition to uncertainties in border delineation due to hut elimination, we clearly observe mismatches between "spatial borders" and "actual borders". This means that in some cases, we identify a single allotment polygon while there are separate allotment gardens per the TN dataset. We define shed clusters based on a distance of 15 meters. Therefore, in areas where the actual borders of two allotment gardens are very close, we falsely identify them as a single allotment area. A good example of such a mismatch between spatial and actual borders can be seen in Figure 8.5, particularly in the allotment gardens located in the central-lower area.

Considering potential mismatches in the identified allotment borders, we incorporate these mismatches into our accuracy assessment procedure. For instance, test scenario three, which we identify as performing better, actually identifies many more false positives com-

pared to the other scenarios. However, the borders of allotment gardens identified in this scenario are much more precisely demarcated and are much closer to the actual, natural borders of allotment gardens. Thus, we include these results in the accuracy assessment, which leads to scenario three being comparatively better performing.
Nonetheless, we state that using the TN dataset for overall accuracy estimation is not very suitable. In Chapter 4, we describe that TN does not include privately owned LUs, and the distinction of small gardens in the dataset is also inconsistent. For example, in Figure 8.4, we can clearly see three nearly perfectly identified allotment gardens that lack corresponding TN allotment polygons. Although these polygons exist in the TN dataset, they are not labeled as small gardens but rather as general gardens, which can include herb gardens, botanical gardens, and others.
Manual digitization of urban gardens has been implemented in numerous studies. For instance, Taylor and Lovell [136] implement this approach to map gardens in Chicago and report that the procedure is highly time-intensive yet also reliable. Similarly, Mathieu et al. [95] note that while automated approaches like geoOBIA for mapping gardens require initial manual adjustments, these become less time-consuming and more feasible over large areas once automated methods are applied. Based on our results and implementation procedures, we agree that manually creating a validation dataset is not a cost-effective method. However, we do not perform any manual improvement on the outlines of identified allotment gardens, as that is not the aim of this study. However, we keep in mind during the validation procedure, that the TN dataset is originally digitized manually based on ground surveys and therefore our results can not exactly match in all areas. Furthermore, we expect the identified accuracy of 66% to drastically increase once manual adjustments are made.
The proximity of allotment gardens to railroads and water bodies is a semantic feature we define, based on the historical development and value of these areas rather than on regulations or laws. We were interested in exploring whether the historical pattern of using unused rail-side areas for extra food production by railroad workers has persisted or changed. Through proximity analysis, we find that in Augsburg, only 52% of the identified allotment gardens are located less than 100 meters from railroads, and 67% are less than 100 meters from water bodies. This observation may indicate that due to high demand, more open spaces were allocated for allotment gardens by the city, especially in areas along the Wertach river.
One of the main goals of this work is to define semantic features of allotment gardens that are universal for at least southern Germany. Therefore, the transferability of the findings to a new study area is a way to validate defined rules. We test the proposed methodology in Wuerzburg, because even though both cities have similar green space coverage, there are peculiarities that could lead to misinterpretations of the rules. To identify allotment gardens in Wuerzburg, we use the same shed height thresholds as in Augsburg, namely 1.93 and 2.62 meters for the minimum and maximum thresholds, respectively. Here, we

also refine our findings by testing whether the identified polygons are intersected by a path network and eliminate those that are not. Unlike Augsburg, only 38% of the mapped allotment gardens in Wuerzburg are false positives, meaning they are not intersected by paths. However, we observe even poorer border delineation of allotment gardens than in Augsburg, leading to lower identification accuracy despite fewer incorrect polygons identified. This phenomenon may be explained by the datasets used, as the DSM is taken at the end of May when the deciduous forest is already green, and large crowns might cover parts of the garden sheds. An example of poor-quality border delineation can be seen in Figure 8.6, in the upper-right polygons located in a generally forested area with densely populated woody vegetation. Therefore, sheds underneath the crowns, if thresholded, are eliminated during the post-processing stage.

In Wuerzburg, we find that 56% of the identified allotment gardens are located closer than 100 meters to railroads and 52% are closer than 100 meters to water bodies. This observation suggests that this city has also likely dedicated more areas for allotment gardening that were initially only alongside rail tracks.

The proposed methodology shows that using shed height thresholds to identify locations of allotment gardens is promising. However, it encounters challenges with the quality of the utilized dataset, especially concerning temporal and spatial resolution. The datasets we use have a 40 centimeters spatial resolution and produce reliable results. However, with even higher resolution, it might be easier to distinguish between garden sheds and terraces, which could improve overall accuracy. Furthermore, we also observe that the transferability of the thresholds, selected based on local SA, is highly promising. However, for areas where allotment gardens might look visually different, or for gardening areas that do not display the same visual-semantic features, new threshold values might be necessary. Moreover, incorporating geoOBIA techniques to perform semantic segmentation, as Mathieu et al. [95] do, or sub-pixel analysis as Haase et al. [63] do, might be beneficial. With the help of segmentation, rectangle-like allotment gardens might be easier to identify. However, segmentation procedures can also be time-consuming, and for the post-classification stage of geoOBIA, new training data for each new study area must be collected. Furthermore, sub-pixel level analysis might help to reduce the information stored in a 40 centimeters large pixel to only shed-relevant information. Yet, utilizing only height data might not be sufficient for such an approach, and a need for multi-spectral high-resolution data might arise. With the approach we propose, shed size and height will generally remain consistent due to existing legislation that is valid across each state of Germany. Thus, with the thresholding approach, we eliminate the need to create new training data for each new study area, making the approach easier to reproduce in other study areas.

In conclusion, the semantic mapping procedure for identifying allotment gardens demonstrates promising results, though it faces challenges with dataset quality and urban feature variability. The proposed methodology effectively identifies sheds within allotment gardens by applying height thresholds, which align well with both legislative criteria for garden shed dimensions and the 5th and 75th height percentiles from sample data. While these thresholds work well in Augsburg, they produce false positives in non-allotment areas like parks and seasonal structures, such as camper parking. We highlight the importance of the data acquisition timeframe, as using a winter dataset could help mitigate seasonal misclassifications by excluding objects that would not meet the height threshold. Winter data could also reduce underestimation of sheds, which may be obscured by dense vegetation crowns in summer seasons.

Testing in Wuerzburg reveals the methodology's transferability, though local adaptations are necessary due to differences in visual-semantic features and proximity to urban elements like railroads. Improved spatial resolution and segmentation techniques could also improve accuracy by allowing more precise shed identification. Although the thresholding approach is not without flaws, it offers a reproducible method for allotment identification, particularly when supplemented with minor local adjustments and refined datasets. Selected semantic features are capable to delineate allotment gardens. In addition, our workflow confirms, that allotment gardens in both study areas store a substantial amount of green spaces, which is otherwise missed if allotment gardens are not recognized as UGS type. The main limitation of the proposed semantic mapping approach remains the accuracy of the available data. Future work should thus prioritize enhancing dataset precision and testing the methodology in new study areas where allotment gardens may exhibit entirely different visual characteristics.

Chapter 9

Urban Agriculture

This chapter deals with semantic-based identification of urban agriculture as a type of UGSs. Therefore, we start by defining urban agriculture using examples from the existing literature. We then, establish spatial-semantic characteristics of urban agriculture that follow the existing definitions and that can be used for their identification. Similarly to the previous investigations, we test the proposed methodological framework both in Augsburg and Wuerzburg.

9.1 Definition of Urban Agriculture

Agriculture is the systematic production of food, fuel, fibers, and fodder, contrasting with nomadic and hunter-gatherer lifestyles. It is typically organized within an economic unit known as a farm, which may be privately or publicly owned and operated individually or collectively. Despite its diversity, all forms of agriculture share common elements including reliance on land and biological processes, human labor, and investments in production facilities [89].

"Green space is not only beautiful but also socially and economically productive" [138]. Especially, throughout the twentieth century, public green spaces have been utilized for food production during periods of crisis [152]. Therefore, urban agriculture is that type of "productive green space". Urban agriculture can take many forms, especially based on the spatial allocation. At the core of various definitions, the fundamental idea is that urban agriculture refers to cultivating food in urban settings. This broad concept uses the term "agriculture" to encompass the types of farming and gardening traditionally associated with rural areas. Peri-Urban Agriculture (PUA) represents a type of farming occurring at the edges of cities. These regions are often characterized as a transitional zone where urban and rural features overlap, with lower population densities and fewer

infrastructural developments than cities, thus not being fully "urban" [109].
A distinction of types of practices and production scales within urban agriculture and PUA is also done by FAO. In their definition, urban agriculture is referred to the practice of cultivating food within city limits. This includes growing produce in various urban spaces such as backyards, rooftops, community gardens, and both vacant and public areas. It is typically characterized by smaller, decentralized operations spread throughout the city. PUA also involves practices that produce food and other agricultural products as well as supply their processing and distribution. In contrast to urban agriculture, PUA is commonly a more intensive variety of rural agriculture and is characterized by short food-supply chains[1]. The latter ones are also refereed to as urban farming [89]. Urban agriculture, based on FAO definition, is more community bounding and education oriented, whereas urban farming is more profit oriented [89].
Urban agriculture often faces displacement and loss due to urban development, expansion of city outskirts, rezoning of agricultural land, green gentrification, and industrialization of food systems [153]. This not only results in the loss of valuable agricultural land but also the loss of local, embedded knowledge. Therefore, more and more urban agriculture is occurring on a LU that is not particularly zoned as such [109]. Frequently, urban agriculture would occur in parks, sport and leisure facility areas, public parks or backyard gardens. Thus, for urban agriculture to be an impactful and integral part of cities' green and blue infrastructures, it needs to be strategically incorporated through planning and design processes [153]. In contrast, PUA takes place on a distinct LU category, usually called agriculture, that has been used for the same purpose for decades [109].
Lohrberg et al. [89] describe different types of urban agriculture as well as PUA. As such, they distinguish between allotment gardens, educational gardens, therapeutic gardens, community gardens, and squatter gardens. Based on their definitions allotment gardens are areas divided into plots rented under a tenancy agreement, often managed by a group or association, whereas educational gardens are located in schools or other educational institutions and serve as a practical learning environment for teaching about food production and environmental sustainability. Moreover, therapeutic gardens are found within healthcare facilities to aid in the treatment of various physical and mental health conditions through horticultural therapy. They are designed to be accessible and engaging to stimulate sensory experiences and emotional well-being. Community gardens are collectively maintained spaces that focus on social engagement, education, and organic production. They are often found in urban settings and emphasize inclusivity and community development. Finally, squatter gardens are utilized by individuals or families who occupy unused land to grow food, often without formal authorization. The authors further highlight a urban farm class that is closely associated with more extensive operations that might include a variety of agricultural activities such as crop production, livestock, and direct sales to consumers. Urban farms adapt to urban demands and often

[1] `https://www.fao.org/unfao/bodies/coag/coag15/x0076e.htm` (accessed on 01.2025)

incorporate elements of social and environmental sustainability.
Apart from making distinctions between various urban agriculture types, Lohrberg et al. [89] also acknowledge the global spatial context of their development and persistence. As such, they note that while the main focus in northern European countries, in terms of urban agriculture, is on preservation and development of green spaces, in southern Europe urban agriculture typically addresses issues such as food insecurity, poverty, and social exclusion. While the societal and environmental benefits of urban agriculture practices are known, there is still a limited understanding of economic dimensions of urban agriculture. Effectively managed urban farms have the potential to become "hidden champions" of urban green development strategies [89].
PUA plays a significant role in shaping the overall landscape of urban vegetation. Furthermore, unlike any other UGSs, PUA can demonstrate multiple growing seasons along a year [20]. The changing seasons of PUA can lead to fluctuations of the total amount of UGSs; increase during in-season and decrease during off-season [91]. Characteristic phenological variations can also be observed with woody perennial crops such as fruit orchards, vineyards, or olive groves. Unlike annual crops that complete their life cycle within one growing season, perennials live and produce over multiple years, undergoing dormancy in winter. In addition to cyclic phenological changes, some PUA sites also exhibit temporal transformations. In this regard, permanent grasslands are of particular interest. Being a type of agricultural use, they are areas dedicated for an extended period to growing herbaceous fodder, forage, or energy crops, whether cultivated or naturally occurring, and not included in the farm's crop rotation. For a crop area left for renaturation and being accepted as a permanent grassland, it should not be cultivated for at least five years. Since 2015, the principle of permanent grassland conservation has been enforced as part of the 'greening' initiative in Germany, with the aim to achieve positive impacts on biodiversity and protection of water, climate, and soil in agricultural landscapes[2]. Consequently, although being referred to as grasslands, these areas are still part of agricultural systems, and serve urban greening purposes.

9.2 Semantic Features of Urban Agriculture

In this work, under PUA we consider arable lands, nurseries, permanent crops as well as orchard lands. Here, we do not include grasslands as a type of PUA, even if it appears as such in the TN dataset. In our ontology, grasslands are represented as a separate UGS type. Selected PUA classes are agricultural production sites, meaning they are actively used for gaining produce for various applications. Furthermore, these classes also constitute to the agriculture category of the TN dataset, which we will later use for

[2] `https://www.umweltbundesamt.de/en/monitoring-on-das/cluster/soil/bo-r-2/indicator#bo-r-2-permanent-grassland` (accessed on 01.2025)

validation of our results. In the following we describe unique semantic characteristics of PUA agriculture that can facilitate to their identification and distinction from other UGS types.
Apart from what PUA refers to, that we previously presented, there are no particular regulations concerning them. This means, that there are no fixed minimum size, or spatial configuration or other requirements specified. Instead, existing definitions mainly focus on how intensive a field can be utilized or what types of vegetation should mainly be planted. Therefore, in order to extract PUA relevant contextual information, we mainly rely on aerial photography and describe them using the most outstanding features. We further utilize the TN dataset in order to extract more specific rules defining PUA. Example of four different PUA classes is illustrated on Figure 9.1.

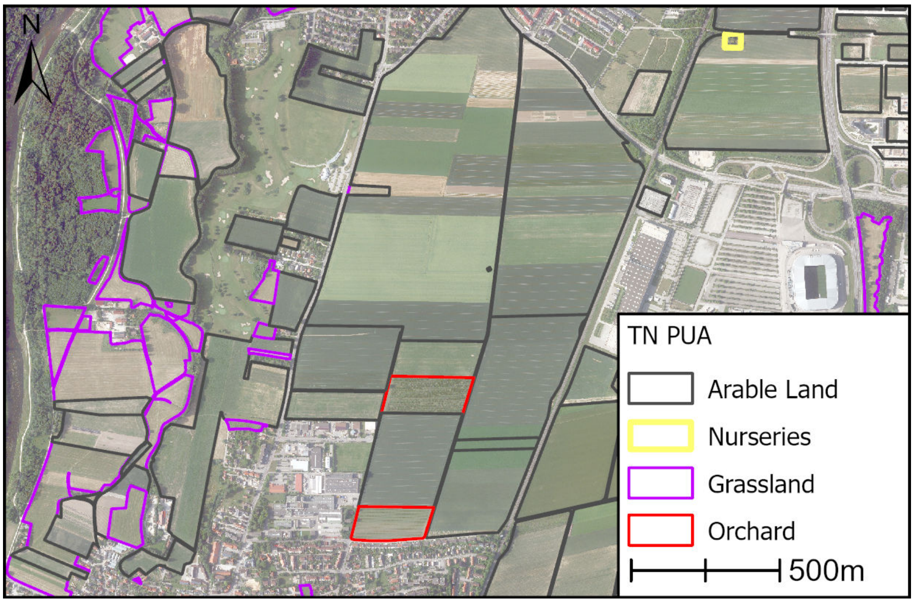

Figure 9.1: Sample area illustrating different types of investigated PUA.

Based on the TN dataset examination, we define the following semantic characteristics of PUA:

- PUA exhibits a predominantly near-rectangular or regular-shaped plot structure, often delineated by clear boundaries such as roads, hedges, or irrigation channels.
- PUA shows very low field heterogeneity as only one crop type dominates in each plot.
- PUA displays distinct, typically three-step, phenological changes throughout the growing season. For annual crops, this includes stages such as seedling emergence, full plant growth, and harvest. For permanent crops, phenological changes include stages such as flowering, fruiting, and harvest cycles.

- PUA demonstrates consistent spatial patterns, such as evenly spaced planting rows or uniform planting density.
- PUA is frequently accompanied by agricultural infrastructure such as irrigation systems, farm buildings, machinery tracks, and access roads, which are indicative of active farming operations.

9.3 Peri-Urban Agriculture modeling

The identification workflow of PUA is based on the insights gained through the mapping of forests in Chapter 7. There, during feature SA, we observe that the utilized texture metrics, height information as well as NDVI highlight either forest or PUA, if different thresholds are set. Consequently, we use all three variables to map PUA. Yet, we modify the procedure in order to better fit the nature of PUA.

Following the workflow depicted in Figure 9.2, we first create temporal vegetation indices. Existing literature, particularly Simonneaux et al. [129], highlights the usefulness of NDVI indices for mapping temporal changes and vegetation status of PUA. Therefore, as a first step, we calculate the NDVI index for each available Sentinel-2 timestamps. For Augsburg, we create NDVI datasets for the following dates in 2022: February 10th, March 27th, April 21st, May 11th, June 15th, July 25th, and December 17th. Furthermore, for Wuerzburg, we calculate NDVI indices for February 28th, March 7th, April 26th, May 31st, June 13th, July 18th, and December 20th of 2021. These datasets were previously calculated for forest mapping, based on Equation 3.4, and already used in Chapter 7.

As noted in the previous section, PUA exhibits phenological changes, with at least three phases within one growing season. By utilizing temporal NDVI data, we create binary change datasets that illustrate pixels where NDVI values change at least three times during the observed time span. To account for even minimal vegetation changes, we define the change threshold for an NDVI dataset as 0.1.

PUA, similarly to forest, showcases low within-field heterogeneity and appears as homogeneous areas in heterogeneous urban fabric. To incorporate this characteristic into the analysis, we implement GLCM-based heterogeneity metrics. Due to observed good predictive results in forest identification, we use the same heterogeneity datasets produced for band two and three of Sentinel-2 imagery from December.

In addition to detecting general PUA, we aim to identify permanent crops such as vineyards and orchards. To achieve this, we utilize nDSM datasets to extract vegetation height, enabling us to distinguish these crops from, for example, forests. The combination of temporal NDVI data and nDSM datasets allows for capturing both seasonal dynamics and structural characteristics. Consequently, we follow a similar procedure as for forests and allotment gardens: observing height variations within known TN polygons

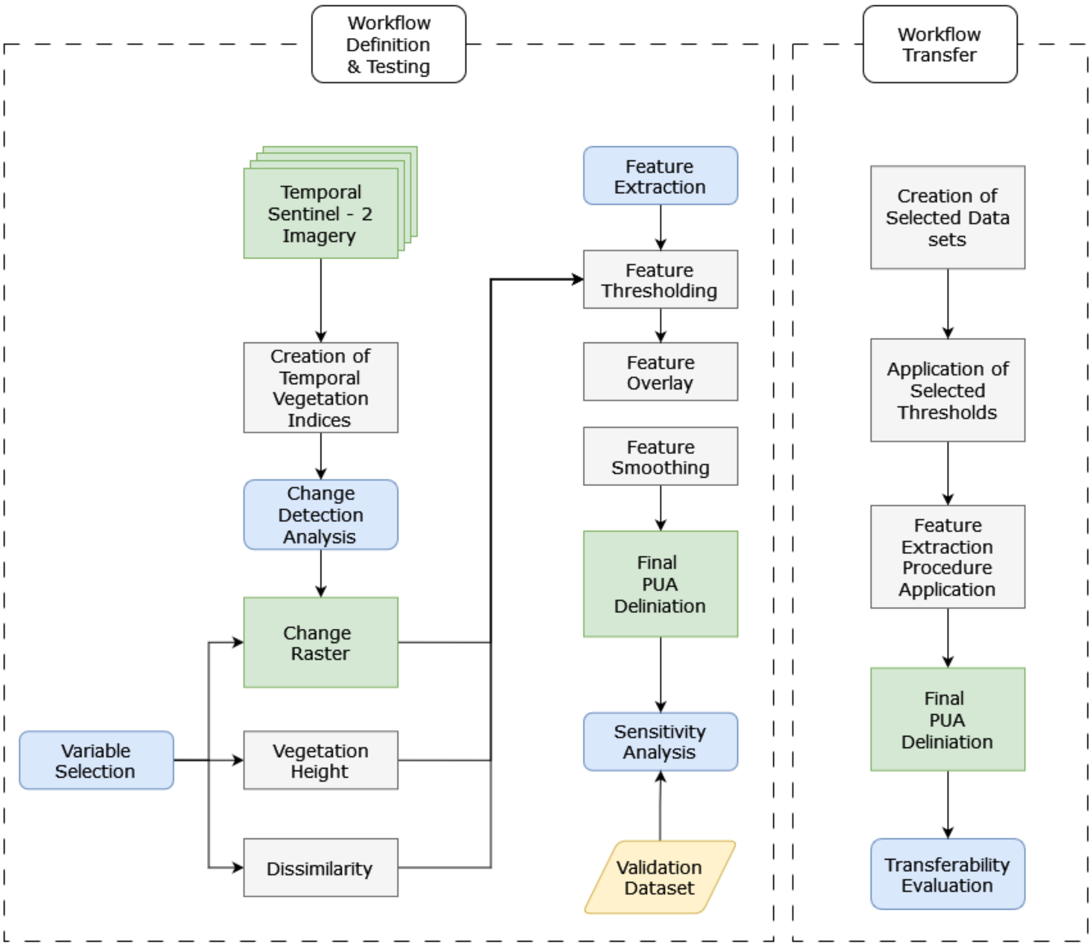

Figure 9.2: Proposed workflow to identify PUA.

and performing percentile-based thresholding. We test four scenarios with different percentile thresholds: 5-95, 5-75, 25-95, and 25-75 percentiles.

The next step in the workflow involves combining the change raster with thresholded height rasters. Our ultimate goal is to identify PUA and non-PUA areas, so we create a multiplication product of the selected layers. This product serves as a basis for creating final PUA polygons. Raster manipulations can often result in patchy and fragmented outputs that do not accurately reflect our description of PUA. To address this, we perform a smoothing operation to improve field boundaries and close any gaps within the fields.

In the previous section, we hypothesize that PUA areas are more rectangular and have roads or hedges at their boundaries. Therefore, we calculate the rectangularity of the fields by dividing area of each polygon by the area of its minimum bounding rectangle, as shown in Equation 9.1.

$$Rectangularity = \frac{\text{Area}}{\text{Area of MBR}} \tag{9.1}$$

Rectangularity values close to 1 indicate that a polygon closely resembles a rectangle, while values less than 1 indicate it is less similar to a rectangle. Additionally, we calculate proximity of the identified fields to roads to establish spatial relationships between fields and roads. To determine this, we utilize road polygons from the TN dataset. Although we mention hedges and irrigation channels as other boundary delineating features, currently such datasets do not exist. Consequently, we are not able to include both of the features into our analysis.

Due to the use of four different percentiles to create minimum and maximum thresholds, we perform an accuracy assessment to identify which thresholds produce the most realistic results. For validation, we rely on the TN dataset, which includes a LU class called "agriculture" that encompasses all the PUA sub-classes we intend to identify. Accuracy assessment is performed based on Equation 8.1. Here, we first eliminate the false positive polygons and then calculate the ratio of true positives against the reference dataset. Apart from calculating and comparing identified PUA agriculture, we also examine how much of urban green these areas store. In order to be able to calculate this, we utilize the urban green map produced using DOP imagery in Chapter 6.

Since we aim to produce a reproducible workflow, we transfer the change detection analysis and nDSM thresholding to Wuerzburg. Unlike Augsburg, Wuerzburg has a considerable amount of permanent vineyards. The height variation of vineyards can differ from that of annual crops and orchards, potentially complicating transferability of the selected height threshold to the new study area. Furthermore, acquiring cloud-free Sentinel-2 datasets on the exact same dates for both cities is extremely challenging. Nevertheless, we use at least one image per season to capture the phenological changes. Additionally, the minimum number of changes and the minimum amount of vegetation change that we use to create a change raster for Augsburg is very low, implying it should be adequately representative for Wuerzburg as well.

As in the case of Augsburg, we calculate the accuracy of the identified PUA in Wuerzburg using the TN dataset. We also examine the extent to which identified polygons are rectangular, as per our PUA definition, and check their spatial relationship to roads. We do not examine proximity to hedges and irrigation channels, since such datasets do not exist for Wuerzburg as well. Finally, we calculate the amount of green stored within identified areas, similarly using the urban green map from Chapter 6.

9.4 Results

We identify PUA in two study areas by first performing a change detection analysis. We set minimum of three-time changes of at least 0.1 as a requirement for a pixel to be counted as changed. The change raster produced based on the temporal change detection visually highlights the PUA areas. However, we further incorporate dissimilarity texture metrics. The maximum threshold values used to reclassify the dissimilarity index of

December is 1.333 and 1.445 for band two and band three accordingly. The minimum threshold for both bands is 0. As we described in Chapter 7, these values suggest a significant textural deviation in vegetation areas during this month, potentially due to seasonal changes affecting leaf-off conditions.

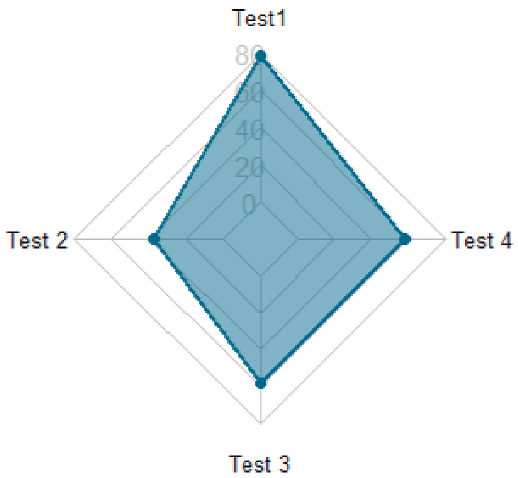

Figure 9.3: A star-plot illustrating accuracy of four implemented threshold settings of height variations.

In order to form the contextual characterization of PUA, we incorporate height information. To observe the height variations, we utilize the known PUA locations from the TN dataset and extract height values using nDSM and various percentiles. Consequently, the 5th percentile of PUA height corresponds to 0.12, whereas the 95th percentiles equals to 1.38 meters. Furthermore, the 25th and 75th percentiles constitute to 0.05 and 0.67 meters respectively. In test one we set the 5th and 95th percentiles as minimum and maximum thresholds, similarly to the 5th and 75th percentiles in test 2. Moreover, in test three we use the 25th and 75th and in test 4 the 75th and 95th percentiles as minimum and maximum thresholds accordingly.

To understand which combination of height, change raster, and texture index produces the most accurate representation of PUA, we perform local SA by exchanging the height layer in each iteration. The accuracy change based on the height threshold iteration is illustrated in Figure 9.3. Consequently, our results show that the height variation based on the 5th and the 95th percentiles, produce the highest identification accuracy. The precision of the identification reduces to nearly 54.43 % for test four, 54.15 % for test 3, and finally 35.39 % for test two. We validate our results using the TN validation dataset, comprised of all four PUA types of interest. The map, illustrating a comparison of the identified PUA against the TN dataset is shown in Figure 9.4.

According to the semantic features we defined previously, PUA consist of nearly rectangular plots. Therefore, we confirm the geometric shape of identified polygons based on

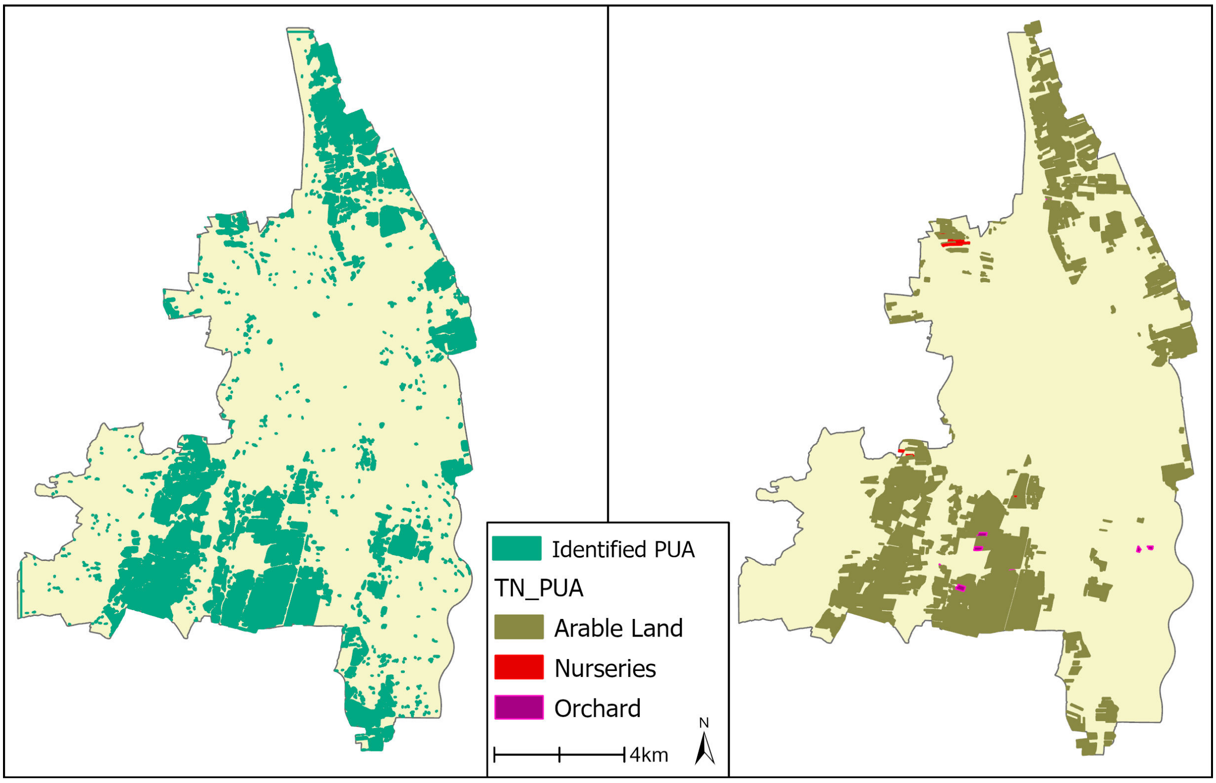

Figure 9.4: Comparative map that illustrates identified PUA as well as PUA in the TN dataset in Augsburg.

the rectangularity equation. It turns out, that the shape of around 88 % of the mapped polygons is very close to rectangular, with shape values being higher than 0.5. Furthermore, the shape of 3% of the identified PUA polygons is nearly perfectly rectangular, with shape measures higher than 0.9.
Further semantic characteristics of PUA indicate, that there are roads present at the boundaries of the polygons. In Augsburg, only 36% of the identified polygons have spatial relationships to roads, by either intersection or boundary touch. In total, the area of PUA in Augsburg based on the TN dataset equals to nearly 37 km^2. By implementing the proposed workflow, PUA covers around 28 km^2. When we examine how much urban green the identified areas store, we calculate approximately 19.5 km^2 of green.
Based on the evaluation, we select PUA height variations from test 1 as the most accurate representation of PUA areas. Thus, we transfer its threshold values to Wuerzburg. As defined for Augsburg, the maximum dissimilarity threshold of December in Wuerzburg for band 2 equals to 1.333. The maximum threshold of band 3 equals to 1.445. For both bands in December, the minimum threshold is set to 0. To produce a binary change raster of NDVI images, we apply the same rule of minimum of three changes of 0.1. Based on the created datasets of Wuerzburg, we produce a multiplication product and apply the same boundary smoothing and gap filling techniques as post-processing steps.

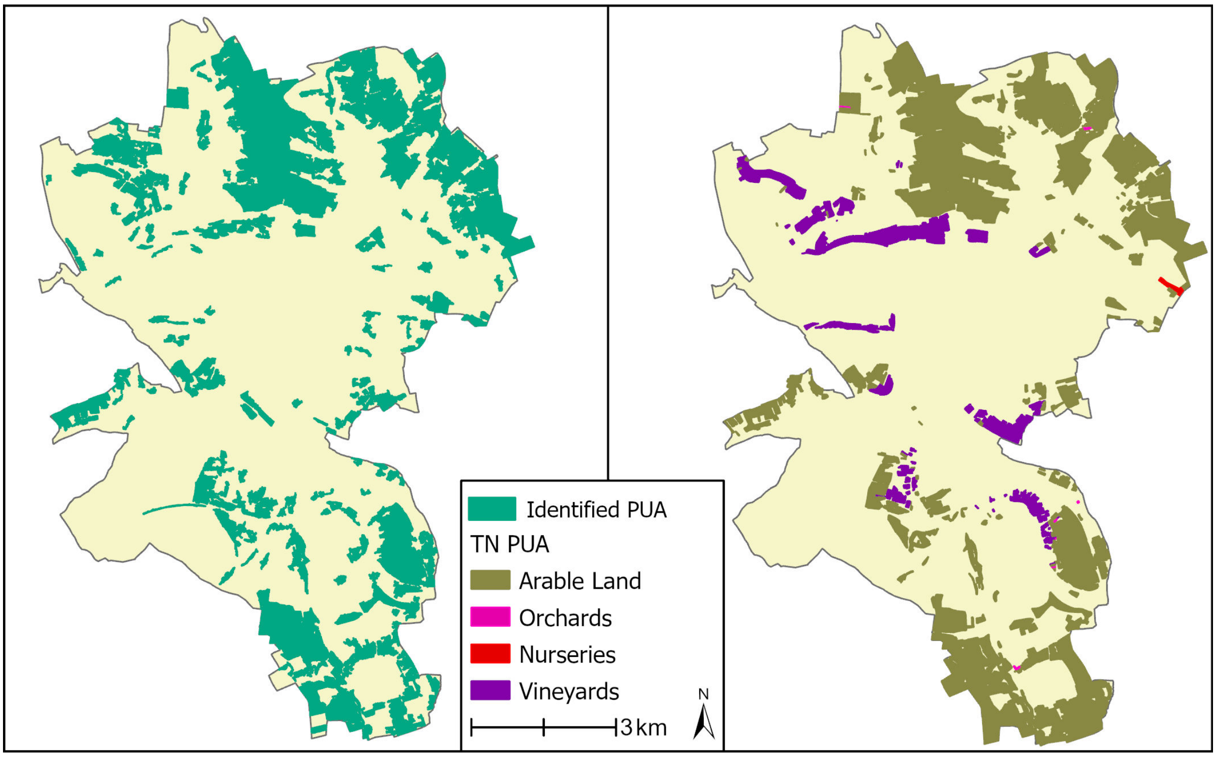

Figure 9.5: Comparative map that illustrates identified PUA as well as PUA in the TN dataset in Wuerzburg.

Following the established workflow in Augsburg, we identify 78 % of PUA in Wuerzburg. The area of PUA in the TN dataset constitutes to 20 km^2. Using the knowledge-based approach that we propose, we also identify nearly 20 km^2 of PUA. A comparative map of TN and identified PUA is shown in Figure 9.5.
From the extracted PUA polygons 78% are near-rectangular, while none of the identified polygons being perfectly rectangular with shape values higher than 0.9. Moreover, 94% of the identified PUA areas have a spatial relationship to roads, in a way of intersection or boundary touch. Furthermore, using the urban green map produced from the DOP imagery, we calculate the amount of actual green available within the identified polygons. It turns out, that the nearly 20 km^2 PUA areal accommodates around 10 km^2 of urban green.

9.5 Discussion and Conclusions

In this chapter, we conduct a workflow to identify PUA areas in Augsburg and test transferability of this approach in Wuerzburg. Based on visual examination, we establish that PUA areas exhibit near-rectangular or regular-shaped plot structures, often delineated by clear boundaries such as roads, hedges, or irrigation channels. These areas typically show very low within-field heterogeneity, as usually only one type of crop is present within each field. The most dominant characteristic of these areas appears to be phenological changes occurring in both annual and perennial crops, although they might progress through slightly different stages. Consequently, we delineate these areas using vegetation change, vegetation height, and vegetation homogeneity features.

To identify areas with vegetation change, we establish that for the same area (or pixel), there should be at least three significant changes, representing three main phases of plant phenology: emergence of seedlings, full plant growth, and harvest. However, it is difficult to establish how drastic these changes are reflected in NDVI values. Thus, we define a slight change as 0.1, which is sufficient to observe vegetation change. This change raster, however, highlights not only PUA areas but also all other vegetation-dominant areas where changes have occurred. This phenomenon is also highlighted by Simonneaux et al. [129], where the authors emphasize that even with set thresholds to delineate vegetation and bare soil, they observe confusions due to overlapping spectral signatures of different crops as well as under-detection of young tree plantations due to low NDVI values. We do not perform SA to identify which change threshold would be the most representative of agricultural fields, as this procedure would be time-intensive and the absence of high-quality validation datasets would always result in high uncertainties. However, another reason for choosing such a low threshold is due to the requirements of the transferability application. Since we are unaware about the extent of seasonal changes in Wuerzburg, setting a low threshold potentially helps to minimize the risk of accidentally excluding relevant data.

To improve results of the change detection, we incorporate texture metrics. The two suitable GLCM texture metrics for this purpose are homogeneity and dissimilarity. Our previous analysis in Chapter 7 illustrates that homogeneity is not capable of highlighting forest areas. Visually and texture-wise, forests appear very similar to crop fields. Therefore, we chose to use the dissimilarity index. Commonly, the lower the dissimilarity value, the higher the homogeneity. The highest dissimilarity value we utilize is nearly 1.4. Although this value is comparatively high for forests, it still adequately represents PUA. Moreover, we only use the dissimilarity index of bands two and three for the month of December. We find December appropriate because it is the leaf-off season in the temperate zone where the study areas are located, which enhances the dissimilarity index and reduces any noise present during the summer months. However, we do not test the temporal change of dissimilarity, as this would require high processing power and time, while we are interested in the most optimal delineation. In addition to the month, we limit texture metric calculations to two Sentinel-2 bands. Bands two, three, four, and eight have the highest resolution (10 meters). Since bands four and eight are already involved in NDVI calculation, we aim to add extra information using bands two and three. Other spectral bands might also be useful for understanding the vegetation health status. Full spectral bands together with NDVI are used by Peña et al. [112], who establish that all the bands used together gives the best results in terms of identifying PUA. Particularly, the short-wave infrared band can assist in understanding water status of plants and identify drought-stressed crops. However, this band has a resolution lower than 10 meters, so we chose not to include it in the analysis.

While using phenological change of vegetation together with texture metrics is a commonly used technique in urban agriculture, using vegetation height is less common. Nevertheless, when mapping forests, we perform a SA where we eliminate height information and observe that crop fields are highlighted. Consequently, we use vegetation height as one of the unique identifiers of PUA, but with different thresholds than for forests. Our results show that the general height variation of PUA in Augsburg lies between 0.12 and 1.38 meters, as these values in combination with other features produce the most realistic results. Although we expect these values to be challenging in terms of transferability, visual inspection of PUA results in Wuerzburg show otherwise. For instance, vineyards can reach up to 1.8-2.7 meters [113], which could presumably lead to the underestimation of these areas due to the 1.38 meter cut-off. Such underestimation of height could originate from the limited temporal resolution of the nDSM datasets. These are calculated from DSM and DTM datasets that are taken on one single date. Therefore, height of only those crops that were present at the time of image capture are evaluated during height thresholding. However, limited identification of vineyards occurs only partially in some areas. We could explain this by the fact that the use of other explanatory variables, such as dissimilarity and change factors, balances the effect of the height. Yet, we acknowledge that the transferability of the height variable might be limited, and further analysis might be needed in Wuerzburg to understand the actual vegetation height distribution.

Phenology, homogeneity, and vegetation change are factors that can be conceptualized, and crisp values or rules can be established. We also refer to the geometric form of PUA and its spatial association with elements such as roads, irrigation channels, and others. These, in turn, are not so easy to characterize using spatial data. Therefore, we calculate the rectangularity of identified polygons. However, in many cases, we are not able to extract single polygons but rather larger areas consisting of a group of polygons. This means that only in areas where single plots are extracted the rectangularity measure is representative. For other areas where a large number of PUA plots occur side by side, this measure does not adequately describe rectangularity. Furthermore, to build spatial associations, such as roads within identified PUA, quality of the utilized road network dataset and the precision of extracted polygons are determining factors. However, the TN dataset does not contain all types of roads. In areas where arable lands are clustered, commonly no roads pass through, but rather biking lanes or walking paths. Therefore, quantitatively defining how many of the identified polygons are associated with the road network while using an incomplete dataset is nearly impossible.

By utilizing the proposed mapping procedure, especially in Wuerzburg, we achieve good PUA identification results. Although these areas do not always overlap, the total amount of the PUA, nearly 20 km^2, matches the TN dataset. In Augsburg, however, we identify much less PUA as the area of it in the TN dataset. We relate these differences to the quality of the utilized data as well as the selected thresholds. Augsburg stores much larger PUA, especially various types of it. However, only NDVI images from one date in some months, or nDSM data from only one date from the whole year are used. Thus, a lot of phenological and structural nuances are lost. Similarly, 20 km^2 of PUA in Wuerzburg stores only 10 km^2 of urban green. This is again due to the temporal factor of the DOP image used for producing the urban green map. Consequently, for adequate translation of all the semantic characteristics of PUA, availability of temporal datasets for all selected features is a must.

Finally, in both study areas, we delineate sub-classes of PUA by referring to the TN dataset. However, the proposed extraction procedure does not allow distinctions between the selected classes. Consequently, some PUA classes might be identified better than others, though we are only able to assess the overall picture.

In this study we develop a workflow to identify Potential PUA areas in Augsburg, assessing its transferability to Wuerzburg. Our key findings suggest that PUA regions tend to be near-rectangular with distinct boundaries, minimal internal variability, and seasonal vegetation changes. Using NDVI to track plant phenology, texture metrics to enhance delineation accuracy, and vegetation height to distinguish PUA from other vegetation types proves to be effective. However, thresholds for NDVI and texture values introduce uncertainty. Similarly, using dissimilarity indices only for December captures PUA more effectively due to reduced vegetation noise but may limit insights into temporal vegetation changes. Another important distinction is the limitation of the road network data, which, by excluding smaller paths, prevents comprehensive spatial associations for all PUA polygons.

We acknowledge, that this approach has limitations, including the lack of SA on NDVI thresholds, which may affect transferability across different agricultural landscapes. Additionally, rectangularity and association with road networks do not apply well in areas where plots cluster, limiting detailed spatial characterization. Therefore, future work should focus on optimizing thresholds for NDVI and texture metrics, particularly in diverse agricultural settings. Furthermore, refining road network datasets could improve PUA identification, while testing the influence of temporal dissimilarity changes might enhance detection stability. Utilizing temporal height data or a urban green map that accounts for temporal changes would be beneficial for accurate PUA mapping. These improvements could allow for more robust, scalable approaches to PUA identification across varied urban regions.

Chapter 10

Urban Green Corridors

In this Chapter we present a practical and systematic approach for mapping urban green corridors in two study areas. We first present the definition of green corridors in the existing literature. However, we only focus on green corridors beneficial for human well-being and allowing human mobility. In the following section, we provide a semantic definition of green corridors as well as present results and discussions of the practical mapping procedure.

10.1 Definition of Urban Green Corridors

For UGSs to provide full range of services, their thorough planning and maintenance is a must. According to the climate adaptation plan of the EU, the creation of a city-wide network of green spaces with interconnected corridors should be prioritized and valued as a fundamental LU type, alongside other essential LU sectors[1]. This statement underlines, that interconnectedness of UGSs is as valuable as the UGSs themselves. Active urbanization is causing rapid habitat fragmentation, and maintaining landscape connectivity is essential for ecosystem health and biodiversity conservation [154]. Urban areas, although comprising a small fraction of land, house significant amounts of various animal species, requiring integrated conservation strategies within urban planning [26].
Although the concept of a green corridor exists for a long time, this term itself is relatively new. Ahern [4] summarizes terms that are used for describing the same concept in both Europe and America. These include ecological network, habitat network, greenways, greenbelts, environmental corridors, and wildlife corridors among others. He also provides a definition of what greenways are, by describing them as "networks of land containing

[1] `https://climate-adapt.eea.europa.eu/en/metadata/adaptation-options/green-spaces-and-corridors-in-urban-areas`(accessed on 01.2025)

linear elements that are planned, designed and managed for multiple purposes including ecological, recreational, cultural, aesthetic, or other purposes compatible with the concept of sustainable LU". Consequently, the concept of greenways stands at a core of ecological studies, and seeks to provide a solution for increasing habitat fragmentation due to rapid urbanization [4].

However, green corridors are not only important from the ecological perspective, but also from a human-nature interactions perspective. Recreative, cultural, and aesthetic functions are among many more services that green corridors provide [102]. Green corridors are placed at a similar level with parks and recreation areas, as they could offer park-like experiences to community residents [126]. Research shows, that green alley projects can foster positive connections between people and places and improve resilience of communities to shocks and stresses, while they help to reduce noise pollution, and generally enhance human well-being [51]. Consequently, from a human well-being, ecological and sustainability perspective, green corridors provide a multitude of functions. They provide safer and more accessible routes for pedestrians, cyclists, and vehicles; foster connections between people and nature; enhance public health; improve air quality; contribute to urban development; promote environmental education; and strengthen a community's sense of place [47].

Interconnectedness among core green areas is also a widely discussed topic in implementation of GI [74], especially in the context of nature-based solutions [76]. Green corridors are defined as linear natural features, like trees and vegetation, that connect various green and open spaces to create an interconnected urban green network [102]. Therefore, green corridors are the key elements of urban landscapes that can enable this connectedness, that is urged for in nature-based solutions for sustainable urban development.

When it comes to specific criteria of green corridor creation, this will vary based on the species of interest. From an ecological perspective, there are some generalizable steps: taking habitat patches as nodes and potential movement paths between these patches as edges, and creating a simplified network of movement between habitat areas [26]. Further modifications on size of patches or characteristics of edges will depend on the particular species. However, green corridor criteria, especially benefiting human movement and well-being, are not as well established. Types of green corridors in cities is yet another, relatively unattended, aspect of green corridor establishment.

One of only few detailed descriptions of green corridor types is given by Yan [150]. The author delineates among green road, green river, and green ribbon corridors. Green road corridors include greenery along urban roads, and are subdivided into main road, secondary road, and railway green corridors. Green river corridors are comprised of vegetation along riverbanks and associated floodplains, dykes, and highlands. Lastly, green ribbon corridors are presented as wide, continuous strips of green space that can be hundreds of meters to kilometers wide, and are typically located on urban outskirts or between urban zones.

Apart from a detailed typology of green corridors, concrete criteria for their identification are as important. By taking human mobility as a key aspect of green corridor design, Moreno et al. [102] provide solid criteria for green corridor mapping. The authors highlight, that the interconnected green spaces can improve urban mobility, particularly pedestrian movement, by linking parks, squares, and green roads. This way their aim is to facilitate easier, safer, and more sustainable pedestrian access across urban areas. Furthermore, they summarize key requirements of green corridor creation for the given purpose as follows:

- Green corridors connect core areas with a minimum size of 2 hectares.
- Core areas are comprised of vegetation, mainly trees (over 50% cover).
- Distance between core areas should not exceed 2 kilometers.
- Green spaces should have surface more than 0.1 hectares.
- Distance between the green spaces must be under 300 meters.

In this definition, core areas refer to large green spaces. Although not exactly specified by the authors, core areas with the given size could be e.g. forests, parks, and cemeteries. Furthermore, the authors refer to green patches along streets and public pathways as green spaces. For allowing better connectedness, the authors require a maximum distance between green patches 300 meters. However, the authors, assess quality of vegetation and from it following connectedness, within 100 meter transects.
This detailed definition of green corridor criteria is one of the very few definitions, especially concerning human movement. Therefore, in our work we will rely on these criteria in order to identify green corridors in the selected study areas.

10.2 Semantic Features of Green Corridors

In order to identify existing green corridors in our study areas, we slightly modify the definition of the Moreno et al. [102] that states: green corridors are linear natural features, like trees and vegetation, that connect various green and open spaces to create an interconnected urban green network. We exclude open spaces from this definition, because the TN dataset includes mixed areas under the "open" class. This class includes open mining areas or open abandoned industrial areas. Consequently, we do not consider such areas as core areas that need to be connected using a network of green corridors. Furthermore, we also make a distinction between green transport and green water body corridors. While transport corridors could be beneficial for human mobility, water corridors can also be important for urban biodiversity. Therefore, by synthesizing and extending the existing green corridor definition, we establish the following semantic identification criteria:

- Green corridors are networks that connect green core areas:
  - Core areas should have a minimum size of 2 hectares
  - Core areas are vegetated areas and are comprised of mainly tree coverage (over 30% cover)
  - Distance between core areas should not exceed 2 kilometers
- Green corridors can be of transport type:
  - Main road corridors
  - Path corridors
  - Railway corridors
- Green corridors can be of water body type:
  - Green corridors along riverbanks
  - Green corridors around lakes
- Green corridors should be comprised of vegetation with an area more than 0.1 hectares per 100 meters

We set 30% tree coverage for core areas, instead of 50% given in the existing literature, because of the structure of UGSs in the study areas. A high tree coverage filter would eliminate many UGSs, that have mixed vegetation coverage, i.e. parks or allotments. However, we are interested in keeping such LUs as core areas due to their importance for human well-being. Excluding those from the core areas might represent only partial connectivity required for human use. Thus, a lower tree coverage threshold would more adequately represent core areas in both cities. Moreover, we expect at least 0.1 hectares of vegetation per 100 meters, for segments to be considered as a corridor. While such criteria do not explicitly exist in the literature, it synthesizes distance and amount of green utilized by Moreno et al. [102].

10.3 Green Corridor Modeling

To identify green corridors, we follow the procedure presented in Figure 10.1. We first select green core areas, which will serve as anchor points for defining green corridors.
During the initial selection of potential core areas, we consider the accessibility of green spaces, opting to exclude those with limited public access. For instance, tree nurseries may appear as large green spaces with nearly 100% tree coverage, fitting our criteria for core areas. Yet, tree nurseries serve commercial purposes rather than recreational use. In

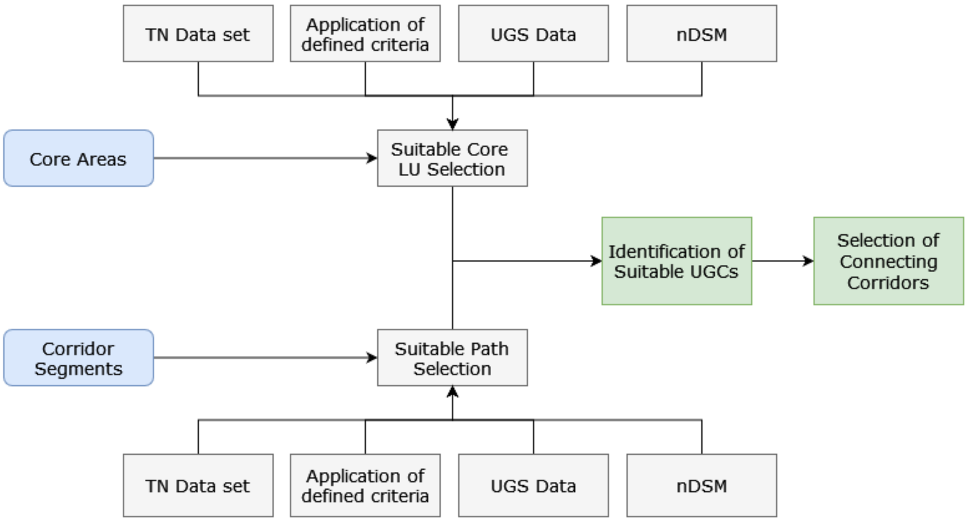

Figure 10.1: Workflow to identify UGSs using two different data sources.

contrast, botanical gardens offer also limited access, only during the opening hours. Yet, these are large green spaces that people attend during opening hours for mostly leisure activity purposes.

Consequently, we refer to the TN dataset and extract all LU classes that we would further asses in terms of their suitability as core areas. The list of classes we extract is given in Table 10.1. While most of the selected classes appear in both cities, vineyards exist only in Wuerzburg, and Zoo only in Augsburg.

We then explore each of the selected classes in terms of their satisfaction of the green corridor criteria. Consequently, we test whether the area of the selected polygons is larger than 2 hectares and whether they are located in maximum 2 kilometers distance from each other. We further take the green space map produced in Chapter 6 and explore the height of vegetation under the remaining polygons. To do so, we extract height values from the nDSM raster for each vegetation polygon within core areas. The nDSM layer was previously produced in Chapter 4, using DSM and DTM rasters. Here, we are aiming for tree-like vegetation composition of more than 30%. There is no exact information as to what height tees in the study area constitute. Nevertheless, in Chapter 7 we use the same nDSM layer to extract the vegetation height under forest areas. Given forest in both study areas are made of coniferous and deciduous trees, we use the same height thresholds as for forest mapping. Consequently, the minimum height threshold of trees in green core areas is set to 0.712 meters. To check whether the selected core areas meet the final criteria, we create a distance table using the Create Near Table tool in ArcGIS pro. This allows us to asses if there are any polygons that are located further than 2 kilometers from at least one other core polygon.

After selection of the core areas, we examine routes that could serve as potential corridors. Therefore, from the TN dataset we extract roads, path, railroads, rivers, and standing

Table 10.1: Initial selection of UGSs to be used as green core areas.

Land Use Type	Cemetery Forest
Designation	Crop Fields Botanical Garden Zoo Recreation Area Leisure Facility Garden Grassland Allotment Garden Orchard Park Children's Playground Vineyard

waters. For networks to be considered green, there should be at least 0.1 hectares of green within 100 meters. TN polygons are already split into sections, especially at the road intersections. However, we further split them in order to obtain 100 meter long transects. This process, is however, cost-intensive as selected datasets are quite large.
Similarly to core areas, we apply the same height threshold to vegetation around the networks. This ensures that we do not falsely classify segments as green corridors, although there is only low, grass vegetation around it. We then reclassify every section of the network into green or non-green corridors based on the amount of green stored in it. Here, we also utilize a buffering approach in order to extract immediate green spaces alongside the network. Consequently, we apply a 5 meters buffer around roads and paths, as well as a 10 meters buffer around railroads and rivers.
We then combine green corridors of all types and examine the connectivity of the core areas with these corridors. This allows to express whether the identified green corridors form continuum within the study areas as per definition. For this, we select all the corridor segments that can connect the majority of the core area continuously. We then identify which of the core areas are isolated and are not connected by any of the identified green corridors.
Here, we do not perform transferability analysis, as we did in the previous chapters. The reason is, that we select green corridor defining criteria from the existing literature. Consequently, we apply the same criteria in both study areas and assess the independent accuracy.

10.4 Results

Green corridors are defined as linear green formations that connect core areas. Therefore, we first identify these core areas. In Augsburg, we select LUs defined in table 10.1, that could potentially serve as core areas. In total we identify 2240 polygons belonging to the defined green space classes. We further narrow down this number by applying core area criteria. Consequently, there remain 218 polygons that are at least 2 hectares large, are closer than 2 kilometers to each other and contain over 30% tree coverage. Differences between originally selected and filtered core areas are shown in Figure 10.2.

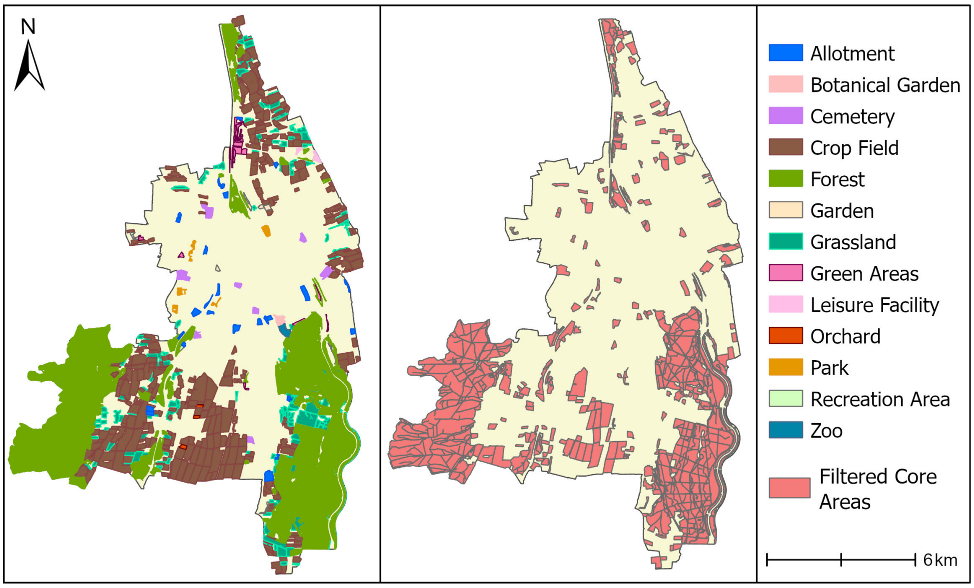

Figure 10.2: Comparative map of selected core areas as well filtered core areas in Augsburg.

The majority of the eliminated core areas belong to crop lands, grasslands, green areas, and gardens. As such, there remain 25 allotment, one botanical garden and one zoo, 9 cemetery, 90 crop field, 58 forest, four garden, five grassland, 15 green area, one leisure facility, two orchard, four park, and 3 recreational area polygons. The total area of these core polygons makes up to 47 km^2.

Furthermore, we identify four types of green corridors, namely path, road, railroad, and water body corridors. For these linear objects to be considered as green corridor, they should store at least 0.1 hectares of green per 100 meters. The TN dataset provides these objects in a polygon geometry, which not consistently covers the whole area of these objects. However, we add buffers around them to even up these inconsistencies, as well as include vegetation that also appears on both sides of pavements. Selected vegetation with the defined buffers go through a filtering process, where vegetation less than 70 centimeters in height is eliminated. This process excludes lower grass and sparse vegetation on bare soils. Consequently, with five meters buffer around roads we identify 4 km^2 of green vegetation, whereas around paths of the same buffer size we identify 4.7

km^2. Through recalculation of the minimum required vegetation amount per 100 meters, we identify that 38% of all road segments fit the green corridor criteria, while this number equals 57% for path segments. Using a 10 meter buffer around water bodies and railroads we identify 2.8 and 0.7 km^2 of green, respectively. Based on the acquired vegetation amount as well as the segment size, 84% of water body and 72% of railroad segments appear to fit the green corridor criteria accordingly. Spatial distribution of all four types of green corridors in Augsburg is illustrated in Figure 10.3.

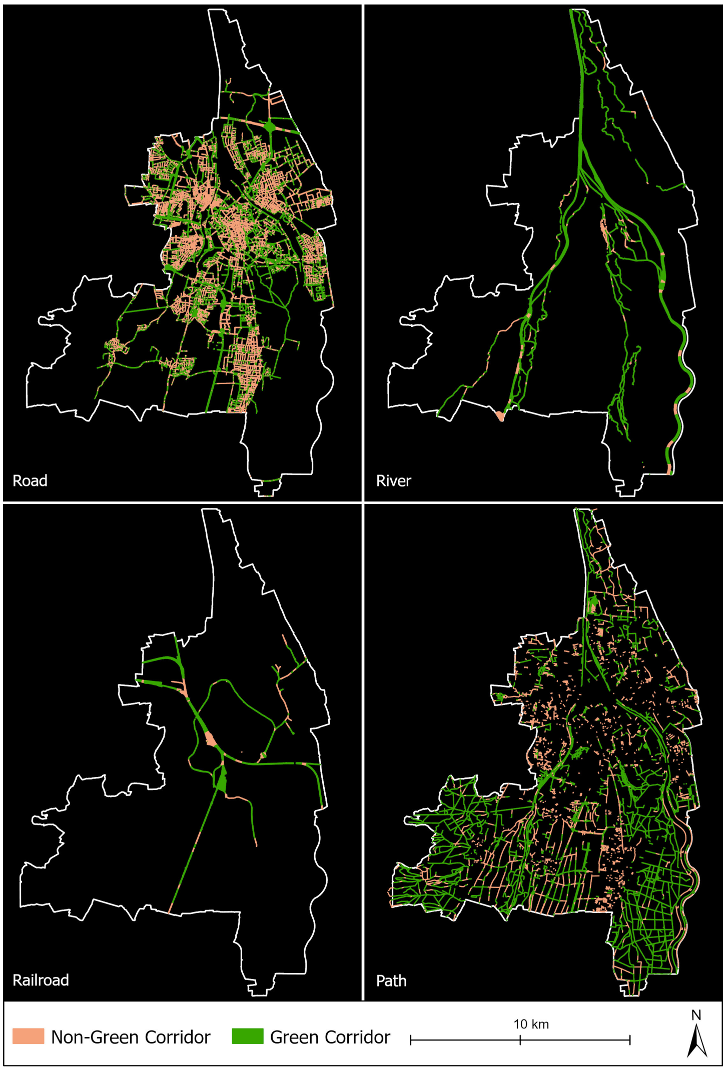

Figure 10.3: Map that illustrates spatial distribution of road, path, water body, and railroad green corridors in Augsburg.

The inherent idea behind green corridors is serving connectivity of core areas. Although originating in ecology, connectivity of green areas also serves for human well-being by allowing safe and pleasant movement of people. Therefore, we examine to what extent selected core areas are connected to each other. It turns out, in Augsburg, 65 of the core area polygons are isolated from the rest of the core areas and cannot be connected through

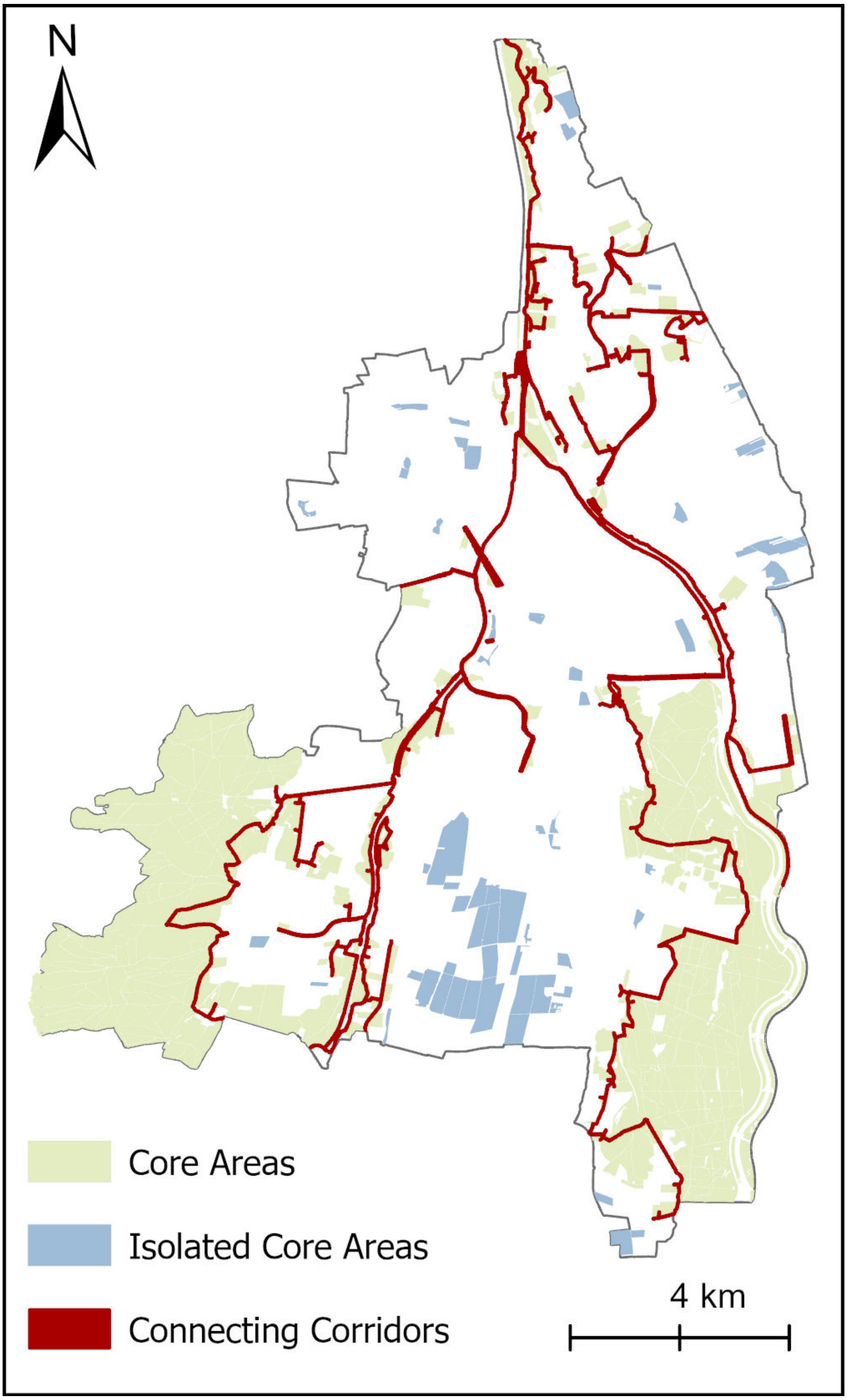

Figure 10.4: Map of the identified green corridor network, made of all four corridor types, that uninterruptedly connects majority of core areas in Augsburg.

the identified corridors. The largest group of core areas, that is isolated, is comprised of 43 crop field polygons. This figure is followed by six allotments and six cemeteries. From the remaining core area classes there are consistently one or two polygons isolated. Moreover, from the two orchard polygons, that were initially selected, none are connected to the rest of the core areas. By following through the green corridor segments of all four types, we establish a route that connects all the 65 core area polygons. Results of the identified corridor route are presented in Figure 10.4. The identified connecting corridor spans in north-south axes and splits into east-west direction in Wolfzahnau, which is a landscape protection area. Main branches of the selected corridor span mainly alongside the Wertach and Lech rivers. From the corridor along the Wertach river another branch splits and connects the forest in the west (westliche wälder) to the rest of the core areas. This connecting corridor is comprised of nearly the same number of road and path segments which make up 42% of the all corridor segments. Furthermore, railroad green corridor segments are on the third place and make 10% of the total corridor segments. Only 6% of the connector corridor segments are made of river segments.

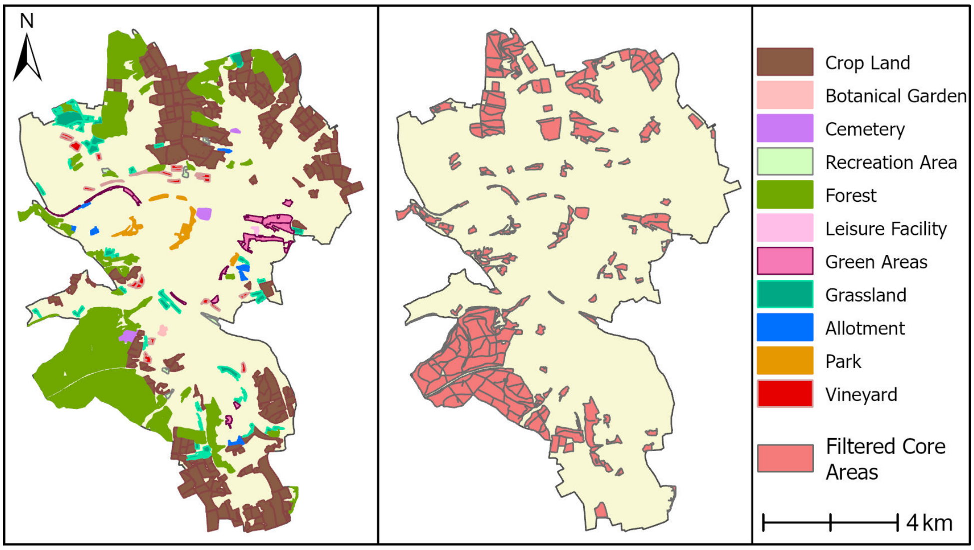

Figure 10.5: Map that illustrates difference between selected and filtered core areas in Wuerzburg.

The identification of green corridors in Wuerzburg follows the same procedure as in Augsburg. Initially, we select 453 polygons from the TN dataset that belong to green space classes defined in Table 10.1. However, here we also filter core polygons based on the size, proximity and tree density. Due to these elimination criteria, we continue our analysis with only 221 UGS polygons from 453 of pre-selected. The largest UGS class that is eliminated, belongs to crop lands. From 201 polygons of crop lands, only 27 fit the set core area criteria. The outcome of the pre and post-selected core areas can be seen in Figure 10.5. We proceeded with the analysis using 146 forest, 27 crop land, seven recreational, one leisure, three cemetery, 12 green space, six grassland, seven allotment, 11 park and one botanical garden polygons. From 23 selected vineyard polygons, none passed through the filtering criteria and are eliminated from the final core area list. In total, filtered core areas constitute nearly 16.6 km^2 of green space.

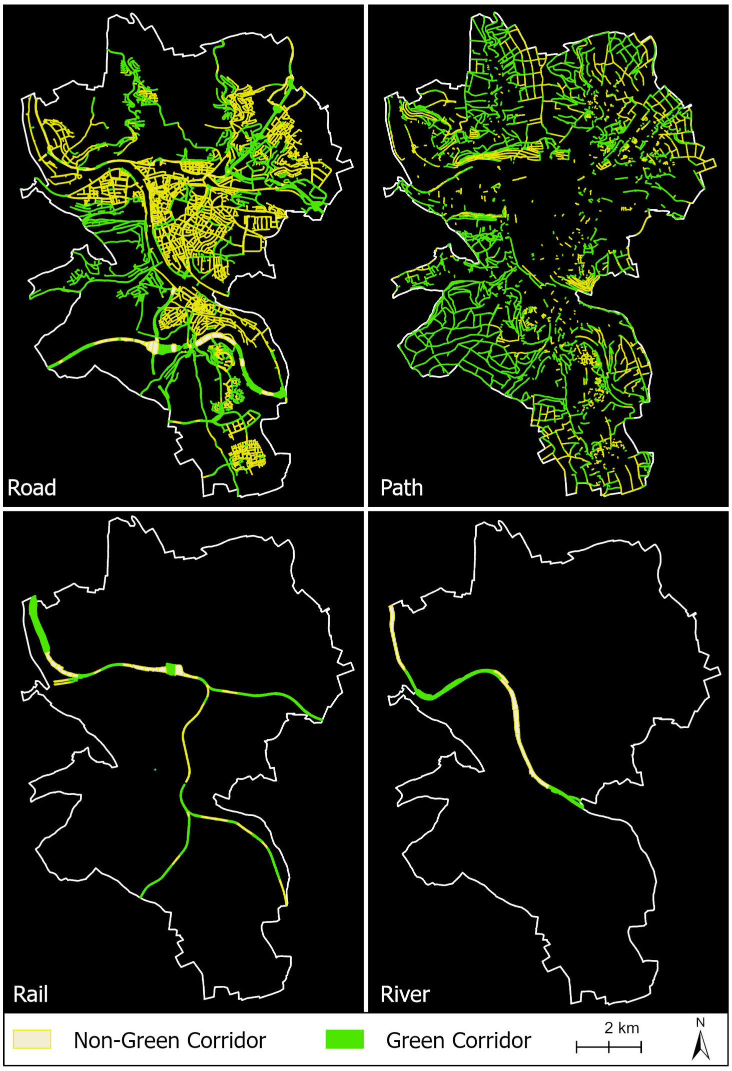

Figure 10.6: Map that illustrates spatial distribution of road, path, water body, and railroad green corridors in Wuerzburg.

To examine the amount of green present alongside the four network types, we utilize buffers around these objects. Consequently, along the existing path network in Wuerzburg and a 5 meter buffer around it, we identify nearly 4.5 km^2 of green that fits the set height threshold. Adjacent to the road segments and a 5 meter buffer around them, we identify 3 km^2 of green. The given number of path segments exceeds the number of road segments by almost 350 segments, there is considerably less green present around paths. Furthermore, parallel to rail network with their 10 meter buffer, there appear 0.3 km^2 of green fulfilling the vegetation height thresholds. These figures constitute 0.2 km^2 of green along the river network and 10 meter buffer around it.

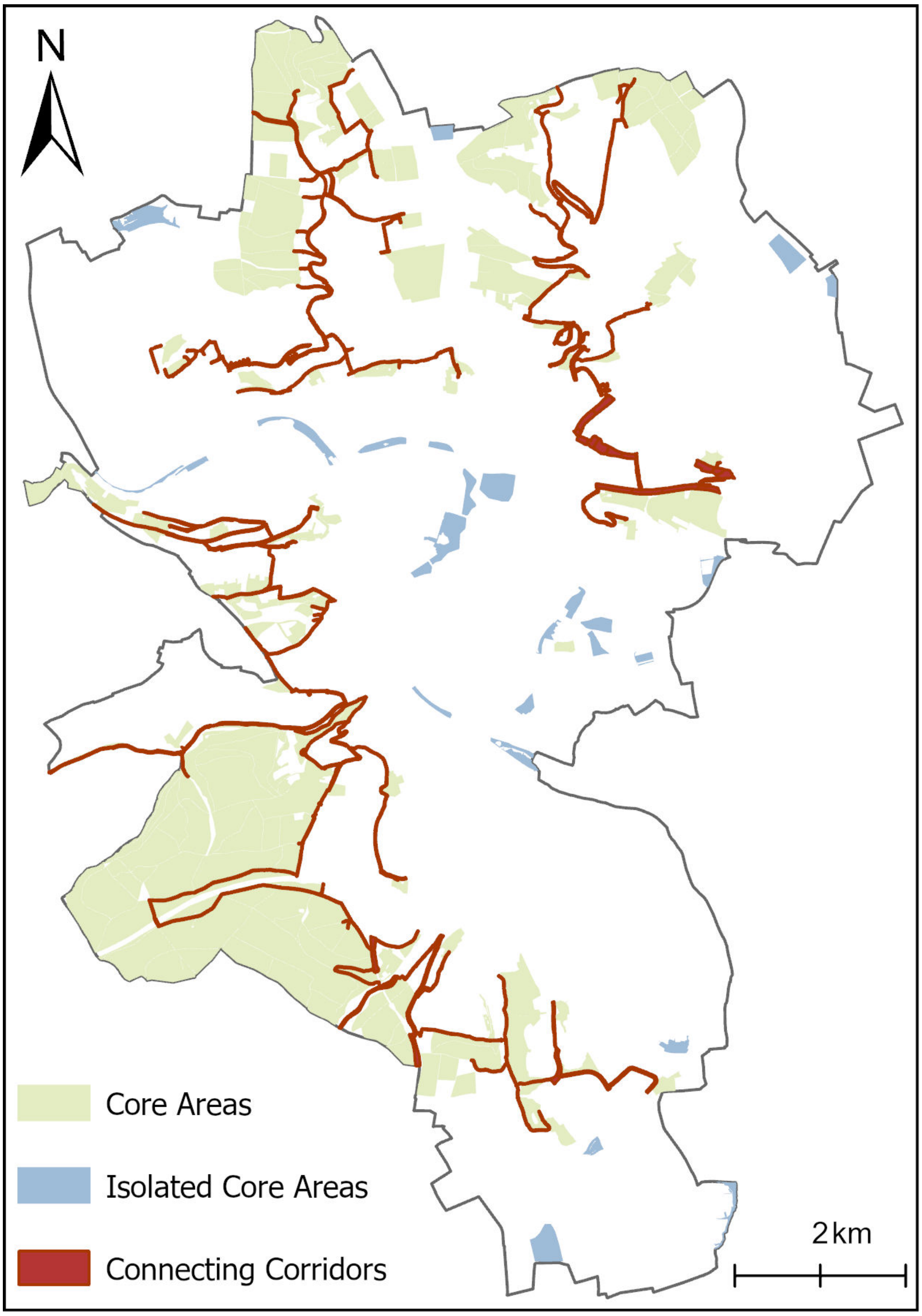

Figure 10.7: Map of the identified green corridor network, made of path, road, and railroad corridor segments, that uninterruptedly connects majority of core areas in Wuerzburg.

In Figure 10.6 we present the identified connector corridors. These corridors are a product of selection of route segments that contain at least 0.1 hectares of green per 100 meters. Consequently, we identify that only 34% of all the road segments within the TN dataset are classified as green corridors. This number constitutes 67% in case of path segments and 46% for the water body segments. From all the railroad segments, 47% fit the green corridor criteria. During the careful visual inspection we reveal that none of the four corridor types can connect core areas uninterruptedly. Furthermore, there is a remarkable insufficiency of green corridors in the central, densely buildup areas of Wuerzburg which can be seen in Figure 10.6. Furthermore, we observe a tendency, that green path corridors mostly appear in places that are already close to other green areas, such as forests and crop fields.

Following the proposed corridor example in Augsburg, we identify a corridor network in Wuerzburg, that is comprised of different green corridor types, and can allow for continuous connection of core areas. The result of this procedure is illustrated in Figure 10.7. It turns out, that utilizing pre-classified green corridor segments, it is not possible to connect core areas located in the northern part of the city with the southern core areas. Moreover, the identified corridors also do not alow a connection of all the core areas in the north. Therefore, we establish three separate green corridor branches that can connect the majority of core areas without interruption. As such, two of such corridors are located in the north and connect mainly two separate clusters of forest and crop field polygons. The third branch of connecting corridors spans from north-west to south-east and connects mainly forest polygons as well. In Wuerzburg we observe better connection of smaller core areas like allotments, recreational areas, cemeteries etc. than in Augsburg. However, parks just like in Augsburg, are the main isolated core type and are followed by green areas. Further isolated core areas, that cannot be connected to any other core areas, are five crop field polygons, one cemetery, two recreational area, two grassland, and three allotment polygons.

Consequently, our results show, that if we rely on only one type of corridor, there is nearly no connection between core areas on both north-south and west-east axes. Therefore, our proposed connecting corridor network with three separate branches, is comprised of 80% of road segments, 19% of path segments, and 1% of railroad segments. The selected connectors are suitable for biodiversity movement, however, within restricted areas. For human mobility, none of the identified green corridors form a continuous green network, by particularly limited distribution within the center of Wuerzburg.

10.5 Discussion and Conclusions

In the existing literature, green corridors are shown to be as important for human well-being as parks and recreational areas. This is because green corridors can provide park-like experiences to community residents [126], can foster positive connections between people and places [51], and provide aesthetic, safe and accessible routes for pedestrians, cyclists, and vehicles [47]. In the light of all the services green corridors provide, they are still not a common green space type that is included in LULC maps.

Identification of green corridors is a straightforward task. In ecological studies, there are two main steps involved into corridor mapping: first perform habitat suitability analysis to identify core habitat areas of the species of interest; then create a connectivity model that establishes or adds linear structures at the critical points that connect the identified core areas [114]. However, mapping green corridors from human perspective is not as frequently performed task and thus there are no hard rules for corridor creation.

In our ontology we differentiate green corridors as a separate UGS type and here perform knowledge-based mapping of them. Therefore, we first define what green corridors mean to us and then implement a workflow to map them. According to our definition, green corridors are networks that connect green core areas. We therefore select potential green spaces in the study areas that can serve as anchor core areas. Moreno et al. [102] in a similar study look for core areas, where more than a half of the areas are covered by trees. However, in both Augsburg and Wuerzburg, there are quite mixed composition green areas ranging from woody forest, to open parks, allotments and grasslands. We therefore, set the threshold of woodiness to 30% to be more inclusive. Our results show, that indeed most of the crop lands and grasslands are eliminated in both cities. This is understandable, as these areas do not have any tree coverage. In contrast, the fact that there are still remaining crop lands after the filter application, could indicate that these areas were covered with high crop vegetation during the time the height dataset was acquired. Croplands exhibit temporal vegetation variations. The nDSM dataset, however, only represents one day, the acquisition date. Therefore, crop fields are dynamic core areas and might change based on the height dataset used. What is however interesting, is that in Wuerzburg none of the allotments are filtered out with only a quarter of allotments remaining in Augsburg. The 30% tree coverage therefore might be location and LU practice dependent.

At the beginning of the analysis we state that we are mainly interested in green corridors for human mobility. Therefore, path and road green corridors are the most relevant corridors from this perspective. Transport green corridors are a very common corridor type extracted in many existing studies. However, similarly to Yan [150], we further delineate railway and water body corridors. It is, however, important to mention, that if there is a possibility to move along the rivers or railroads, then this can be mainly done by using paths or roads. Given path and road datasets are not totally complete, we hope to compensate through using railroad and water body corridors. From the sustainable urban development viewpoint, both human and biodiversity require good living circumstances. Therefore, those sections of rivers and railways that are not accessible to humans, might still be usable for animals.

To identify how much green is stored adjacent to the selected movement network, we use the green space map that we create in Chapter 6. There are many data sources used for this purposes in the existing literate. This list ranges from CORINE LC [24], to Landsat imagery [33]. Both Moreno et al. [102] and Zhang et al. [154] experience under-detection of green spaces due to the datasets' spatial resolution. The authors conclude that smaller

vegetation patches might not have been captured accurately. Our green space map is created using 20 centimeters DOP. Consequently, it is highly detailed and includes all the types of vegetation (trees, grass, bushes) with a high precision. In contrast, our dataset might even include shadows of green spaces, which might result in over-estimation of actual greenness alongside the transport networks. The accuracy of the utilized dataset has already been discussed in Chapter 6 and it has not been validated entirely due to the absence of accurate validation datasets.
What does not seem to be a drawback in other green corridor studies, is the amount of greenness expected per 100 meters. Our results show that there are two main frequent issues around network segments. Firstly, the TN dataset is not consistent in digitizing the full width of all four types of networks. As it can be seen in Figure 10.8(a), one segment of a railroad is digitized by following the actual width of the road, whereas the second section is digitized much larger. LU in the TN dataset does not only consider the actual use but also its ownership. As such, it might be in that section, that area around the railway also belongs to the same owner as the tracks themselves. But it might also be just an error in the digitization. Railway tracks in both cities are not as complex as path and road networks. Therefore, it is feasible to correct railroad and water body polygons, yet extremely time consuming to improve road and path networks.

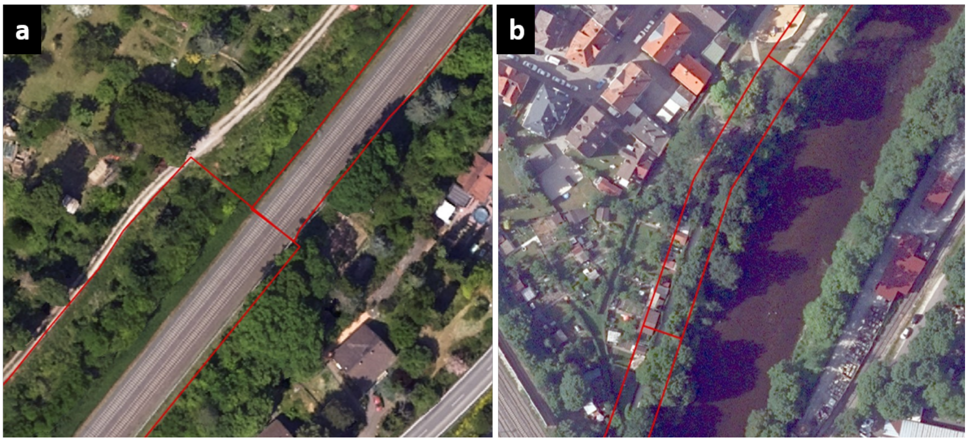

Figure 10.8: Figure illustrating inconsistencies in network digitization in the TN dataset (a), as well as false positive green corridor identification (b) in Augsburg.

Mentioned inconsistencies lead to the fact that some segments of the same network count for more green that the others (narrow digitized ones) which is directly linked to under- and overestimation of vegetation. We attempt to compensate for these differences by improving as many network segments as possible, as well as by creating buffers around the segments. Nevertheless, we still observe that in areas with low digitization accuracy, buffers contribute to overestimation of vegetation. Consequently, for optimal greenness judgment alongside transport networks, the accuracy of the underlying datasets is crucial. Secondly, our results indicate, that the availability of 0.1 hectares of vegetation per 100 meters can be a very sensitive threshold. In Figure 10.8(b) we highlight in red three path segments that are identified as non-green corridors. However, also from the figure, it is obvious, that these segments pass through a densely vegetated riverside. During detailed examination, we observe that there is missing only around 0.0005 hectares for these segments to be classified as a green corridor. Moreno et al. [102] set a requirement of 0.1 hectares of green spaces within 300 meter proximity. This approach requires slightly less vegetation per 100 meters. However, reducing minimum required vegetation amount per 100 meters, might again result in overestimation in areas with sparse vegetation and might again lead to missclassifications. Therefore, it is extremely important to validate the outcome and maybe utilize location-based thresholding. Furthermore, existing studies do not differentiate between sides of the roads. Given the same example, for large roads considering every side separately might help to represent the reality more adequately. Carver et al. [24] differentiate between "line" and "strip" corridors by considering their width and connectivity, which they find significant for conservation efforts. Thus involving width of network segments might result in a totally different picture of green corridors.

What we do not consider in this analysis, but is done previously and might be important to explore as well, is the quality of vegetation on the road segments. Moreno et al. [102] utilize NDVI derived thresholds in order to assess the quality of vegetation. However, the DOP dataset used to create the urban green map contains only three spectral bands. Yet, we use the GLI index during urban green map creation, which can be used as a substitute for NDVI. Therefore, we do not further analyze the state of vegetation.

Our analysis, especially around road and path networks, indicates a considerable amount of qualified green corridors. Yet their distribution is uneven, with significant gaps particularly in city centers. This highlights a common urbanization issue where green spaces appear more fragmented or sparse in highly urbanized areas, affecting the continuity of green corridors [154]. This discontinuity of green corridors not only prevents ecological connectivity but also limits the corridors' effectiveness in providing ecosystem services to more densely populated urban areas. The fact that in both cities, only around 40% of road segments, and less than 70% of path segments are green corridors, further emphasizes the challenge of integrating GI into existing urban settings. Moreover, the spatial distribution of these green segments further complicates connectivity throughout buildup city centers.

We however, still try to trace, whether there are any potential, already existing green corridors. From the human perspective, it is questionable whether green corridors should always aim to connect large green core areas. For pedestrian movement or cycling, the question would potentially be if the route between point A and point B is a green corridor, where it is nicer to cycle. However, if we consider climate change effects such as hotter and drier summers, availability of ways with green provided shadows, might immensely improve day-to-day life in hectic cities. This would, of course, indirectly also facilitate for stronger ecological connectivity. As such, we conclude that in Augsburg it is still possible to highlight continuous corridor networks that connect a majority of core areas. In Wuerzburg, however, there is an immense fragmentation of green corridors. There are three dominant core area clusters that show some sort of within cluster connectivity. Nevertheless, they are not connected with each other. This could be due to the large river crossing the city of Wuerzburg that further disables connectivity. In contrast, two rivers in Augsburg rather facilitate connectivity that disabling it. Although the approach we take to assess connectivity is used on an example of core areas, it can still be implemented in other settings, for connecting different anchor points too.

In conclusion, while the intent to map and connect green corridors for enhancing urban livability and biodiversity is clear, the approach is impaired by poor data quality, inappropriate or vague parameter settings, and a lack of comprehensive validation datasets. We initially state that urban areas contain much more green space than is included into LULC maps. We also pinpoint in the previous chapters, that some of the "unknown" green is street level green. With the performed analysis, we can confirm, that portions of this unnamed vegetation belong to green corridors. Particularly in Augsburg the area of vegetation along corridors equals nearly 13 km^2 while in Wuerzburg around 8 km^2. Consecutively, if we continue excluding green corridors from LULC maps, then we are indeed missing a substantial amount of green that cities store. Nonetheless, at its current state, the identified green corridors fall short in connecting fragmented green core areas. Therefore, future research should focus on improving underlying data quality as well as establishing more robust thresholds for green corridor identification. Further exploring vegetation composition of selected corridors can help to build a better picture as to what extent these corridors support human well-being and biodiversity.

Chapter 11

Synthesis

Throughout the thesis, we perform knowledge-based identification workflows to map urban forests, allotment gardens, peri-urban agriculture, and green corridors. For all performed analyses, we also present their results as well as provide discussions and conclusions for them. In this chapter, however, we address the key points we establish through the analysis and elaborate on them from an overarching perspective of the thesis. These include the usability of the created ontology, particularly in populating its feature properties. Furthermore, we elaborate on the identified semantic characteristics of UGSs and assess the extent to which they supported green space mapping. Additional discussion points include quality requirements for the utilized spatial datasets and the methodologies selected. We conclude this chapter by answering research questions and addressing our hypotheses.

11.1 Conceptual Implementation

In everyday life of bustling cities, human well-being can be compromised. Above average hot summers and scarce shadow opportunities, extreme flooding due to highly sealed surfaces, fragmented natural habitats as a result of intensive constructions are only few of the adverse effects of city life [45][12]. With urban populations on the rise, these challenges are further intensified[1]. Only nature can help nature, can it? A solution to the majority of listed problems is indeed seen in nature itself. That is why the concept of nature-based solutions is popular as never before. This includes establishing green roofs and rain gardens, or construction of wetlands can minimize damaging runoff by absorbing storm water, reducing flood risks and others. Altered city structures and systems make

[1] `https://www.un.org/en/development/desa/population/publications/pdf/urbanization/WUP2011_Report.pdf` (accessed on 01.2025)

it, however, not easy to implement [76].
UGSs serve as breaths of fresh air in congested urban areas. Their importance for human well-being is undeniable. Parks and recreational areas significantly enhance physical and social well-being by providing spaces for physical activities such as walking and jogging, which help to reduce the obesity rates and other health issues, and foster social interactions through community engagement and activities [73]. Urban forests and green corridors contribute notably to mental well-being by offering serene environments that help to reduce stress and anxiety, promote relaxation, support cognitive recuperation, and allow the brain to rest [77][116][148]. Moreover, community gardens enhance subjective well-being by increasing life satisfaction and personal happiness through frequent visits and interactions, which also promote physical activity and healthy eating, thereby supporting overall quality of life [105][46]. The relevance of UGSs is amplified at times of crisis. The COVID-19 pandemic was almost a proof of concept, since UGSs were seen as safe places to attend without the fear of getting infected [117].
However, we establish, that there is still a misunderstanding of types of green spaces and their importance. How would it be even possible to make informed decisions, if there is no knowledge of how much green a city accommodates? We also identify, that the confusion of types of green spaces originates from a long discussed question on what is LU and what is LC [50], as well as what is the smallest size of an object that we can represented on LULC maps. Some UGSs represent LC e.g. forest. Others represent LU, e.g. allotment. Given there are no maps that represent purely LU or only LC [5], shouldn't then UGSs appear on them? Most of the maps utilize a minimum mapping unit to represent information. However, some green spaces can be simply too small to be included into such maps. These include, for instance, street level trees or back and front yard gardens. The latter ones are privately owned areas, which adds on an additional level of exclusion criteria. Furthermore, another reason why certain UGS types are not considered as such, is due to limited understanding of them [127]. If we acknowledge, that LULC maps are the most common data sources to perform various urban analyses, their precision might directly impact decisions made based on them.

11.1.1 Towards a Urban Green Space Ontology

Numerous attempts have been made to establish a common typology of UGSs. However, this commonality is limited only to the topic of interest. Thus, UGS typologies are developed to serve specific purposes. For instance, Degerickx et al. [37] propose a green typology that highlights the services provided by these spaces, Bell et al. [15] suggest a typology of UGSs suitable for hedonic house price estimation, and Cvejić et al. [35] develop a typology to understand the functional linkages between UGSs and ecosystem services as well as biodiversity.
Purpose-oriented typologies are useful for highlighting specific features within a domain

that might otherwise be overlooked. Yet, no such typology exists for enhancing human well-being, making the development of a common classification framework essential. Without this, new typologies are continually proposed, however none of which cover all relevant UGSs comprehensively. Therefore, we consider geographic information ontologies as a reasonable solution for avoiding yet another typology or classification.

Ontologies provide a structured framework that enhances information sharing and collaboration by defining domain-specific terminology. They capture key meanings within a domain and promote semantic consistency across various systems [139]. Therefore, in this work, we propose developing a UGS ontology rather than a typology. Effective ontologies should include the core vocabulary of the domain but also be capable of extension [58]. This feature of ontologies eliminates the need to create a new UGS classification from scratch each time, allowing for adjustments based on specific needs. In contrast, typologies do not aim to define core, universal concepts, and terms can vary based on applications, for example "riverbank green" and "linear green" can be used interchangeably. Moreover, unlike typologies, ontologies are formalized into a machine-understandable format, which simplifies access to the structure of the UGS ontology for various applications without the need to provide the same information repeatedly.

In order to define a common UGS vocabulary, we explore existing UGS typologies and identify the most commonly occurring UGS classes. We also add classes that may appear in one typology but not in another, yet still represent a relevant and distinguishable UGS class. Our domain ontology consists of 7 classes including forest, park, grassland, cemetery, urban agriculture, green corridor, and amenity, each further subdivided into corresponding hierarchical subclasses. From these, only forest, park, and grassland are commonly represented in LULC maps. Urban agriculture, referred to as intensive crop production sites in and around cities, is never marked as UGS in existing maps. Nevertheless, there are many subclasses that represent a significant amount of green and are proven beneficial for human well-being.

As an example, we define allotment gardens as a subclass of urban agriculture. Our analysis reveals that in Augsburg they encompass almost one km^2 of green, whereas in Wuerzburg nearly 0.7 km^2. Furthermore, green corridors also do not appear as a subclass of UGSs. Yet, in almost every city such linear green spaces exist. Only in Wuerzburg, based on our analysis, green corridors encompass nearly 17 km^2 of green, which constitutes about 40% of total green spaces. Consequently, we consider the proposed ontology an important tool that can help to name different types of green spaces, but also helps to estimate the actual green space status of cities. Furthermore, this ontology is adapted to UGSs in southern German cities. Yet, if applied to a different geographic area, it can be extended. For instance, one could add mangroves if the analysis is performed in a Southeast-Asian city. This will not change the structure of the ontology, but rather make it more complete for different geographic locations.

Defining classes and subclasses of UGSs is only one part of the proposed ontology. What makes this ontology distinguishable from typologies, is that it also provides object property specifications. There are examples of attempts to perform ontology-based classification of RS data [7]. While existing RS data classification approaches focus on numeric data, ontologies integrate symbolic knowledge (e.g., "Forest" has "HighNPP" or "HighNDVI" values) with numeric thresholds to enhance knowledge representation and sharing [23]. Consequently, the object property, that we attach to the UGS ontology, supports exactly that knowledge representation with additional numeric information. Since our overall goal is UGS mapping, we define geometry, texture, position, and thematic properties of UGSs. This could further hold values for e.g., texture metrics, form, height, and others. Moreover, the properties can be extended as well in order to more accurately describe UGSs in certain locations.

11.1.2 Integrating Semantic Characteristics

To enrich the proposed ontology with very specific, green space relevant, object properties, we perform four UGS mapping studies. We choose forests, allotments, green corridors, and peri-urban agriculture from our ontology as example green spaces. These, apart from being underrepresented in LULC maps, also exhibit additional characteristics such as temporal dynamics, heterogeneousness, and in some cases small size. In the existing literature, there are not many examples of finding exact thresholds for certain UGS characteristics. Our analysis exhibits that it is indeed extremely challenging to establish one single threshold for a certain property which would remain consistent over different spatial locations. For example, we explore the height property of trees in a forest. The threshold we derive based on the samples in Augsburg shows that the height ranges between 70 centimeters to nearly 29 meters. However, we do not acquire as accurate results when these values are transferred to another city. In contrast, NDVI values of summer months of around 0.6 are in line with the existing literature [9] and clearly represent tree species in forests. Yet, we acquire totally different winter NDVI values as in the existing literature, which again makes it difficult to set certain NDVI values as a crisp identifier of forests both in summer and winter. It could, however, also be that for some properties it is simply not possible to establish exact thresholds at all. While we expect that woody vegetation in general constitutes to NDVI values of 0.6, this can fluctuate by weather conditions, solar illumination, altitude, and others. At its current state, the proposed ontology, even if formalized, cannot be directly used for ontology-based classification because we do not populate this ontology with exact values for their properties. We see the need for these factors to be tested in many different study areas before exact threshold values can be fixed. Alternatively, location-specific properties can be established and applied to the UGS ontology without the need of defining such properties uniquely for all locations and for all circumstances.

Ontologies represent semantic information. To determine if certain green spaces have unique semantic characteristics, we conduct separate studies for four UGS classes. First, we identify and describe their unique "faces" or identifiable features, that is suitable for spatial analysis. Then, we test whether these characteristics are distinct across different study areas.

Forest

To define selected UGSs, we heavily rely on existing literature, which is critical because it builds upon tested methodologies. However, definitions related to green spaces can be too vague for direct implementation in spatial analysis. For example, the FAO definition of a forest suggests that forest canopy coverage should exceed 10%, or have the potential to meet these criteria in situ. This highlights the importance of an area's natural capacity to support a forest ecosystem under local environmental conditions, without the need for human-driven restoration or alteration. While calculating canopy coverage is feasible, incorporating in situ predictions adds a layer of complexity. This process not only requires high-quality data but also local knowledge about the forest regeneration potential in specific areas. Such conditions might vary significantly not just from region to region, but also from city to city, complicating the development of a universally applicable methodology. Consequently, we select semantic features of forests that might not include all the required criteria by FAO, yet are better suited for spatial analysis. However, to prove that the selected features are adequate, we validate our results using TN forest data.

Our results illustrate that some semantic features, validated through OAT SA, provide consistent results in both locations, while others demonstrate varying degrees of effectiveness. Specifically, our analysis shows that the height data (nDSM) and the NDVI values are highly influential across both study areas, confirming their robustness and transferability. However, the textural dissimilarity indices, especially those derived during the leaf-off season in December, are less consistent between the two study areas. In Wuerzburg, these indices do not perform as effectively as in Augsburg, possibly due to different forest compositions or phenological patterns influenced by the local climate and ecological conditions.

Consequently, semantic criteria, which include the presence of tree species, minimum area requirements, tree height, and absence of agricultural or urban LU, among others, are indeed very forest-specific and identifiable using nDSM, NDVI, and TN datasets in both cities. However, some characteristics such as the pattern of tree distribution and proximity to non-forest areas (e.g., agricultural lands) pose challenges in certain cases, indicating that while the semantic definitions are generally specific, it would be beneficial to adjust them based on local ecological and geographical variations.

Allotment

When defining semantic criteria for allotments, we face several challenges. The concept of allotments is clear, and there is even a national law on allotments in Germany. Yet, these mostly describe regulations concerning the use of allotments. Therefore, we utilize the concepts defined within the legislative framework but also include visual observation in-

puts. In contrast to forests, no global definition of allotment gardens exists. Historically, they developed differently in every part of the world, in Europe being an act of counteracting post-war famine [43][52]. Thus, we acknowledge from the beginning that the semantic features of allotments we select are specific to southern Germany. Our feature extraction approach centers around garden sheds as primary indicators, but also considers other features like shed presence, size, height, clustering, and their relationship with other landscape elements such as path networks and proximity to major roads and water bodies. Reflecting on the defined criteria and analyzing the outcomes of our studies, the results confirm that using defined criteria, it is possible with considerable accuracy, to identify allotment gardens in Augsburg. However, the experiment also reveals the variability in the transferability of these features to different areas.
The height thresholds established from the Augsburg data (between 1.93 and 2.62 meters) are somewhat effective in Wuerzburg. Yet there are also discrepancies in accuracy and the prevalence of false positives. Moreover, our results also reveal challenges in meeting one of our key criteria - the presence of path networks. A significant number of the allotment gardens identified in each test does not have intersecting paths, despite this being an essential feature in our allotment definition. Here, we do not observe limitations of selected semantic features, but rather limitations in the utilized datasets to confirm the semantic features. Although selected semantic features of allotment gardens are specific enough to facilitate effective mapping, they still require careful adjustment and validation when applied to different urban settings.

Peri-urban Agriculture

PUA represents a type of "productive" green space primarily characterized as a transitional zone from urban to rural. Due to lower population densities and fewer infrastructural developments, these areas are also seen as not fully "urban" [109]. Similar to forests, the FAO provides a global definition of PUA, referring to it as the practice of cultivating food within city limits. Unlike allotments, where food can also be grown, PUA is a more intensive food production system[2]. We characterize PUA by its near-rectangular plot structures delineated by distinct boundaries, low within-field heterogeneity with a single crop type dominating, and observable phenological changes throughout the growing season. Additionally, consistent spatial patterns and the presence of agricultural infrastructure are key indicators. To test the derived semantic criteria, we perform a change detection approach, setting a threshold to recognize changes in vegetation cover. This analysis is enhanced by incorporating texture metrics that help to refine our identification based on the distinct textural properties of agricultural fields, especially during the leaf-off season. The height data derived from nDSM further refines our ability to differentiate between various types of vegetation and confirm the agricultural use of the identified plots.
However, here we also encounter challenges in aligning all identified PUA plots with the

[2] `https://www.fao.org/unfao/bodies/coag/coag15/x0076e.htm` (accessed on 01.2025)

full range of semantic characteristics. For instance, while a significant number of plots closely matches the near-rectangular shape criteria, fewer plots show the expected proximity to roads or other specified boundaries. Additionally, selected change thresholds might be too sensitive to the smallest changes, thus overestimating overall temporal changes. This suggests that while the overall semantic model is effective, certain aspects such as spatial relationships may require adjustments. Moreover, we observe a good level of transferability between two cities, indicating that the selected semantic characteristics are specific and effective. Yet, we again highlight the necessity for local calibration, especially in terms of infrastructure elements and plot arrangements, which may differ significantly between regions.

Green Corridors

Defining semantic characteristics and mapping green corridors is the most challenging among the selected UGSs due to the limited availability of ground truth data. While some ground truth data exists to prove the robustness of the defined criteria to a certain extent, green corridors have never been mapped for the selected study areas, leaving no data for validation. Moreover, green corridors designed for human mobility in cities are rare, as they commonly serve biodiversity objectives, aiming to connect green areas fragmented by urbanization. We base our green corridor definition on Moreno et al. [102], but modify it to better represent green corridors in our areas of interest. Our semantic characteristics for green corridors include defining corridors as connectors of core green areas, which must be at least 2 hectares in size, have more than 30% tree coverage, and be spaced no more than 2 kilometers apart. Additionally, we categorize corridors by their association with transport routes like main roads, paths, railways, and water bodies such as riverbanks and lakes. At a more detailed level, there should be at least 0.1 hectares of green space per every 100 meters. We establish a non-typical list of core areas compared to existing literature. While parks and forests are the most common green spaces in cities, we also consider allotments, grasslands, botanical gardens, zoos, crop fields, cemeteries, and even children's playgrounds as core areas. These spaces not only provide shelter for animals and serve as anchor points for ecological corridors, but are also actively used by people for their relaxing properties.

Based on our established workflow, we observe that in urban centers and along railway segments, the amount of green is often insufficient to qualify as corridors, leading to gaps in connectivity. This is particularly evident in central Wuerzburg, where urban density reduces the continuity of green corridors. Additionally, we experience variations due to insufficient vegetation between selected corridor types. While path and water body corridors generally meet selected criteria well and demonstrate higher connectivity, road and railway corridors often do not. Urban infrastructure is identified as another probable cause of disconnectedness, along with vegetation quantity. We do not perform a transferability analysis of green corridors because the semantic criteria primarily originate from existing literature and are thus the same for both study areas. The selected semantic

characteristics prove to be good identifiers of green corridors, especially for human mobility. Nevertheless, we find that 0.1 hectares of green vegetation per 100 meters is relatively low, particularly for wider primary roads and railroads. To confirm this, the proposed workflow must be tested in more study areas.
By undertaking knowledge-based mapping, we are able to confirm that selected UGS types indeed possess unique characteristics that make them distinguishable and identifiable within complex urban environments. Looking ahead, the precision in identifying these green space types could be optimized by modifying several aspects. Firstly, acquiring more comprehensive datasets that better represent green spaces. This includes utilizing measurements of temporal vegetation height or incorporating Sentinel-2 datasets spanning multiple years. Since currently no better sources for validation datasets are available apart from TN, manually creating such a dataset could be an alternative way to go. Secondly, revisiting the results of performed analyses and enhancing the feature properties in the ontology could be advantageous. We acknowledge that our ontology is currently incomplete in a sense that it is not directly applicable for ontology-based mapping. However, we do not perform further analysis to complete ontological properties. Nonetheless, through repeated applications of the mapping procedures in various spatial contexts and consistently updating stable feature properties in the ontology, its utility can be significantly enhanced. This iterative refinement can ensure that the proposed ontology becomes genuinely useful, rather than being just another forgotten framework. Consequently, taking into consideration these two points could be a starting point for possible future research in the field.

11.2 Technical Implementation

The importance and challenges of the technical implementation within our analysis evolves around several key aspects of data and methods, which are generally applicable across all identified UGS types.
Data
Regardless of the type of green space we aim to identify, spatial, temporal, and spectral resolution emerge as the main determining factors. This is, however, already known in the existing literature [127]. Sun et al. [133] note that UGSs can be effectively mapped using data with resolutions as fine as two meters and up to 16 meters, beyond which effectiveness diminishes. However, Huang et al. [66] state that adequate results can be achieved even with a 30 meter resolution if a sub-pixel approach is taken. These studies generally focus on large common green spaces and do not provide an elaborated discussion of classification rates per UGS classes. We perform green space mapping using Sentinel-2 data, with visible and NIR bands having 10 meter resolution, which literature confirms is within a suitable range for green space mapping. Nevertheless, we derive two major

outcomes from using this dataset. Firstly, it is suitable for mapping green spaces that are large enough to be accurately captured with a 10 meter resolution, such as forests, crop fields, and grasslands. Secondly, given the resolution is suitable in terms of processing time intensity; even if the analysis is performed for two cities as well as temporal bands and vegetation indices are used, the data processing time remains under 24 hours. However, we identify a major disadvantage of using Sentinel-2 data for green space mapping. Vegetation in areas like allotments or front- and backyard gardens cannot be identified precisely, because within a 10 by 10 meters area, there could be a tree crown, part of a garden shed, pavement, and a crop plot. Since the reflectance of all these objects is different, it is challenging to pinpoint a spectral signature in such small areas. The resolution of Sentinel-2 data also appears to be inadequate for recognizing single trees at street level. It could be that by adopting the sub-pixel approach of Huang et al. [66], it would be possible to extract more detail from mixed pixels. Alternatively, it is fair to say that a 10 meter resolution is only suitable for mapping large homogeneous UGSs. For other green spaces, which do not form a continuous green surface and are heterogeneous, different data sources should be used, if available.

In the existing literature, e.g., Haase et al. [63] and Huerta et al. [67] explore capabilities of very high-resolution data in capturing detailed green space characteristics that are often overlooked by coarser satellite imagery. Therefore, we also test a very high-resolution DOP dataset. We observe that this dataset can identify urban green within all the UGS classes defined in our ontology, especially those that Sentinel-2 failed to identify. DOP with 20 centimeters resolution is capable of not only identifying green or non-green areas but also allows for precise delineation of tree crowns. This is true for both homogeneous forest areas and street level vegetation, where single standing trees are present. It also proves useful in areas where tree shadows appear very similar to some dark green vegetation. However, the major drawback of using this dataset is the processing time. Performing straightforward binary classification of green/non-green areas requires over 24 hours in Augsburg. In Wuerzburg, this number is slightly lower since the area of Wuerzburg is smaller than that of Augsburg. Consequently, based on our results, we understand that the choice of data resolution should be in accordance with the question of interest. If the aim is to map large green areas like forests, cemeteries, or parks, or if the exact delineation of green space boundaries is not of relevance, then Sentinel-2 data is a better choice. However, if the focus is to exactly delineate every type of green space, or to delineate only trees or sparse vegetation in gardening areas, then a DOP with 20 centimeters resolution could be a more suitable choice.

Green vegetation, unlike other objects on the earth's surface, has distinguishing spectral characteristics. Chlorophyll in the leaves absorbs blue and red light, while the mesophyll leaf structure scatters NIR [151]. Therefore, utilizing vegetation indices that highlight these characteristics can be beneficial for vegetation detection. Many studies use NDVI alongside the spectral bands to maximize information gain [37][104]. However, to calculate

vegetation indices, especially NDVI, NIR or other non-visible spectral bands are required. Sentinel-2 provides a wide range of spectral bands, but only red, green, blue, and NIR bands have 10 meters resolution. Our analysis of urban green mapping illustrates that NDVI is indeed a key predictor variable. There are, however, other vegetation indices that could help highlight, for example, water stress in plants or reduce soil background effects in reflectance values. Based on the results of our analysis, including those vegetation indices might not necessarily improve the outcomes. If a 10 meter resolution is already too low for some green spaces, using bands with 20 or 60 meters resolution, which are needed for other indices, might deteriorate the results even more.
A disadvantage of using DOP is that it only contains visible light information. Agapiou [3] illustrates that indices like GLI and NGRDI, derived from the basic RGB bands, can effectively differentiate various forms of vegetation. Based on our analysis, we can state that GLI is one of the most influential predictors of green vegetation. Therefore, we can confirm that even though DOP offers limited spectral resolution, using the GLI index can produce much better results than Sentinel-2 data, which has many more spectral bands.
Apart from the reflective and absorption properties of green vegetation, in the temperate climate zone they also exhibit phenological changes. This is particularly true for herbaceous and deciduous vegetation. Vegetation in both study areas comprises a mix of deciduous and coniferous types, so some seasonal changes in plant appearance are expected. Therefore, temporal data is critical for capturing phenological changes that can significantly influence the classification accuracy of UGSs [1]. We utilize temporal Sentinel-2 data for several purposes: to improve classification gain when mapping overall green spaces, and to map forests as well as PUA. We observe that the use of multi-temporal NDVI effectively captures seasonal dynamics of vegetation, and therefore, even with lower spatial resolution, it can identify a majority of green spaces. Moreover, temporal Sentinel-2 datasets appear to be the key identifier of agricultural fields in the case of PUA analysis. Through the use of change detection approaches, we are able to accurately establish which areas illustrate vegetation change at least three times per year. The DOP dataset does not provide seasonal information. Its acquisition is costly and therefore is commonly done only once per year.
The temporal factor of the utilized datasets extends beyond DOP and Sentinel-2 data. In all our studies, we use vegetation height as a semantic indicator. Utilizing Airborne Lidar datasets in conjunction with NDVI and spectral bands has proven advantageous for vegetation delineation [37]. However, point cloud datasets can be very expensive to acquire. Therefore, we opt for the more cost-effective nDSM dataset. By using DTM and DSM models, nDSM represents the height of objects above the ground. As a result, nDSM is used more often for vegetation detection than Lidar data [10][83]. Nevertheless, we observe that nDSM, due to its limited temporal resolution, can be more of a limiting than an improving factor. For instance, when performing forest identification, nDSM appears to be a key parameter that helps to distinguish between forests and crop fields. In

contrast, when mapping crop fields, we observe that some fields are incorrectly eliminated due to the height factor. This should not have been the case, but the height information from a single date fails to recognize this. Consequently, we see here an improvement potential for all the performed analyses, to include temporal nDSM and DOP datasets.

Availability of datasets is another significant decision factor, alongside resolution. The Sentinel-2 dataset is freely available and can be utilized at no cost. In Bavaria, the DOP dataset is also freely available and can be acquired in 40 and 20 centimeters resolutions. However, nDSM is not a readily available product. We calculate it using DTM and DSM datasets. While DTM is available at a 1 meter resolution for free, DSM is not free of charge at the time of performing the practical analysis. The free availability of selected datasets is crucial for conducting transferability analysis. We were able to perform this analysis for two study areas because we acquired the DSM dataset. However, for future knowledge-based mapping efforts, the availability of these selected datasets could become a limitation that should be considered in advance.

Validation of results is an essential step in mapping procedures. We utilize the TN dataset for validation purposes; however, due to inherent inaccuracies within the TN dataset and its failure to recognize some UGSs as green areas, we achieve only partial validation of our findings. Consequently, enhancing the accuracy of validation datasets or utilizing alternative validation methods, such as through DL applications, could provide deeper insights into the final results.

Methods

Besides data resolution, it is crucial to consider the methods used or applicable for such datasets. ML methods are increasingly utilized for mapping UGSs, due to their capacity to handle large datasets and complex classification tasks. RF and SVM are two of the most popular choices for their robustness and accuracy in classifying LULC types in general [75][27]. Another established approach for such tasks is geoOBIA [18]. We chose to use RF in combination with Sentinel-2 and DOP data, as it has proven to be very promising in achieving good classification outcomes [147]. Availability of training and validation data is a primary requirement for assessing the quality of a classification. We collect these manually, as there are currently no accurate training datasets available for the study areas. Looking at the results and processing steps, we can also confirm that RF is a suitable ML method for urban green detection. However, we observe that in the followed set up, RF does not require building more than 500 trees to achieve very accurate results. This suggests that the classification task we perform is relatively simple and straightforward. Especially when using DOP data, where only values between 0 and 255 are possible, RF does not require many trees to learn the green space pattern. Here, the use of the RF model can be argued. However, in previous research, we also test a simple rule-based classification approach [69]. Although we generally reach good results for mapping forests, we find this approach not very suitable for transferability analysis. Contrary, RF trained using training data from one study area, can be utilized for other geographic contexts. Therefore, we find the RF model superior to other techniques, especially under consideration of transparency in ML mapping procedures.

To eliminate the possibility of over-fitting, where the model learns the data instead of the pattern, we assess OOB accuracies. These clearly indicate that the RF model is not over-fitting. To further prove that the model can recognize green areas under new circumstances, we apply models trained in Augsburg to predict green vegetation in Wuerzburg. When using Sentinel-2 data and the RF model from Augsburg, we classify 9 km^2 more green space in Wuerzburg than if we were to train the model directly with data from Wuerzburg. However, using the DOP and RF model, we identify nearly 8 km^2 more green space than with the model trained in Wuerzburg. Given that Sentinel-2 generally fails to adequately identify all green spaces, 9 km^2 of over-prediction is actually a high number. What the DOP and RF model combination fails to recognize are tree shadows, especially in forests. Consequently, we confirm that our model is not over-fitting, but we also establish that for more accurate transfer-learning results, models should be trained with training data from the study area of application.

Additional Techniques

In addition to the RF model, we face challenges with many of the techniques we use. For instance, GLCM matrices prove sensitive to gray levels in different study areas, necessitating further exploration of their parameters. Similarly, clustering of garden sheds and defining optimal cluster parameters is similar to the challenges observed with GLCM. We select clustering parameters based on available evidence. For example, the minimum number of clusters for shed clustering is set based on our knowledge of the number of plots in the smallest allotment garden in both cities. However, the distance between sheds is measured in some sample gardening areas. Consequently, when discussing quality of the derived semantic features and their transferability to other cities, it is important to consider that it may not be the features themselves, but rather the parameter settings in intermediate steps that affect the final outcome.

From the methodological perspective, the provided ontology at its current state does not support ontology-based mapping procedures. We formally conceptualize it by presenting it in OWL language through the Protégé software. This means, that it is already in a machine-comprehendible form. Nevertheless, we do not populate feature properties that can be used for mapping actions. Therefore, we see a tremendous need for reapplication of the proposed method, so that the feature properties can be confirmed and entered into our ontology. By exploring only two study areas and the minimum adequate list of semantic features, the ontology-based mapping goal is out-of-scope of this thesis.

In addition, our ontology contains seven UGS types, four of which we detect in this thesis. The proposed knowledge-based mapping can be applied to the other three classes as well. For this, existing regulations and definitions of these UGS types need to be examined and relevant semantic information should be extracted. Especially identifying types that are not recognized as green space, the majority of which appears under the agricultural and

amenity class, is crucial for human well-being as well as for sustainable city development under climate change.
The techniques and results presented in this work serve as valuable references for urban planners and decision makers. Our experience and insights confirm that this approach is not only promising but also a useful supplementary tool for both understanding and managing UGSs.

11.3 Answer to the Research Questions

Hereafter, based on the performed analysis we answer our research questions. Furthermore, here we also address our hypotheses.

RQ 1: To what extent is it possible to develop a unified vocabulary for urban green spaces to form the basis of an ontology that facilitates domain-standardized knowledge sharing?

Many UGS typologies exist, but they do not always overlap because they are developed for various use cases. When these classes are combined, a large variety of UGS vocabulary can be created. However, regional differences may appear, as the type of green spaces is closely related to climatic and soil conditions. Therefore, based on our synthesis of existing typologies, we can state that it is possible to develop a common vocabulary for a domain-specific ontology. Its span is however limited to southern Germany. Nevertheless, the ontology we provide aligns with the requirements for ontology development, meaning it can easily be extended, if needed, to different spatial locations.

RQ 2: What unique spatial semantic characteristics of forests, allotments, peri-urban agriculture, and green corridors can be derived to assist their identification?

We examine four types of UGSs and develop their unique spatial semantic characteristics. These types include forests, allotment gardens, PUA, and green corridors. Below, we will detail the semantic characteristics we use for their identification.
A forest is defined primarily by its vegetation, consisting of tree species that cover areas larger than 0.5 hectares and typically exceed 5 meters in height. These areas must not overlap with other LUs such as agriculture or urban environments. Forests may also include younger tree populations that have not yet reached the expected heights but are anticipated to do so. Additionally, these spaces might temporarily lack trees; however, natural regeneration is expected within five years. The definition specifically excludes agricultural production systems like olive orchards or vineyards, as well as woody vegetation patterns such as scattered trees, tree lines, or hedges, to distinguish forests from

agricultural or ornamental landscapes. Forests are also not located adjacent to railway paths. Moreover, areas covered with linear tree formations such as windbreaks and shelterbelts are considered as part of forests if they cover an area greater than 0.5 hectares and are wider than 20 meters.
An allotment garden is characterized by specific structural and locational features that support its designation and functionality. Each allotment garden is defined by the presence of garden sheds, with every allotment containing at least one shed. These sheds are restricted in size to not exceed 24 square meters and have a maximum height of 3.5 meters. Organizationally, an allotment should feature a cluster of at least five garden sheds, indicating the presence of minimum five separate allotment plots within the garden. The allotments are designed with a network of intersecting paths to facilitate access and mobility within the area, enhancing the functionality of the space. Locationally, allotment gardens are typically situated away from major roads but are often found close to railroads and/or water bodies.
PUA is a unique type of UGSs that integrates agricultural productivity within an urban environment. The plot structures in PUA areas are predominantly near-rectangular or regularly shaped, usually demarcated by clear and precise boundaries such as roads, hedges, or irrigation channels. Within these plots, there is very low heterogeneity, as typically only one type of crop dominates each field. PUA exhibits distinct phenological changes throughout the growing season, which are essential for crop management. For annual crops, these stages include seedling emergence, full plant growth, and harvest, while permanent crops go through phases such as flowering, fruiting, and subsequent harvest cycles. Spatially, PUA is characterized by consistent patterns, such as evenly spaced planting rows or uniform planting densities. Additional distinctive features of PUA include the presence of agricultural infrastructure, such as irrigation systems, farm buildings, machinery tracks, and access roads.
Green corridors function as networks that enhance connectivity between larger green spaces, referred to as core areas, within urban landscapes. These corridors primarily serve to link core areas that are each at least 2 hectares in size and substantially vegetated, with tree coverage exceeding 30%. Furthermore, the distance between any two core areas does not exceed 2 kilometers. Green corridors manifest in various forms, including green transport and green water body types. The green transport type includes main road corridors, path road corridors, and railway green corridors. Green water body corridors encompass those along riverbanks and around lakes. To qualify as green corridors, every 100 meter segment of the network must encompass more than 0.1 hectares of vegetation.

- H1: Integrating the unique spatial semantic characteristics of urban green spaces into existing mapping methodologies enhances the effective identification of these spaces within urban areas.

To be able to prove this hypothesis we perform four studies, where we combine semantic characteristics with the existing methods. While the selected semantic characteristics help to enhance one or another aspect during the identification process, these do not result in a 100% identification accuracy. Therefore, we establish that the selected characteristics are useful for highlighting certain aspects of green spaces that otherwise would be lost or ignored if traditional mapping procedures are used. Nevertheless, they do no allow very precise identification without a need of further improvement. Therefore, we reject this hypothesis.

- H2: The selected spatial semantic characteristics remain consistent across different spatial locations.

We test selected semantic characteristics in two cities, Augsburg and Wuerzburg. We identify that some of the selected features are consistent in both cities. These are mostly structural characteristics like shed or vegetation height, form of fields and others. However, semantic features that describe the vegetation itself or dataset, frequently failed during the transferability analysis. For instance NDVI values, texture metrics, and phenology are highly location, weather condition and acquisition time sensitive. Consequently, we reject this hypothesis, as selected semantic characteristics are not consistent through spatial locations.

- H3: Utilizing freely available high-resolution Sentinel-2 imagery provides a comparable level of accuracy in identifying urban green spaces' coverage as does using freely available very-high resolution aerial imagery.

To prove this hypothesis, we perform a comparative study of green space mapping using Sentinel-2 data and DOP data. If we consider all the green spaces that appear in our ontology, then we observe substantial differences in the classification results. DOP provides much higher definition of green spaces, thus the produced product has higher level of detail. This is particularly relevant in areas where only scattered trees appear, like sidewalks or allotments. Sentinel-2 data fails to represent such fine information. Although, using Sentinel-2 it is possible to acquire good detection results of larger and more homogeneous green spaces. While we are only partially able to validate the results, it still allows us to conclude that Sentinel-2 and DOP data provide different classification outcomes. Thus, we reject this hypothesis.

Chapter 12

Conclusions and Outlook

Today there are more people living in cities than ever before. In bustling urban centers, UGSs provide unique opportunities for human well-being. Allowing cognitive restoration, reducing stress-induced adverse health effects, enhancing mental productivity, providing areas for recreation, physical activity, and social interaction are only fractions of services provided by UGSs. However, we identify that there is no universal agreement of what types of UGSs exist. Due to the persistent trend of exploration of large homogeneous green areas, smaller or fragmented green areas are frequently overlooked. Underrepresentation or exclusion of some types of UGSs is frequently connected either to their size or to our limited understanding of them. Yet, by excluding such green spaces from spatial analysis, we are missing on a considerable amount of green that exists in cites. Moreover, methods for their identification can vary depending on the type of UGS. However, current trends in UGS mapping predominantly implement machine or deep learning techniques. These methods achieve good identification outcomes. Nevertheless, they are highly cost-intensive and difficult to interpret. To overcome discussed issues, in this thesis, we propose two solutions and use conceptual and applied examples to illustrate their feasibility.

12.0.1 Urban Green Space Ontology

Types of UGSs are commonly organized in typologies. However, in order to organize UGS types, we propose a UGS ontology. By doing so, we also seek an answer to our first research question that asks to what extent it is possible to develop a unified vocabulary for UGSs to form the basis of an ontology that facilitates domain-standardized knowledge sharing.

Unlike typologies, ontologies are extendable and usable by machines due to their formalization. We further enrich the UGS ontology though object properties. These properties contain descriptive information, such as height, distance, that can be used to uniquely identify various UGS types. However, our analysis indicate that it is not easy to establish crisp feature ranges that could be applicable at various spatial locations. While we are capable to identify ranges of values for some features, others are nearly impossible to narrow down. For instance, NDVI values of around 0.6 can accurately describe woody vegetation. This is stated in the existing literature, and is also confirmed throughout our forest identification procedure. Yet, other properties, such as texture metrics are highly image quality dependent and their values are extremely challenging to transfer to new study areas. In contrast, non-numeric features, such as presence of sheds and path networks in allotments, can be accurately identified and confirmed, as well as can be fixed within the ontology. Consequently, our study confirms the possibility of developing a unified vocabulary for a domain-specific ontology to facilitate standardized knowledge sharing among UGSs. Moreover, our ontology also allows for organizing UGS classes into a common hierarchy. Through the definition of seven main UGS types and 28 sub-types, we capture all possible UGS types southern German cities can accommodate. These classes, defined under consideration of human well-being, consider not only common large UGSs, but also commonly neglected smaller green spaces. The ontology we develop is adaptable and can be extended to different geographical locations, though initially it is tailored for southern Germany. However, the difficulty of establishing crisp properties makes this ontology not yet ready for ontology-based classifications.

12.0.2 Knowledge-Based Mapping of Urban Green Spaces

Given the underrepresentation of some UGS types is related to our limited understanding of them, we recognize machine and deep learning approaches for UGSs mapping as poorly suitable due to their limited interpretability. In this regard, we propose knowledge-based mapping of UGSs. Through performing this novel green space identification procedure, we also aim to find answers to our second research question, namely what unique spatial semantic characteristics of UGSs can be derived to assist their identification. This approach considers first understanding the semantics of various types of green spaces. We achieve this by exploring existing official definitions as well as investigating legal regulations. We then extract spatial-semantic characteristics that we further use for their identification. To establish to what extent the proposed identification approach is suitable, we test it in a new study area.

In this thesis, we identify four types of green spaces, namely forests, allotments, peri-urban agriculture, and green corridors. Overall, we determine, that some of the defined semantic characteristics are specific enough to effectively map selected green space types. Parameters such as tree height and NDVI are examples of transferable parameters across two study areas. For most of the other features like texture measures, we experience a need for adjustments to improve their specificity and applicability in varying geographic contexts. Moreover, from a parameter definition perspective, we also experience some limitations. As such, the definition of sensitivity thresholds, or spatial proximity thresholds influences final identification results. Therefore, we see a need for adjustments in spatial relationships and sensitivity settings to ensure the criteria are fully applicable and effective in various urban contexts.

Our findings emphasize a need for a flexible application of selected semantic criteria. This means, that during semantic feature selection process in new study areas, it should always be accounted for regional differences, because these differences can significantly affect the identification accuracy. An example of such accountability could be considering different crop production and harvest cycles or temporal precipitation fluctuations. In addition, investigating local regulations can further help to refine semantic characteristics. For instance, height of sheds in allotments, or minimum and maximum height of trees in forests could be locally regulated. Therefore, identifying such fixed features can diminish vagueness in threshold selection and increase final mapping accuracy.

Semantic-feature based mapping, in our experience, can be time intensive, especially when considering that the required feature sets as well as tailored spatial datasets must be created beforehand. Furthermore, it requires different techniques to identify different semantic features. Consequently, incorporating more traditional, e.g. geoOBIA techniques might reduce some intermediate steps. The availability of pre-calculated datasets, such as nDSM, NDVI, could also facilitate cutting down the processing costs. Consequently, in terms of the research question, we do identify various semantic characteristics for all four selected UGS types. However, their applicability in other regions requires further investigation.

In order to be able to communicate how much green is stored within various UGS types, we perform an RF-based classification procedure. Here we also explore to what extend the spatial, spectral, and temporal resolution of datasets affect final classification accuracy. While there are suggestions in the existing literature, there are no precise definitions as at what scale of the datasets which types of UGSs can be mapped. We identify, that the choice of datasets should be based on the final goal. We establish, that DOP provides the most accurate results, in comparison to Sentinel-2 datasets. This is especially evident across heterogeneous and small green space types. However, it requires much higher processing capabilities and is extremely cost intensive. In contrast, Sentinel-2 can achieve similarly good results, but only for large homogeneous green spaces. Consequently, if the final goal of analysis is to identify large green space types, like forests, then Sentinel-2 can be a more suitable solution. Yet, if the goal is to explore the vegetation composition of e.g. allotments, a DOP with 20 centimeters spatial resolution can more adequately represent green areas. In addition, if seasonal changes are unique characteristics of UGS types, then DOP images can fall short. Nevertheless, this limitation can be compensated using additional datasets, such as vegetation height.

12.0.3 Results of Hypothesis Tests

In this thesis, we test three hypotheses. We first test whether integrating the unique spatial semantic characteristics of UGSs into existing mapping methodologies enhances the effective identification of these spaces within urban areas. In this work, we observe mixed results. While some characteristics enhance the identification process of UGS, they do not achieve 100% identification accuracy and require further refinement. Consequently, this hypothesis is rejected, indicating the need for improvements in how these characteristics are implemented within mapping methodologies. We further test our second hypothesis stating that the selected spatial semantic characteristics remain consistent across different spatial locations. Testing in Augsburg and Wuerzburg reveals that structural characteristics like vegetation height and form remain consistent, but other semantic features related to the vegetation itself show variability due to location-specific factors like climate and acquisition time. This leads to the rejection of this hypothesis, suggesting that semantic features need to be adaptable to local conditions for effective transferability. Finally, our third hypothesis states that utilizing freely available high-resolution Sentinel-2 imagery provides a comparable level of accuracy in identifying UGS coverage as does using freely available very-high resolution aerial imagery. However, our comparative study of green space mapping with Sentinel-2 and high-resolution DOP imagery indicates significant differences in classification results. DOP provides more detailed identification of green spaces, particularly in complex urban settings with scattered trees and smaller green patches. Sentinel-2, while effective for larger, more homogeneous green spaces, does not match DOP in detail. This hypothesis is therefore also rejected, underscoring the limitations of freely available high-resolution satellite imagery for detailed green space mapping.

12.0.4 Contributions

This thesis represents a significant advancement in GIScience, starting with its demonstration of the critical importance of establishing a common vocabulary for UGSs. Our work successfully develops and introduces a comprehensive UGS ontology and sets a foundational framework for further exploration. Furthermore, we provide and showcase an approach for organizing UGS classes that has not been attempted previously. By doing so, we illustrate that UGS classes can vary depending on spatial locations and thus require organizational techniques that allow for modifications and adjustments. Additionally, by establishing the UGS ontology, we demonstrate how UGS features could be organized and associated to enable machine-aided detection of these spaces in the future.

We significantly advance the field by demonstrating the effective utilization of unique semantic characteristics of UGSs to enhance their identification. Our research reveals that existing definitions of UGSs are not immediately suitable for identification purposes.

However, with minor modifications, these definitions can facilitate the extraction of semantic information and improve the detection of these spaces. We show that forests can be precisely identified using area and height information, as well as spatial relationships to other land uses, such as agricultural areas and railroads. Allotment gardens, with their distinctive features including the presence of sheds, their area and height, and a network of intersecting paths, also offer unique characteristics that aid in their detection. Additionally, PUA can be characterized and identified through phenological vegetation changes, within-field textural variability, and field shape. Finally, green corridors are distinguishable by their linear shape, the presence of 0.1 hectares of vegetation every 100 meters, and their role in connecting large green areas.
This study takes an innovative step by integrating traditional geoinformatics tools with modern machine learning techniques within our identification workflows, thereby enriching the methodological toolkit available for UGS mapping. Moreover, by testing our methodological approaches in two distinct study areas, this thesis not only contributes to the GIScience community but also significantly impacts the domain of UGSs. These tests confirm the essential role of methodological testing and validation, ensuring that our contributions are both practical and theoretically robust. Through the established UGS identification approach, we open new dimensions for leveraging existing analytical tools as well as enhancing their utility in the dynamic field of UGS mapping.

12.0.5 Future Research

Results of this thesis might concern city planners as well as decision makers at various scales, because it can equip them with a robust, knowledge-based mapping tool that enables more effective monitoring and management of UGSs. With this approach, planners can proactively oversee developments within these areas and implement necessary changes in a timely manner. Nevertheless, this study also opens up several avenues for further research. Future investigations should aim to refine the feature parameters of our ontology to ensure its applicability across broader regions. This step is essential for the ontology to reach its full potential in supporting ontology-aided identification of UGSs. Moreover, the spatial-semantic features developed here must undergo extensive testing in various regions to validate their effectiveness and adaptability. Beyond mere testing, there is a pressing need to explore and define new semantic features that more accurately describe the evolving dynamics of UGSs. Identifying and integrating such features will be pivotal in enhancing the livability and relevance of the proposed UGS ontology, ultimately reinforcing its utility in urban planning and development.
From a practical standpoint, optimizing parameter settings and enhancing the quality and quantity of training data for the RF model represents a crucial advancement. Such refinements are essential for developing more precise and transferable models. In our tests, the transfer model utilizing RF does not perform as anticipated, highlighting the need

for further development in this area. By focusing on improving transfer models, we can achieve more spatially generalizable models, which in turn will significantly lower both production and implementation costs. Additionally, conducting a comprehensive SA on all selected semantic features will greatly enhance the reliability of our approach. Future efforts should therefore include detailed sensitivity analyses across all features, and more rigorous testing of defined threshold values. This will also facilitate more accurate knowledge sharing, and will not only refine our current methodologies but also set a new standard for precision in the field.

We have undertaken a thorough and comprehensive analysis of UGSs, acknowledging their vital role in enhancing human well-being. Given their significant impact, it is crucial that our findings are carefully assessed from the lenses of urban planning and strategic decision-making. Such an evaluation is crucial to ensure that our insights and recommendations can drive transformative changes in urban planning practices across selected study areas. This research serves as a foundation upon which future urban environments can be designed to be more sustainable and resilient to serve well-being.

Bibliography

[1] A. M. Abdi. Land cover and land use classification performance of machine learning algorithms in a boreal landscape using sentinel-2 data. *GIScience & Remote Sensing*, 57(1):1–20, 2020.

[2] A. Abdollahi and B. Pradhan. Urban vegetation mapping from aerial imagery using explainable ai (x). *Sensors*, 21(14):4738, 2021.

[3] A. Agapiou. Vegetation extraction using visible-bands from openly licensed unmanned aerial vehicle imagery. *Drones*, 4(2):27, 2020.

[4] J. Ahern. Greenways as a planning strategy. *Landscape and Urban Planning*, 33 (1-3):131–155, 1995.

[5] J. R. Anderson. A land use and land cover classification system for use with remote sensor data, 1976. URL `https://pubs.usgs.gov/pp/0964/report.pdf`. Accessed on 01.2025.

[6] K. J. Archer and R. V. Kimes. Empirical characterization of random forest variable importance measures. *Computational Statistics & Data Analysis*, 52(4):2249–2260, 2008.

[7] D. Arvor, L. Durieux, S. Andrés, and M.-A. Laporte. Advances in geographic object-based image analysis with ontologies: A review of main contributions and limitations from a remote sensing perspective. *ISPRS Journal of Photogrammetry and Remote Sensing*, 82:125–137, 2013.

[8] D. Arvor, M. Belgiu, Z. Falomir, I. Mougenot, and L. Durieux. Ontologies to interpret remote sensing images: why do we need them? *GIScience & Remote Sensing*, 56(6):911–939, 2019.

[9] J. Aryal, C. Sitaula, and S. Aryal. Ndvi threshold-based urban green space mapping from sentinel-2a at the local governmental area (lga) level of victoria, australia. *Land*, 11(3):351, 2022.

[10] I. Balenović, A. Seletković, R. Pernar, and A. Jazbec. Estimation of the mean tree height of forest stands by photogrammetric measurement using digital aerial images of high spatial resolution. *Annals of Forest Research*, 58(1):125–143, 2015.

[11] A. Bannari, D. Morin, F. Bonn, and A. Huete. A review of vegetation indices. *Remote sensing reviews*, 13(1-2):95–120, 1995.

[12] F. Baró and E. Gómez-Baggethun. Assessing the potential of regulating ecosystem services as nature-based solutions in urban areas. In *Nature-based solutions to climate change adaptation in urban areas: linkages between science, policy and practice*, pages 139 – 158. Springer, 2017.

[13] C. Bartesaghi Koc, P. Osmond, and A. Peters. Towards a comprehensive green infrastructure typology: a systematic review of approaches, methods and typologies. *Urban Ecosystems*, 20:15–35, 2017.

[14] C. Bartesaghi-Koc, P. Osmond, and A. Peters. Mapping and classifying green infrastructure typologies for climate-related studies based on remote sensing data. *Urban Forestry & Urban Greening*, 37:154–167, 2019.

[15] S. Bell, A. Montarzino, and P. Travlou. Mapping research priorities for green and public urban space in the uk. *Urban Forestry & Urban Greening*, 6(2):103–115, 2007.

[16] J. Bendig, K. Yu, H. Aasen, A. Bolten, S. Bennertz, J. Broscheit, M. L. Gnyp, and G. Bareth. Combining uav-based plant height from crop surface models, visible, and near infrared vegetation indices for biomass monitoring in barley. *International Journal of Applied Earth Observation and Geoinformation*, 39:79–87, 2015.

[17] F. Beute, M. Andreucci, A. Lammel, Z. G. Davies, J. Glanville, H. Keune, M. Marselle, L. O'Brien, A. Olszewska-Guizzo, R. Remmen, A. Russo, and S. de Vries. Types and characteristics of urban and peri-urban green spaces having an impact on human mental health and wellbeing: a systematic review. Technical report, EKLIPSE Expert Working Group, 2020. URL `https://kar.kent.ac.uk/89644/`. Kent Academic Repository. Accessed on 01.2025.

[18] T. Blaschke. Object based image analysis for remote sensing. *ISPRS journal of Photogrammetry and Remote Sensing*, 65(1):2–16, 2010.

[19] L. Blickensdörfer, M. Schwieder, D. Pflugmacher, C. Nendel, S. Erasmi, and P. Hostert. Mapping of crop types and crop sequences with combined time series of sentinel-1, sentinel-2 and landsat 8 data for germany. *Remote Sensing of Environment*, 269:112831, 2022.

[20] E. Borgogno-Mondino and V. Fissore. Reading greenness in urban areas: Possible roles of phenological metrics from the copernicus hr-vpp dataset. *Remote Sensing*, 14(18):4517, 2022.

[21] L. Breiman. Bagging predictors. *Machine Learning*, 24:123–140, 1996.

[22] L. Breiman. Random forests. *Machine Learning*, 45:5–32, 2001.

[23] G. Camara. On the semantics of big earth observation data for land classification. *Journal of Spatial Information Science*, (20):21–34, 2020.

[24] S. Carver, I. Convery, S. Hawkins, R. Beyers, A. Eagle, Z. Kun, E. Van Maanen, Y. Cao, M. Fisher, S. R. Edwards, et al. Guiding principles for rewilding. *Conservation Biology*, 35(6):1882–1893, 2021.

[25] G. Chen, Q. Weng, G. J. Hay, and Y. He. Geographic object-based image analysis (geobia): Emerging trends and future opportunities. *GIScience & Remote Sensing*, 55(2):159–182, 2018.

[26] R. Chen, J. Carruthers-Jones, S. Carver, and J. Wu. Constructing urban ecological corridors to reflect local species diversity and conservation objectives. *Science of The Total Environment*, 907:167987, 2024.

[27] Y. Chen, Q. Weng, L. Tang, Q. Liu, X. Zhang, and M. Bilal. Automatic mapping of urban green spaces using a geospatial neural network. *GIScience & Remote Sensing*, 58(4):624–642, 2021.

[28] C. Coburn and A. C. Roberts. A multiscale texture analysis procedure for improved forest stand classification. *International journal of remote sensing*, 25(20):4287–4308, 2004.

[29] D. Comaniciu and P. Meer. Mean shift: A robust approach toward feature space analysis. *IEEE Transactions on Pattern Analysis and Machine Intelligence*, 24(5): 603–619, 2002.

[30] A. Comber, C. Brunsdon, and E. Green. Using a gis-based network analysis to determine urban greenspace accessibility for different ethnic and religious groups. *Landscape and Urban Planning*, 86(1):103–114, 2008.

[31] H. Couclelis. Ontologies of geographic information. *International Journal of Geographical Information Science*, 24(12):1785–1809, 2010.

[32] M. Crosetto, S. Tarantola, and A. Saltelli. Sensitivity and uncertainty analysis in spatial modelling based on gis. *Agriculture, Ecosystems & Environment*, 81(1): 71–79, 2000.

[33] L. Cui, J. Wang, L. Sun, and C. Lv. Construction and optimization of green space ecological networks in urban fringe areas: A case study with the urban fringe area of tongzhou district in beijing. *Journal of Cleaner Production*, 276:124266, 2020.

[34] R. Cukier, C. Fortuin, K. E. Shuler, A. Petschek, and J. H. Schaibly. Study of the sensitivity of coupled reaction systems to uncertainties in rate coefficients. i theory. *The Journal of Chemical Physics*, 59(8):3873–3878, 1973.

[35] R. Cvejić, K. Eler, M. Pintar, Š. Železnikar, D. Haase, N. Kabisch, and M. Strohbach. A typology of urban green spaces, eco-system services provisioning services and demands. Technical Report D3.1, GREEN SURGE, 2015. URL https://web.archive.org/web/20190430143550id_/https://greensurge.eu/working-packages/wp3/files/D3.1_Typology_of_urban_green_spaces_1_.pdf/D3.1_Typology_of_urban_green_spaces_v2_.pdf. Accessed on 01.2025.

[36] M. Dash and H. Liu. Feature selection for classification. *Intelligent Data Analysis*, 1(1-4):131–156, 1997.

[37] J. Degerickx, M. Hermy, and B. Somers. Mapping functional urban green types using high resolution remote sensing data. *Sustainability*, 12(5):2144, 2020.

[38] C. Delgado. Mapping urban agriculture in portugal: Lessons from practice and their relevance for european post-crisis contexts. *Moravian Geographical Reports*, 25(3):139–153, 2017.

[39] A. Di Gregorio. *Land cover classification system: classification concepts and user manual: LCCS*, volume 2. Food & Agriculture Organization, 2005.

[40] O. Diedershagen, B. Koch, and H. Weinacker. Automatic segmentation and characterisation of forest stand parameters using airborne lidar data, multispectral and fogis data. In *International Archives of Photogrammetry, Remote Sensing and Spatial Information Sciences*, volume 36, pages 208–212, 2004.

[41] T. G. Dietterich. Machine-learning research. *AI magazine*, 18(4):97–97, 1997.

[42] J. Douet. *The water industry as world heritage*. TICCIH, 2018.

[43] M. Drilling, R. Giedych, L. Poniży, M. Benson, M. Bihunova, D. d. Mata, S. Meeres, P. Oehler, R. Štěpánková, N. Thomas, et al. The idea of allotment gardens and the role of spatial and urban planning. In *Urban Allotment Gardens in Europe*, pages 35–61. Routledge, 2016.

[44] L. El Hoummaidi, A. Larabi, and K. Alam. Using unmanned aerial systems and deep learning for agriculture mapping in dubai. *Heliyon*, 7(10), 2021.

[45] T. Emilsson and Å. Ode Sang. Impacts of climate change on urban areas and nature-based solutions for adaptation. In *Nature-based solutions to climate change adaptation in urban areas: linkages between science, policy and practice*, pages 15–27. Springer, 2017.

[46] F. Enssle and N. Kabisch. Urban green spaces for the social interaction, health and well-being of older people—an integrated view of urban ecosystem services and socio-environmental justice. *Environmental Science & Policy*, 109:36–44, 2020.

[47] S. G. Eraghi, M. Meschi, and S. Gholampour. Studying the relationship between urban green corridors and sustainable urban landscape. *International Journal of Science, Technology and Society*, 3(2-1):36–40, 2015.

[48] M. Ester, H.-P. Kriegel, J. Sander, and X. Xu. A density-based algorithm for discovering clusters in large spatial databases with noise. In *Proceedings of the Second International Conference on Knowledge Discovery and Data Mining*, volume 96, pages 226–231, 1996.

[49] F. Ferretti, A. Saltelli, and S. Tarantola. Trends in sensitivity analysis practice in the last decade. *Science of the Total Environment*, 568:666–670, 2016.

[50] P. Fisher, A. J. Comber, and R. Wadsworth. Land use and land cover: contradiction or complement. *Re-presenting GIS*, 85:98, 2005.

[51] D. Forde, L. McElduff, and G. Rafferty. Alley greening: a tool for enhancing community resilience? *Local Environment*, 29(9):1150–1169, 2024.

[52] M. Forrest. Allotments in dublin 1900–1950. *Irish Geography*, 44(2-3):265–290, 2011.

[53] D. Forster, T. W. Kellenberger, Y. Buehler, and B. Lennartz. Mapping diversified peri-urban agriculture–potential of object-based versus per-field land cover/land use classification. *Geocarto International*, 25(3):171–186, 2010.

[54] S. Freire, T. Santos, and J. A. Tenedório. Agriculture and food availability–cultivating the city: Mapping and characterizing urban agriculture with satellite imagery. Technical report, Earthzine, 2009. URL `https://earthzine.org/agriculture-and-food-availability-cultivating-the-city-mapping-and-\characterizing-urban-agriculture-with-satellite-imagery/`. Accessed on 01.2025.

[55] K. Fukunaga and L. Hostetler. The estimation of the gradient of a density function, with applications in pattern recognition. *IEEE Transactions on Information Theory*, 21(1):32–40, 1975.

[56] M. Gascon, M. Triguero-Mas, D. Martínez, P. Dadvand, J. Forns, A. Plasència, and M. J. Nieuwenhuijsen. Mental health benefits of long-term exposure to residential green and blue spaces: a systematic review. *International journal of Environmental Research and Public Health*, 12(4):4354–4379, 2015.

[57] A. Gebejes and R. Huertas. Texture characterization based on grey-level co-occurrence matrix. *Conference of Informatics and Management Sciences*, 9(10): 375–378, 2013.

[58] T. R. Gruber. Toward principles for the design of ontologies used for knowledge sharing? *International journal of Human-Computer Studies*, 43(5-6):907–928, 1995.

[59] N. Guarino. Semantic matching: Formal ontological distinctions for information organization, extraction, and integration. In *Information Extraction A Multidisciplinary Approach to an Emerging Information Technology*, pages 139–170. Springer, 1997.

[60] N. Guarino. *Formal ontology in information systems: Proceedings of the first international conference (FOIS'98)*, volume 46. IOS press, 1998.

[61] D. Gülçin and A. Akpinar. Mapping urban green spaces based on an object-oriented approach. *Bilge International Journal of Science and Technology Research*, 2:71–81, 2018.

[62] N. Guneroglu, C. Acar, M. Dihkan, F. Karsli, and A. Guneroglu. Green corridors and fragmentation in south eastern black sea coastal landscape. *Ocean & Coastal management*, 83:67–74, 2013.

[63] D. Haase, C. Jänicke, and T. Wellmann. Front and back yard green analysis with subpixel vegetation fractions from earth observation data in a city. *Landscape and Urban Planning*, 182:44–54, 2019.

[64] M. Hall-Beyer. Practical guidelines for choosing glcm textures to use in landscape classification tasks over a range of moderate spatial scales. *International Journal of Remote Sensing*, 38(5):1312–1338, 2017.

[65] R. M. Haralick. Statistical and structural approaches to texture. *Proceedings of the IEEE*, 67(5):786–804, 1979.

[66] C. Huang, J. Yang, and P. Jiang. Assessing impacts of urban form on landscape structure of urban green spaces in china using landsat images based on google earth engine. *Remote Sensing*, 10(10):1569, 2018.

[67] R. E. Huerta, F. D. Yépez, D. F. Lozano-García, V. H. Guerra Cobián, A. L. Ferriño Fierro, H. de León Gómez, R. A. Cavazos González, and A. Vargas-Martínez.

Mapping urban green spaces at the metropolitan level using very high resolution satellite imagery and deep learning techniques for semantic segmentation. *Remote Sensing*, 13(11):2031, 2021.

[68] I. Ismayilova and S. Timpf. Classifying urban green spaces using a combined sentinel-2 and random forest approach. *AGILE: GIScience Series*, 3:38, 2022.

[69] I. Ismayilova and S. Timpf. Semantic identification of urban green spaces: forest. *AGILE: GIScience Series*, 4:28, 2023.

[70] I. Ismayilova and S. Timpf. Towards an ontology of urban green spaces. *GI Forum 2022*, 10:47–57, 2023.

[71] I. Ismayilova and S. Timpf. Knowledge-based identification of urban green spaces: Allotments. *AGILE: GIScience Series*, 5:8, 2024.

[72] I. Ismayilova and S. Timpf. Identification of green corridors as a type of urban green spaces. Technical report, Zenodo, 2024. URL `https://zenodo.org/records/10927987`. Accessed on 01.2025.

[73] M. Jabbar, M. M. Yusoff, and A. Shafie. Assessing the role of urban green spaces for human well-being: A systematic review. *GeoJournal*, 87:4405–4423, 2022.

[74] L. Jones, S. Anderson, J. Læssøe, E. Banzhaf, A. Jensen, D. N. Bird, J. Miller, M. G. Hutchins, J. Yang, J. Garrett, T. Tim, W. Benedict W., L. Rebecca, F. David, Q. Yueming, V. Massimo, and Z. Marianne. A typology for urban green infrastructure to guide multifunctional planning of nature-based solutions. *Nature-Based Solutions*, 2:100041, 2022.

[75] Y. Ju, I. Dronova, and X. Delclòs-Alió. A 10 m resolution urban green space map for major latin american cities from sentinel-2 remote sensing images and openstreetmap. *Scientific Data*, 9(1):586, 2022.

[76] N. Kabisch and M. A. Van Den Bosch. Urban green spaces and the potential for health improvement and environmental justice in a changing climate. In *Nature-Based Solutions to Climate Change Adaptation in Urban Areas: Linkages between Science, Policy and Practice*, pages 207–220. Springer, 2017.

[77] R. Kaplan. The nature of the view from home: Psychological benefits. *Environment and Bbehavior*, 33(4):507–542, 2001.

[78] R. Kaplan and S. Kaplan. *The experience of nature: A psychological perspective*. Cambridge University press, 1989.

[79] S. Kaplan. The restorative benefits of nature: Toward an integrative framework. *Journal of Environmental Psychology*, 15(3):169–182, 1995.

[80] J. G. Kelcey and N. Müller. *Plants and habitats of European cities*. Springer Science & Business Media, 2011.

[81] N. Kelly and S. Di Tommaso. Mapping forests with lidar provides flexible, accurate data with many uses. *California Agriculture*, 69(1):14–20, 2015.

[82] L. Kettner, K. Mehlhorn, S. Pion, S. Schirra, and C. Yap. Classroom examples of robustness problems in geometric computations. *Computational Geometry*, 40(1): 61–78, 2008.

[83] K. Kim. Estimation of stand height and forest volume using high resolution stereo photography and forest type map. *The International Archives of the Photogrammetry, Remote Sensing and Spatial Information Sciences*, 41:695–698, 2016.

[84] C. B. Koc, P. Osmond, and A. Peters. A green infrastructure typology matrix to support urban microclimate studies. *Procedia Engineering*, 169:183–190, 2016.

[85] S. Korpilo, A. Kajosaari, T. Rinne, K. Hasanzadeh, C. M. Raymond, and M. Kyttä. Coping with crisis: green space use in helsinki before and during the covid-19 pandemic. *Frontiers in Sustainable Cities*, 3:713977, 2021.

[86] H.-P. Kriegel, P. Kröger, J. Sander, and A. Zimek. Density-based clustering. *Wiley interdisciplinary reviews: data mining and knowledge discovery*, 1(3):231–240, 2011.

[87] S. Labib and A. Harris. The potentials of sentinel-2 and landsat-8 data in green infrastructure extraction, using object based image analysis (obia) method. *European Journal of Remote Sensing*, 51(1):231–240, 2018.

[88] L. Lilburne and S. Tarantola. Sensitivity analysis of spatial models. *International Journal of Geographical Information Science*, 23(2):151–168, 2009.

[89] F. Lohrberg, L. Lička, L. Scazzosi, A. Timpe, and J. Verlag. *Urban agriculture europe*, volume 38. Jovis Berlin, 2016.

[90] M. Louhaichi, M. M. Borman, and D. E. Johnson. Spatially located platform and aerial photography for documentation of grazing impacts on wheat. *Geocarto International*, 16(1):65–70, 2001.

[91] S. T. Lovell and J. R. Taylor. Supplying urban ecosystem services through multifunctional green infrastructure in the united states. *Landscape Ecology*, 28:1447–1463, 2013.

[92] C. Ludwig, R. Hecht, S. Lautenbach, M. Schorcht, and A. Zipf. Mapping public urban green spaces based on openstreetmap and sentinel-2 imagery using belief functions. *ISPRS International Journal of Geo-Information*, 10(4):251, 2021.

[93] S. Lundberg. A unified approach to interpreting model predictions. Technical report, ArXiv, 2017. URL `https://arxiv.org/pdf/1705.07874`. Accessed on 01.2025.

[94] S. M. Lundberg, G. Erion, H. Chen, A. DeGrave, J. M. Prutkin, B. Nair, R. Katz, J. Himmelfarb, N. Bansal, and S.-I. Lee. From local explanations to global understanding with explainable ai for trees. *Nature Machine Intelligence*, 2(1):56–67, 2020.

[95] R. Mathieu, C. Freeman, and J. Aryal. Mapping private gardens in urban areas using object-oriented techniques and very high-resolution satellite imagery. *Landscape and Urban Planning*, 81(3):179–192, 2007.

[96] L. Matikainen, J. Hyyppä, E. Ahokas, L. Markelin, and H. Kaartinen. Automatic detection of buildings and changes in buildings for updating of maps. *Remote Sensing*, 2(5):1217–1248, 2010.

[97] J. McEldowney. Urban agriculture in europe: Patterns, challenges and policies. In *European Parliamentary Research Service*, volume PE 614.641, 2017.

[98] K. Millard and M. Richardson. On the importance of training data sample selection in random forest image classification: A case study in peatland ecosystem mapping. *Remote sensing*, 7(7):8489–8515, 2015.

[99] P. Mohammadpour, D. X. Viegas, and C. Viegas. Vegetation mapping with random forest using sentinel 2 and glcm texture feature—a case study for lousã region, portugal. *Remote Sensing*, 14(18):4585, 2022.

[100] M. Monmonier. *How to lie with maps*. University of Chicago Press, 2018.

[101] E. Montero, J. Van Wolvelaer, and A. Garzón. The european urban atlas. In *Land Use and Land Cover Mapping in Europe: Practices & Trends*, pages 115–124. Springer, 2014.

[102] R. Moreno, N. Ojeda, J. Azócar, C. Venegas, and L. Inostroza. Application of ndvi for identify potentiality of the urban forest for the design of a green corridors system in intermediary cities of latin america: Case study, temuco, chile. *Urban Forestry & Urban Greening*, 55:126821, 2020.

[103] J. Morpurgo, R. P. Remme, and P. M. Van B. Cugic: The consolidated urban green infrastructure classification for assessing ecosystem services and biodiversity. *Landscape and Urban Planning*, 234:104726, 2023.

[104] T. Motohka, K. N. Nasahara, H. Oguma, and S. Tsuchida. Applicability of green-red vegetation index for remote sensing of vegetation phenology. *Remote Sensing*, 2(10):2369–2387, 2010.

[105] I. Mourão, M. Moreira, T. Almeida, and L. M. Brito. Perceived changes in well-being and happiness with gardening in urban organic allotments in portugal. *International Journal of Sustainable Development & World Ecology*, 26(1):79–89, 2019.

[106] R. B. Myneni, F. G. Hall, P. J. Sellers, and A. L. Marshak. The interpretation of spectral vegetation indexes. *IEEE Transactions on Geoscience and Remote Sensing*, 33(2):481–486, 1995.

[107] E. Næsset. Determination of mean tree height of forest stands by digital photogrammetry. *Scandinavian Journal of Forest Research*, 17(5):446–459, 2002.

[108] R. Neyns and F. Canters. Mapping of urban vegetation with high-resolution remote sensing: A review. *Remote Sensing*, 14(4):1031, 2022.

[109] I. Opitz, R. Berges, A. Piorr, and T. Krikser. Contributing to food security in urban areas: differences between urban agriculture and peri-urban agriculture in the global north. *Agriculture and Human Values*, 33:341–358, 2016.

[110] T. E. Panduro and K. L. Veie. Classification and valuation of urban green spaces—a hedonic house price valuation. *Landscape and Urban planning*, 120:119–128, 2013.

[111] Y. Park and J.-M. Guldmann. Measuring continuous landscape patterns with gray-level co-occurrence matrix (glcm) indices: An alternative to patch metrics? *Ecological Indicators*, 109:105802, 2020.

[112] M. Peña, R. Liao, and A. Brenning. Using spectrotemporal indices to improve the fruit-tree crop classification accuracy. *ISPRS Journal of Photogrammetry and Remote Sensing*, 128:158–169, 2017.

[113] M. Pereira and M. Lee. Identification of genomic regions affecting plant height in sorghum and maize. *Theoretical and Applied Genetics*, 90(3):380–388, 1995.

[114] O.-C. Popescu, A.-V. Tache, and A.-I. Petrișor. Methodology for identifying ecological corridors: A spatial planning perspective. *Land*, 11(7):1013, 2022.

[115] A. Puissant, S. Rougier, and A. Stumpf. Object-oriented mapping of urban trees using random forest classifiers. *International Journal of Applied Earth Observation and Geoinformation*, 26:235–245, 2014.

[116] J. Rathmann. *Therapeutic Landscapes: An Interdisciplinary Perspective on Landscape and Health*. Springer, 2021.

[117] F. Reinwald, D. Haluza, U. Pitha, and R. Stangl. Urban green infrastructure and green open spaces: An issue of social fairness in times of covid-19 crisis. *Sustainability*, 13(19):10606, 2021.

[118] R. Reyes-Riveros, A. Altamirano, F. De La Barrera, D. Rozas-Vásquez, L. Vieli, and P. Meli. Linking public urban green spaces and human well-being: A systematic review. *Urban Forestry & Urban Greening*, 61:127105, 2021.

[119] D. Robertson, Laura, King, and D. J. Comparison of pixel-and object-based classification in land cover change mapping. *International Journal of Remote Sensing*, 32(6):1505–1529, 2011.

[120] A. Rosenqvist, M. Shimada, B. Chapman, A. Freeman, G. De Grandi, S. Saatchi, and Y. Rauste. The global rain forest mapping project-a review. *International Journal of Remote Sensing*, 21(6-7):1375–1387, 2000.

[121] Y. Saeys, T. Abeel, and Y. Van de Peer. Robust feature selection using ensemble feature selection techniques. In *Machine Learning and Knowledge Discovery in Databases*, pages 313–325. Springer, 2008.

[122] A. Saltelli and P. Annoni. How to avoid a perfunctory sensitivity analysis. *Environmental Modelling & Software*, 25(12):1508–1517, 2010.

[123] A. Saltelli, S. Tarantola, and F. Campolongo. Sensitivity analysis as an ingredient of modeling. *Statistical Science*, 15(4):377–395, 2000.

[124] A. Saltelli, M. Ratto, S. Tarantola, F. Campolongo, and J. R. C. o. I. European Commission. Sensitivity analysis practices: Strategies for model-based inference. *Reliability Engineering & System Safety*, 91(10-11):1109–1125, 2006.

[125] T. Semeraro, A. Scarano, R. Buccolieri, A. Santino, and E. Aarrevaara. Planning of urban green spaces: An ecological perspective on human benefits. *Land*, 10(2): 105, 2021.

[126] C. S. Shafer, D. Scott, and J. Mixon. A greenway classification system: Defining the function and character of greenways in urban areas. *Journal of Park & Recreation Administration*, 18(2), 2000.

[127] A. R. Shahtahmassebi, C. Li, Y. Fan, Y. Wu, M. Gan, K. Wang, A. Malik, and G. A. Blackburn. Remote sensing of urban green spaces: A review. *Urban Forestry & Urban Greening*, 57:126946, 2021.

[128] M. Simard, N. Pinto, J. B. Fisher, and A. Baccini. Mapping forest canopy height globally with spaceborne lidar. *Journal of Geophysical Research: Biogeosciences*, 116(G4), 2011.

[129] V. Simonneaux, B. Duchemin, D. Helson, S. Er-Raki, A. Olioso, and A. Chehbouni. The use of high-resolution image time series for crop classification and evapotranspiration estimate over an irrigated area in central morocco. *International Journal of Remote Sensing*, 29(1):95–116, 2008.

[130] R. K. Singh, P. Singh, M. Drews, P. Kumar, H. Singh, A. K. Gupta, H. Govil, A. Kaur, and M. Kumar. A machine learning-based classification of landsat images to map land use and land cover of india. *Remote Sensing Applications: Society and Environment*, 24:100624, 2021.

[131] I. M. Sobol'. On sensitivity estimation for nonlinear mathematical models. *Matematicheskoe Modelirovanie*, 2(1):112–118, 1990.

[132] G. Sun, K. J. Ranson, Z. Guo, Z. Zhang, P. Montesano, and D. Kimes. Forest biomass mapping from lidar and radar synergies. *Remote Sensing of Environment*, 115(11):2906–2916, 2011.

[133] Y. Sun, Q. Meng, Z. Sun, J. Zhang, and L. Zhang. Assessing the impacts of grain sizes on landscape pattern of urban green space. In *AOPC 2017: Optical Sensing and Imaging Technology and Applications*, volume 10462, pages 934–940. SPIE, 2017.

[134] C. Swanwick, N. Dunnett, and H. Woolley. Nature, role and value of green space in towns and cities: An overview. *Built Environment (1978-)*, 120(2):94–106, 2003.

[135] H. Taubenböck, M. Reiter, F. Dosch, T. Leichtle, M. Weigand, and M. Wurm. Which city is the greenest? a multi-dimensional deconstruction of city rankings. *Computers, Environment and Urban Systems*, 89:101687, 2021.

[136] J. R. Taylor and S. T. Lovell. Mapping public and private spaces of urban agriculture in chicago through the analysis of high-resolution aerial images in google earth. *Landscape and Urban Planning*, 108(1):57–70, 2012.

[137] A. Temenos, N. Temenos, M. Kaselimi, A. Doulamis, and N. Doulamis. Interpretable deep learning framework for land use and land cover classification in remote sensing using shap. *IEEE Geoscience and Remote Sensing Letters*, 20:1–5, 2023.

[138] H. Thierfelder and N. Kabisch. Viewpoint berlin: Strategic urban development in berlin–challenges for future urban green space development. *Environmental Science & Policy*, 62:120–122, 2016.

[139] S. Timpf. Ontologies of wayfinding: a traveler's perspective. *Networks and Spatial Economics*, 2:9–33, 2002.

[140] C. J. Tucker. Red and photographic infrared linear combinations for monitoring vegetation. *Remote Sensing of Environment*, 8(2):127–150, 1979.

[141] K. Tzoulas, K. Korpela, S. Venn, V. Yli-Pelkonen, A. Kaźmierczak, J. Niemela, and P. James. Promoting ecosystem and human health in urban areas using green

infrastructure: A literature review. *Landscape and Urban Planning*, 81(3):167–178, 2007.

[142] P. Vogt, K. H. Riitters, M. Iwanowski, C. Estreguil, J. Kozak, and P. Soille. Mapping landscape corridors. *Ecological Indicators*, 7(2):481–488, 2007.

[143] T. T. Vu, M. Matsuoka, and F. Yamazaki. Lidar-based change detection of buildings in dense urban areas. In *IEEE International Geoscience and Remote Sensing Symposium*, volume 5, pages 3413–3416. IEEE, 2004.

[144] B. Wagner and M. Egerer. Application of uav remote sensing and machine learning to model and map land use in urban gardens. *Journal of Urban Ecology*, 8(1): juac008, 2022.

[145] H. Wang and Z. Pei. Urban green corridors analysis for a rapid urbanization city exemplified in gaoyou city, jiangsu. *Forests*, 11(12):1374, 2020.

[146] L. Wang, C. Shi, C. Diao, W. Ji, and D. Yin. A survey of methods incorporating spatial information in image classification and spectral unmixing. *International Journal of Remote Sensing*, 37(16):3870–3910, 2016.

[147] M. Weigand, J. Staab, M. Wurm, and H. Taubenböck. Spatial and semantic effects of lucas samples on fully automated land use/land cover classification in high-resolution sentinel-2 data. *International Journal of Applied Earth Observation and Geoinformation*, 88:102065, 2020.

[148] C. J. Wood, J. Pretty, and M. Griffin. A case–control study of the health and well-being benefits of allotment gardening. *Journal of Public Health*, 38(3):e336–e344, 2016.

[149] C. Xie, J. Wang, D. Haase, T. Wellmann, and A. Lausch. Measuring spatio-temporal heterogeneity and interior characteristics of green spaces in urban neighborhoods: A new approach using gray level co-occurrence matrix. *Science of the Total Environment*, 855:158608, 2023.

[150] Z. Yan. Establishment of urban green corridor network based on neural network and landscape ecological security. *Journal of Computational Science*, 79:102315, 2024.

[151] Y. Zeng, D. Hao, A. Huete, B. Dechant, J. Berry, J. M. Chen, J. Joiner, C. Frankenberg, B. Bond-Lamberty, Y. Ryu, J. Xiao, G. R. Asrar, and M. Chen. Optical vegetation indices for monitoring terrestrial ecosystems globally. *Nature Reviews Earth & Environment*, 3(7):477–493, 2022.

[152] J. Zeunert. Urban agriculture up-scaled: economically and socially productive public green space. In *Sustainable urban agriculture and food planning*, pages 121–139. Routledge, 2016.

[153] J. Zeunert. Dimensions of urban agriculture. In *Routledge handbook of landscape and food*, pages 160–184. Routledge, 2018.

[154] Z. Zhang, S. Meerow, J. P. Newell, and M. Lindquist. Enhancing landscape connectivity through multifunctional green infrastructure corridor modeling and design. *Urban forestry & Urban Greening*, 38:305–317, 2019.

[155] L. Zheng, J. Zhang, and Q. Wang. Mean-shift-based color segmentation of images containing green vegetation. *Computers and Electronics in Agriculture*, 65(1):93–98, 2009.

[156] Zylshal, S. Sulma, F. Yulianto, J. T. Nugroho, and P. Sofan. A support vector machine object based image analysis approach on urban green space extraction using pleiades-1a imagery. *Modeling Earth Systems and Environment*, 2:1–12, 2016.